Ontario

Ontario Geological Survey
Open File Report 6156

# Volcanic Stratigraphy and Controls on Mineralization in the Genex Mine Area, Kamiskotia Area: Discover Abitibi Initiative

2005

105-03973/

Ontario

ONTARIO GEOLOGICAL SURVEY

Open File Report 6156

# Volcanic Stratigraphy and Controls on Mineralization in the Genex Mine Area, Kamiskotia Area: Discover Abitibi Initiative

by

S.M. Hocker, P.C. Thurston and H.L. Gibson

2005

Parts of this publication may be quoted if credit is given. It is recommended that reference to this publication be made in the following form:

Hocker, S.M., Thurston, P.C. and Gibson, H.L. 2005. Volcanic stratigraphy and controls on mineralization in the Genex Mine area, Kamiskotia area: Discover Abitibi Initiative; Ontario Geological Survey, Open File Report 6156, 143p.

Discover Abitibi
A project of innovation, cooperation and revitalization

Découvrons l' Abitibi
Un projet d' innovation, de coopération et de renouvellement

Discover Abitibi Initiative
The Discover Abitibi Initiative is a regional, cluster economic development project based on geoscientific investigations of the western Abitibi greenstone belt. The initiative, centred on the Kirkland Lake and Timmins mining camps, will complete 19 projects developed and directed by the local stakeholders. FedNor, Northern Ontario Heritage Fund Corporation, municipalities and private sector investors have provided the funding for the initiative.

Initiative Découvrons l'Abitibi
L'initiative Découvrons l'Abitibi est un project de développment économique régional dans une grappe d'industries, projet fondé sur des études géoscientifiques de la ceinture de roches vertes de l'Abitibi occidental. Cette initiative, centrée sur les zones minières de Kirkland Lake et de Timmins, mènera à bien 19 projets élaborés et dirigés par des intervenants locaux. FedNor, la Société de gestion du Fonds du patrimoine du Nord de l'Ontario, municipalités et des investisseurs du secteur privé ont fourni les fonds de cette initiative.

FedNor
Canada

Timmins

KIRKLAND LAKE

Ontario
Northern Ontario Heritage Fund
Fonds du patrimoine du Nord de l'Ontario

© Queen's Printer for Ontario, 2005

© Queen's Printer for Ontario, 2005.

Open File Reports of the Ontario Geological Survey are available for viewing at the Mines Library in Sudbury, at the Mines and Minerals Information Centre in Toronto, and at the regional Mines and Minerals office whose district includes the area covered by the report (see below).

Copies can be purchased at Publication Sales and the office whose district includes the area covered by the report. Although a particular report may not be in stock at locations other than the Publication Sales office in Sudbury, they can generally be obtained within 3 working days. All telephone, fax, mail and e-mail orders should be directed to the Publication Sales office in Sudbury. Use of VISA or MasterCard ensures the fastest possible service. Cheques or money orders should be made payable to the *Minister of Finance*.

Mines and Minerals Information Centre (MMIC)
Macdonald Block, Room M2-17
900 Bay St.
Toronto, Ontario M7A 1C3
Tel: (416) 314-3800

Mines Library
933 Ramsey Lake Road, Level A3
Sudbury, Ontario P3E 6B5
Tel: (705) 670-5615

Publication Sales
933 Ramsey Lake Rd., Level A3
Sudbury, Ontario P3E 6B5
Tel: (705) 670-5691(local)
1-888-415-9845(toll-free)
Fax: (705) 670-5770
E-mail: pubsales@ndm.gov.on.ca

**Regional Mines and Minerals Offices:**

Kenora - Suite 104, 810 Robertson St., Kenora P9N 4J2

Kirkland Lake - 10 Government Rd. E., Kirkland Lake P2N 1A8

Red Lake - Box 324, Ontario Government Building, Red Lake P0V 2M0

Sault Ste. Marie - 70 Foster Dr., Ste. 200, Sault Ste. Marie P6A 6V8

Southern Ontario - P.O. Bag Service 43, 126 Old Troy Rd., Tweed K0K 3J0

Sudbury - Level B3, 933 Ramsey Lake Rd., Sudbury P3E 6B5

Thunder Bay - Suite B002, 435 James St. S., Thunder Bay P7E 6S7

Timmins - Ontario Government Complex, P.O. Bag 3060, Hwy. 101 East, South Porcupine P0N 1H0

Toronto - MMIC, Macdonald Block, Room M2-17, 900 Bay St., Toronto M7A 1C3

This report has not received a technical edit. Discrepancies may occur for which the Ontario Ministry of Northern Development and Mines does not assume any liability. Source references are included in the report and users are urged to verify critical information. Recommendations and statements of opinions expressed are those of the author or authors and are not to be construed as statements of government policy.

If you wish to reproduce any of the text, tables or illustrations in this report, please write for permission to the Team Leader, Publication Services, Ministry of Northern Development and Mines, 933 Ramsey Lake Road, Level B4, Sudbury, Ontario P3E 6B5.

**Cette publication est disponible en anglais seulement.**

Parts of this report may be quoted if credit is given. It is recommended that reference be made in the following form:

**Hocker, S.M., Thurston, P.C. and Gibson, H.L. 2005. Volcanic stratigraphy and controls on mineralization in the Genex Mine area, Kamiskotia area: Discover Abitibi Initiative; Ontario Geological Survey, Open File Report 6156, 143p.**

# Contents

Abstract ..... xvii

Introduction ..... 1
  Goals and Objectives of Study ..... 1
  Location and Access ..... 3
  Field and Analytical Methods ..... 3
  Previous Work and History of the Genex Mine ..... 4
  Structure of Report ..... 4
  Regional Geology ..... 5
    The Abitibi Greenstone Belt ..... 5
    The Kamiskotia Volcanic Complex ..... 7

Stratigraphy in the Genex Area ..... 8
  Introduction ..... 8
  Felsic Metavolcanic Rocks ..... 8
  Mafic Metavolcanic Rocks ..... 13
  Mafic Intrusive Rocks ..... 20
  Intermediate Intrusive Rocks ..... 24
  Volcaniclastic and Epiclastic Rocks ..... 26
  Late Diabase Intrusive Rocks (Matachewan) ..... 28

Deformation ..... 29
  Faults ..... 29
  Shear Zones ..... 29

Geochemistry ..... 29
  Introduction ..... 29
  Element Mobility ..... 30
  Fractionation Trends ..... 37
  Rare Earth Element Trends ..... 43
    Felsic Metavolcanic Rocks ..... 43
    Mafic Metavolcanic Rocks ..... 47
    Synvolcanic Intrusive Rocks ..... 50
  Contamination ..... 53
  Geologic Setting ..... 56

Hydrothermal Alteration ..... 61
  Introduction ..... 61
  Sericitization ..... 63
  Chloritization ..... 64
  Epidotization ..... 66
  Silicification ..... 67
  Fe-Carbonate Alteration ..... 69
  Alteration Chemistry ..... 70

Controls on Mineralization ........ 72
  Introduction ........ 72
  Controls on C-Zone Mineralization ........ 73
  Controls on H-Zone and A-Zone Mineralization ........ 74
  Shear Zone Mineralization ........ 75
  Intrusions and Mineralization ........ 76
  Discussion of the Genex Mineralization ........ 77

Summary ........ 78

Recommendations ........ 81

References ........ 81

Appendix 1. Petrographic Descriptions of Samples ........ 87

Appendix 2. Drill Hole Identifications ........ 103

Appendix 3. Listing of Geochemical Data from the Genex Mine Area ........ 105

Appendix 4. Previous Ownership and Exploration History of the Genex Mine Area ........ 133

Appendix 5. Outcrop, Drill Hole and Waypoint UTM Locations ........ 135

Metric Conversion Table ........ 143

## FIGURES

1. Generalized map of Ontario ........ 1
2. Location map of the Genex area showing lots, concessions, claims, and dispositions ........ 2
3. Location map of access to the Kamiskotia area ........ 3
4. Generalized map of the Abitibi greenstone belt ........ 6
5. Distribution of supracrustal groups in the southern Abitibi greenstone belt ........ 6
6. Regional geology of the Kamiskotia volcanic complex ........ 7
7. Stratigraphic section through the Genex deposit ........ 9
8. Sketch map of graded felsic lapilli and ash-tuff from unit 3 ........ 10
9. Schematic block diagram of pillow morphology and size as a function of slope ........ 14
10. 1:100 scale map of pillowed basalts ........ 15
11. 1:100 scale map of pillowed basalts and hyaloclastite breccia ........ 16
12. 1:50 scale map of contact between synvolcanic mafic intrusion and felsic flow breccia ........ 23
13. Selected variation diagrams of immobile elements in Genex felsic metavolcanic rocks ........ 32
14. Selected variation diagrams of immobile elements in Genex mafic metavolcanic rocks ........ 33
15. Selected variation diagrams of immobile elements in the Genex synvolcanic mafic intrusion ........ 34
16. Selected variation diagrams of immobile elements in the Genex synvolcanic intermediate intrusion ........ 35
17. $Na_2O + K_2O$ (total alkalis) versus $SiO_2$ plots of felsic and mafic metavolcanic rocks in the Genex area ... 36
18. $Zr/TiO_2$ versus Nb/Y plot of felsic and mafic metavolcanic rocks in the Genex area ........ 36
19. Fractionation trends in Genex footwall mafic metavolcanic rocks ........ 39

20. Fractionation trends in Genex hanging-wall mafic metavolcanic rocks ........ 40
21. Fractionation trends in Genex synvolcanic mafic intrusion ........ 41
22. Fractionation trends in Genex synvolcanic intermediate intrusion ........ 42
23. Plagioclase fractionation trends in Genex felsic metavolcanic rocks ........ 43
24. Zr/$TiO_2$ versus Nb/Y classification of felsic volcanic rocks ........ 44
25. Zr/Y versus Y plot for classification of rhyolites ........ 45
26. Chondrite-normalized spider plot of Genex felsic metavolcanic rocks ........ 46
27. Primitive mantle-normalized spider plot of Genex felsic metavolcanic rocks ........ 46
28. Zr/$TiO_2$ versus Nb/Y classification of mafic volcanic rocks ........ 47
29. Tectonic environment of formation for Genex mafic metavolcanic rocks ........ 48
30. $P_2O_5$ versus Zr discrimination diagram for mafic rocks ........ 48
31. Nb/Y versus Zr/($P_2O_5$ × 10000) discrimination diagram for mafic volcanic rocks ........ 49
32. Chondrite-normalized spider plot of Genex mafic metavolcanic rocks ........ 49
33. Zr/$TiO_2$ versus Nb/Y classification of intrusive rocks ........ 50
34. $P_2O_5$ versus Zr discrimination diagram for intrusive rocks ........ 51
35. Nb/Y versus Zr/($P_2O_5$ × 10000) discrimination diagram for intrusive rocks ........ 51
36. Chondrite-normalized spider diagram of the Genex synvolcanic mafic intrusion ........ 52
37. Chondrite-normalized spider diagram of the Genex synvolcanic intermediate intrusion ........ 52
38. Chondrite-normalized spider plot of Genex synvolcanic mafic intrusions and intermediate intrusion compared to trends in the Kamiskotia gabbroic complex ........ 53
39. Y–Nb–Ce felsic derivative magma composition ternary plot ........ 54
40. Zr–Ti/100–Y*3 magma–upper crust interaction ternary plot [for] mafic metavolcanic rocks ........ 55
41. Zr–Ti/100–Y*3 magma–upper crust interaction ternary plot [for] synvolcanic mafic intrusion ........ 55
42. Zr–Ti/100–Y*3 magma–upper crust interaction ternary plot [for] synvolcanic intermediate intrusion ..... 56
43. Nb versus Y tectonic discrimination diagram for rocks of granitic composition ........ 57
44. Ta versus Yb tectonic discrimination diagram for felsic rocks ........ 57
45. Rb versus Y + Nb tectonic discrimination diagram for felsic rocks ........ 58
46. Rb versus Yb + Ta tectonic discrimination diagram for felsic rocks ........ 58
47. Th–Zr/117–Nb/16 discrimination diagram for mafic rocks ........ 59
48. Th–Hf/3–Ta discrimination diagram for mafic rocks ........ 59
49. Th–Zr/117–Nb/16 discrimination diagram for intrusive rocks ........ 60
50. Nb versus Y tectonic discrimination diagram for intrusive rocks ........ 60
51. Generalized model of a hydrothermal system associated with the genesis of VMS deposits ........ 62
52. Alteration box plot of felsic metavolcanic rocks and mafic metavolcanic rocks ........ 65
53. Alteration box plot of mafic synvolcanic intrusion, intermediate synvolcanic intrusion and Matachewan diabase dike ........ 66
54. $K_2O + Na_2O$ versus ($100^* K_2O$)/($K_2O + Na_2O$) Harker diagram showing alteration of felsic metavolcanic rocks in the Genex area ........ 71

55. MgO versus $SiO_2$ plot of footwall and hanging-wall mafic metavolcanic rocks in the Genex area .......... 72
56. 1:2500 scale geological map of the Genex Mine area .......... back pocket

## PHOTOS

1. Felsic lapilli- and block-tuff .......... 11
2. Bedded felsic-tuff .......... 11
3. *In situ* brecciated felsic-tuff .......... 12
4. Flow banded felsic flow breccia .......... 12
5. Spherulites in felsic flow .......... 12
6. Felsic hyaloclastite .......... 13
7. Well-defined pillows .......... 17
8. Pillow lobe, in footwall .......... 17
9. Quartz amygdules in pillowed flow .......... 18
10. Budding in pillowed flow, with interpreted flow direction .......... 18
11. Concentric cooling cracks in pillowed flow .......... 18
12. Spherulitic margin and bleached selvage in hanging-wall pillows .......... 19
13. Irregular shaped pillows and hyaloclastite breccia, with interpreted flow direction .......... 19
14. Pillow breccia with silicified fragments and sulphides in matrix .......... 19
15. Bedded mafic-tuff overlain by pillowed flow .......... 20
16. Coarse- to medium-grained intrusion .......... 21
17. Mineralization in the lower mafic intrusion .......... 21
18. Brecciation at the base of the lower intrusion .......... 22
19. Amoeboid dikes in unconsolidated felsic-tuff .......... 22
20. Peperite .......... 22
21. Polygonal joints and pyrite mineralization in the north-trending sill .......... 25
22. Mixed zone in upper contact of north-trending sill .......... 25
23. Coherent block of lapilli-tuff in upper contact of north-trending sill .......... 25
24. Shattered fragments of intermediate intrusion in a glassy matrix .......... 26
25. Heterolithic lapilli-tuff breccia .......... 27
26. Bedded-tuff .......... 27
27. Finely laminated mudstone .......... 27
28. Mineralized mudstone fragment in lapilli-tuff .......... 28
29. Matachewan diabase dike .......... 28
30. Sericite alteration if felsic lapilli-tuff .......... 63
31. Sericite alteration in felsic-tuff .......... 63
32. Chlorite alteration in pillowed mafic metavolcanic rocks .......... 64
33. Chlorite alteration concentrated in pillow selvages .......... 65

34. Epidote-filled amygdule in pillowed mafic metavolcanic rock ........ 67
35. Quartz-filled amygdules in pillowed metavolcanic rock ........ 67
36. Quartz veins and epidote alteration in pillowed mafic metavolcanic rock ........ 68
37. Quartz filled amygdules in intermediate intrusion ........ 68
38. "Lacy" silicification in intermediate intrusion ........ 68
39. Outcrop appearance of Fe-carbonate alteration in massive mafic unit ........ 69
40. Photomicrograph of Fe-carbonate rhombs ........ 69
41. Fe-carbonate veins in mafic unit ........ 70
42. Massive Fe-carbonate alteration in mafic intrusion ........ 70
43. Mineralized pillow breccia in the C-zone ........ 73
44. C-zone stringer sulphide mineralization contained within a pillow selvage ........ 74
45. H-zone sulphide mineralization in felsic lapilli-tuff ........ 75
46. A-zone sulphide mineralization in intermediate synvolcanic intrusions ........ 75
47. Shear-hosted mineralization in claim post zone ........ 76
48. Black sphalerite mineralization in "Claim Post zone" ........ 76

**Appendix 1**

49. Photomicrographs, in crossed polarized light, of A) fragmental felsic flow; B) felsic lapilli tuff; C) ash-rich felsic lapilli tuff; D) felsic lapilli tuff with pumice and felsic fragments ........ 88
50. Photomicrographs, in crossed polarized light, of A) quartz amygdaloidal fine-grained mafic volcanic rock; B) medium-grained mafic volcanic rock; C) diabasic mafic volcanic rock; D) pillow breccia ........ 91
51. Photomicrographs, in crossed polarized light, of A) medium-grained mafic intrusion; B) coarse-grained mafic intrusion ........ 94
52. Photomicrographs, in crossed polarized light, of A) medium-grained intermediate intrusion; B) coarse-grained intermediate intrusion ........ 96
53. Photomicrographs of A) finely laminated mudstone in plane polarized light; B) bedded tuff in plane polarized light; C) polymict lapilli-tuff in crossed polarized light. ........ 98
54. Photomicrograph of coarse-grained Matachewan diabase intrusion in crossed polarized light. ........ 100

## TABLES

1. Highlights of previous work and history of the Genex Mine area ........ 4
2. Trace element classification and behaviour during alteration ........ 30
3. Correlation coefficients for selected variation diagrams of Genex rocks ........ 31
4. Summary of element mobility trends in Genex rocks ........ 31
5. Classification of felsic volcanic rocks in the Abitibi belt ........ 44
6. Classification of Abitibi belt igneous rocks ........ 61
7. Classification of VMS deposits based on host rock composition ........ 77

**Appendix 4**

8. Table of ownership and exploration history in the Genex mine area ........ 134

Miscellaneous Release—Data 144

## Geochemical, Petrographic and Compilation Data from the Genex Mine Area, Kamiskotia Area: Discover Abitibi Initiative

by S.M. Hocker, P.C. Thurston and H.L. Gibson

This digital data release, produced as part of the Discover Abitibi Initiative, is being released in conjunction with Open File Report 6156. This release contains 1) ArcMap® files for a 1:2500 scale geological map of the Genex Mine area in Godfrey Township (Figure 56 in OFR 6156); 2) colour versions (*.tif*) of two 1:100 scale maps and a 1:50 scale map (Figures 10, 11 and 12, respectively, in OFR 6156); 3) drill core photographs; 4) drill logs; 5) geochemical analyses; 6) outcrop photographs; 7) petrographic descriptions; and 8) photomicrographs. The data are available as Microsoft® Word 2002 (*.doc*), Microsoft® Access 97 and 2002 (*.mdb*), Microsoft® Excel 2002 (*.xls*), ArcMap® 8.3 (*.mxd*), and image (*.jpg* and *.tif*) files on one CD-ROM.

# Abstract

As part of the Base Metal Subproject of the Discover Abitibi Initiative, a two-year study has been conducted in the Genex Mine area, in the Kamiskotia area of the western part of the Abitibi greenstone belt. Geologic mapping and core logging has been conducted to better define the stratigraphy, deformation, and hydrothermal alteration in the Genex area and to determine the controls on the volcanogenic massive sulphide mineralization in the Genex Mine area. The Genex deposit consists of 3 lenses of mineralization that were mined from 1964 to 1966, producing approximately 242 tonnes (218 tons) of copper concentrate containing 21 to 27% Cu. The deposit is hosted in a bimodal sequence of metavolcanic rocks correlated with the Blake River assemblage based on a U/Pb age of 2698.6±1.3 Ma obtained on a felsic metavolcanic rock located south-southwest of the Genex Mine, as well as the bimodal character of the stratigraphy. The volcanic rocks are overlain by a volcaniclastic and epiclastic unit, and cut by Proterozoic (2454±2 Ma) diabase dikes of the Matachewan swarm. The sequence is a north-trending, eastward-younging succession approximately 2 km thick, bounded by the availability of outcrop to the west, and by the volcaniclastic and epiclastic succession to the east.

Felsic metavolcanic rocks are prevalent in the area surrounding the Genex deposit and represent a generally fining-upward succession. Tuff-breccias are common at the base of the mine stratigraphy, with lapilli- to block-size fragments that are commonly of the same composition as their matrix. Normally graded lapilli-tuff to bedded-tuff sequences are found throughout the stratigraphy. Small felsic flows and flow breccias occur in the footwall of the Genex deposit and also cutting the volcaniclastic units in the hanging wall of the Genex deposit. Whole rock geochemical analysis indicates that the felsic metavolcanic rocks are FIIIa rhyolites, and were erupted or emplaced in an arc environment.

Mafic metavolcanic rocks are present in both the footwall and the hanging wall of the Genex strata, and overlie the felsic sequence. Mafic metavolcanic rocks consist of pillowed and massive flows as well as minor mafic tuffs. Significant variations in pillow size, morphology, strike, and flow direction documented in pillows in the immediate footwall of the deposit indicate downslope movement of the flow from a paleotopographic high, with the crest located at or near the C-zone orebody. Small pillow breccia units and massive basal flow units are also found associated with the pillow flows. Disconformable massive mafic units in the Genex area represent feeders for the mafic flows. Mafic fragmental rocks range from fine-grained tuffs to lapilli-tuffs. Whole rock analysis indicates that the mafic volcanic rocks are tholeiitic in composition, and were erupted or emplaced in an arc environment.

The metavolcanic rocks in the Genex area are cut by 2 mafic synvolcanic sills and a series of intermediate synvolcanic intrusions. The synvolcanic timing of the mafic intrusions is evidenced by the presence of peperite, a pillowed base, irregular contacts, amoeboid dikes, and incorporation of felsic material. The synvolcanic nature of the intermediate intrusions is evidenced by the presence of a mixed zone near the upper contact, abundant spherulites and amygdules, and localization within synvolcanic faults.

Synvolcanic faulting occurred after emplacement of the mafic synvolcanic intrusions but prior to emplacement of the intermediate synvolcanic intrusions. The synvolcanic faults provided conduits for the intermediate synvolcanic intrusions and for the hydrothermal fluids responsible for the base-metal mineralization and alteration at Genex. The mineralization is distributed in 3 major zones: the C-zone, H-zone, and A-zone. The C-zone is hosted in pillow breccia and hyaloclastite. The H-zone occurs within felsic tuff and at the contact of the tuff with the surrounding intermediate intrusion. The A-zone mineralization is hosted dominantly in the intermediate intrusion with some mineralization in the matrix of a felsic lapilli-tuff. The Genex mineralization represents subseafloor replacement of sulphides localized within zones of higher permeability, with no massive sulphide present.

Petrography and geochemistry reveals that all rocks have experienced hydrothermal alteration in the form of sericitization, chloritization, epidotization, silicification, and Fe-carbonitization. The small size of the synvolcanic intrusions prohibits them from being the primary heat source that drove the hydrothermal system, but these intrusions do indicate the presence of a high-temperature thermal corridor that is permissive for the formation of a high-temperature hydrothermal system. Mapping of these intrusions is important in defining synvolcanic structures, and new zones of potential volcanogenic massive sulphide mineralization.

# Volcanic Stratigraphy and Controls on Mineralization in the Genex Mine Area, Kamiskotia Area: Discover Abitibi

S.M. Hocker[1], P.C. Thurston[1] and H.L. Gibson[1]

Ontario Geological Survey
Open File Report 6156
2005

---

[1] Mineral Exploration Research Centre, Laurentian University, Sudbury, Ontario
steph_hocker@yahoo.com or pthurston@laurentian.ca

# Introduction

## GOALS AND OBJECTIVES OF STUDY

This study is completed as part of a MSc thesis at Laurentian University. Funding is provided by the Base Metal Subproject of the Greenstone Architecture Project, a \$1.2 million regional geoscience investigation of the Abitibi greenstone belt, within the Discover Abitibi Initiative. The Base Metal Subproject is a group of projects aimed at addressing the volcanic facies, lithology, structure and alteration of the Kamiskotia and Blake River areas in order to establish stratigraphic, geochemical and volcanological controls on base metal mineralization, and thereby characterize key mineralized assemblages within the Abitibi greenstone belt.

The purpose of this study is to assess the controls on mineralization in the Genex deposit through a combination of detailed surface mapping (1:1000, 1:100 and 1:50 scale), diamond drill core logging, and petrographic and geochemical analysis of the volcanic stratigraphy, alteration mineralogy and geochemistry, and deformation in both the hanging wall and the footwall of the deposit. Particular attention is paid to 2 previously poorly understood intrusive bodies in the area. The objectives of this part of the study are to define the relationship and relative timing of the 2 intrusions relative to each other, to the overlying volcanic rocks, to the Genex mineralization, and to the Kamiskotia gabbroic complex.

Of the 4 mines in the Kamiskotia area, the Genex Mine was chosen for this study due to the abundance of outcrop, the large amount of drill core available, and the desire to improve our knowledge of the volcanic and alteration history in the Genex area.

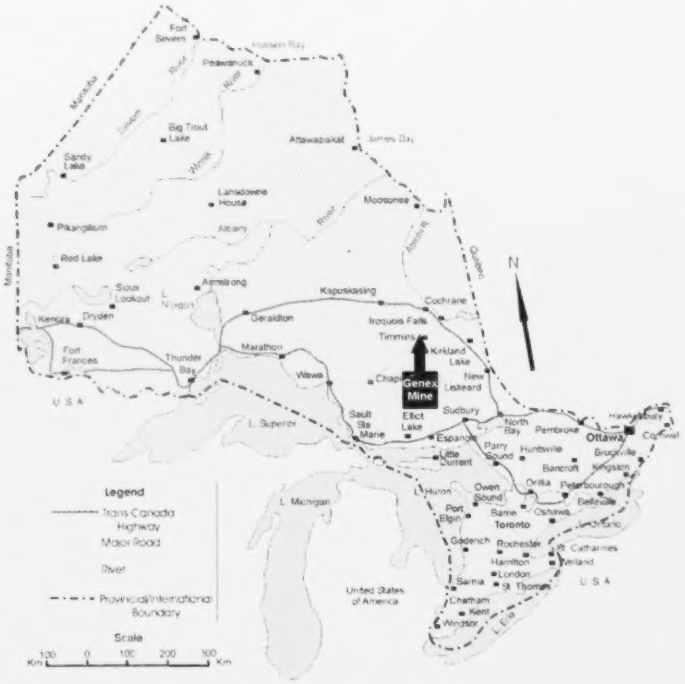

**Figure 1.** Generalized map of Ontario (*modified from* map of Ontario published by Natural Resources Canada, available at http://atlas.gc.ca/site/english/maps/reference/provincesterritories/ontario).

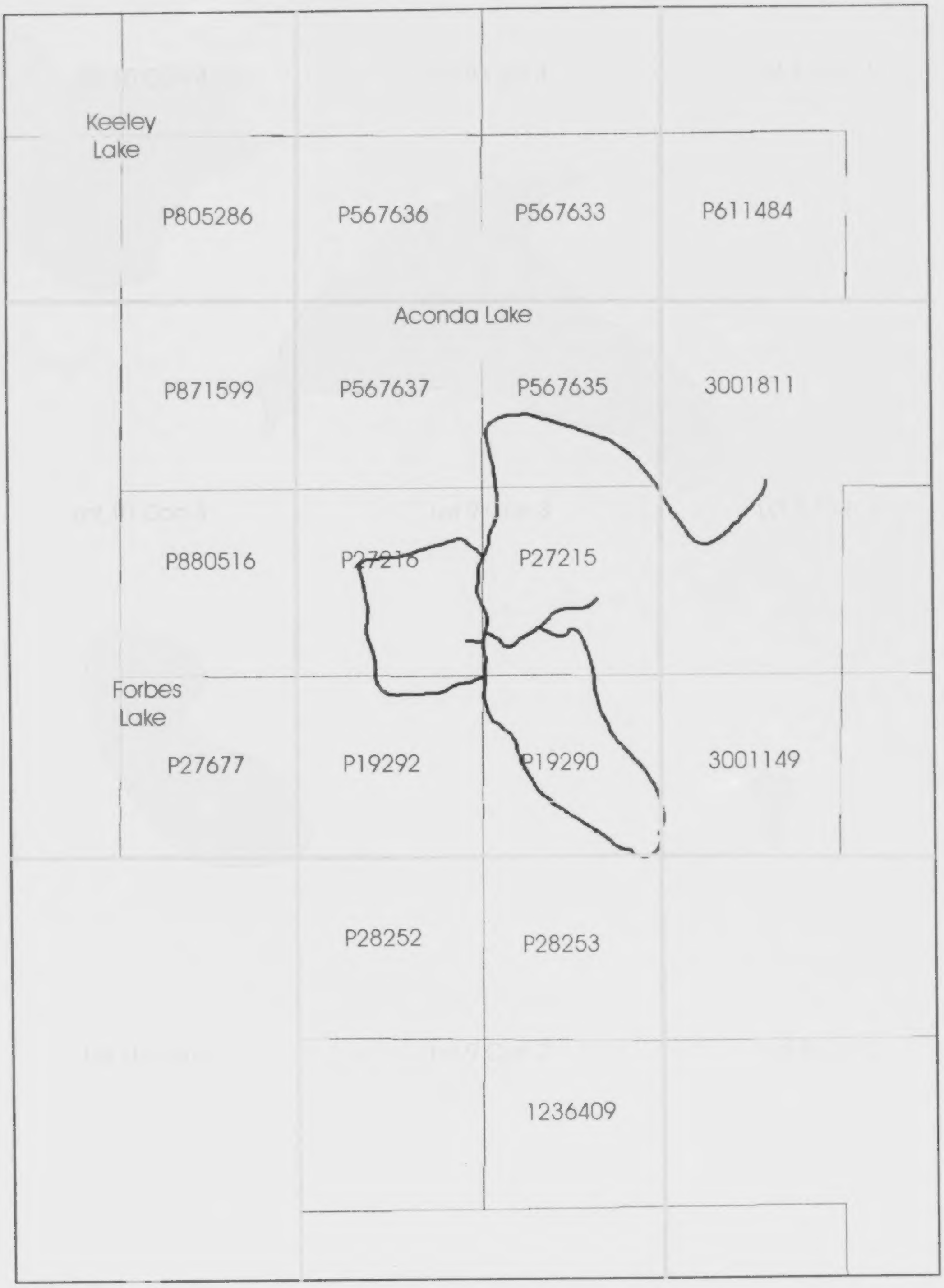

**Figure 2.** Location map of the Genex area showing lots, concessions, claims (7-digit numbers), and dispositions (5- and 6-digit numbers) (P = pending). Information from the Ontario Ministry of Northern Development and Mines, CLAIMaps III (current as of January 17, 2005).

## LOCATION AND ACCESS

The Genex mine area, located in the eastern portion of the Kamiskotia area, is in the west-central portion of Godfrey Township, about 16 km west of the city of Timmins, Ontario (Figure 1). The area covers Lots 8, 9, and 10, Concessions 2 and 3, and is covered by numerous mining claims and dispositions (Figure 2).

The main access to the area is via highway 101 west from Timmins (for 8 km), then to highway 576 west (Kamiskotia road). An unnamed gravel road (the Genex road) extends west from the highway about 20 m southeast of the turn for the Kamiskotia Ski Resort. Many smaller tracks splay off of this gravel road, but the main road leads around Aconda Lake to the Genex mine site (Figure 3). Several small logging roads within the Genex area provide easy access to outcrop.

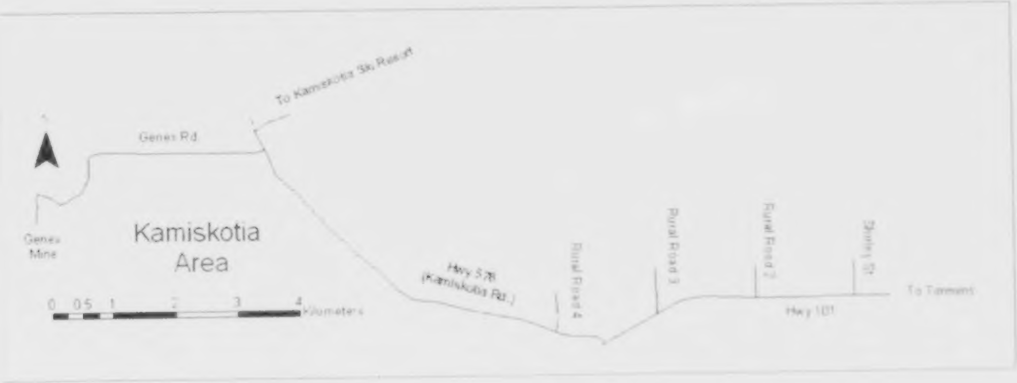

**Figure 3.** Location map of access to the Kamiskotia area.

## FIELD AND ANALYTICAL METHODS

During the months of June through August, 2003, 1:1000 scale surface mapping was completed in the area bounded by Aconda Lake to the north, Forbes Lake to the west and the availability of outcrop to the south and east. Selected outcrops were mapped at 1:100 scale. Over this time period, 236 samples were collected, and 100 thin sections were made from these samples. 100 samples were analyzed by the Ontario Geoscience Laboratories using a geological sample preparation and closed-beaker digest. Major elements were analyzed by X-ray fluorescence (XRF), trace elements were analyzed by XRF and inductively coupled plasma mass spectroscopy (ICP–MS), and loss-on-ignition (LOI) was analyzed by a two-step program.

During May 2004, diamond drill core logging was completed on 18 Falconbridge Ltd. drill holes and 9 Explorers Alliance drill holes. Detailed drill logs and drill core photographs are available on MRD 144. During August, 2004, 1:1000 and 1:50 scale surface mapping was completed in the areas south and east of Forbes Lake and west of Aconda Lake. Several outcrops from the 2003 field season were also re-visited. During the 2004 field season, 130 samples were collected, and 83 thin sections were made from these samples. Eighty-nine samples were analyzed by Activation Laboratories Limited and by the Ontario Geoscience Laboratories. The samples were crushed using mild steel, and analyzed for major elements and trace elements by XRF at Activation Laboratories. Trace and rare earth elements were analyzed by ICP–MS using a closed-beaker digest at the Ontario Geoscience Laboratories. Full geochemical analyses are presented in Appendix 3, and also on MRD 144. Precision and accuracy calculations can be found in MacDonald, Piercey and Hamilton (2005).

## PREVIOUS WORK AND HISTORY OF THE GENEX MINE

A brief history of ownership and exploration history in the Genex mine area is outlined in Table 1. Complete table of ownership and exploration history can be found in Appendix 4 (Table 8).

**Table 1.** Highlights of previous work and history of the Genex Mine area.

| **Dates** | **Company or Individual's Name** | **Highlights of Activity** |
|---|---|---|
| Prior to 1926 | Prospector Fred Steep | Noticed sulphide mineralization in the area south of Aconda Lake while trapping |
| 1964–1967 | Genex Mines Ltd. | Purchased area, 50 diamond drill holes, induced polarization survey. Shaft sunk to 84 m with levels at 38 and 76 m. Total 807 m of drifts, 211 m of raises, 95 m of crosscuts, and 82 m of underground diamond drilling |
| September 1966 | Genex Mines Ltd. | Name changed to Irvington Mines Ltd. |
| November 1966 | Irvington Mines Ltd. | Operations ceased |
| February 1967 | | Company declared bankruptcy |
| 1975 | R.S. Middleton | Geologic mapping for the Ontario Department of Mines (Middleton 1975) |
| 1985 | Mark H. Legault | Detailed surface mapping as a MSc thesis (Legault 1985) |
| 1985–1991 | Falconbridge Ltd. (Kidd) | Purchased property, diamond drilling, mechanical stripping, power stripping, geophysics |
| 1999 | Prospectors Alliance Corp. | Mapping, drilling |
| 2001 | Falconbridge Ltd., joint venture with Explorers Alliance, Campbell Resources | Diamond drilling, assaying of grab samples |
| The claims in the area are presently held by Explorers Alliance | | |

## STRUCTURE OF REPORT

This report is organized such that there is a general introduction which includes methods of study, previous work, as well as the regional context for the study. This is followed by a detailed description of the volcanic stratigraphy, deformation, geochemistry, hydrothermal alteration, and controls on mineralization in the Genex area. Appendixes contain petrographic descriptions (Appendix 1), drill logs (Appendix 2), geochemical data (Appendix 3), a table of previous work and history of the Genex mine area (Appendix 4), and a table of outcrop, waypoint, and drill hole UTM locations (Appendix 5). A 1:2500 scale geological map of the Genex mine area (Figure 56) accompanies this report (*see* back pocket).

Miscellaneous Release—Data 144 complements this report and contains colour versions of Figures 10, 11 and 12, ArcMap® files for Figure 56 (back pocket figure in OFR 6156), petrographic descriptions, and photomicrographs (to accompany Appendix 1), drill core photographs and drill logs (to accompany Appendix 2), geochemical analyses (to accompany Appendix 3), and outcrop photographs.

# REGIONAL GEOLOGY

## The Abitibi Greenstone Belt

The Abitibi greenstone belt is the largest coherent greenstone belt in the world and is located in the eastern part of Ontario and extends into the western part of Quebec (Figure 4) (Wyman, Kerrich and Polat 2002; Dostal and Mueller 1997). The belt is unique in that it contains a high proportion of volcanic rocks representing multiple crystallization ages, minor associated sedimentary rocks and numerous granitic intrusions (Ayer et al. 2002; Chown, Harrap and Moukhsil 2002).

The western part of the Abitibi greenstone belt experienced semi-continuous volcanism from 2750 to 2697 Ma with a broad range of lava compositions ranging from komatiite and tholeiitic basalt to calc-alkaline mafic and felsic (Ayer et al. 2002). The belt experienced regional-scale deformation since 2725 Ma (Ayer et al. 2002). Numerous granitic plutons and batholiths are present throughout the Abitibi and correspond in age to the volcanic events (Ayer et al. 2002; Chown, Harrap and Moukhsil 2002).

The belt is interpreted to have formed over a low-angle, north-dipping Archean subduction zone as a broad oceanic arc, which was then enhanced and modified by mantle plume processes (Ayer et al. 2002; Wyman, Kerrich and Polat 2002; Dostal and Mueller 1997). The interaction of a mantle plume with the oceanic arc is important in understanding the tectonic history of the Abitibi greenstone belt. Geochronological analyses of komatiite flows in the western Abitibi indicates that the mantle plume was active for about 20 million years (Wyman, Kerrich and Polat 2002). During that time, the plume generated both extensive komatiite and tholeiitic basalt flows (Dostal and Mueller 1997). The komatiites are interpreted to be derived from the hotter axial parts of the plume, whereas the tholeiitic basalt flows are derived from the cooler plume head and also from the entrained material in the upwelling plume (Dostal and Mueller 1997). The presence of interstratified komatiitic and basaltic flows throughout the Abitibi is interpreted to be the result of pulsing on the plume during the 20 million years that it was active (Dostal and Mueller 1997). The komatiitic flows are interpreted to result from times when the plume was tapping a deeper mantle source. As the plume rose through the mantle, it began to tap sources higher in the mantle, resulting in production of tholeiitic basalt flows. The plume would then proceed to "pulse" and a deeper mantle source was again tapped (Dostal and Mueller 1997). As the mantle plume cut up through the volcanic arc complex early in the history of the evolution of the Abitibi, it is interpreted to have either initiated or enhanced rifting within the belt (Dostal and Mueller 1997).

Historically, the Ontario portion of the Abitibi greenstone belt (southern portion of the Abitibi) was subdivided into 55 fault-bounded supracrustal lithotectonic assemblages (e.g., Jackson and Fyon 1991). However, recent field work and geochronological analyses by Ayer et al. (2002) has simplified these 55 assemblages into 9 supracrustal assemblages, on the basis of similar geochronological ages (Figure 5). These 9 assemblages can be looked upon as stratigraphic groups instead of fault-bounded slices as previously considered. The Kamiskotia volcanic complex is located within the Tisdale assemblage in the far western edge of the southern Abitibi greenstone belt (*see* Figure 5).

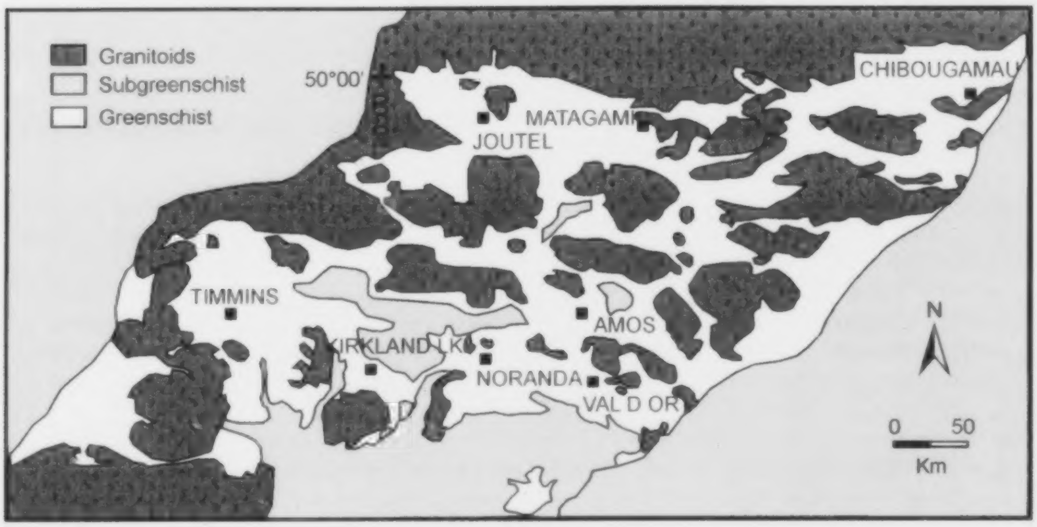

**Figure 4.** Generalized map of the Abitibi greenstone belt (*modified from* Hannington and Kjarsgaard 2001).

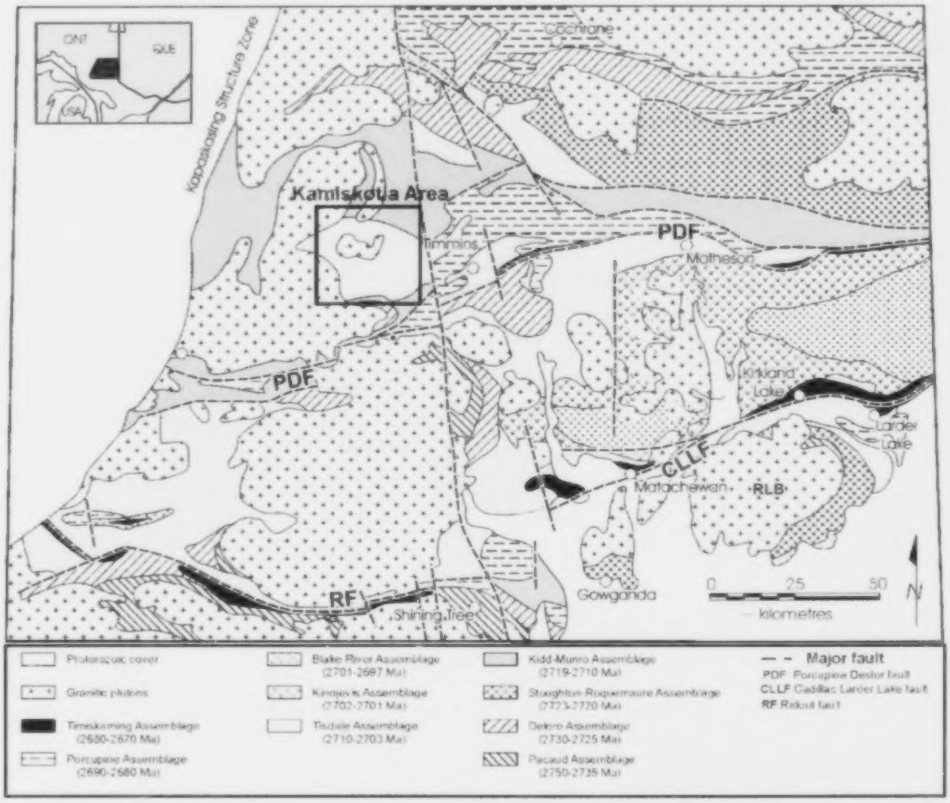

ONT
QUE
USA
Kapuskasing Structure Zone
Cochrane
Kamiskotia Area
Timmins
PDF
Matheson
PDF
Kirkland Lake
Larder Lake
CLLF
Matachewan
RLB
Gowganda
RF
Shining Tree
0
25
50
kilometres
N
Proterozoic cover
Granitic plutons
Timiskaming Assemblage (2680-2670 Ma)
Porcupine Assemblage (2690-2680 Ma)
Blake River Assemblage (2701-2697 Ma)
Kinojevis Assemblage (2702-2701 Ma)
Tisdale Assemblage (2710-2703 Ma)
Kidd-Munro Assemblage (2719-2710 Ma)
Stoughton-Roquemaure Assemblage (2723-2720 Ma)
Deloro Assemblage (2730-2725 Ma)
Pacaud Assemblage (2750-2735 Ma)
Major fault
PDF Porcupine Destor fault
CLLF Cadillac Larder Lake fault
RF Ridout fault

**Figure 5.** Distribution of supracrustal groups in the southern Abitibi greenstone belt (*modified from* Ayer et al. 2002). The Kamiskotia gabbroic complex is located in the Tisdale assemblage.

## The Kamiskotia Volcanic Complex

The Kamiskotia volcanic complex lies within the westernmost extension of the Archean Abitibi greenstone belt (*see* Figure 5) and covers all of Whitesides, Carscallen, Massey, Turnbull, Cote and Robb townships and parts of Enid, Fortune, Bristol, Jamieson, Frey and Godfrey townships in the district of Cochrane, near Timmins, Ontario (Barrie 1992). A volcanic complex is defined as a site "of persistent volcanic activity commonly . . . characterized by a diverse assemblage of extrusive volcanic rocks, related intrusions, and their weathering products" (North American Commission on Stratigraphic Nomenclature 1983). The Kamiskotia complex is a bimodal succession of felsic and mafic volcanic rocks originally interpreted to span the ages of the Tisdale (2710–2703 Ma) and Kidd–Munro (2719–2711 Ma) assemblages (Ayer et al. 2002) (Figures 5 and 6). Recent work by Hathway, Hudak and Hamilton (2005) has shown that the Genex rocks (2698.6±1.3 Ma), as well as a portion of the Kamiskotia complex, are similar in age to the Blake River assemblage (2699 Ma). There are also minor associated sedimentary rocks, and several large, multi-phase (gabbroic to granitic) intrusions (Barrie 1992; Legault 1985).

The region has been strongly deformed and altered, and hosts 4 volcanic-hosted massive sulphide deposits with production ranging in size from the Kam-Kotia deposit (6.0 million tonnes of ore: Binney and Barrie 1991) to the Genex deposit (242 tonnes of Cu concentrate: Binney and Barrie 1991). Five small gold deposits and 3 Ni-Cu occurrences are also present in the Kamiskotia area (*see* Figure 6; Barrie 1992). Regional mapping by Hathway, Hudak and Hamilton (2005) has indicated that at least part of the Kamiskotia volcanic complex may represent a caldera-type environment.

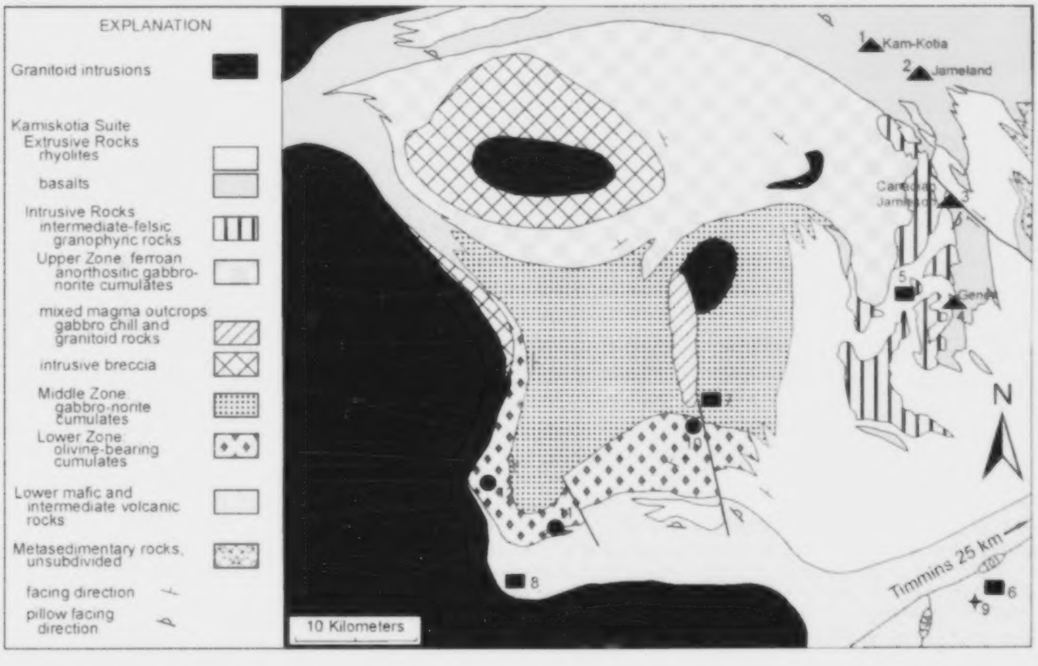
EXPLANATION
Granitoid intrusions
Kamiskotia Suite
Extrusive Rocks
rhyolites
basalts
Intrusive Rocks
intermediate-felsic granophyric rocks
Upper Zone: ferroan anorthositic gabbro-norite cumulates
mixed magma outcrops gabbro chill and granitoid rocks
intrusive breccia
Middle Zone: gabbro-norite cumulates
Lower Zone: olivine-bearing cumulates
Lower mafic and intermediate volcanic rocks
Metasedimentary rocks, unsubdivided
facing direction
pillow facing direction
1 Kam-Kotia
2 Jameland
Canadian Jamieson
3
4
Genex
5
6
7
8
9
10
11
N
Timmins 25 km
10 Kilometers

**Figure 6.** Regional geology of the Kamiskotia volcanic complex (*modified from* Barrie 1992). 1) Kam-Kotia Cu-Zn mine; 2) Jameland Cu-Zn mine; 3) Canadian Jamieson Cu-Zn mine; 4) Genex Cu-Zn mine; 5) Lally Gold Mine; 6) Holmer Gold Mine; 7) De Santis gold property; 8) Union Gold Mine; 9) Croxall REE and gold property; 10-12) Ni-Cu occurrences.

# Stratigraphy in the Genex Area

## INTRODUCTION

The stratigraphy in the Genex area is an approximately 2 km thick sequence that is north striking, east facing, and steeply dipping to slightly overturned (Figure 56, back pocket). Stratigraphic descriptions have been determined through outcrop mapping and diamond drill core logging (Figure 7 illustrates a stratigraphic column through the Genex stratigraphy). In general, the base of the Genex stratigraphy (footwall) comprises a thick (approximately 590 m) felsic unit, which ranges from felsic-tuff breccias to lapilli-tuffs, and tuffs with minor flows and flow breccias. This unit is cut by numerous dikes and sills of mafic and intermediate compositions. Overlying the felsic unit is a massive basalt flow approximately 130 m thick, which then becomes a 200 m thick pillowed sequence. The bulk of the Genex mineralization is hosted within an 8 m thick pillow breccia overlying the pillowed flow. Mineralization is also contained within a fault-bounded felsic unit comprised of felsic-tuff, lapilli-tuff, and flows. Dikes of intermediate intrusion are present along the faults in the immediate footwall of the deposit. Two 20 m thick mafic sills define the immediate hanging wall of the deposit. The uppermost mafic sill cuts a 52 m thick massive mafic flow, which is then overlain by a 35 m thick lens of felsic-tuff and lapilli-tuff. The lapilli-tuff is overlain by a 70 m thick massive mafic flow, which grades to a 360 m thick pillowed flow. Immediately overlying the pillowed flow unit is a thick (at least 370 m) volcaniclastic and epiclastic unit composed of numerous depositional sequences that grade from heterolithic tuff-breccia and lapilli-tuff to tuff to mudstone or graphitic argillite. The volcaniclastic and epiclastic unit is cut by a few mafic and felsic flows. The entire Genex stratigraphy is cut by 4 late diabase dikes.

## FELSIC METAVOLCANIC ROCKS

Felsic metavolcanic rocks are prevalent in the area surrounding the Genex deposit and range from felsic-tuffs to felsic breccias, to felsic flows and flow breccias. All felsic units are east facing, with sharp contacts, and can be subdivided into 3 major stratigraphic units: the laterally extensive footwall felsic unit (unit 1), the fault-bounded felsic units in the immediate footwall (unit 2), and the felsic lens in the hanging wall of the deposit (unit 3) (units 1 and 3 are shown in Figure 7; unit 2 is not present along the section line). Small felsic flows have also been observed in drill core cutting the volcaniclastic strata to the east of the Genex area. Felsic volcaniclastic rocks are described using Fisher's 1966 non-genetic classification. Representative photomicrographs, as well as selected petrographic descriptions, can be found in Appendix 1 (Photo 49).

Felsic-tuffs, lapilli-tuffs, and tuff-breccias are found throughout the Genex area. Tuff-breccias are more common at the base of the mine stratigraphy, in the footwall of the deposit (unit 1) whereas lapilli-tuffs and tuffs occur in both the footwall and hanging wall of the deposit (units 1, 2, and 3). Tuff-breccias contain felsic blocks up to 2 m in size, in an ash-sized matrix and locally exhibit broken and contorted flow banding, locally contain flow-banded fragments, and are *in situ* brecciated. Block size decreases up section. Lapilli-tuffs are commonly normally graded, and grade to tuff with bed thickness ranging from 0.5 to about 10 m (Figure 8). Lapilli are mostly felsic in composition (Photo 1), although accidental mafic fragments have been observed in drill core. Petrographically, lapilli compositions include altered pumice, cherty felsic lithic fragments, chloritized mafic lithic fragments, altered volcanic glass, and felsic lithic fragments of the same composition as the matrix with a large range of sizes and morphology for

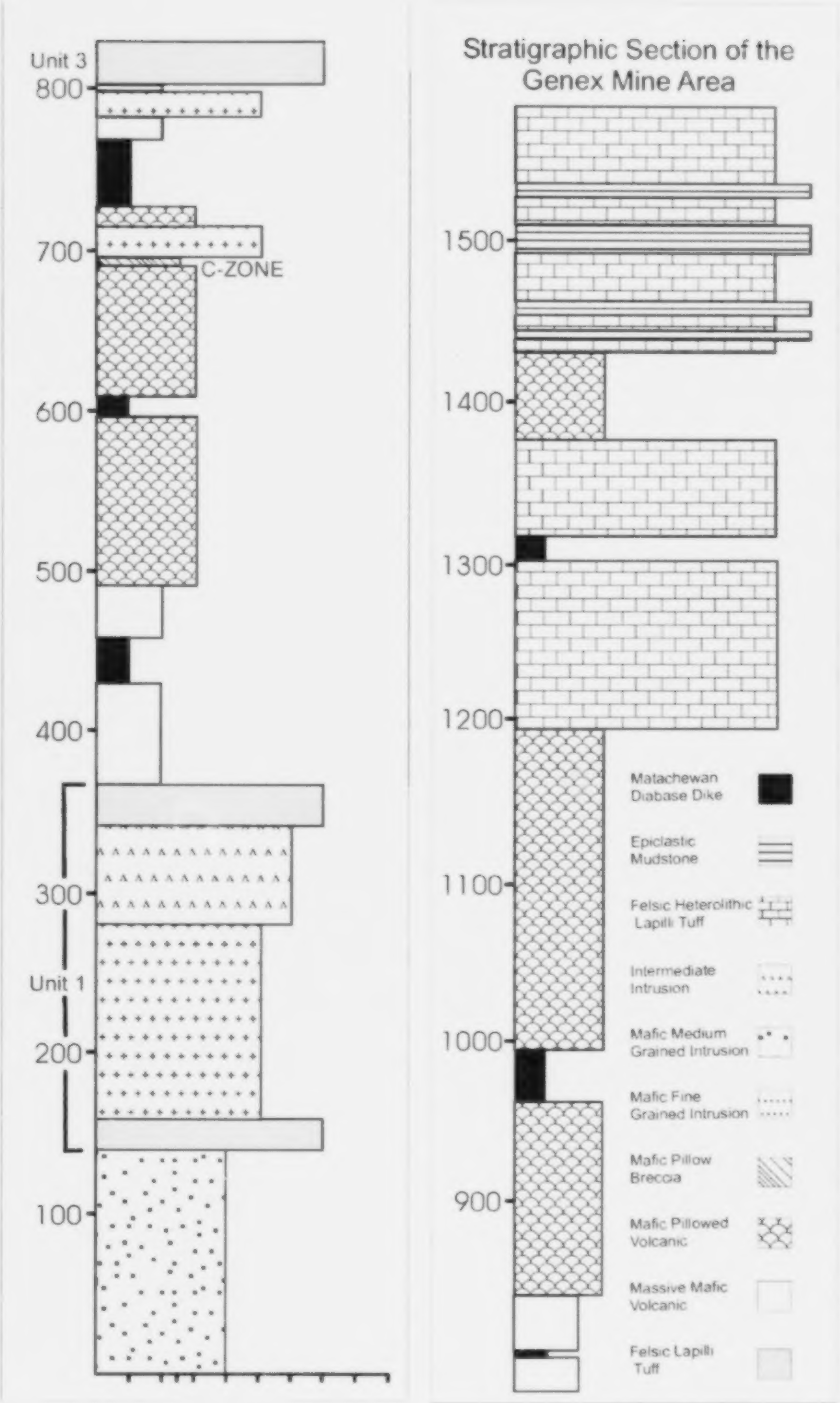

**Figure 7.** Stratigraphic section through the Genex mine area stratigraphy (*see* Figure 56, back pocket, for location of section).

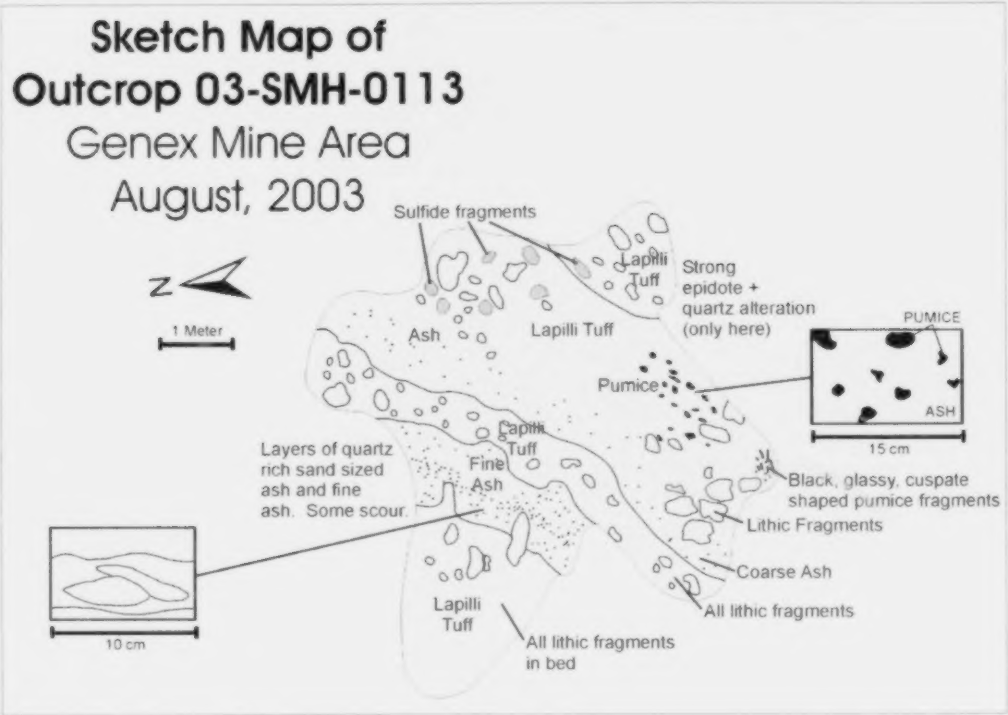

**Figure 8.** Sketch map of graded felsic lapilli and ash-tuff from unit 3 (outcrop 03-SMH-0113).

each fragment type. No chilled margins have observed on any fragments. Bedding is commonly contorted and broken, but grading and cross-bedding are present in both outcrop and in drill core (Photo 2). Bedding is generally at a scale too large to be visible in thin section, but one sample (03-SMH-0110-1) displays normally graded, ash-sized material in beds about 12 mm thick. In thin section, spherulites are visible in the matrices of some lapilli-tuff units (up to 5%), and are generally small (few millimetres). Large (tens of millimetres) quartz phenocrysts are present in all felsic lithologies (up to 15%), and are highly microfractured and locally broken. The ash-sized matrix of lapilli-tuffs and tuffs is heavily silicified and sericitized, and is locally carbonitized.

The overall lack of internal bedding, and large thickness of the felsic breccias, especially at the base of the Genex stratigraphy (unit 1), suggests that the breccias may be the result of a large collapse event (i.e., caldera collapse: Troll, Emeleus and Donaldson (2000)). In the north-trending lens of felsic ash and lapilli-tuff in the hanging wall of the deposit (unit 3), an *in situ* brecciated zone crosscuts stratigraphy perpendicular to strike. This zone is believed to represent fluid interaction along either a fault or shear zone cutting stratigraphy at a high angle (Photo 3).

Felsic flows and flow breccias are present in both the footwall (units 1 and 2) and hanging wall of the Genex deposit (cutting volcaniclastic rocks), and are much less common than felsic fragmental rocks. Phenocryst content varies within the different flows and flow breccias. Quartz phenocryst content ranges from a trace to 30%, whereas feldspar phenocryst content ranges from a trace to 10%. Flows are locally fragmental with 5–7% pumice and 5–7% felsic lithic fragments in a crystalline siliceous matrix. Flows are commonly flow banded (Photo 4) and spherulitic (Photo 5). In thin section, felsic flows look very similar to felsic-tuffs except that the siliceous matrix appears crystalline. In drill core, minor felsic hyaloclastite (Photo 6) is present where the flow is in contact with the mafic intrusion (units 1 and 2). Flow breccias commonly contain flow banded fragments, and locally have flow banding in the matrix. In general, the fragments are angular, indicating little transport. On the far southern side of outcrop 03-SMH-0034 (unit 2), a lobe and breccia facies flow is present. Although the outcrop of the lobe and breccia facies is very small and poorly exposed, the lobes are greater than 0.25 m, and are surrounded by felsic breccia and hyaloclastite.

Although no coherent domes have been identified in outcrop or in drill core, the textures of the fragments in the flow breccias indicate a proximal environment (Gibson, Morton and Hudak 1999) in that the fragments are flow banded, all similar in composition, and have experienced little transport (angular). It can be inferred that the flow breccias in outcrops 03-SMH-0112 and 03-SMH-0109 are dome proximal as is outcrop 03-SMH-0034 (in units 1 and 2).

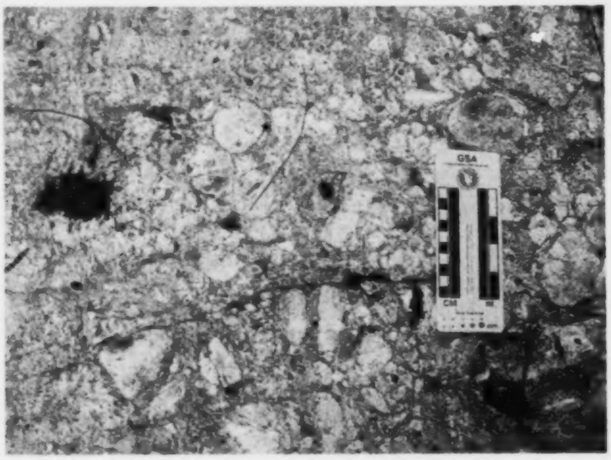

**Photo 1.** Felsic lapilli- and block-tuff (outcrop 03-SMH-0130).

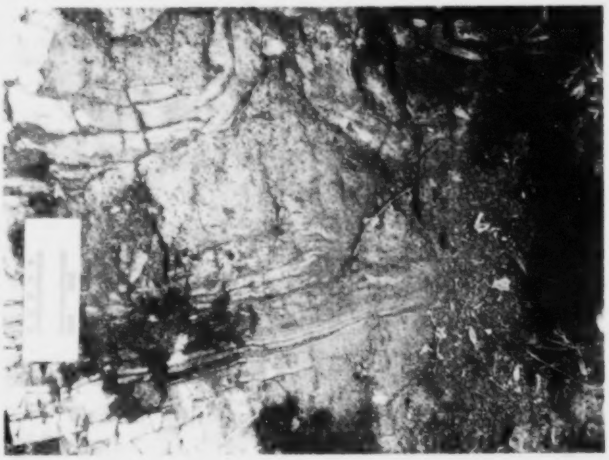

**Photo 2.** Bedded felsic-tuff (outcrop 03-SMH-0103).

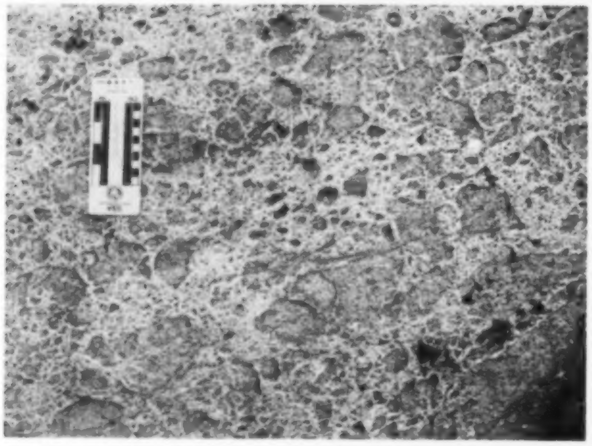

**Photo 3.** *In situ* brecciated felsic-tuff (outcrop 03-SMH-0122).

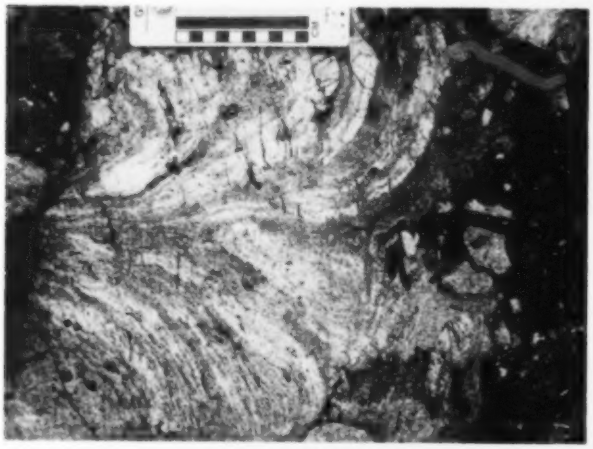

**Photo 4.** Flow banded felsic flow breccia (outcrop 03-SMH-0109).

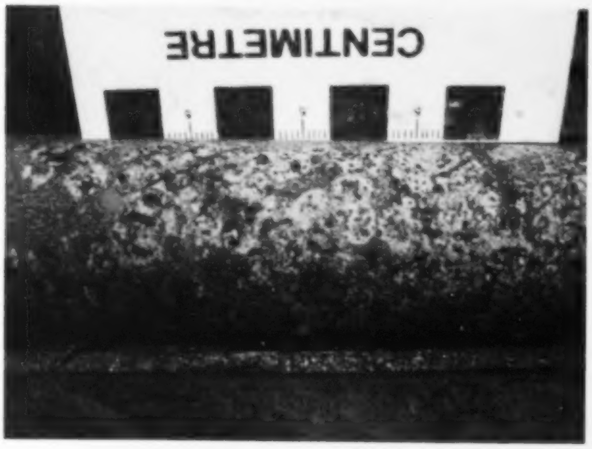

**Photo 5.** Spherulites in felsic flow from Falconbridge drill hole G22-12 (04-SMH-0005).

**Photo 6.** Felsic hyaloclastite from Falconbridge drill hole G32-25 (04-SMH-0001).

## MAFIC METAVOLCANIC ROCKS

Mafic metavolcanic rocks consist of pillowed and massive flows as well as minor mafic-tuffs, which are present throughout the Genex area. Within the pillowed units, there is great variability in pillow size, pillow hyaloclastite thickness, amygdule percentage and degree of alteration. Pillowed flows in the footwall of the deposit range in size from small (25 cm) well-defined pillows (Photo 7) to large (248 cm) irregularly shaped pillow lobes (Photo 8). Pillow hyaloclastite thickness ranges from 2 to 18 cm and is generally well defined with perlitic, cuspate glass shards, and altered glass. Amygdules in footwall pillows are quartz, chlorite, and carbonate filled, range from a trace to 50%, and are 1–40 mm in size (Photo 9). Mafic flows are massive, fine to medium grained, and locally diabasic. The mineralogy of most samples is now represented by chlorite, epidote, sericite, quartz, and ankerite. However, in a few samples, primary plagioclase (up to 60% in diabasic samples) and pyroxene (up to 5%) are preserved. Up to 10% very small spherulites, visible in thin section, are present in some samples. Budding and concentric cooling cracks are common (Photos 10 and 11). Overall, the footwall pillows are blue green on a fresh surface and light brown on a weathered surface. Representative photomicrographs, as well as selected petrographic descriptions, can be found in Appendix 1 (Photo 50).

Hanging-wall pillowed flows show a lesser degree of variability than their footwall counterparts. Pillows range in size from 24 to 200 cm and are generally irregularly shaped. Pillow hyaloclastite thickness ranges from 1.5 to 7 cm, and is generally marked by an abundance (up to 90%) of spherulites (Photo 12), giving the selvages a bleached appearance. Amygdules in hanging-wall pillows are mainly carbonate filled with minor quartz, constitute 1–55% of the pillows, and range in size from 1–10 mm. Budding and concentric cooling cracks are not common. Overall, the hanging-wall pillows are reddish green on a fresh surface and tan on a weathered surface.

Mapping of two pillowed outcrops (1:100 scale) in the immediate footwall of the deposit, near the C-zone, indicates that the flow mantles the paleotopography of the seafloor, and that it moved down a relatively steep slope (similar features have been observed by Dimroth et al. (1978); Eddy et al. (1998) and Walker (1992)). According to Walker (1992), the overall pillow morphology and size in a flow, as well as the occurrence of pipe vesicles are useful indicators of the presence of a paleo-slope (Figure 9). Mafic flows erupted onto a horizontal surface (less than 4°), are dominated by small and closely packed pillows, which lack strong evidence of unidirectional flow, and quite commonly contain well-defined pipe vesicles (Walker 1992). In contrast, mafic flows erupted onto a steep slope (15 to 40°) tend to be dominated by hyaloclastite breccia, with associated highly elongate tubular pillows, which display strong evidence for unidirectional flow and rarely contain pipe vesicles (Walker 1992). There is a continuum between these two end members for flows erupted onto a moderate slope (Walker 1992).

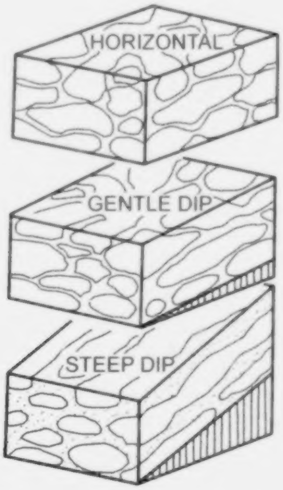

**Figure 9.** Schematic block diagram of pillow morphology and size as a function of slope (*adapted from* Walker 1992).

The morphology of pillowed flows in the footwall of the Genex deposit near the C-zone (Figures 10 and 11) indicates that the pillowed flows were erupted onto a moderately to steeply dipping slope with the crest of the slope near the C-zone (*see* Figure 56, back pocket). As shown in Figures 10 and 11, there is abundant evidence for the interpretation, from north to south (along strike), for an east-trending flow direction with the smaller bun-shaped pillows giving way to larger pillow tubes and amoeboid-shaped pillows and finally to hyaloclastite breccia (Photo 13). Although vesicles and amygdules are prevalent throughout the flow (concentrated in the margin at the base of the pillow), no pipe vesicles have been recognized. The transition from pillowed flow to hyaloclastite breccia indicates an increase of slope which became too great for the formation of pillows. The flow instead moved rapidly downslope and was instantly quenched by the seawater, forming hyaloclastite (Cas and Wright 1988).

Massive mafic units can be subdivided into those which are conformable to stratigraphy and those which are disconformable to stratigraphy. All massive mafic units are fine grained and contain 1 to 15% quartz- and carbonate-filled amygdules. Conformable massive mafic units are found stratigraphically below pillowed flows. Although the contacts between the conformable massive mafic units and the overlying pillowed flows are poorly exposed in outcrop, drill core logging has revealed the contacts to be gradational, indicating that the conformable massive mafic units are basal flow units (Dimroth et al. 1978). Disconformable massive mafic units are in close proximity to the east-trending faults in the Genex area. These units represent feeders for the mafic flows in the area, and utilized the faults as conduits (similar features have been described by Binney and Barrie (1991) and Stix et al. (2003)).

Small pillow-breccia units are also found associated with the pillowed flows, generally at the top of a pillowed flow. Flow breccias are similar in composition to the flows, but also contain

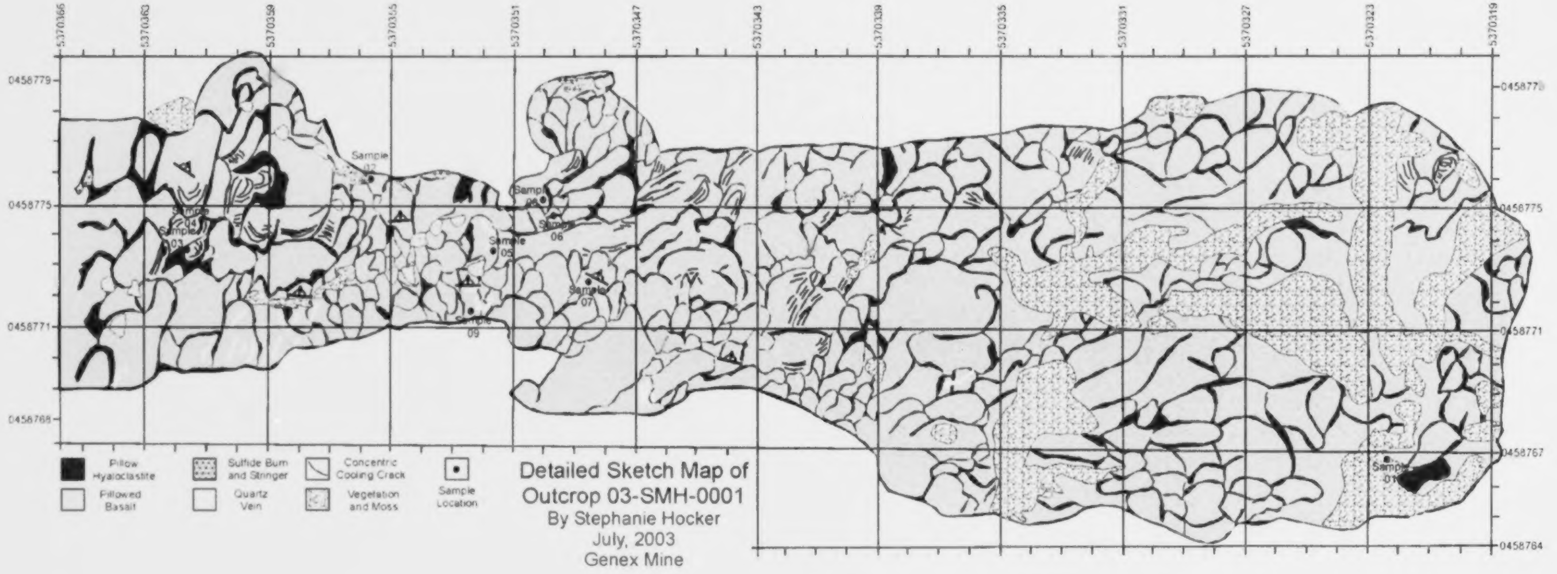

Figure 10. 1:100 scale map of pillowed basalts (outcrop 03-SMH-0001). Colour version of Figure 10 can be found on MRD 144.

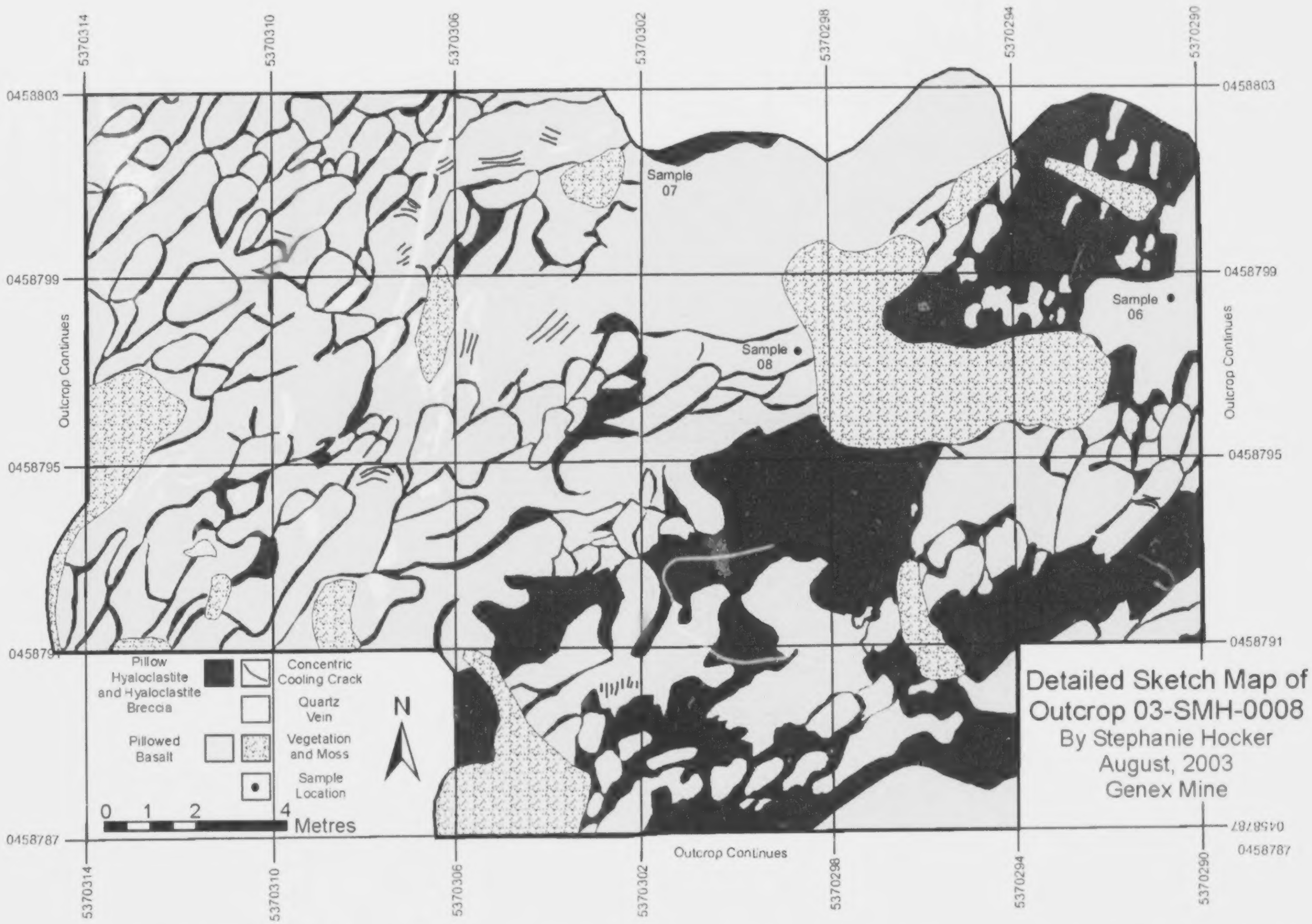

**Figure 11.** 1:100 scale map of pillowed basalts and hyaloclastite breccia (outcrop 03-SMH-0008). Outcrop is 7 m east, along strike, from outcrop 03-SMH-0001 (*see* Figure 10). Colour version of Figure 11 can be found on MRD 144.

highly silicified, amygdaloidal mafic fragments (up to 5%), 1–15 mm in size in a fine-grained matrix (Photo 14). The matrix contains 1–10% quartz-filled amygdules. Previously, some of the pillow breccias have been mistaken for felsic breccias. However, the presence of amygdaloidal fragments, amygdules in the matrix, and an absence of quartz phenocrysts all indicate that these breccias are mafic. In the Genex deposit, the C-zone is hosted within the matrix of one such pillow breccia.

Mafic-tuffs, although rare, are found in proximity to pillowed and massive flows, and range from fine-grained tuffs to lapilli-tuffs. Bedding and cross-bedding are present in the fine-grained tuffs (Photo 15). Lapilli are mafic in composition, and are commonly silicified. Juvenile fragments are also present.

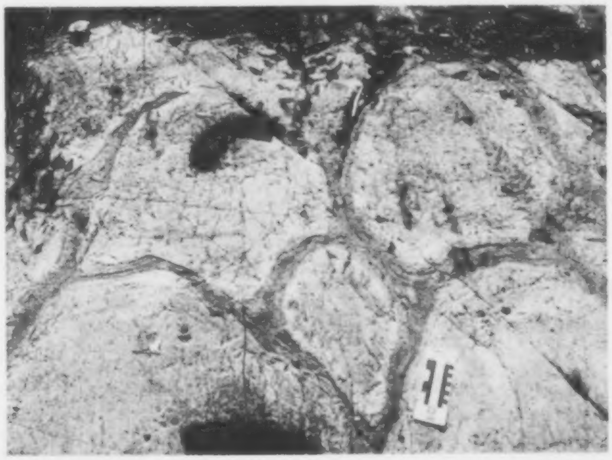

**Photo 7.** Well-defined pillows (outcrop 03-SMH-0057).

**Photo 8.** Pillow lobe, in footwall (outcrop 03-SMH-0017).

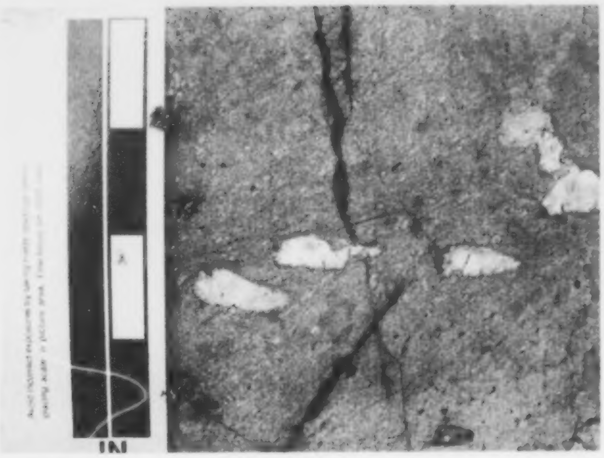

**Photo 9.** Quartz amygdules in pillowed flow (outcrop 03-SMH-0001).

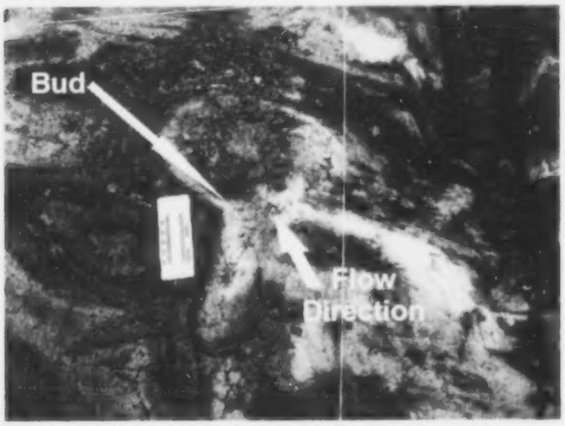

**Photo 10.** Budding in pillowed flow, with interpreted flow direction (outcrop 03-SMH-0001).

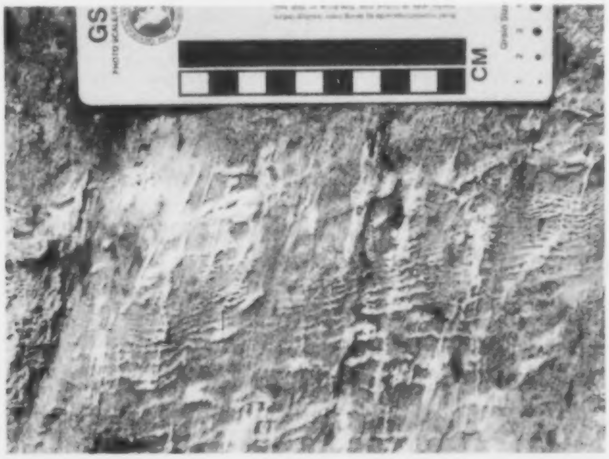

**Photo 11.** Concentric cooling cracks in pillowed flow (outcrop 03-SMH-0088). Cracks run left to right on photo, crosscut by veins.

**Photo 12.** Spherulitic margin and bleached selvage in hanging-wall pillows from Explorers Alliance drill hole 6G-04-2 (04-SMH-0085).

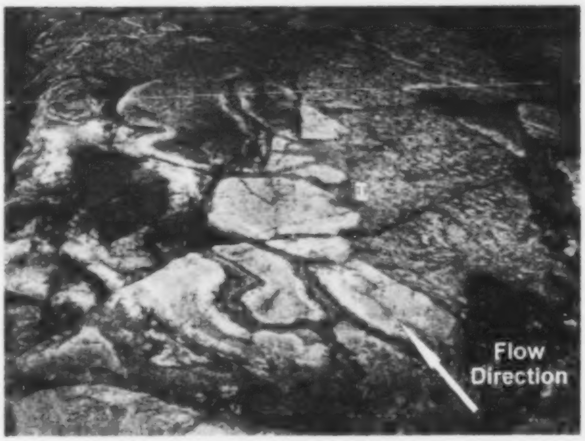

**Photo 13.** Irregular shaped pillows and hyaloclastite breccia, with interpreted flow direction (east side of Figure 11, outcrop 03-SMH-0008).

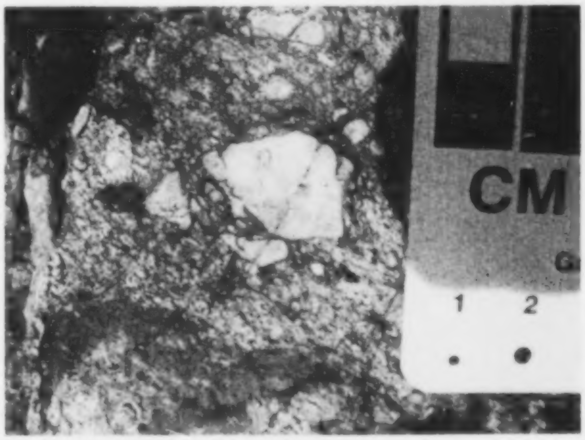

**Photo 14.** Pillow breccia with silicified fragments and sulphides in matrix (outcrop 03-SMH-0003).

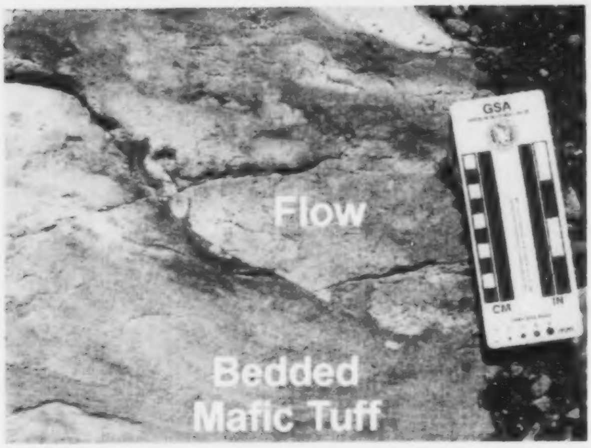

**Photo 15.** Bedded mafic-tuff overlain by pillowed flow (outcrop 03-SMH-0057).

## MAFIC INTRUSIVE ROCKS

Mafic intrusive rocks can be subdivided into those which are dominantly fine grained and those which are dominantly medium grained. The fine-grained mafic intrusive rocks can be subdivided into the upper and lower intrusions. The upper fine-grained intrusions are 2 north-trending sills located in the immediate hanging wall of the Genex deposit, whereas the lower fine-grained intrusions are 2 north-trending sills in the footwall of the deposit with numerous small apophyses stemming from the main body. Toward the northern portion of the field area, the 2 lower fine-grained sills coalesce into a single sill. The medium-grained mafic intrusive rocks occur in the far eastern portion of the field area, and cut the fine-grained sills. The mafic intrusions are fine to coarse grained, and gabbroic to quartz gabbroic in composition. Most of the primary minerals have been altered to epidote, chlorite, quartz, ankerite, sericite, and in one sample, muscovite. However, in some samples, remnant primary minerals are observed including <1 mm clinopyroxene phenocrysts (5–40%), 1–3 mm quartz phenocrysts (up to 30%), and <1 mm plagioclase phenocrysts (up to 40%) (Photo 16). Small 1–3 mm spherulites are present in some samples (up to 5%), visible mainly in thin section. Up to 50% quartz- and carbonate-filled amygdules are present along the margins of the intrusions. The gabbro is dark grey to green grey when fresh and light brown to blue grey when weathered. Locally, the lower fine-grained intrusion has abundant fracture-controlled and stringer mineralization (Photo 17), whereas the upper intrusions are unmineralized. Photomicrographs, as well as selected petrographic descriptions, can be found in Appendix 1 (Photo 51).

The lower contact of the lower fine-grained intrusion is brecciated (visible only in drill core) with chilled and chloritized irregularly shaped fragments (Photo 18) and is locally pillowed. The upper contact is also irregular with numerous dikes stemming from the main intrusive body. These dikes are amoeboid (Photo 19) and are also locally peperitic (Photo 20) where they intruded the overlying unconsolidated felsic volcaniclastic rocks. Near the upper part of the fine-grained intrusions, felsic volcaniclastic rocks are incorporated in the intrusion. The presence of peperite, a pillowed base, irregular contacts, amoeboid dikes, and incorporation of felsic volcaniclastic rocks all indicates that the lower fine-grained intrusion is a high level synvolcanic sill (Gibson, Morton and Hudak 1999).

The contacts of the upper fine-grained intrusions are poorly exposed in outcrop. The lower contact of the upper intrusions is peperitic (visible in outcrop) with chilled and irregularly shaped intrusion fragments in felsic lapilli-tuff. The upper contact is irregular with numerous, amoeboid dikes stemming from the main intrusive body. Although the upper intrusions are synvolcanic, they do not incorporate felsic material, which suggests that the upper intrusions are slightly later than the lower intrusion.

The synvolcanic nature of the mafic synvolcanic intrusions is best exemplified in outcrop 03-SMH-0112 (Figure 12) where the upper contact of the north-trending lower mafic intrusion with an overlying felsic flow breccia is exposed. Numerous amoeboid dikes of mafic synvolcanic intrusion cut across the outcrop and show various degrees of interaction with the felsic flow breccia. This is a phenomenon where successive pulses of the same intrusion interact less and less with the host rock, as the host becomes indurated and more consolidated during successive development of peperite (H.L. Gibson, unpublished data, 2004). This is likely the case in outcrop 03-SMH-0112. The earliest pulse of intrusion shows a high degree of interaction with the unconsolidated felsic flow breccia, in which a peperite is developed as the intrusion rapidly quenches and brecciates in contact with the felsic breccia. The next pulse surrounds the peperite, and instead of quenching against the felsic flow breccia, incorporates numerous xenoliths of felsic material. Subsequent pulses of intrusion cut through the felsic flow breccia with little to no interaction.

**Photo 16.** Coarse- to medium-grained intrusion from Falconbridge drill hole G32-26 (04-SMH-0023).

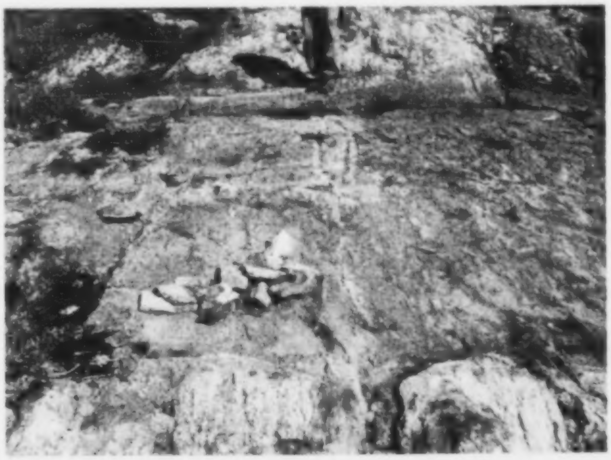

**Photo 17.** Mineralization in the lower mafic intrusion (outcrop 04-SMH-0052). Dark colouration is due to sulphide burn.

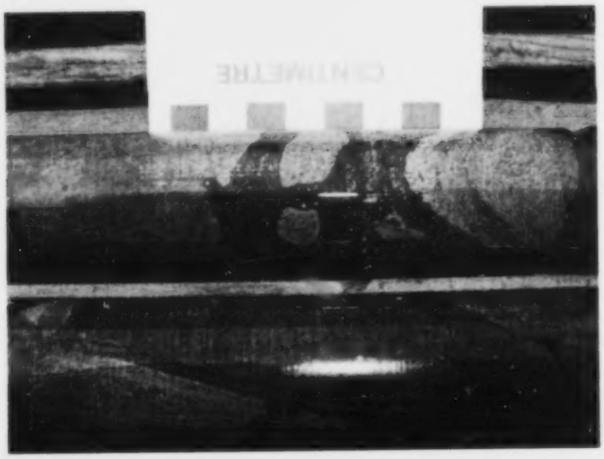

**Photo 18.** Brecciation at the base of the lower intrusion from Falconbridge drill hole G32-25 (04-SMH-0001).

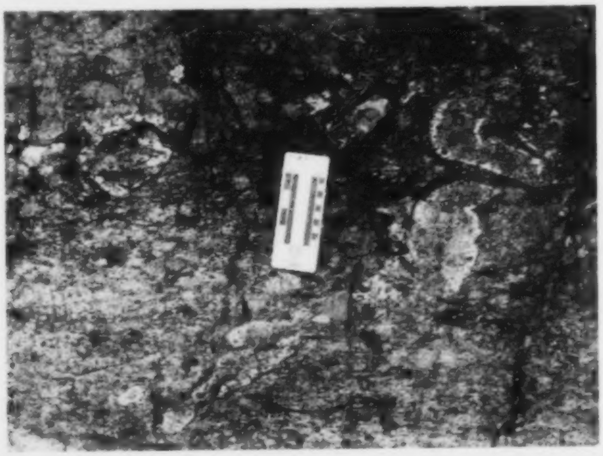

**Photo 19.** Amoeboid dikes in unconsolidated felsic-tuff (outcrop 03-SMH-0112).

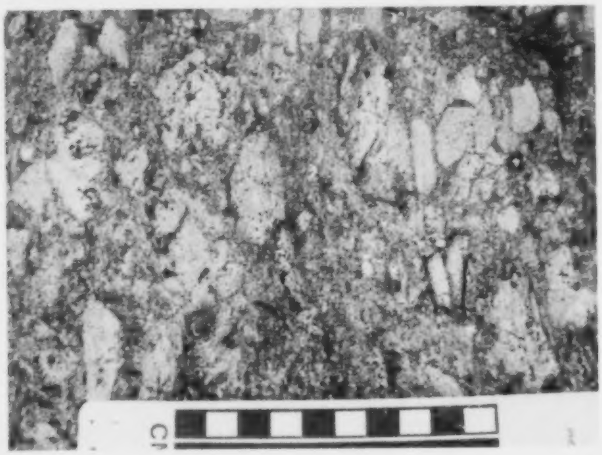

**Photo 20.** Peperite (outcrop 03-SMH-0112).

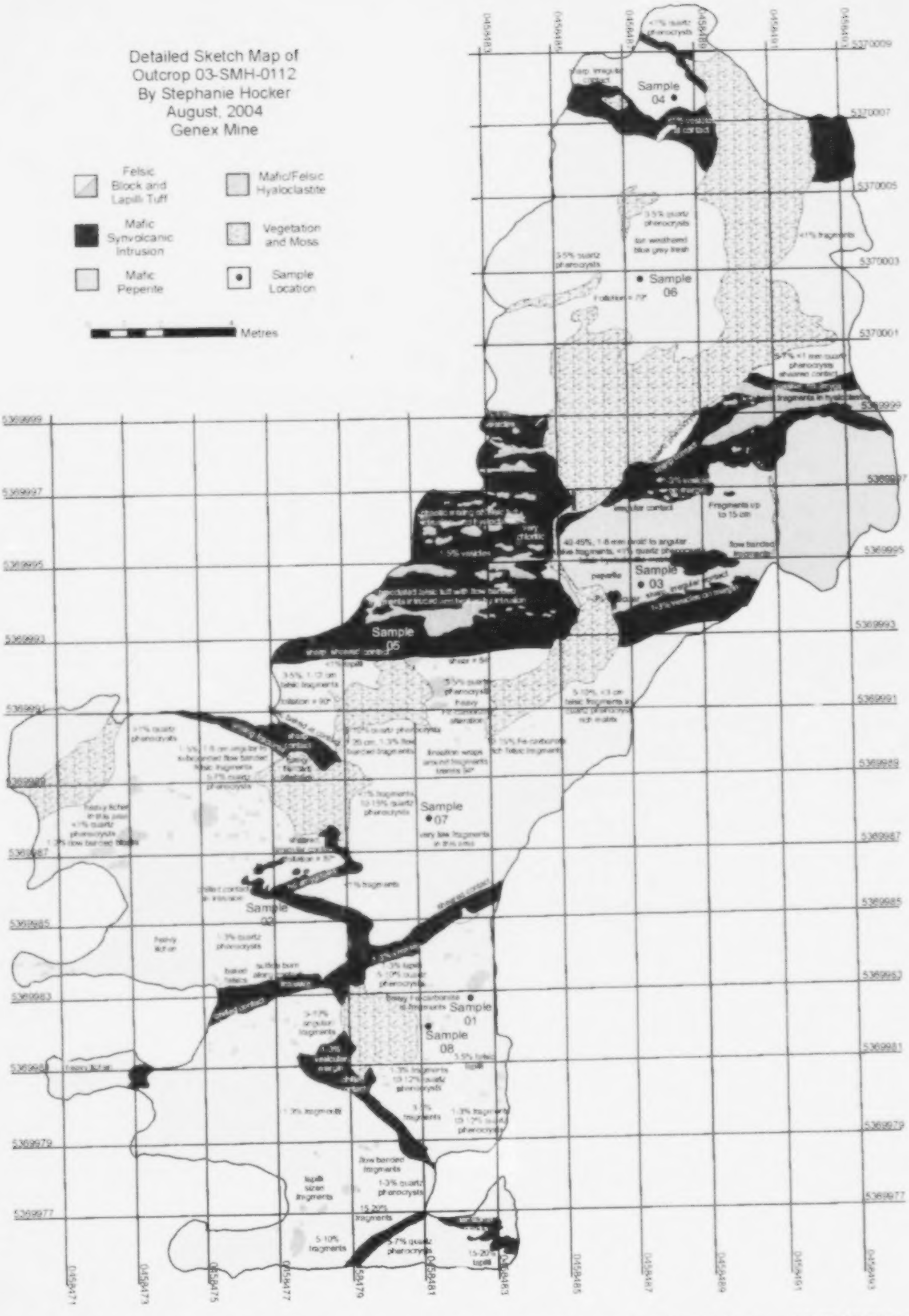

**Figure 12.** 1:50 scale map of contact between synvolcanic mafic intrusion and felsic flow breccia (outcrop 03-SMH-0112). Colour version of Figure 12 can be found on MRD 144.

## INTERMEDIATE INTRUSIVE ROCKS

Intermediate intrusive rocks are manifested as a north-trending sill with numerous east-trending dikes stemming from the main intrusive body, parallel to faults in the Genex area. The intermediate intrusion is a fine- to coarse-grained rhyodacite to dacite. Most of the primary minerals have been altered to ankerite, chlorite, quartz, epidote and sericite. Primary minerals include 15–30%, <1 mm plagioclase phenocrysts, 10–30%, <1 mm quartz phenocrysts, and <1 mm orthopyroxene phenocrysts, up to 5%, all in a very fine-grained groundmass. Most samples contain up to 20%, 1–2 mm spherulites, indicating that the intrusion was glassy upon emplacement. Up to 40% quartz and carbonate amygdules are locally concentrated on the margins of the east-trending dikes. Polygonal joints are present in the thicker sections of the north-trending sill at the base of the Genex stratigraphy (Photo 21). The intrusion is dark to light grey on a fresh surface, and light tan on a weathered surface. The main sill may be composed of multiple intrusions, all utilizing the same conduit. The contacts between individual intrusions can be distinguished by the presence of *in situ* brecciated zones representing seawater interaction, which also suggests that the intrusion is high level (emplaced relatively close to the seafloor) and synvolcanic. The intermediate intrusion can be distinguished from the mafic intrusion by a smaller degree of epidotization, a higher degree of carbonitization, a greater abundance of quartz, and a greater abundance of spherulites. Photomicrographs, as well as selected petrographic descriptions, can be found in Appendix 1 (Photo 52).

The lower contact of the main north-trending sill is characterized by numerous apophyses which intrude the underlying volcanic rocks and the lower mafic intrusion. The upper contact of the north-trending sill, as well as the contacts of the east-trending dikes are characterized by a mixed zone up to 25 m wide in which the intrusion and the overlying rocks are chaotically mixed (Photo 22). However, blocks of felsic-tuff caught up in the intrusion are intact, suggesting that they were lithified prior to incorporation, and thus indicating that the intermediate intrusion is synvolcanic in its timing, but is slightly later than the mafic intrusion (Photo 23). In the immediate footwall of the Genex deposit, the east-trending dikes are shattered against the host rock (a felsic lapilli-tuff) with fragments of the intrusion in an altered glass matrix (Photo 24).

The numerous east-trending synvolcanic faults in the area do not cut the intrusion, but the intrusion does appear to be utilizing the faults as conduits as many of the dikes stemming from the main sill follow the faults (also described by Binney and Barrie 1991). The east-trending dikes commonly contain abundant sulphides higher up in the mine stratigraphy, while the lower parts of the intrusion are unmineralized.

The presence of a mixed zone, abundant spherulites and amygdules, and the utilization of the faults as conduits all indicate that the intrusion is a high level synvolcanic intrusion (Gibson, Morton and Hudak 1999). However, the intrusion is slightly later than the mafic intrusion as it is not cut by all the faults in the area, and cuts the mafic intrusion.

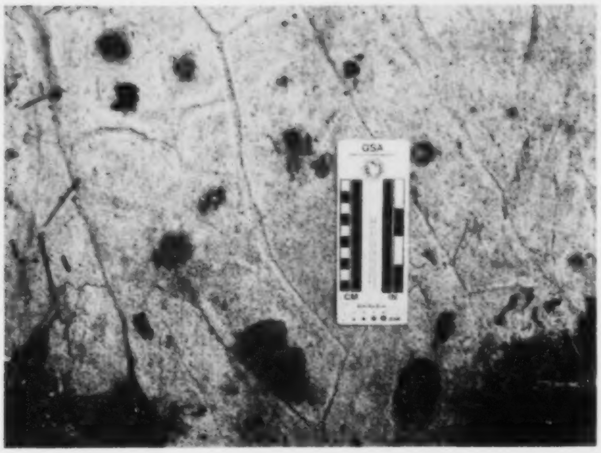

**Photo 21.** Polygonal joints and pyrite mineralization in the north-trending sill (outcrop 03-SMH-0102).

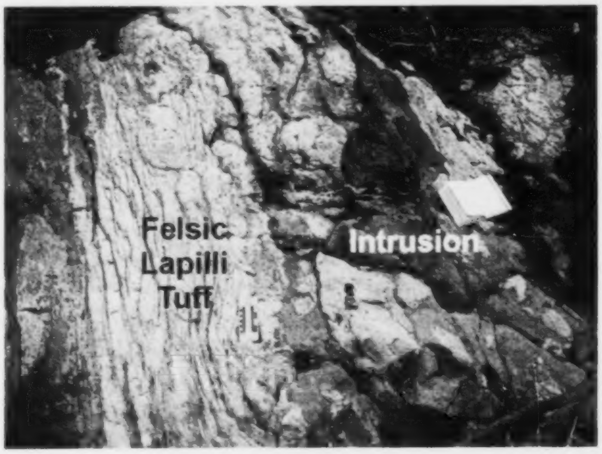

**Photo 22.** Mixed zone in upper contact of north-trending sill (outcrop 03-SMH-0125).

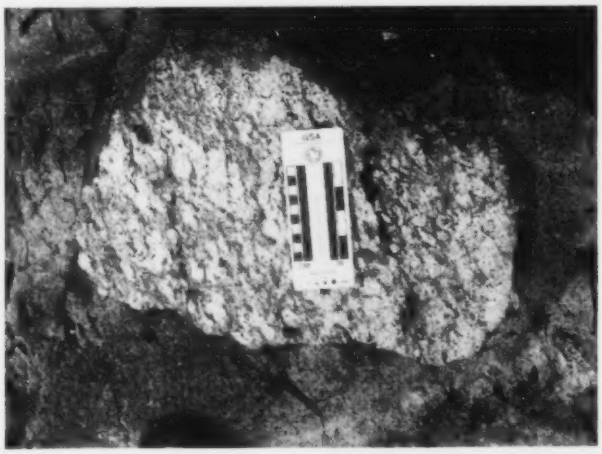

**Photo 23.** Coherent block of lapilli-tuff in upper contact of north-trending sill (outcrop 03-SMH-0102).

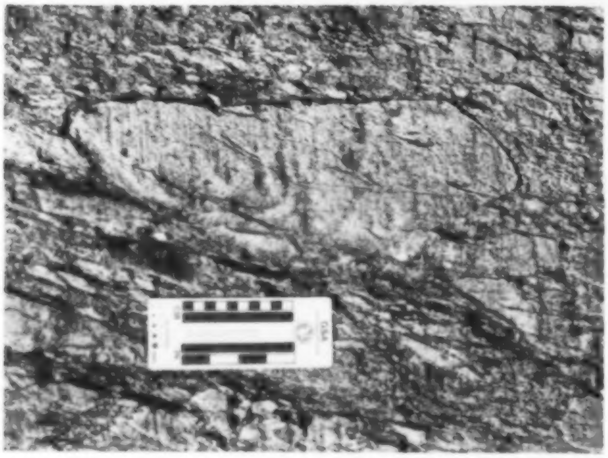

**Photo 24.** Shattered fragments of intermediate intrusion in a glassy matrix (outcrop 03-SMH-0034).

## VOLCANICLASTIC AND EPICLASTIC ROCKS

Volcaniclastic and epiclastic rocks occur east of the Genex mine area, and are visible only in drill core. Volcaniclastic rocks are classified using Fisher's 1966 non-genetic classification scheme. The hundreds of metres thick sequence is composed of numerous metre-thick, normally graded sequences grading from felsic heterolithic tuff-breccia and lapilli-tuff (Photo 25) to locally bedded-tuff (Photo 26) to black, finely laminated, locally pyritic, epiclastic mudstone or graphitic argillite (Photo 27). Tuff-breccias and lapilli-tuffs are heterolithic and contain felsic fragments of numerous compositions, mafic lithic fragments, massive mudstone fragments, and highly mineralized mudstone fragments (Photo 28). The matrix is fine felsic ash. The heterolithic nature of the tuff-breccias suggests that the rock is not a primary deposit. Tuffs are fine felsic ash and are locally thinly bedded. The tuffs commonly contain a small mudstone component. Like the tuff-breccias and lapilli-tuffs, the tuffs are not primary and have been redeposited. Laminated (6 mm thick) mudstones or graphitic argillites are black with evidence of cross-bedding and soft-sediment deformation. The graphitic component of the mudstones, as well as the presence of cross-bedding and soft-sediment deformation suggest that the mudstones are epiclastic in origin. Throughout the volcaniclastic and epiclastic succession, there is abundant evidence of soft-sediment deformation, graded beds, bedding, and cross-bedding, all which suggest that the volcaniclastic rocks were deposited as a series of subaqueous debris flows. Felsic flows, mafic pillowed flows, and intrusions commonly disrupt the volcaniclastic sequences. Photomicrographs, as well as selected petrographic descriptions, can be found in Appendix 1 (Photo 53).

The presence of the volcaniclastic and epiclastic rocks suggests a period of quiescence in which volcanism was not as prominent, and was replaced by mass debris flows as the primary depositional mechanism. Mudstone beds reveal a hiatus in mass flow sedimentation that allowed relatively calm suspension deposition and pelagic background sedimentation (Mueller and Mortensen 2002). The few felsic flows and mafic flows which disrupt the volcaniclastic sequence indicate that bimodal volcanism was still occurring.

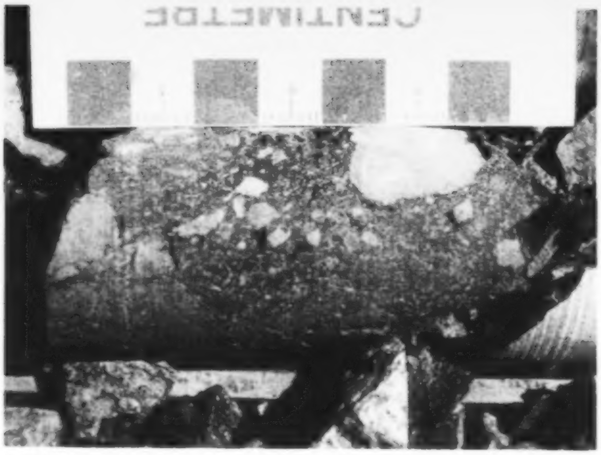

**Photo 25.** Heterolithic lapilli-tuff breccia from Falconbridge drill hole G32-10 (04-SMH-0024).

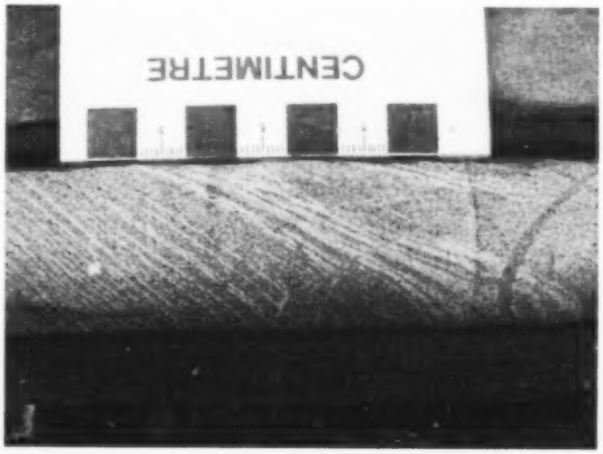

**Photo 26.** Bedded-tuff from Falconbridge drill hole G22-12 (04-SMH-0005).

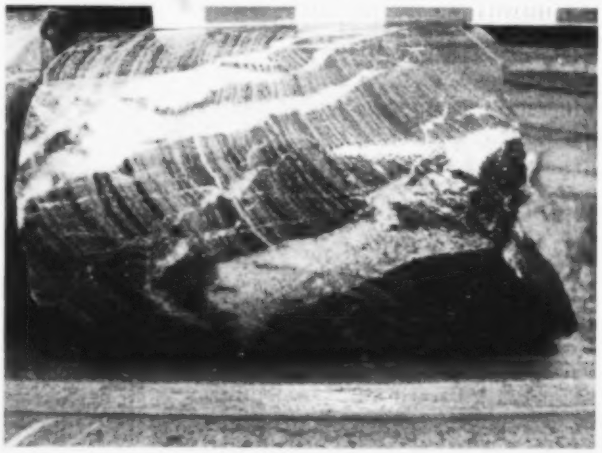

**Photo 27.** Finely laminated mudstone from Falconbridge drill hole G22-11 (04-SMH-0015).

**Photo 28.** Mineralized mudstone fragment in lapilli-tuff from Falconbridge drill hole G22-12 (04-SMH-0005).

## LATE DIABASE INTRUSIVE ROCKS (MATACHEWAN)

Based on their trend, presence of epidotized plagioclase glomerocrysts, and magnetic nature, the north-trending diabase dikes in the Genex area are part of the Proterozoic (2454±2 Ma: Heaman 1988) Matachewan dike swarm that covers the Kamiskotia and surrounding area. In the Genex area, the dikes are fine- to coarse-grained diabase, with an average modal mineralogy of 40–55%, 1–3 mm plagioclase phenocrysts, 5–7%, <1 mm quartz phenocrysts, and 20–60%, 1–5 mm clinopyroxene phenocrysts (Photo 29). Much of the plagioclase has been altered to epidote, zoisite, and sericite, whereas most of the pyroxene has been altered to chlorite, actinolite, and epidote. Disseminated pyrite (5–10%) is visible in thin section. The diabase dikes are all relatively fresh and unaltered, and weakly to strongly magnetic. A photomicrograph, as well as the petrographic description of the sample, can be found in Appendix 1 (Photo 54).

**Photo 29.** Matachewan diabase dike (outcrop 03-SMH-0059).

# Deformation

## FAULTS

Two types of faults have been recognized in the Genex area: synvolcanic faults and late faults. Four synvolcanic faults have been recognized, and can be distinguished by 3 key factors. The first line of evidence is that the synvolcanic intermediate intrusion utilizes these faults as conduits (*see* Figure 56, back pocket). Because the intrusion is synvolcanic in its timing, the structure along which the intrusion is emplaced must also be synvolcanic. The second line of evidence is the disconformable nature of the A- and H-zones of the Genex deposit (*see* "Controls on Mineralization"). Not only are both zones disconformable to stratigraphy, but they are parallel to a fault which served as a conduit for the hydrothermal mineralizing fluid. Since the Genex mineralization is synvolcanic, it follows that the synvolcanic structure must also be synvolcanic. The third line of evidence is that the faults do not extend far into the hanging wall of the deposit. The synvolcanic fault just south of Aconda Lake may have experienced later reactivation, as evidenced by the offset observed in the mafic and intermediate intrusions. This is a phenomenon common in caldera environments (Rytuba 1994) in which later, caldera-related deformation is focused along synvolcanic structures.

Five late faults have been recognized in the Genex area which predate the intrusion of the Proterozoic Matachewan dikes. The late faults are continuous across the field area, and offset all Archean lithologies (*see* Figure 56, back pocket). The offset observed along all 5 late faults in the Genex area represent faulting during continued subsidence. The latest fault identified in the Genex area is the east-trending Aconda Lake fault that passes through Aconda Lake, north of the Genex mine area, and postdates the intrusion of the Matachewan diabase dikes. The Aconda Lake fault is recognized by a large displacement of stratigraphy (regional-scale work by Hathway, Hudak and Hamilton (2005) has been unable to follow the Genex stratigraphy across the fault, presumably due to the large displacement) and displacement of the Proterozoic Matachewan dikes.

## SHEAR ZONES

There are numerous east-trending shear zones in the Genex area, many of which are proximal to faults and synvolcanic structures. Mineralization along these shear zones (*see* "Controls on Mineralization") is synvolcanic, but is related to lower temperature hydrothermal fluids than the fluids responsible for the main zone of mineralization. However, the presence of mineralization in these shear zones indicates that they are related to the synvolcanic structures and not to later deformation.

# Geochemistry

## INTRODUCTION

For this project, 189 samples were submitted for whole rock geochemical analysis using ICP–MS and XRF techniques. Major rock types (felsic metavolcanic rocks, mafic metavolcanic rocks, synvolcanic mafic intrusive rocks, synvolcanic intermediate intrusive rocks) were defined based on field observations, petrographic descriptions, and geochemical trends. Complete geochemical analyses can be found in Appendix 3 (and on MRD 144). Qualitative accuracy and precision of geochemical data can be found in MacDonald, Piercey and Hamilton (2005).

Because the rocks in the Genex area have experienced hydrothermal alteration and metasomatism (*see* "Hydrothermal Alteration"), it cannot be assumed that the concentrations of each element analyzed represents the initial concentration of that element when the rock was emplaced or deposited (Franklin 1996; Hudak et al. 2003; Jenner 1996; Pearce 1996). Thus, we must consider element mobility to assess mass gains and losses in each rock type. Once element mobility has been taken into account, fractionation trends, major and trace element trends, and geodynamic environment can all be evaluated.

## ELEMENT MOBILITY

Many of the major elements, as well as some trace elements, are mobile during hydrothermal alteration (Franklin 1996; Hudak et al. 2003; Pearce 1996), and a study of mobility should be undertaken prior to interpretation of geochemical data. Most high field strength elements (HFSE) and rare earth elements (REE) are generally immobile during hydrothermal alteration, and are highly useful for chemostratigraphic correlation, and for plotting discrimination diagrams. Table 2 displays the relative mobility of trace elements during hydrothermal alteration processes. However, an independent assessment of trace element mobility should still be undertaken to support the trends presented in Table 2.

Cann (1970) developed a method to screen elements that may have been mobile during hydrothermal alteration that has since been utilized by numerous researchers (i.e., Hudak et al. 2003; Pearce 1996). The approach examines the correlation coefficients of variation diagrams (X–Y plots of individual elements). A high correlation coefficient (approaching 1 or negative 1) indicates that both of the plotted elements are immobile. A low correlation coefficient (approaching 0) indicates that at least one of the plotted elements is mobile. For example, if a Zr–Hf variation diagram has a high correlation coefficient, than both Hf and Zr can be assumed immobile. If, however, a Zr–Y variation diagram has a low correlation coefficient, than Y must be a mobile element (since Zr is immobile).

Numerous variation diagrams of trace and major element data have been constructed for the felsic metavolcanic rocks and mafic metavolcanic rocks in the Genex area, as well as for the mafic intrusion and the intermediate intrusion (Table 3, Figures 13, 14, 15 and 16). The data set for the volcaniclastic and epiclastic rocks and the Matachewan diabase dikes is too small for this evaluation. Correlation coefficients were determined using the Igpet 2001 computer program (*see* Table 3). The Pearson's Product Moment Correlation Coefficient (r) ranges from 0 to 1, and is a measure of the linear association between the two variables (Hudak et al. 2003).

**Table 2.** Trace element classification and behaviour during alteration (*from* Jenner 1996). LFSE = low field strength elements; HFSE = high field strength elements; REE = rare earth elements; TE = transitional elements. Seawater (SWD) or Rock (RD) Dominated is related to water:rock ratio during alteration.

| | **Seawater (SWD) or Rock (RD) Dominated** | **Comments** |
|---|---|---|
| **LFSE** | | |
| K, Rb, Cs, U, Pb | Mobile SWD and RD | Assume mobile |
| Ba, Sr | Mobile SWD? and RD | Consider mobile |
| Th | Immobile RD? and SWD | Potentially mobile, generally immobile |
| **HFSE** | | |
| Ti, Zr, Hf, Nb, Ta | Immobile RD and SWD | Immobile |
| P | Immobile RD? mobile SWD | Immobile to slightly mobile |
| Y | Immobile RD and SWD | Immobile |
| **REE** | | |
| La, Ce, Nd, Sm | Immobile RD? mobile SWD | Generally immobile, but can be mobile |
| Eu | Slightly mobile to mobile RD and SWD | Unreliable for petrogenesis |
| Gd, Tb, Dy, Er, Yb, Lu | Immobile RD, slightly mobile SWD | Generally immobile, addition of carbonate can make mobile |
| **TE** | | |
| Cr, Ni, Sc, V | Immobile RD and SWD | Ti-V ratio is useful |

According to Table 3, Ti, Y, Ni, Sc and V should all be immobile during hydrothermal alteration. However, according to Table 4, these elements are mobile to moderately mobile. This inconsistency has been recognized in work done by Hudak et al. (2003) as well, and indicates that geochemical trends,

**Table 3.** Correlation coefficients for selected variation diagrams of Genex rocks. High r values indicate element immobility, whereas low r values indicate element mobility.

| Plot | Felsic Volcanic Rocks | Mafic Volcanic Rocks | Mafic Intrusion | Intermediate Intrusion |
|---|---|---|---|---|
| | r | r | r | r |
| Zr–$TiO_2$ | 3.6 | –0.31 | 0.56 | 0.33 |
| Zr–Hf | 1 | 0.99 | 0.99 | 0.92 |
| Zr–Nb | 0.95 | 0.92 | 0.90 | 0.93 |
| Zr–Ta | 0.96 | 0.85 | 0.58 | 0.66 |
| Zr–$P_2O_5$ | –0.34 | 0.31 | 0.74 | 0.67 |
| Zr–Yr | 0.23 | 0.11 | 0.40 | 0.38 |
| Zr–Ga | –0.01 | –0.07 | 0.63 | 0.42 |
| Zr–Ce | 0.18 | 0.42 | 0.31 | 0.22 |
| Zr–La | 0.17 | 0.43 | 0.29 | 0.21 |
| Zr–Yb | 0.56 | 0.31 | 0.54 | 0.43 |
| Zr–Th | 0.65 | 0.85 | 0.87 | 0.74 |
| Zr–V | –0.45 | –0.50 | 0.44 | 0.37 |
| Zr–MgO | –0.32 | 0.11 | –0.26 | 0.48 |
| Zr–$Na_2O$ | –0.35 | –0.06 | 0.10 | –0.28 |
| Zr–$K_2O$ | 0.33 | 0.39 | –0.04 | 0.31 |
| Zr–$Fe_2O_3$ | –0.51 | –0.18 | –0.26 | 0.17 |
| Zr–$SiO_2$ | 0.32 | 0.15 | 0.66 | –0.20 |
| Zr–Rb | 0.49 | 0.30 | –0.16 | 0.21 |
| Zr–CaO | –0.09 | –0.24 | –0.19 | 0.37 |
| Zr–$Al_2O_3$ | 0.29 | 0.51 | –0.51 | 0.63 |
| Nb–Hf | 0.96 | 0.94 | 0.90 | 0.73 |
| Nb–Ta | 0.94 | 0.9 | 0.89 | 0.89 |
| Hf–Ta | 0.94 | 0.91 | 0.84 | 0.59 |
| Nb–$Al_2O_3$ | 0.22 | 0.41 | –0.16 | 0.55 |
| Hf–$Al_2O_3$ | 0.25 | 0.55 | –0.3 | 0.61 |
| Ta–$Al_2O_3$ | 0.12 | 0.50 | –0.23 | 0.42 |
| Zr–Ni | –0.39 | –0.09 | –0.36 | 0.39 |
| Zr–Sc | –0.58 | –0.39 | –0.91 | 0.2 |
| Zr–Cs | 0.1 | 0.31 | 0.01 | 0.34 |
| Zr–Gd | 0.11 | 0.20 | 0.44 | 0.28 |
| Nd–Zr | 0.21 | 0.34 | 0.63 | 0.26 |
| Zr–Sm | 0.2 | 0.29 | 0.67 | 0.47 |

**Table 4.** Summary of element mobility trends in Genex rocks.

| | Felsic Volcanic Rocks | Mafic Volcanics Rocks | Mafic Intrusion | Intermediate Intrusion |
|---|---|---|---|---|
| **Immobile Elements ($r > 0.60$)** | Zr, Hf, Nb, Ta, Th | Zr, Hf, Nb, Ta, Th | Zr, Hf, Nb, Ta, $P_2O_5$, Th, Sc, Nd, Sm, $SiO_2$ | Zr, Hf, Nb, Ta, Th, $P_2O_5$ |
| **Moderately Mobile Elements ($0.60 > r > 0.40$)** | Yb, Cr, V, $Fe_2O_3$, Rb, Sc | Ce, La, V, $Al_2O_3$ | $TiO_2$, Y, Ga, Yb, V, $Al_2O_3$, Gd | Ga, Yb, MgO, $Al_2O_3$, Gd |
| **Mobile Elements ($r < 0.40$)** | $TiO_2$, $P_2O_5$, Y, Ga, Ce, La, MgO, $Na_2O$, $K_2O$, $SiO_2$, CaO, $Al_2O_3$, Ni, Cs, Gd, Nd, Sm | $TiO_2$,$P_2O_5$, Y, Ga, Yb, MgO, $Na_2O$, $K_2O$, $Fe_2O_3$, $SiO_2$, Rb, CaO, Ni, Sc, Cs, Gd, Sm, Nd | Ce, La, MgO, $Na_2O$, $K_2O$, $Fe_2O_3$, Rb, CaO, Cs, Ni | $TiO_2$, Ce, La, V, $Na_2O$, $K_2O$, $Fe_2O_3$, $SiO_2$, Rb, CaO, Sc, Cs, Nd, Y, Ni, Sm |

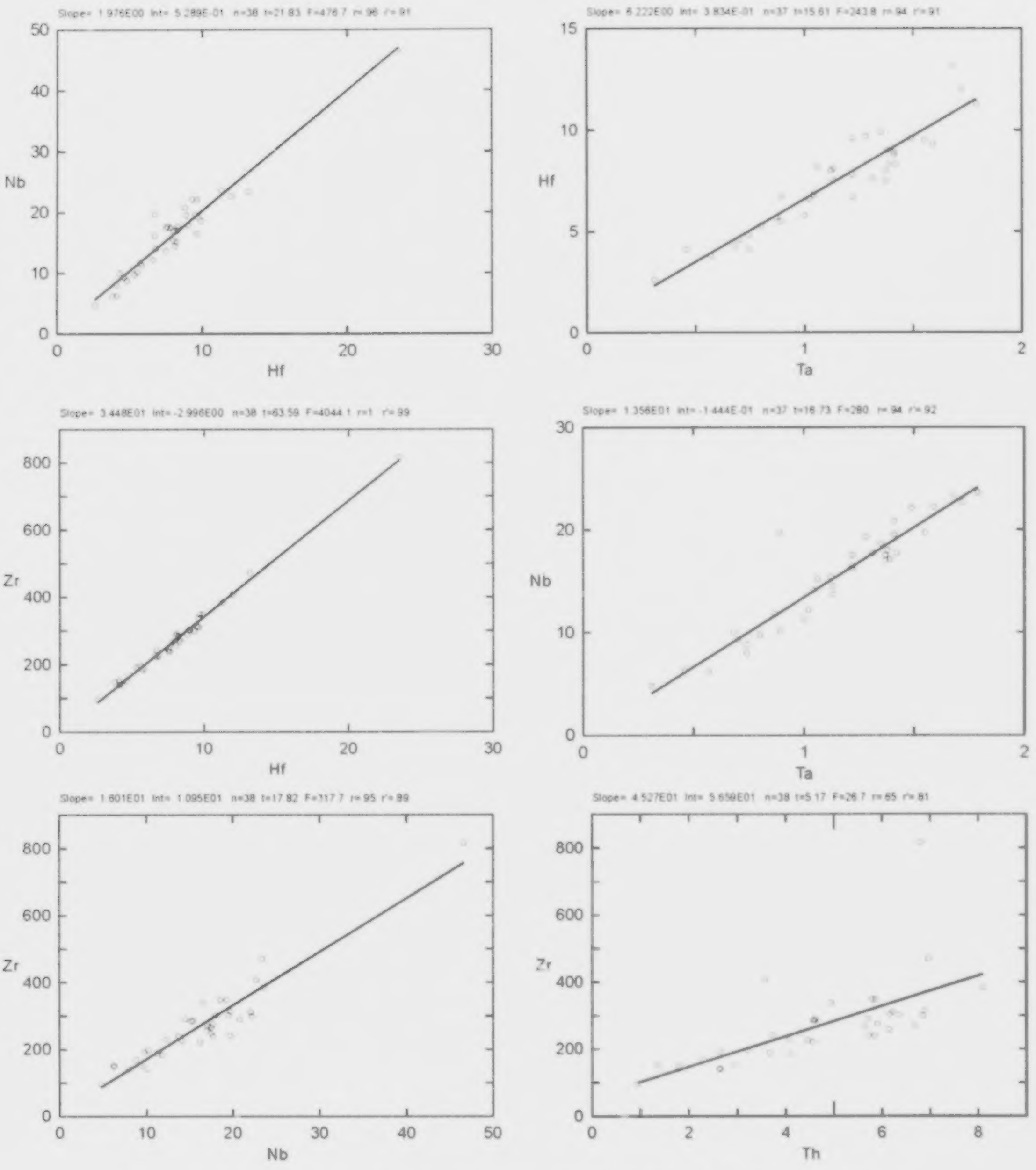

**Figure 13.** Selected variation diagrams of immobile elements in Genex felsic metavolcanic rocks.

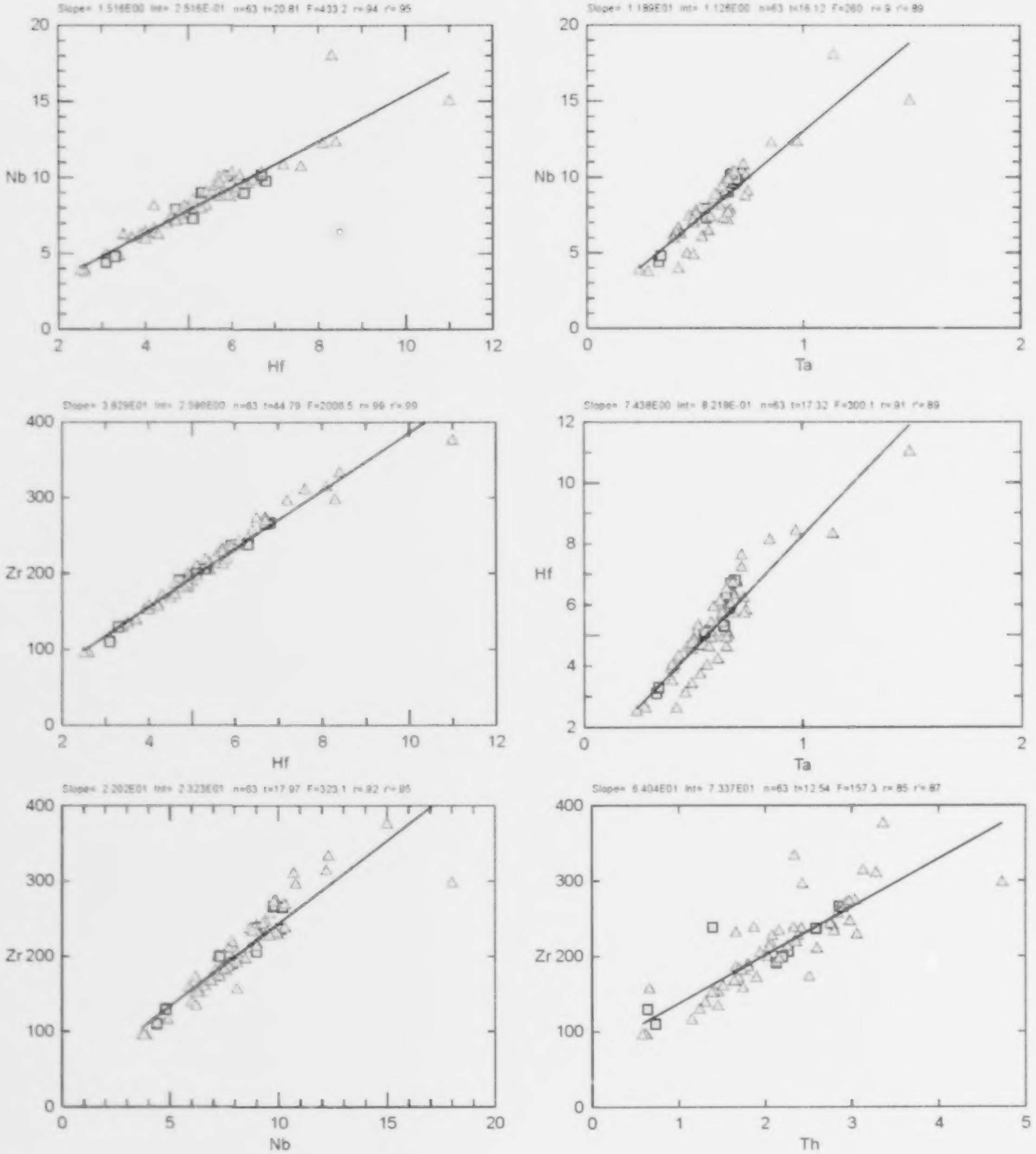

**Figure 14.** Selected variation diagrams of immobile elements in Genex mafic metavolcanic rocks. Triangles represent footwall samples, squares represent hanging-wall samples.

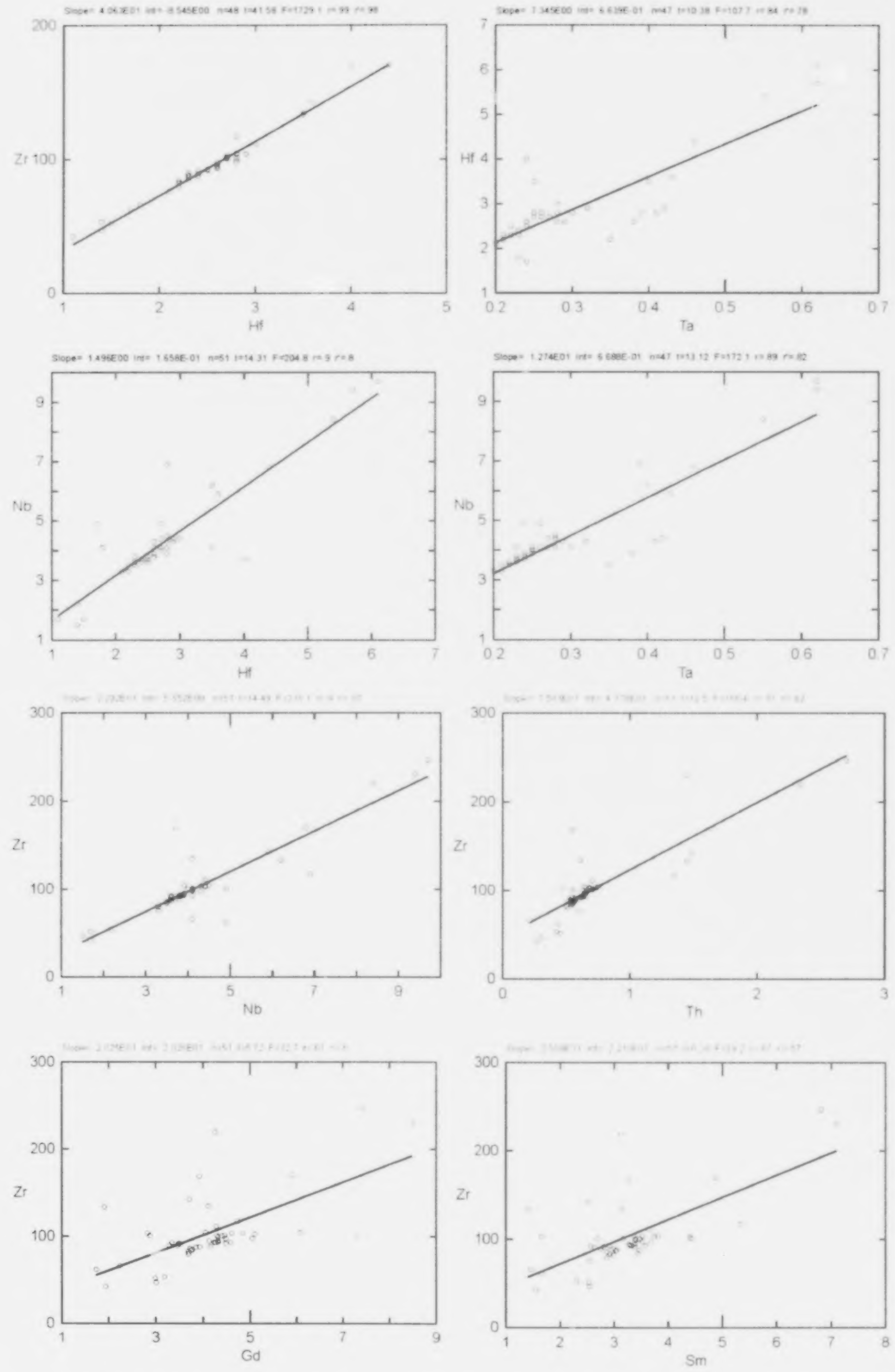

**Figure 15.** Selected variation diagrams of immobile elements in the Genex synvolcanic mafic intrusion.

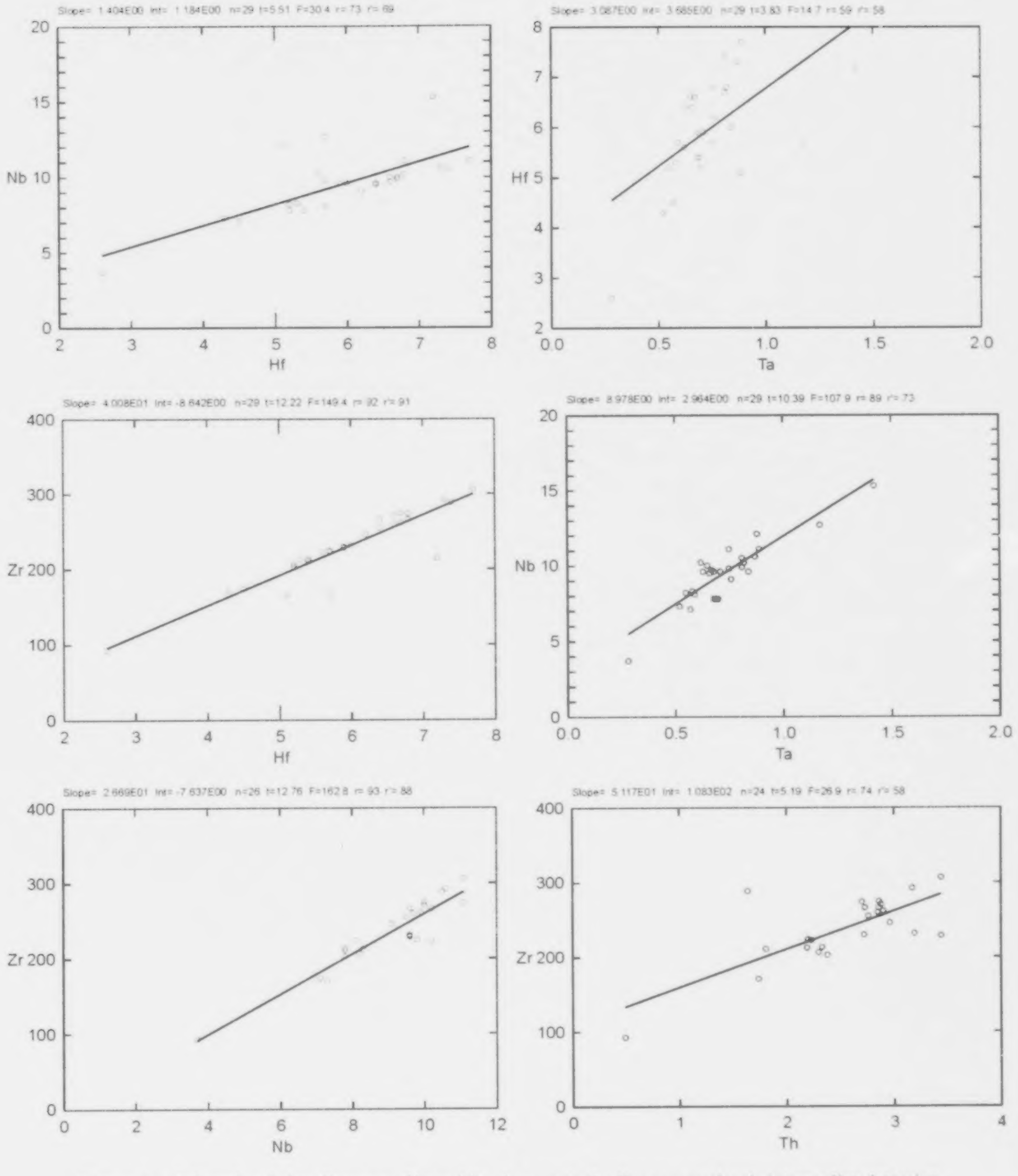

**Figure 16.** Selected variation diagrams of immobile elements in the Genex synvolcanic intermediate intrusion.

especially in areas that have experienced hydrothermal alteration, are rarely consistent from one location to another, and great care should be taken in making gross generalizations. It should be noted, however, that there is a greater number of immobile elements in the mafic intrusion (i.e., Sc, Gd, Nd, Sm and $SiO_2$) than in the other rock types, indicating a lesser degree of hydrothermal alteration in the intrusion, relative to the volcanic rocks and to the intermediate intrusion. This is also evident in outcrop and drill core as the mafic intrusion appears to be less altered (*see* "Stratigraphy in the Genex Area" and "Hydrothermal Alteration") than the surrounding rock types.

Further analysis of major element mobility is displayed in Figures 17 and 18. In Figure 17, felsic and mafic rocks, respectively, are plotted on a classification diagram that utilizes major element data ($SiO_2$, $Na_2O$, $K_2O$). Conversely, Figure 18 plots the same data on a classification diagram that utilizes trace element data (Nb, Y, Zr, $TiO_2$). The significant variations between the two diagrams suggests that the major elements are relatively mobile.

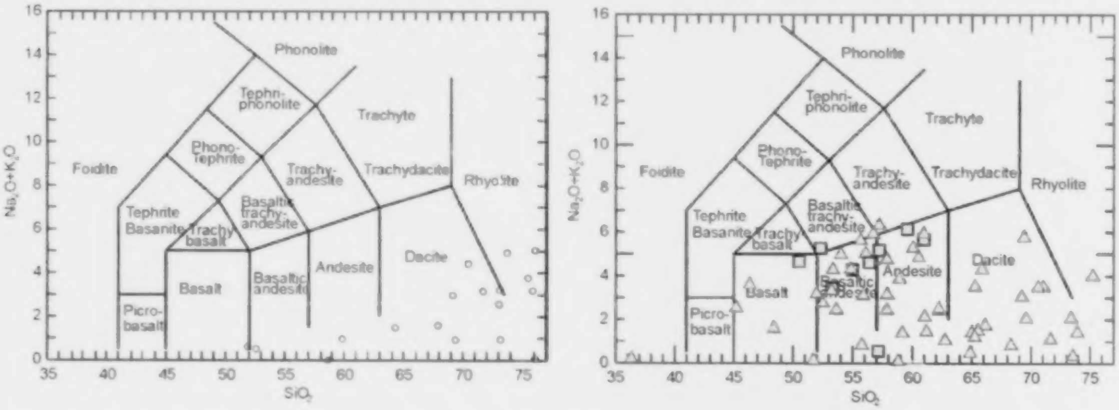

**Figure 17.** $Na_2O + K_2O$ (total alkalis) versus $SiO_2$ plots of felsic (left) and mafic (right) metavolcanic rocks in the Genex area (*after* Le Bas et al. 1986).

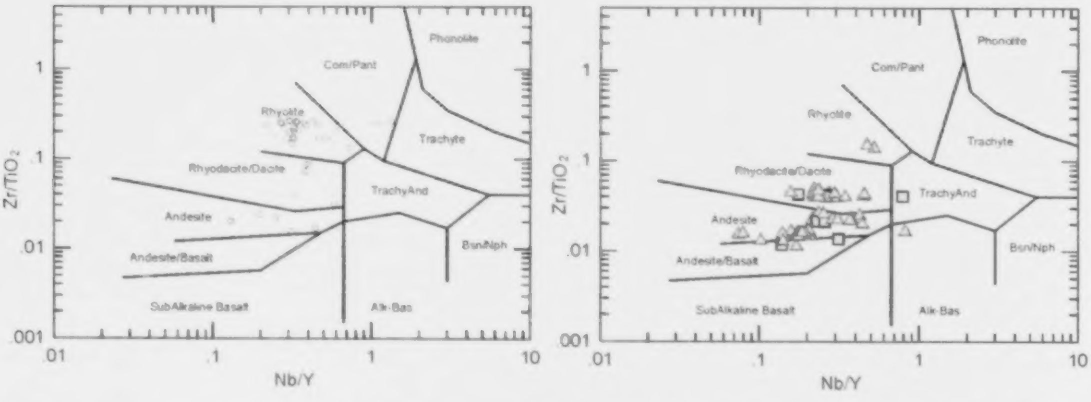

**Figure 18.** $Zr/TiO_2$ versus Nb/Y plot of felsic (left) and mafic (right) metavolcanic rocks in the Genex area (*after* Winchester and Floyd 1977).

# FRACTIONATION TRENDS

Pearce element ratios (Pearce 1968) are highly useful in discerning fractionation trends in mafic igneous rocks. Ratios are constructed using oxides ($SiO_2$ for example) or cations (Si) converted to mole units (refer to Stanley (1990) for method), plotted on x–y plots (i.e., (2Ca+Na)/K versus Al/K). Variables are based on mineral stoichiometry (i.e., plagioclase fractionation is based on $Al_2O_3$, CaO, $Na_2O$, $K_2O$), and ratio denominators use a single conserved element (i.e., $TiO_2$) that is common to both axes (Nicholls and Russell 1990). Correlation coefficients (r-values) for x–y plots are calculated according to the method outlined in the previous subsection. For the fractionation diagrams used in this study, an r-value approaching 1 indicates that the plotted mineral(s) are fractionating phases of the magma. Highly altered samples are identified based on petrographic analysis and field observations, and are omitted from the fractionation diagrams.

Fractionation diagrams in the Genex area have been constructed for mafic metavolcanic rocks (footwall and hanging wall) and the synvolcanic mafic and intermediate intrusions. Pearce element numbers (p) were calculated by dividing the weight percent of an oxide (wt %) by the gram formula weight (g), for example, $Al_2O_{3p} = Al_2O_{3\,wt\%} / 101.96_g$. In cases where Pearce element numbers (p) were reported as elements, the numerator of the aforementioned formula is multiplied by the number of cations in the chemical formula, for example, $Al_p = [Al_2O_{3\,wt\%} * 2] / 101.96_g$. It should be noted that Pearce element ratios are constructed using molar percentages of major oxides, which are mobile in the Genex rocks. Thus, we do not expect to see r-values close to 1 due to hydrothermal alteration processes. However, it is still possible to identify fractionating mineral phases in the Genex rocks using Pearce element ratios, because the relative elemental abundances remain generally constant.

Fractionation trends in the footwall mafic metavolcanic rocks of the Genex area are shown in Figure 19. The r-value in Figure 19A is near 0 (0.04), indicating that olivine alone is not a fractionating phase. The r-value in Figure 19B is also relatively low (0.23) indicating the plagioclase alone is not a fractionating phase either. Thus, there must be a combination of olivine, plagioclase, and clinopyroxene fractionating. Figure 19C and 19D both have relatively low r-values indicating that is not just olivine + plagioclase fractionation, nor is it just olivine + clinopyroxene. The highest r-value (0.99) is illustrated in Figure 19E, which models fractionation of olivine + plagioclase + clinopyroxene. This almost perfect correlation indicates that the Genex mafic metavolcanic rocks are derived from fractionation of all three mineral phases (olivine, plagioclase, and clinopyroxene). Petrographic analysis of the Genex footwall mafic metavolcanic rocks confirms the presence of plagioclase and clinopyroxene. However, no olivine is observed in thin section.

Fractionation trends in the hanging-wall mafic metavolcanic rocks are slightly different from those in the footwall rocks. Figure 20A has a low r-value (0.04) which indicates that olivine alone is not a fractionating phase. However, the r-values in Figures 20B and 20C are both high (0.83 and 0.87, respectively) which support the interpretation that the fractionating phases are plagioclase + olivine. The low r-value in Figure 20D (0.22) indicates that clinopyroxene is either entirely absent or a minor fractionating phase. Lastly, the high r-value in Figure 20E (0.88) supports the presence of plagioclase + olivine ± clinopyroxene (minor). Both plagioclase and clinopyroxene have been observed petrographically in the hanging-wall mafic metavolcanic rocks. However, olivine has not been observed in thin section. These fractionation trends would suggest that the hanging-wall mafic metavolcanic rocks are derived from a slightly less evolved magma than the footwall mafic metavolcanic rocks. These trends will be further evaluated in a planned journal paper by the authors of this report (S.M. Hocker, H.L. Gibson and P.C. Thurston).

Fractionation trends in the synvolcanic mafic intrusions are shown in Figure 21. Figure 21A has a low r-value (0.29) whereas Figure 21B has a slightly higher r-value (0.41). This suggests that while olivine alone is not a fractionating phase, plagioclase may be a dominant phase. Further analysis of fractionation trends shown in Figure 21C (r-value 0.02) and 21D (r-value 0.31) indicate that neither olivine + plagioclase nor olivine + clinopyroxene are the dominant fractionating phases. However, the highest r-value (0.91) is derived from modeling olivine ± plagioclase ± clinopyroxene fractionation (Figure 21E). This suggests that, as has already been shown, plagioclase is a major fractionating phase, whereas olivine and clinopyroxene are minor fractionating phases. The lack of strong fractionation trends in the intrusions indicates that the Genex synvolcanic mafic intrusions are derived from a relatively primitive melt that experienced minimal fractionation. Fractionation trends in the mafic intrusions are most similar to those in the hanging-wall mafic metavolcanic rocks. Petrographically, both plagioclase and clinopyroxene have been observed. Olivine, however, has not been observed in thin section.

Figure 22 shows fractionating trends in the synvolcanic intermediate intrusion. Figure 22A and 22B both have relatively low r-values (0.14 and 0.23, respectively) which indicate that neither olivine nor plagioclase alone are fractionating phases. The olivine + plagioclase diagram (Figure 22C) also has a low r-value (0.22). The olivine + clinopyroxene diagram (Figure 22D) has a slightly higher r-value (0.48). The highest r-value is derived from Figure 22E, the olivine ± plagioclase ± clinopyroxene diagram (0.81). These trends suggest that olivine + clinopyroxene are the dominant fractionating phases in the intermediate intrusion. Plagioclase is either absent or is a minor fractionating phase. The overall low r-values in the intermediate intrusive rocks are likely due to element mobility (discussed in the previous subsection).

Fractionation trends in the Genex felsic metavolcanic rocks are not easily distinguished using Pearce element ratios. Figure 23 displays plagioclase fractionation trends, and the relatively high r-value (0.60) suggests that plagioclase is a fractionating phase in the Genex felsic metavolcanic rocks. Quartz is also a likely fractionating phase in the Genex felsic metavolcanic rocks. However, Pearce element ratios cannot model quartz fractionation due to the simple chemical composition of the mineral. In thin section, both quartz and plagioclase have been observed.

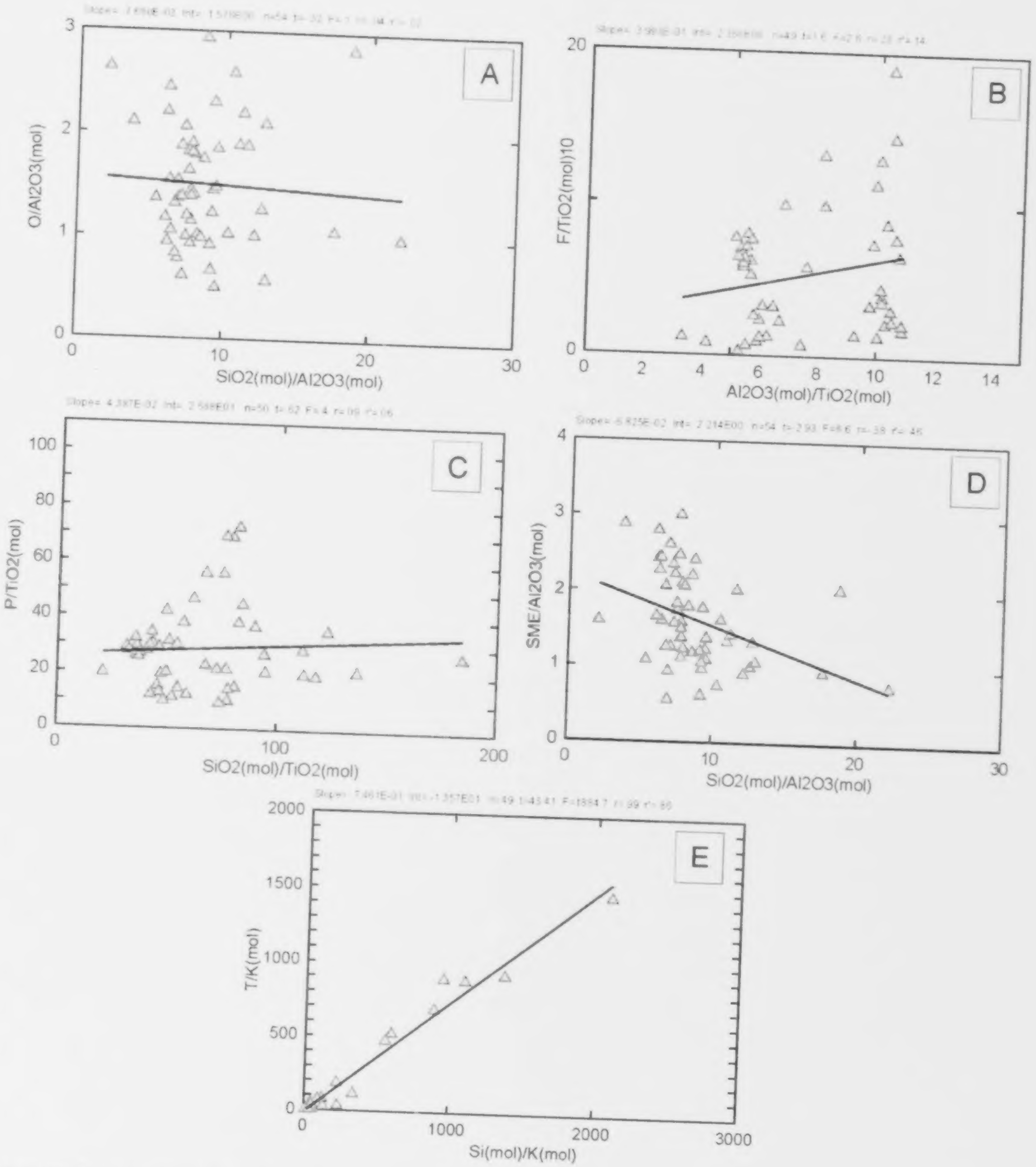

**Figure 19.** Fractionation trends in Genex footwall mafic metavolcanic rocks.
A) Olivine fractionation trends (*from* Pearce 1990). O = 0.5(FeO) + MgO.
B) Plagioclase fractionation trends (*from* Pearce 1990). F = CaO + $Na_2O$ + $K_2O$.
C) Olivine ± plagioclase fractionation trends (*from* Pearce 1990). P = 0.5(FeO + MgO) + 6($Na_2O$ + $K_2O$) + 2CaO.
D) Olivine ± clinopyroxene fractionation trends (*from* Pearce 1990). SME = 1.5CaO + 0.5(FeO + MgO).
E) Olivine ± plagioclase ± clinopyroxene fractionation trends (*from* Nicholls 1990). T = 0.25Al + 0.5(Fe + Mg) + 1.5Ca + 2.75Na.

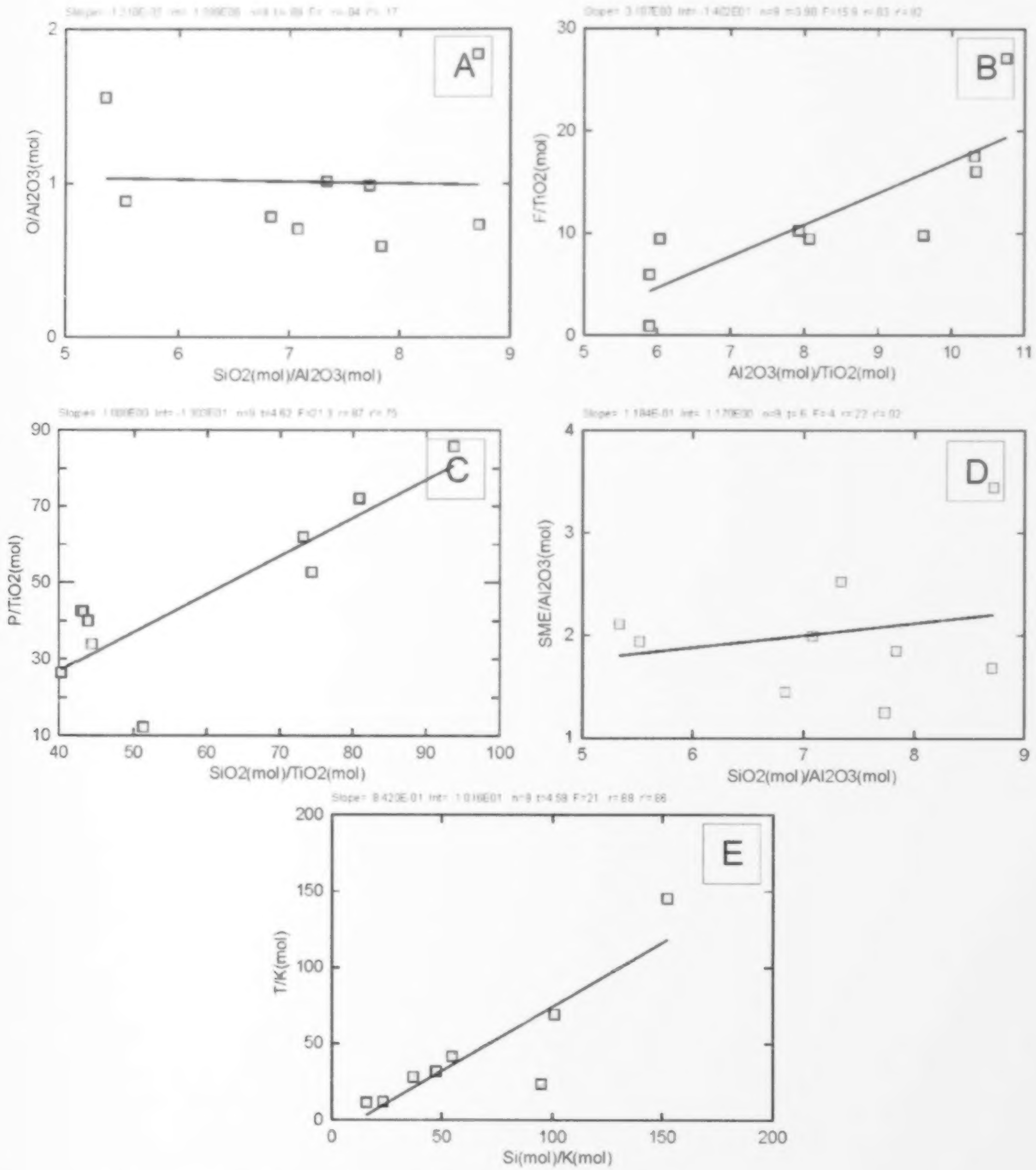

**Figure 20.** Fractionation trends in Genex hanging-wall mafic metavolcanic rocks.
A) Olivine fractionation trends (*from* Pearce 1990). O = 0.5(FeO) + MgO.
B) Plagioclase fractionation trends (*from* Pearce 1990). F = CaO + $Na_2O$ + $K_2O$.
C) Olivine ± plagioclase fractionation trends (*from* Pearce 1990). P = 0.5(FeO + MgO) + 6($Na_2O$ + $K_2O$) + 2CaO.
D) Olivine ± clinopyroxene fractionation trends (*from* Pearce 1990). SME = 1.5CaO + 0.5(FeO + MgO).
E) Olivine ± plagioclase ± clinopyroxene fractionation trends (*from* Nicholls 1990). T = 0.25Al + 0.5(Fe + Mg) + 1.5Ca + 2.75Na.

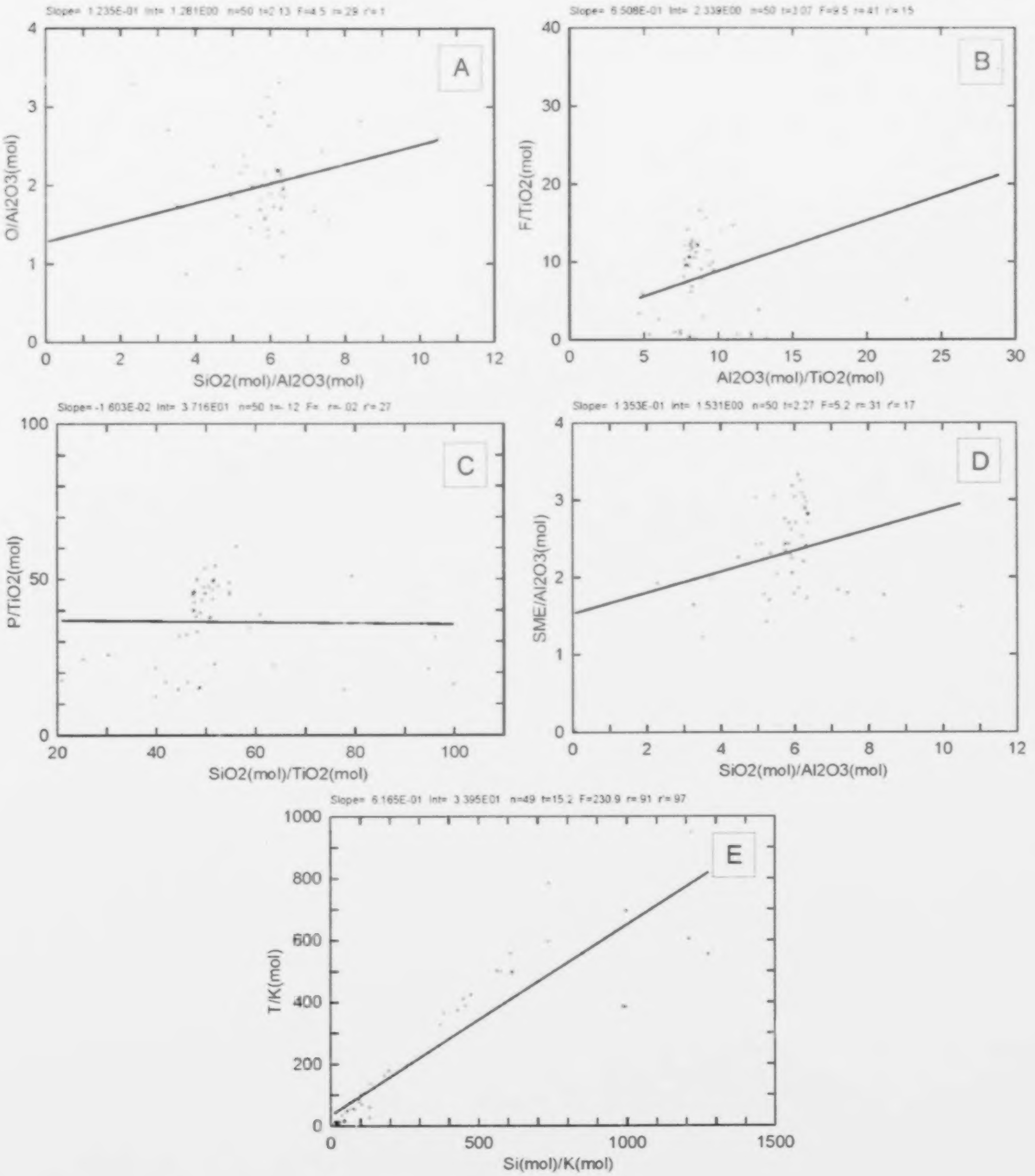

**Figure 21.** Fractionation trends in Genex synvolcanic mafic intrusion.
A) Olivine fractionation trends (*from* Pearce 1990). O = 0.5(FeO) + MgO.
B) Plagioclase fractionation trends (*from* Pearce 1990). F = CaO + $Na_2O$ + $K_2O$.
C) Olivine ± plagioclase fractionation trends (*from* Pearce 1990). P = 0.5(FeO + MgO) + 6($Na_2O$ + $K_2O$) + 2CaO.
D) Olivine ± clinopyroxene fractionation trends (*from* Pearce 1990). SME = 1.5CaO + 0.5(FeO + MgO).
E) Olivine ± plagioclase ± clinopyroxene fractionation trends (*from* Nicholls 1990). T = 0.25Al + 0.5(Fe + Mg) + 1.5Ca + 2.75Na.

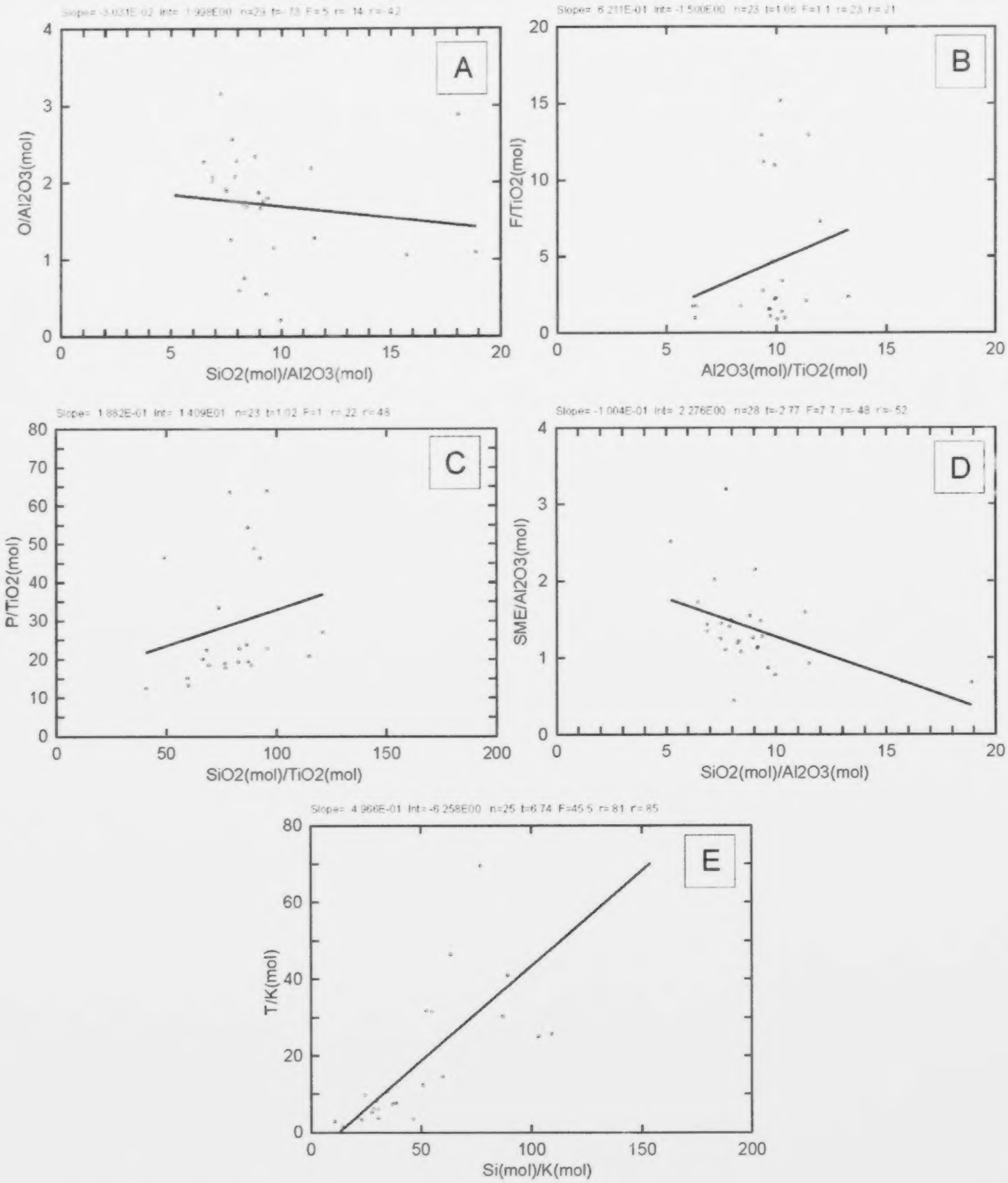

**Figure 22.** Fractionation trends in Genex synvolcanic intermediate intrusion.
A) Olivine fractionation trends (*from* Pearce 1990). O = 0.5(FeO) + MgO.
B) Plagioclase fractionation trends (*from* Pearce 1990). F = CaO + $Na_2O$ + $K_2O$.
C) Olivine ± plagioclase fractionation trends (*from* Pearce 1990). P = 0.5(FeO + MgO) + 6($Na_2O$ + $K_2O$) + 2CaO.
D) Olivine ± clinopyroxene fractionation trends (*from* Pearce 1990). SME = 1.5CaO + 0.5(FeO + MgO).
E) Olivine ± plagioclase ± clinopyroxene fractionation trends (*from* Nicholls 1990). T = 0.25Al + 0.5(Fe + Mg) + 1.5Ca + 2.75Na.

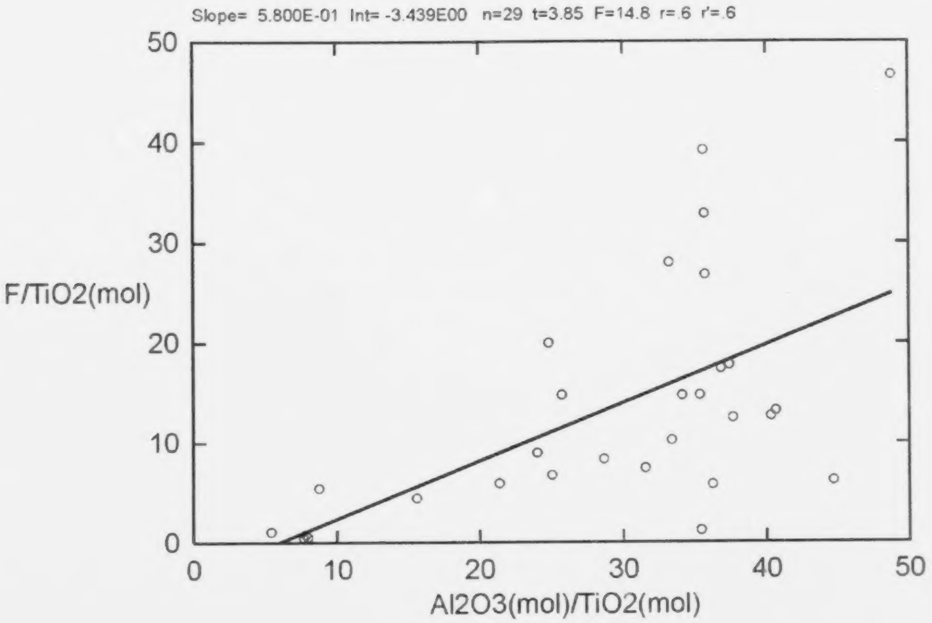

**Figure 23.** Plagioclase fractionation trends in Genex felsic metavolcanic rocks (*after* Pearce 1990). F = $CaO + Na_2O + K_2O$.

# RARE EARTH ELEMENT TRENDS

## Felsic Metavolcanic Rocks

Felsic metavolcanic rocks in the Genex area are classified as rhyolites and dacites using a $Zr/TiO_2$ versus Nb/Y diagram developed by Winchester and Floyd (1977) and modified by Pearce (1996) (Figure 24). This diagram is especially useful in classifying altered rocks since it utilizes relatively immobile trace element data. Petrographic and field observations indicate that all samples plotted in Figure 24 are felsic. Therefore, the few outliers that plot in more mafic fields reflect element mobility during hydrothermal alteration.

Work by Lesher et al. (1986) has classified Archean felsic metavolcanic rocks into 4 main types based on geochemical trends: FI, FII, and FIIIa and FIIIb rhyolites (Table 5). The Kamiskotia felsic volcanic rocks have been classified as FIIIb rhyolites (Hart, Gibson and Lesher 2004; Lesher et al. 1986). The Genex felsic metavolcanic rocks are, however, classified as FIIIa rhyolites.

Overall, FIII rhyolites have relatively unfractionated REE patterns and are derived from either a) low-pressure partial melting of a tholeiitic basalt without residual amphibole or garnet in a subvolcanic magma chamber (Barrie, Ludden and Green 1993; Campbell et al. 1981, 1982; Hart 1984; Hart, Gibson and Lesher 2004; Lesher et al. 1986); b) low-pressure plagioclase-dominated fractional crystallization of an intermediate magma (Hart, Gibson and Lesher 2004; Lesher et al. 1986); or c) partial melting of continental crust with minor assimilation fractional crystallization (Barrett and MacLean 1999; Hart, Gibson and Lesher 2004). Generally, FIII rhyolites are derived from high-level magma chambers

(<10 km), whereas FI and FII rhyolites are derived from deeper sources without high-level fractionation (Hart, Gibson and Lesher 2004; Lesher et al. 1986). Overall, FIII rhyolites are considered prime exploration targets, as they host many of Canada's Archean volcanogenic massive sulphide (VMS) deposits (for example, Kidd Creek, Noranda, and Kamiskotia in the Abitibi belt, and Confederation Lake in the Uchi belt; Hart, Gibson and Lesher 2004; Lesher et al. 1986).

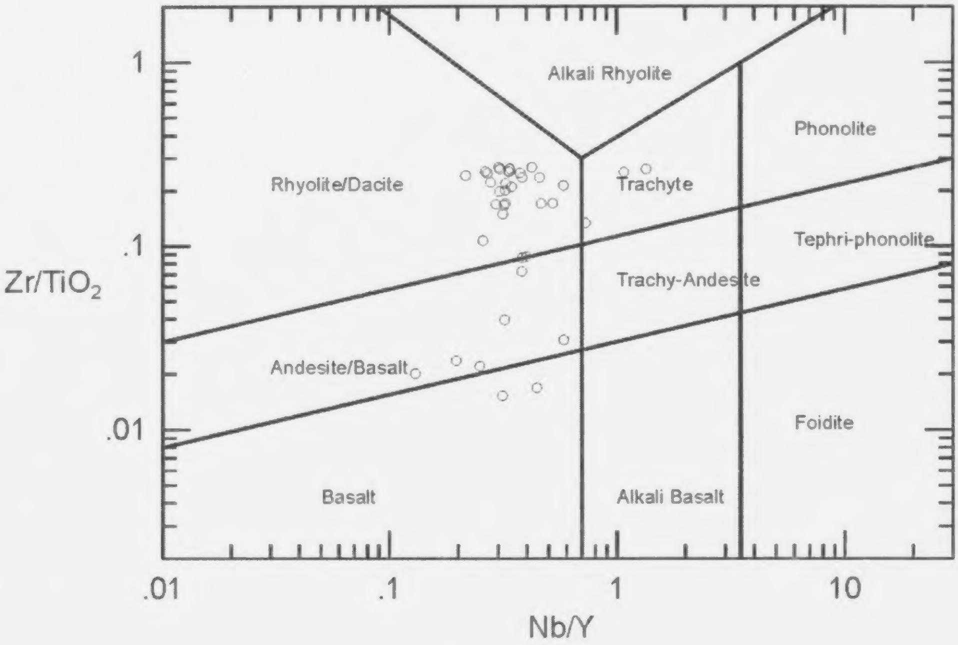

**Figure 24.** Zr/TiO$_2$ versus Nb/Y classification of felsic volcanic rocks (*after* Winchester and Floyd 1977; Pearce 1996). Genex felsic metavolcanic rocks plot primarily in the rhyolite/dacite field.

**Table 5.** Classification of felsic volcanic rocks in the Abitibi belt (*from* Lesher et al. 1986). Genex felsic metavolcanic rocks are most similar to FIIIa rhyolites, contrary to the rest of the Kamiskotia rhyolites.

| SiO$_2$ wt % | TiO$_2$ wt % | Rb ppm | Sr ppm | Y ppm | Zr ppm | La ppm | Yb ppm | Th ppm | Hf ppm | Sc ppm | La/Yb ppm | Zr/Y ppm |
|---|---|---|---|---|---|---|---|---|---|---|---|---|
| **FI** | | | | | | | | | | | | |
| 64-69 | 0.31-0.55 | 8-89 | 147-514 | 6-12 | 110-142 | 7.2-14 | 0.46-0.87 | 0.6-2.0 | 2.4-3.5 | 2.4-12 | 5.8-20 | 9.2-24 |
| **FII** | | | | | | | | | | | | |
| 66-73 | 0.39-0.79 | 5-60 | 43-175 | 17-48 | 96 | 9.1 | 1.7-5.8 | 1.3-4.3 | 2.3-8.3 | 7.8-25 | 2.3-3.6 | 5.6-7.0 |
| **FIIIa** | | | | | | | | | | | | |
| 67-78 | 0.21-0.99 | 1-62 | 4.8-101 | 25-70 | 170-370 | 9.8-37 | 3.4-9.3 | 1.5-7.3 | 3.9-8.6 | 7.0-20 | 1.5-2.8 | 3.9-6.8 |
| **FIIIb** | | | | | | | | | | | | |
| 67-84 | 0.09-0.47 | 1-157 | 7-73 | 72-188 | 194-442 | 26-67 | 7.3-22 | 3.2-12 | 5.8-16 | 1.4-11 | 1.1-4.9 | 2.0-3.8 |
| **GENEX FELSIC VOLCANIC ROCKS (averages)** | | | | | | | | | | | | |
| 72.99 | 0.46 | 31.03 | 14.94 | 42.75 | 262.78 | 28.58 | 4.92 | 4.58 | 7.73 | 32.52 | 5.80 | 6.76 |

Based on the criteria outlined in Table 5, and shown on Figure 25, the felsic metavolcanic rocks in the Genex area are classified as FIIIa rhyolites. The chondrite-normalized spider plot of the felsic metavolcanics (Figure 26) indicates a relatively unfractionated REE pattern, as well as a pronounced Eu anomaly. The primitive mantle-normalized spider plot (Figure 27) displays a large Sr anomaly, common in FIII rhyolites. According to Hart, Gibson and Lesher (2004) and Lesher et al. (1986), pronounced Eu and Sr anomalies suggest retention of plagioclase in the residue. Fractionation trends, outlined in the previous subsection, indicate that plagioclase is likely a fractionating phase during the evolution of the Genex felsic metavolcanic rocks, or was a residual phase during melting. The Sr anomaly, however, may be due to carbonate alteration (*see* "Hydrothermal Alteration").

The Kamiskotia area, of which the Genex stratigraphy is a part, has traditionally been included in the Tisdale and Kidd–Munro assemblages. According to the classification scheme developed by Lesher et al. (1986), the Kamiskotia rocks are classified as FIIIb rhyolites. However, the Genex rocks are most similar to FIIIa rhyolites (*see* Table 5). Canadian examples of Archean FIIIa rhyolites include the Noranda camp (Quebec; Blake River assemblage), Winston Lake (Ontario), and Manitouwadge (Ontario) (Hart, Gibson and Lesher 2004; Lesher et al. 1986). This discrepancy suggests that the Genex rocks may be more similar to those of the Blake River assemblage, than to those of the Tisdale and Kidd–Munro assemblages, as has been previously thought (Ayer et al. 2002). The full implications of this discrepancy are beyond the scope of this project, but are discussed in detail in Hathway, Hudak and Hamilton (2005).

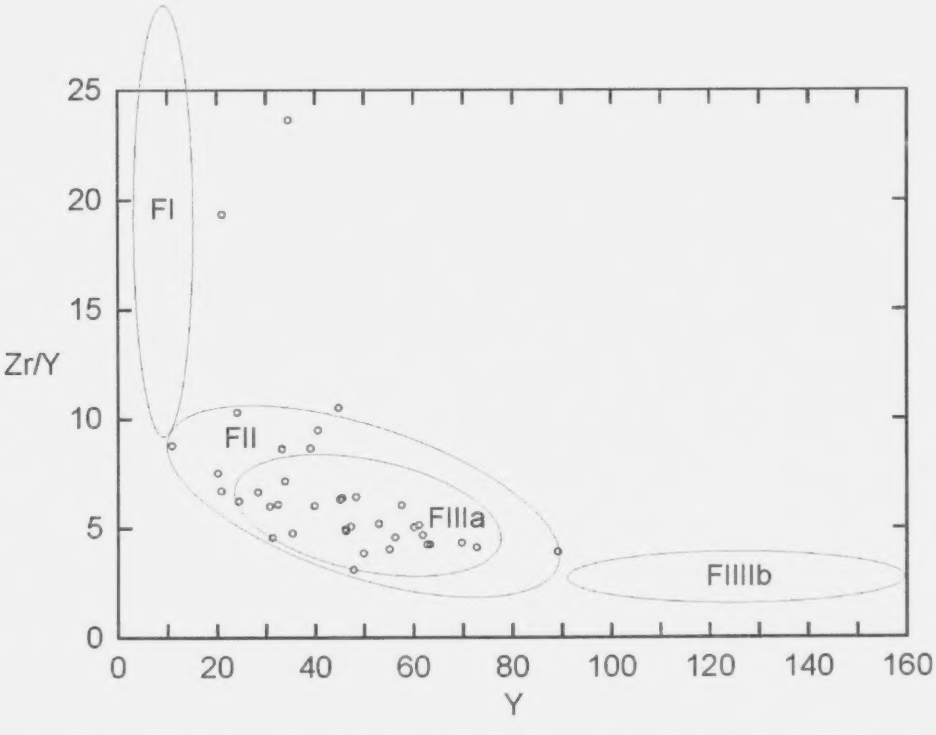

**Figure 25.** Zr/Y versus Y plot for classification of rhyolites (Lesher et al. 1986; Piercey et al. 2001b). Genex felsic metavolcanic rocks plot in the FIIIa field.

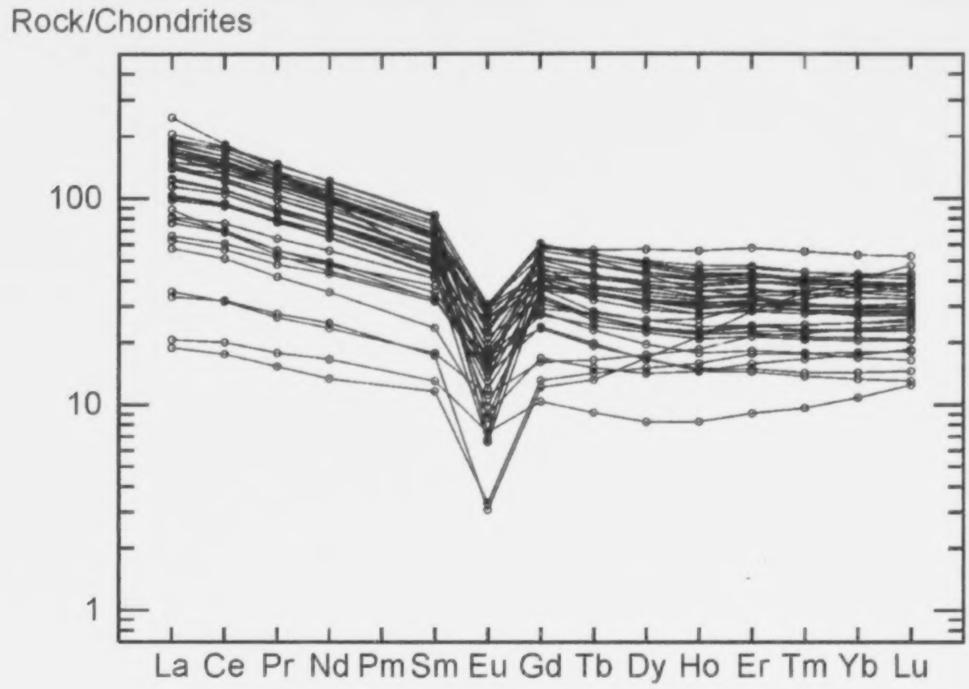

**Figure 26.** Chondrite-normalized spider plot of Genex felsic metavolcanic rocks (*after* Sun and McDonough 1989).

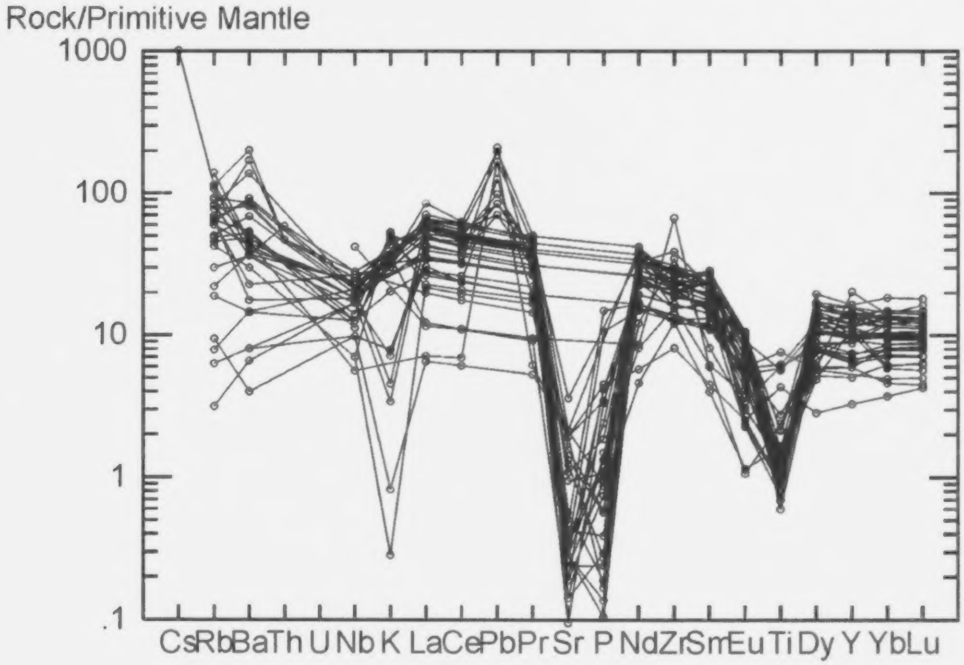

**Figure 27.** Primitive mantle-normalized spider plot of Genex felsic metavolcanic rocks (*after* Sun and McDonough 1989).

## Mafic Metavolcanic Rocks

Mafic metavolcanic rocks in the footwall and hanging wall of the Genex deposit plot in the basalt to basaltic andesite fields of the $Zr/TiO_2$ versus Nb/Y discrimination diagram developed by Winchester and Floyd (1977), and modified by Pearce (1996) (Figure 28). Further analysis of the Genex mafic metavolcanic rocks using primitive mantle-normalized spider plots indicates that the mafic metavolcanic rocks are most similar to boninites (Figure 29). However, plotting the Genex mafic metavolcanic rocks on other boninite discrimination diagrams (i.e., Ti/V versus Ti/Sc and La/Sm versus $TiO_2$ (Piercey et al. 2001a)) reveals no correlation with boninite compositions. Instead, the Zr versus $P_2O_5$ plot by Winchester and Floyd (1976) and the Nb/Y versus $Zr/P_2O_5$ plot by Floyd and Winchester (1975) indicate that the footwall and hanging-wall mafic metavolcanic rocks are oceanic tholeiitic basalts (Figures 30 and 31). Thus, the Genex mafic metavolcanic rocks are not boninites, but oceanic tholeiites.

Chondrite-normalized spider diagrams for Genex mafic rocks (Figure 32) display a relatively flat pattern, indicating an unevolved and unfractionated magma. Hanging-wall rocks are slightly depleted in all REE and are especially depleted in HREE relative to footwall rocks.

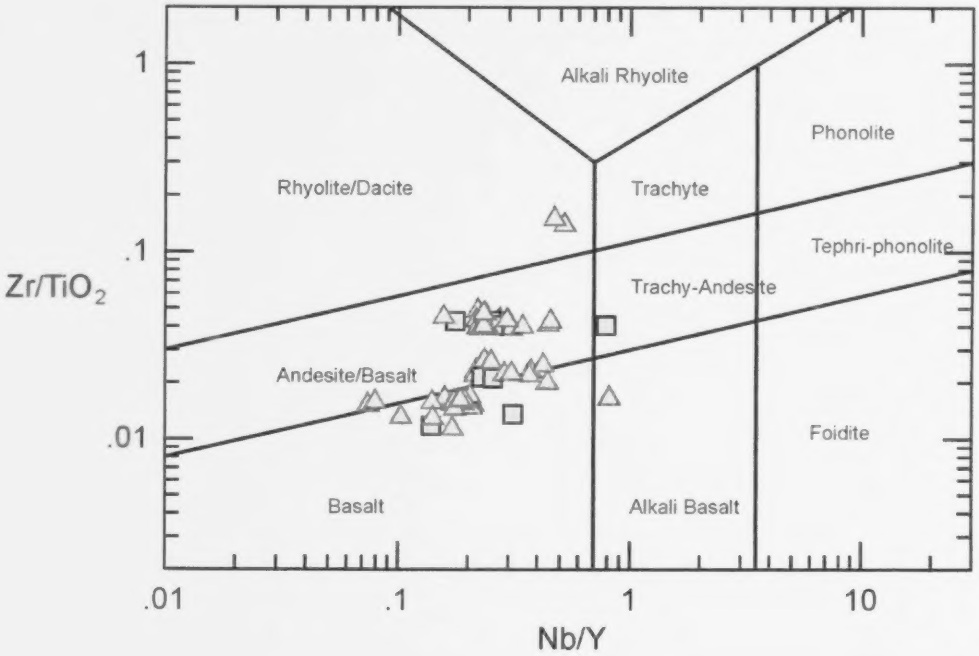

**Figure 28.** $Zr/TiO_2$ versus Nb/Y classification of mafic volcanic rocks (*after* Winchester and Floyd 1977; Pearce 1996). Triangles are footwall samples, boxes are hanging-wall samples. Genex mafic metavolcanic rocks plot dominantly in the andesite/basalt field.

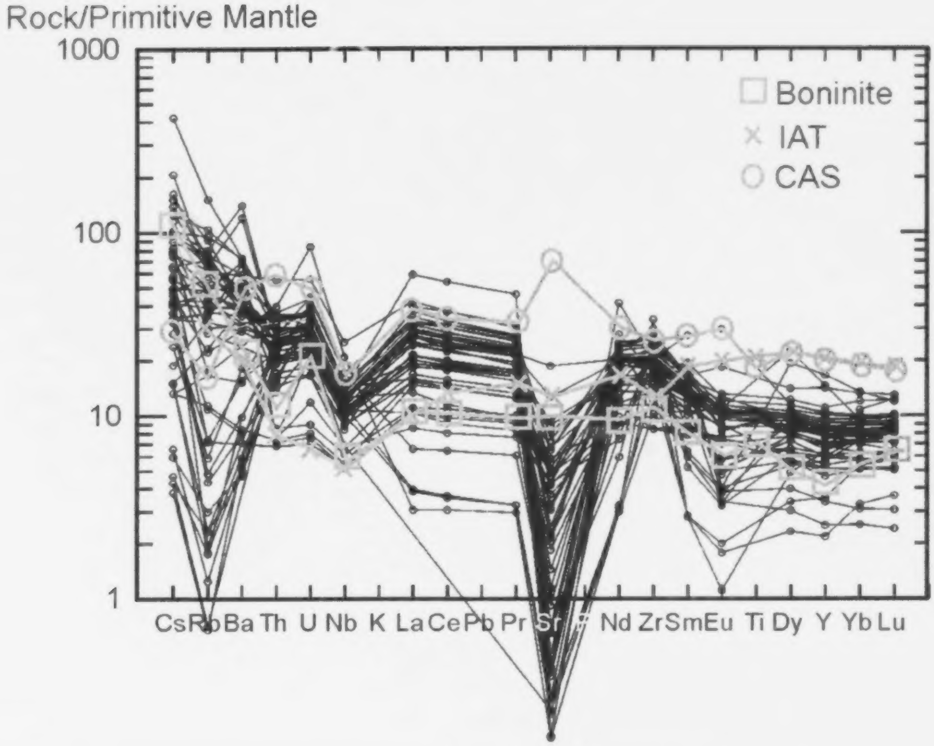

**Figure 29.** Tectonic environment of formation for Genex mafic metavolcanic rocks (*after* Sun and McDonough 1989; Jenner 1996). Genex rocks are most similar to the boninite field. IAT = island arc tholeiite. CAS = calc-alkaline series.

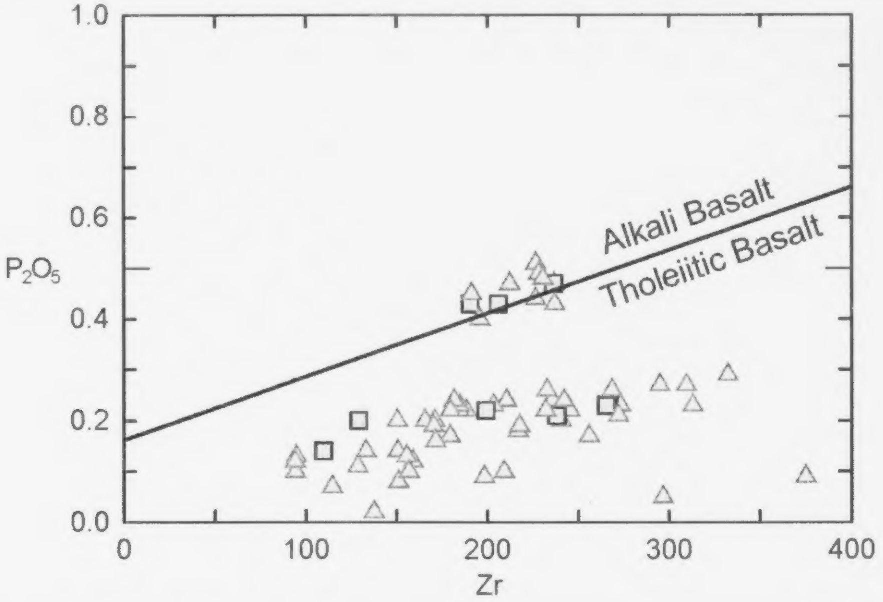

**Figure 30.** $P_2O_5$ (wt %) versus Zr (ppm) discrimination diagram for mafic rocks (*after* Winchester and Floyd 1976). Genex mafic metavolcanic rocks plot in the tholeiitic basalt field. Triangles are footwall metavolcanic rocks. Squares are hanging-wall metavolcanic rocks.

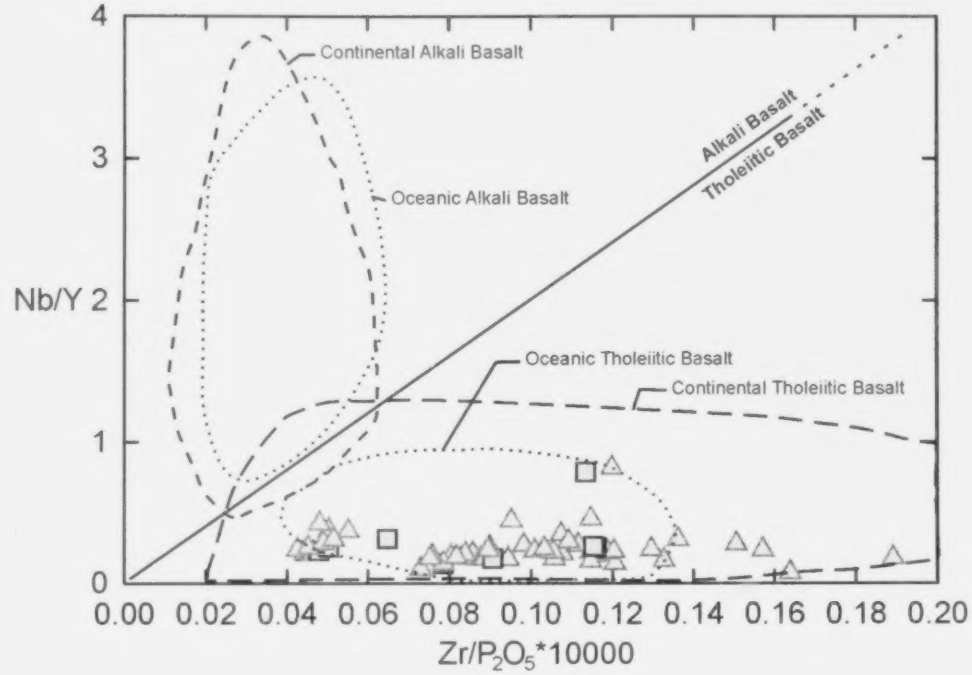

**Figure 31.** Nb/Y versus Zr/($P_2O_5$ × 10000) discrimination diagram for mafic volcanic rocks (*after* Floyd and Winchester 1975). Triangles are footwall rocks, squares are hanging-wall rocks. Genex mafic metavolcanic rocks plot in the oceanic tholeiitic basalt field.

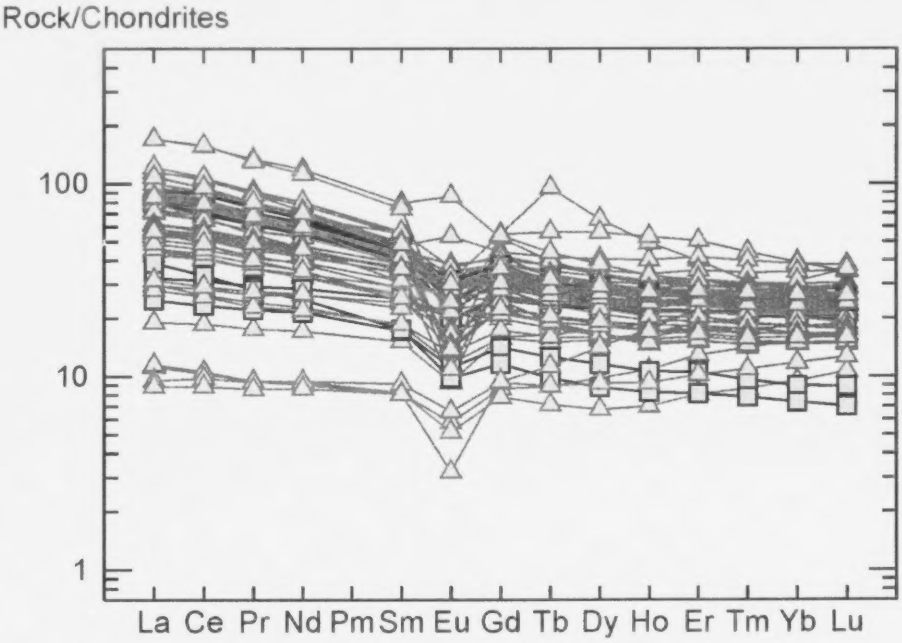

**Figure 32.** Chondrite-normalized spider plot of Genex mafic metavolcanic rocks (*after* Sun and McDonough 1989). Triangles are footwall rocks, squares are hanging-wall rocks.

## Synvolcanic Intrusive Rocks

Using a $Zr/TiO_2$ versus Nb/Y diagram (Winchester and Floyd 1977; Pearce 1996), the mafic intrusive rocks plot mainly in the basalt field, whereas the intermediate intrusive rocks plot mainly in the andesite/basalt field (Figure 33). Further analysis of the two intrusions using a $P_2O_5$ versus Zr plot (Figure 34) indicates that both intrusions are tholeiitic, and have an oceanic tholeiitic affinity (Figure 35). It is expected that both intrusions would be oceanic tholeiites since they are synvolcanic in their timing, and should be derived from a source similar to the Genex metavolcanic rocks.

A chondrite-normalized spider diagram of the synvolcanic mafic intrusion (Figure 36) indicates derivation from a primitive, relatively unevolved magma (relative to the Genex mafic metavolcanic rocks). Fractionation trends discussed in previous subsections support this hypothesis. Conversely, a chondrite-normalized spider diagram of the Genex synvolcanic intermediate intrusion (Figure 37) indicates derivation from a more evolved source (similar to the mafic metavolcanic rocks). This idea is also supported by fractionation trends discussed previously.

Further analysis of chondrite-normalized REE trends indicates that the Genex synvolcanic mafic and intermediate intrusions are similar to the upper zone of the Kamiskotia gabbroic complex (Figure 38) (Barrie et al. 1991; Campbell et al. 1981). This similarity may suggest a relation between the Genex synvolcanic intermediate intrusions and the Kamiskotia gabbroic complex, and will be explored in a planned journal paper by the authors of this report (S.M. Hocker, H.L. Gibson and P.C. Thurston).

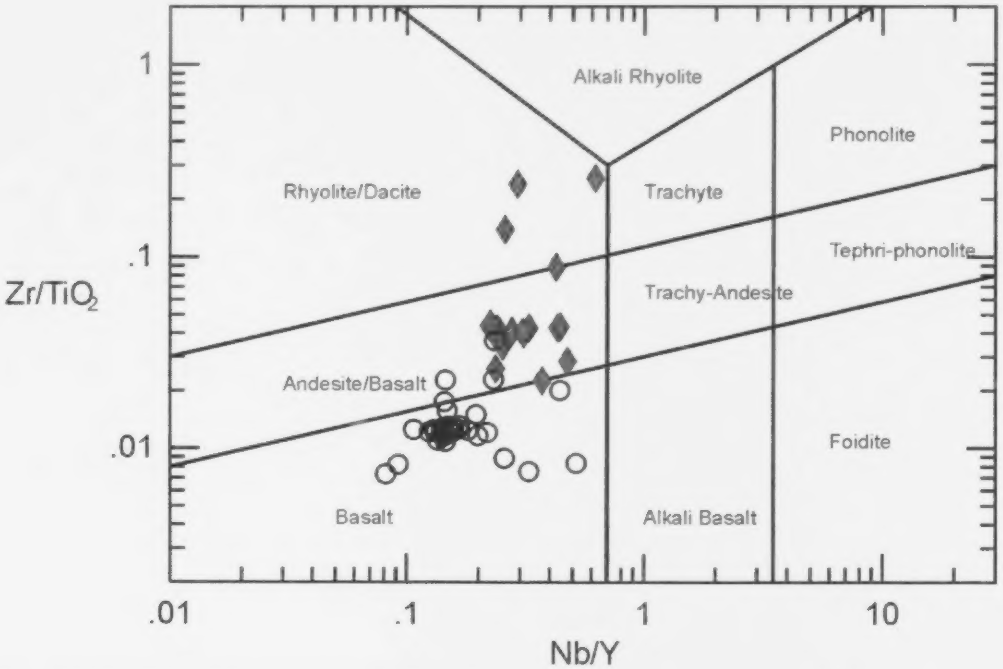

**Figure 33.** $Zr/TiO_2$ versus Nb/Y classification of intrusive rocks (*after* Winchester and Floyd 1977; Pearce 1996). Genex mafic synvolcanic intrusion (circles) plot dominantly in the basalt field, intermediate intrusion (diamonds) plot dominantly in the andesite/basalt field.

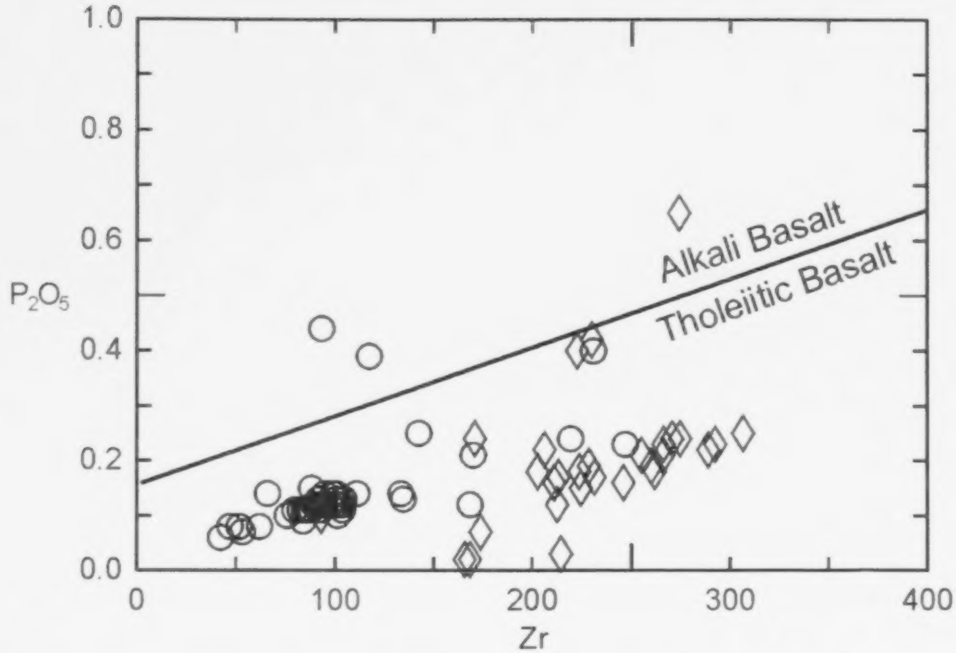

**Figure 34.** $P_2O_5$ (wt %) versus Zr (ppm) discrimination diagram for intrusive rocks (*after* Winchester and Floyd 1976). Genex synvolcanic mafic intrusive rocks (circles) and intermediate intrusive rocks (diamonds) plot in the tholeiitic basalt field.

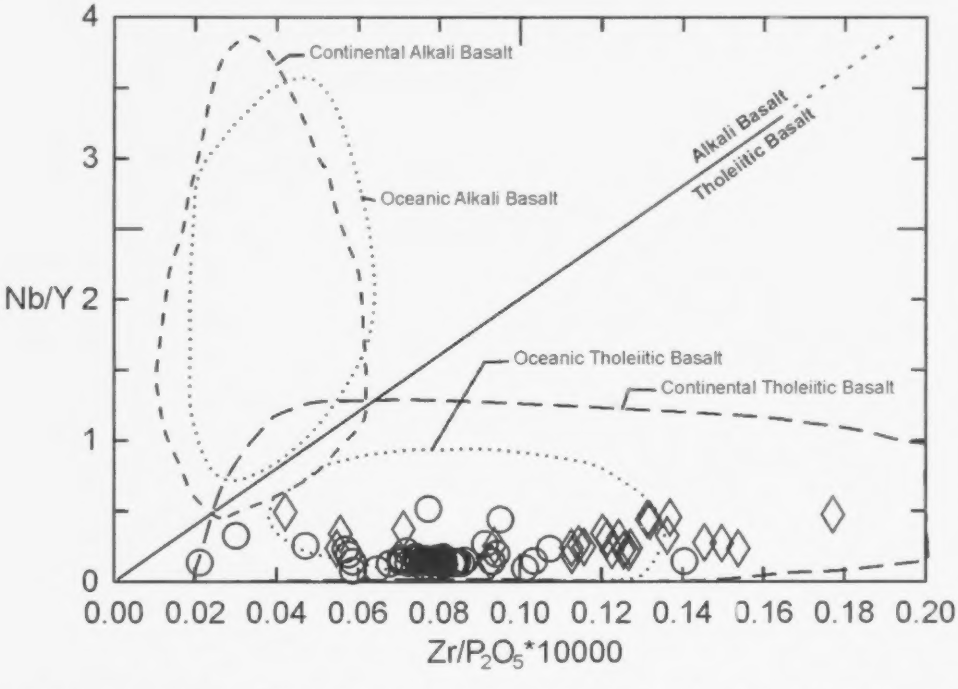

**Figure 35.** Nb/Y versus Zr/($P_2O_5$ × 10000) discrimination diagram for intrusive rocks (*after* Floyd and Winchester 1975). Genex synvolcanic mafic intrusive rocks (circles) and intermediate intrusive rocks (diamonds) plot in the oceanic tholeiitic basalt field.

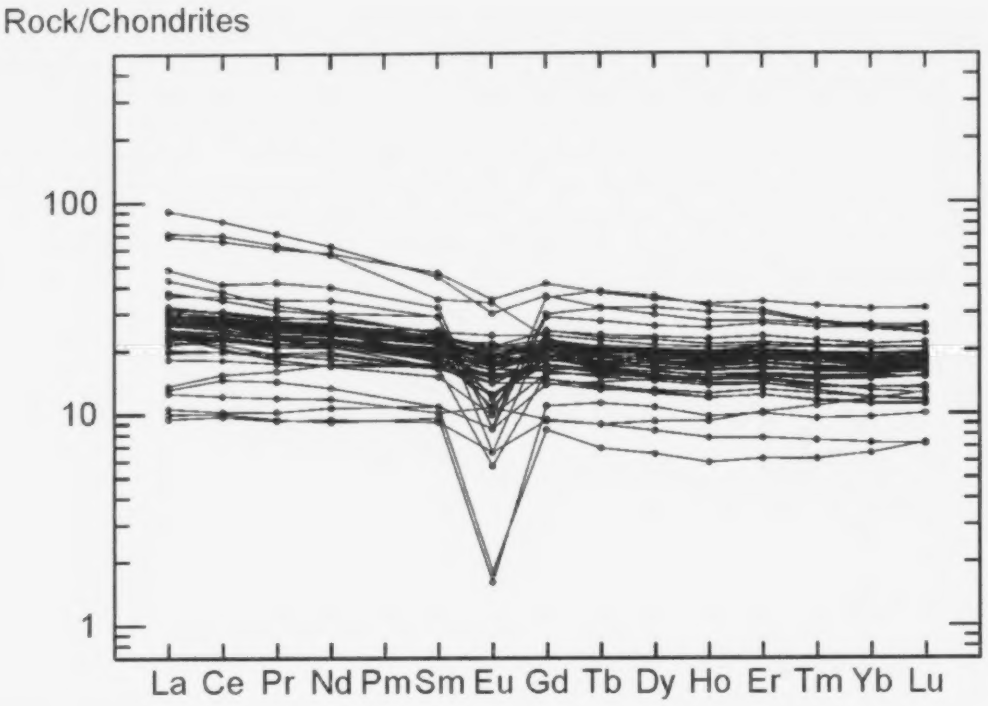

**Figure 36.** Chondrite-normalized spider diagram of the Genex synvolcanic mafic intrusion (*after* Sun and McDonough 1989).

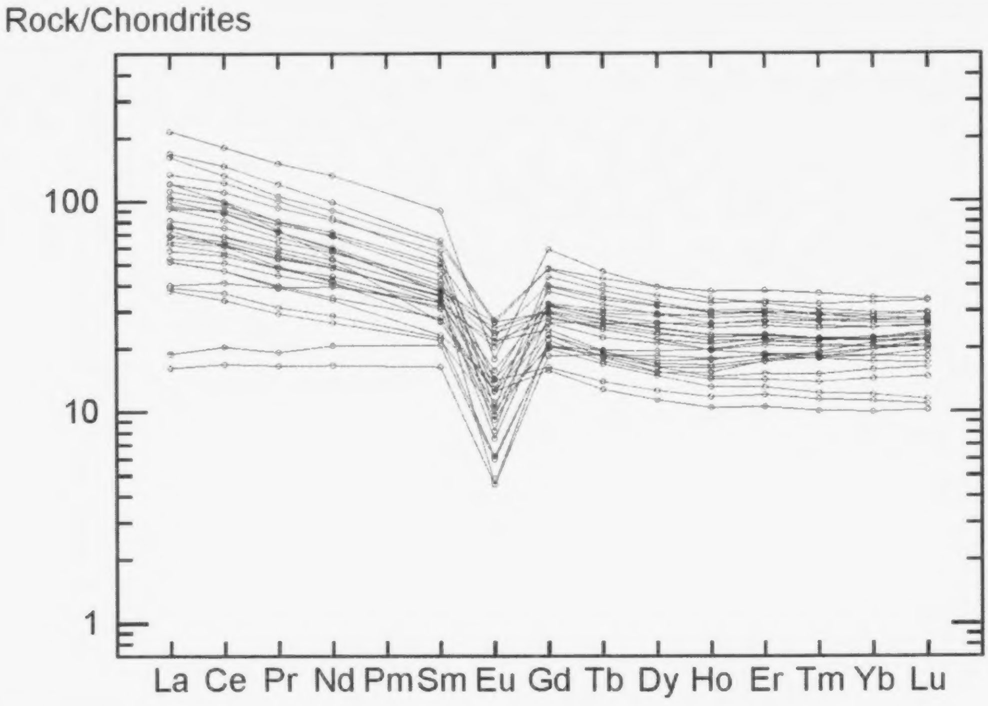

**Figure 37.** Chondrite-normalized spider diagram of the Genex synvolcanic intermediate intrusion (*after* Sun and McDonough 1989).

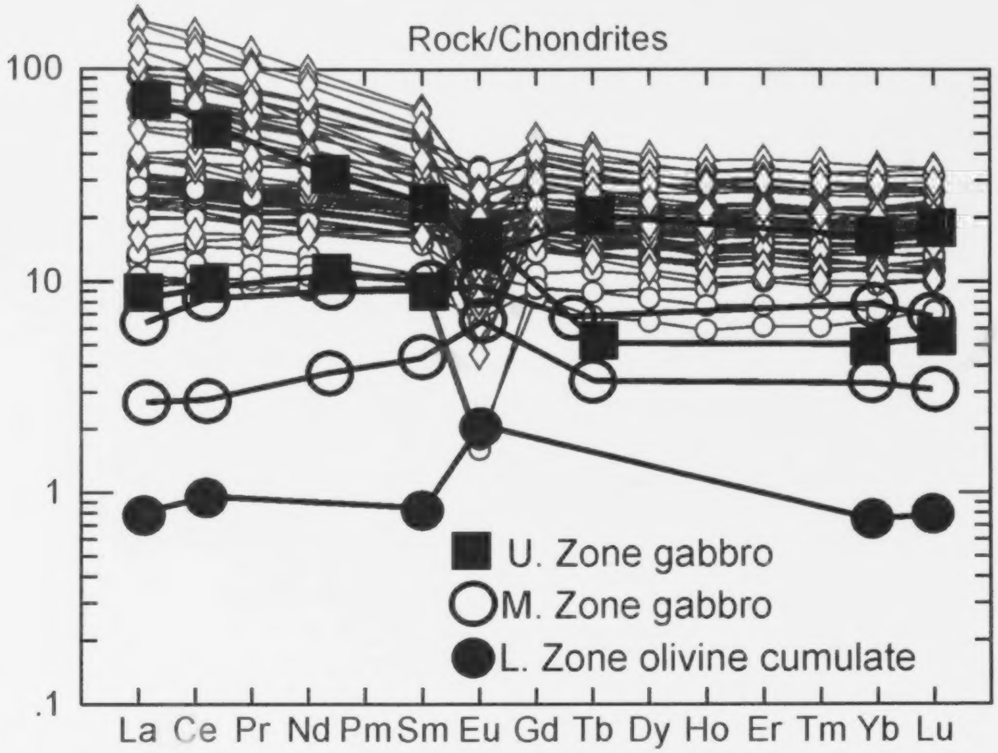

**Figure 38.** Chondrite-normalized spider plot of Genex synvolcanic mafic intrusions (circles) and intermediate intrusion (diamonds) compared to trends in the Kamiskotia gabbroic complex (*after* Barrie et al. 1991; Galley 1996; Sun and McDonough 1989). Genex intrusive rocks are most similar to the upper zone gabbro (U. Zone gabbro) of the Kamiskotia gabbroic complex.

## CONTAMINATION

Crustal contamination of felsic metavolcanic rocks in the Genex area can is postulated based on the Y–Nb–Ce ternary plot developed by Eby (1992) (Figure 39). This plot indicates whether a sample is derived from a crustal-contaminated source or from a mantle derived source. Genex felsic metavolcanic rocks plot almost exclusively in the A-type crustal field, indicating that all samples are from either a crustal-contaminated derivative magma, or from partial melting of the crust.

Crustal contamination in mafic metavolcanic rocks can be identified using the Zr–Ti/100–Y*3 ternary plot developed by Pearce and Cann (1973) and modified by Pearce (1996) (Figures 40, 41 and 42). The MM point is the composition of average N-MORB mantle, whereas the UC point is the composition of average upper crust (Pearce 1996). A sample that plots near the MM point is derived from a mantle melt without crustal contamination, whereas a sample that plots near the UC point is derived from a magma which has undergone upper crust interaction, or is derived from a crustal-derived source. For mantle-derived sources, the relative enrichment of the mantle, and the degree of melting can also be ascertained from the diagram.

The Genex mafic metavolcanic rocks plot near the UC point, indicating that they are derived from either a crustal-contaminated source, or a crustal-derived source (*see* Figure 40). The outliers are more altered samples, that have experienced slight mobility in the elements plotted (*see* "Element Mobility").

Conversely, the synvolcanic mafic intrusion samples plot almost exclusively in field B, near the MM point (*see* Figure 41). This dissimilarity could be due to 2 possible factors: the first factor is that the synvolcanic mafic intrusion is derived from a different magma source than the volcanic rocks in the Genex area. The second factor is that the mafic intrusion is derived from a less evolved phase of the magma than the volcanic rocks. Spider diagrams, discussed in the previous subsection, support this interpretation. REE trends for the intrusion suggest derivation from a primitive, unfractionated source, whereas REE trends in the volcanics suggest derivation from a more evolved, and more crustal contaminated, source.

Lastly, samples from the synvolcanic intermediate intrusion plot almost exclusively on or very near the UC point, suggesting that these samples are also derived from a more evolved source which was either crustal derived or experienced a large degree of crustal contamination (*see* Figure 42).

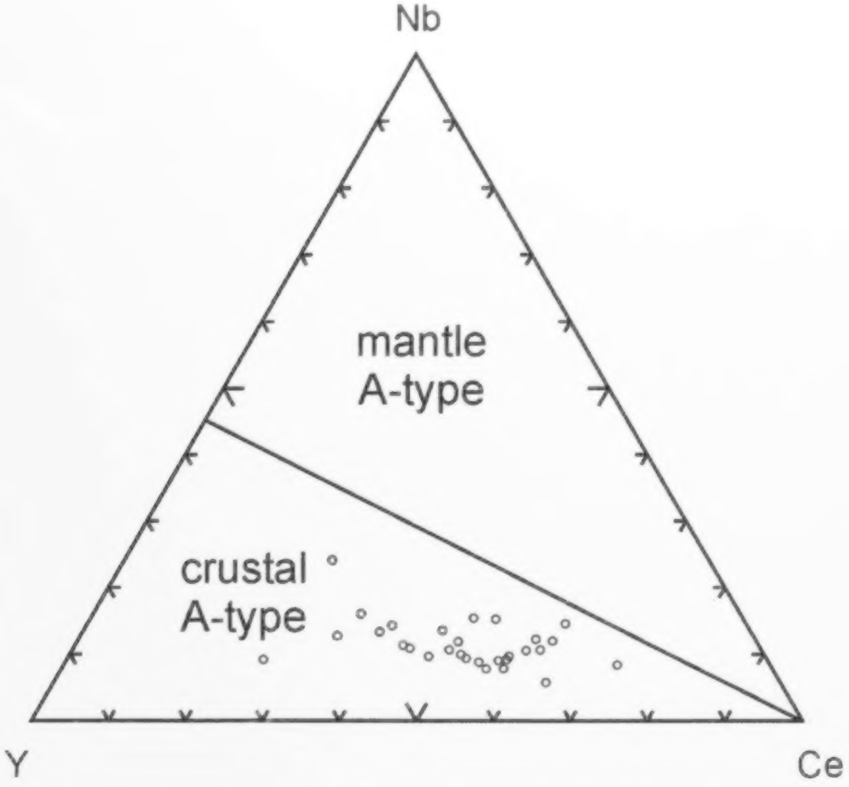

**Figure 39.** Y–Nb–Ce felsic derivative magma composition ternary plot (*from* Eby 1992). Genex rocks fall within the crustal A-type magma field.

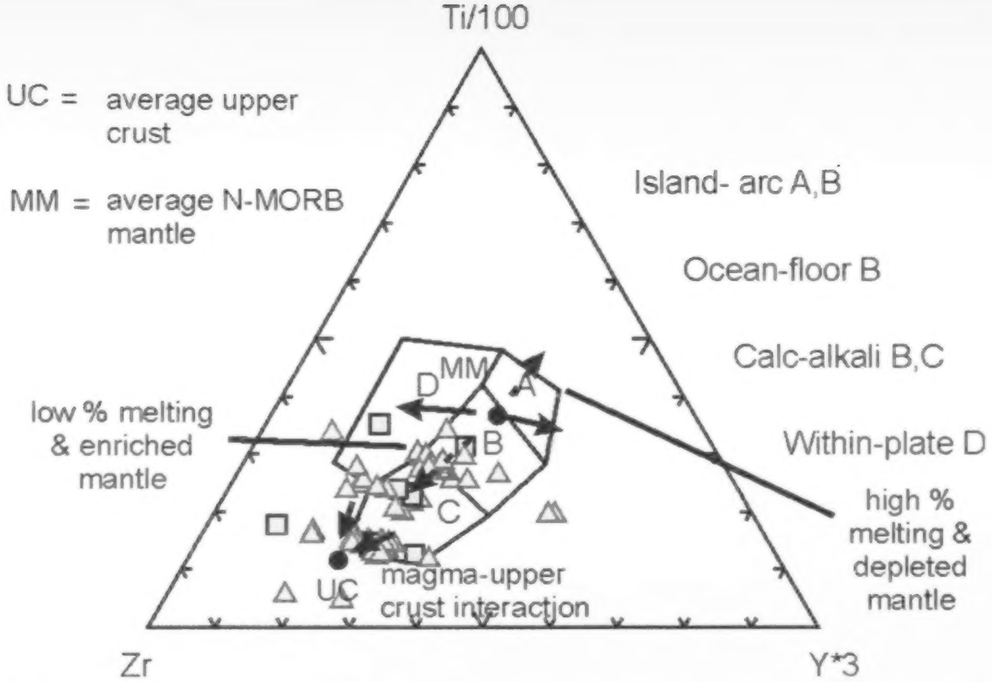

**Figure 40.** Zr–Ti/100–Y*3 magma–upper crust interaction ternary plot (*after* Pearce 1996; Pearce and Cann 1973). The Genex mafic metavolcanic rocks are derived from a crustal-contaminated source.

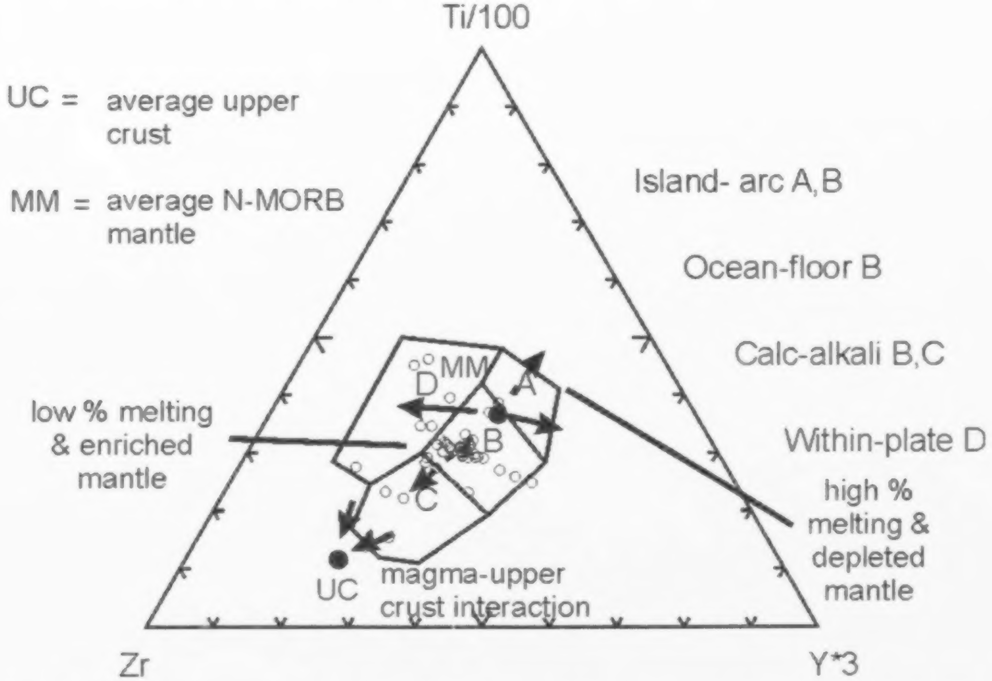

**Figure 41.** Zr–Ti/100–Y*3 magma–upper crust interaction ternary plot (*after* Pearce 1996; Pearce and Cann 1973). The Genex synvolcanic mafic intrusion is derived from a mantle source without crustal contamination.

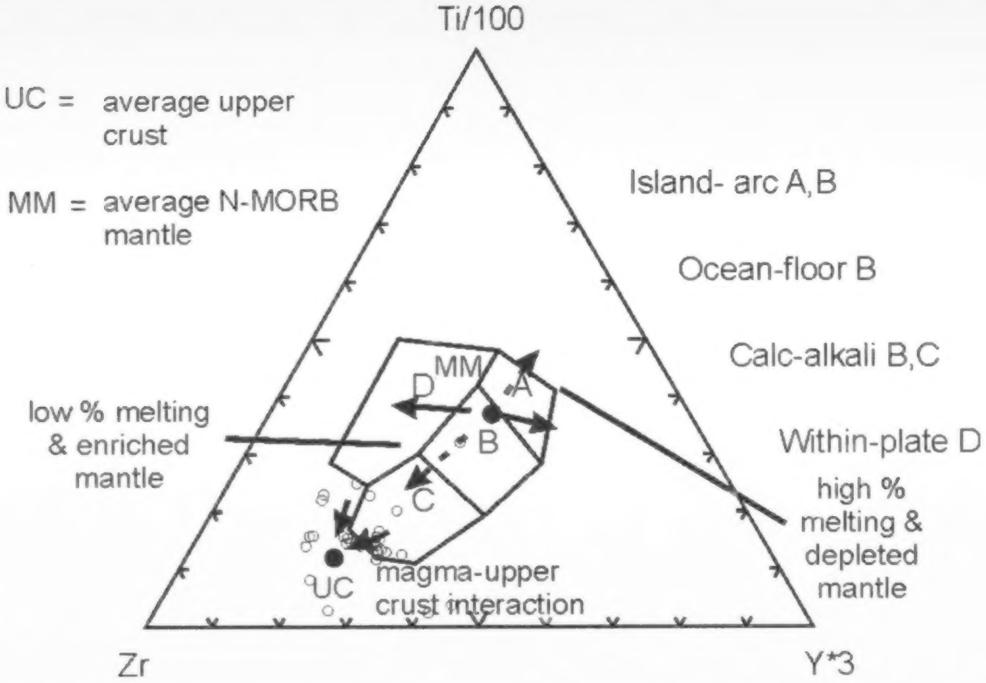

**Figure 42.** Zr–Ti/100–Y*3 magma–upper crust interaction ternary plot (*after* Pearce 1996; Pearce and Cann 1973). The Genex synvolcanic intermediate intrusion is derived from a crustal-contaminated source.

## GEOLOGIC SETTING

Based on trace element plots using Nb, Y, Ta, Rb, and Yb (Figures 43 to 46), the Genex felsic metavolcanic rocks are of arc origin. The slight translation of felsic rocks into within-plate fields (*see* Figures 43 to 46) reflects crustal contamination in the derivative magma, as discussed in the previous subsection, or a crustal source. Trace element plots using Th, Zr, Nb, Hf, Ta, and Y (Figures 47 to 50), indicate that the Genex mafic metavolcanic rocks, the synvolcanic mafic intrusion, and the synvolcanic intermediate intrusion are also of arc origin.

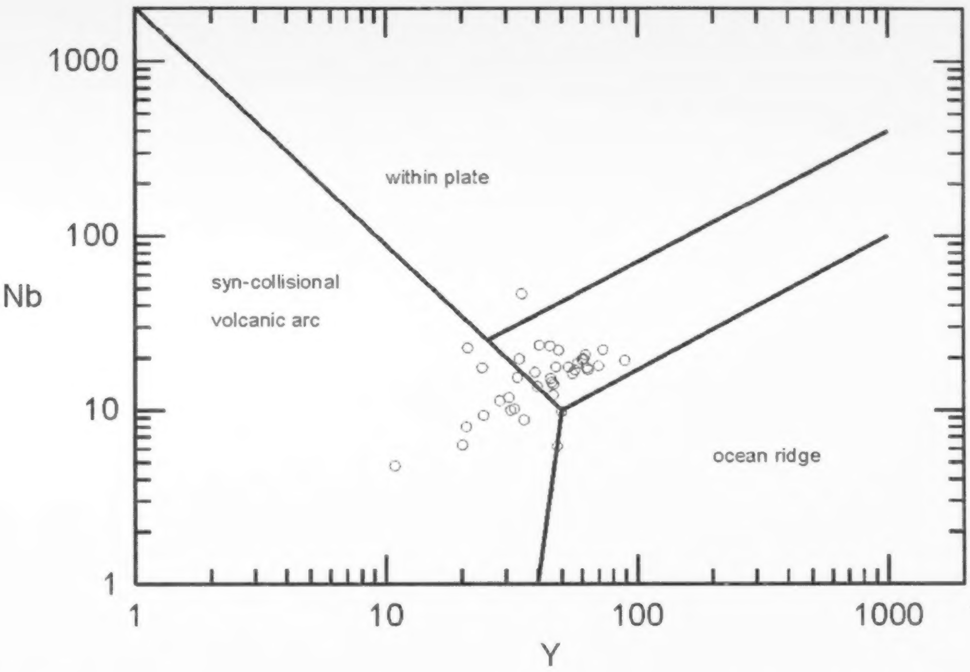

**Figure 43.** Nb versus Y tectonic discrimination diagram for rocks of granitic composition (*after* Pearce, Harris and Tindle 1984). Genex felsic metavolcanic rocks plot within the syncollisional volcanic arc field.

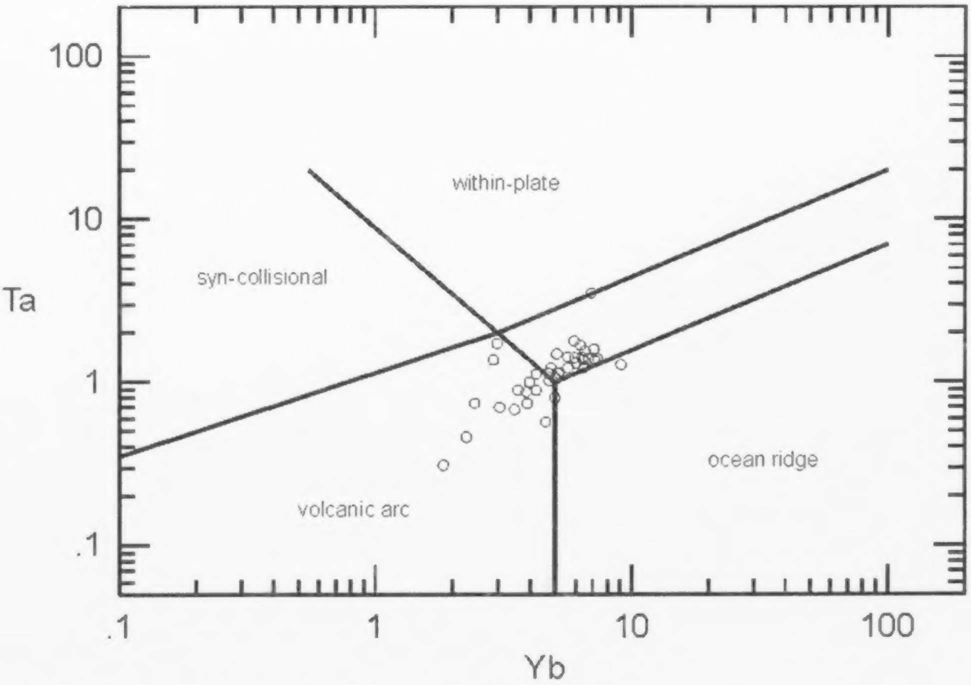

**Figure 44.** Ta versus Yb tectonic discrimination diagram for felsic rocks (*after* Pearce, Harris and Tindle 1984). Genex felsic metavolcanic rocks plot in the volcanic arc field.

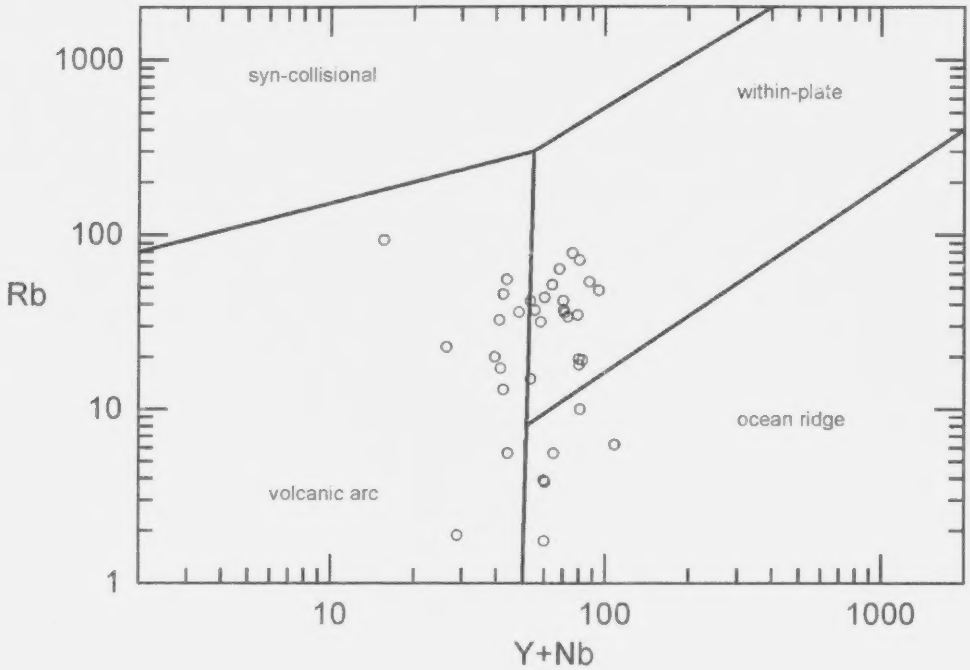

**Figure 45.** Rb versus Y + Nb tectonic discrimination diagram for felsic rocks (*after* Pearce, Harris and Tindle 1984). Genex metavolcanic rocks plot in the volcanic arc and within-plate fields.

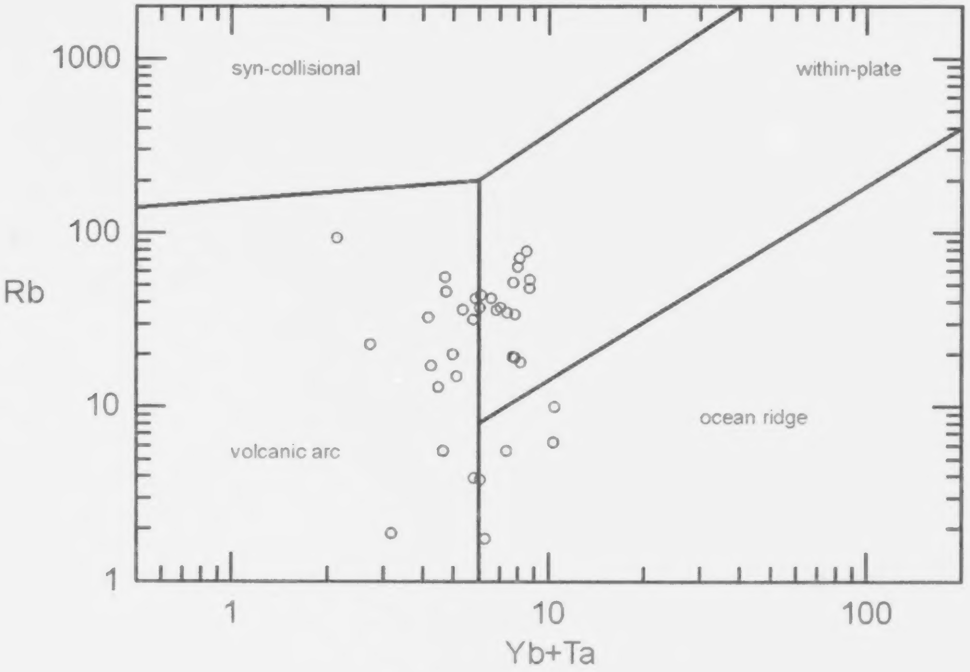

**Figure 46.** Rb versus Yb + Ta tectonic discrimination diagram for felsic rocks (*after* Pearce, Harris and Tindle 1984). Genex felsic metavolcanic rocks plot within the volcanic arc and within-plate fields.

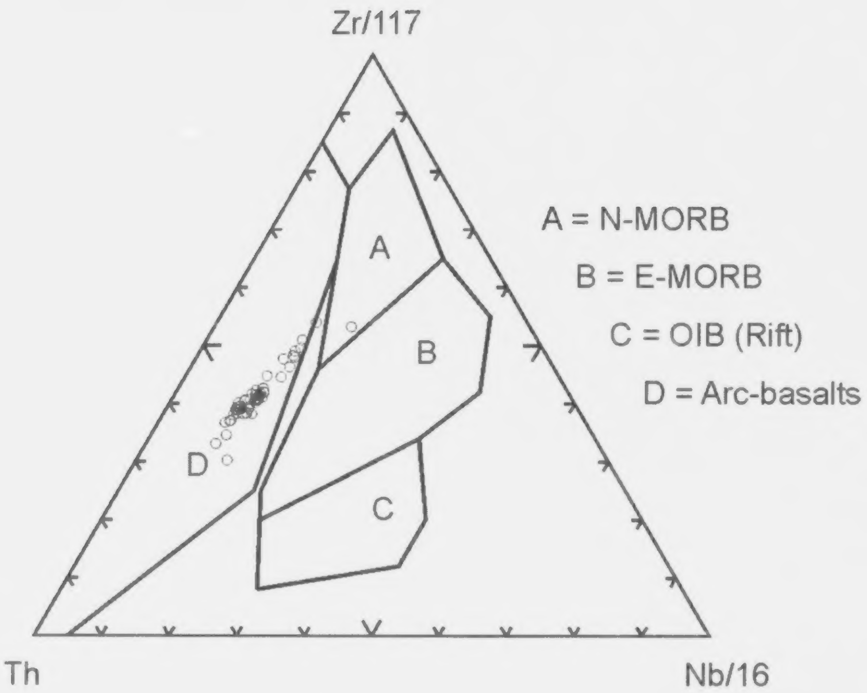

**Figure 47.** Th–Zr/117–Nb/16 discrimination diagram for mafic rocks (*after* Wood 1980). Genex mafic metavolcanic rocks plot within the arc-basalt field.

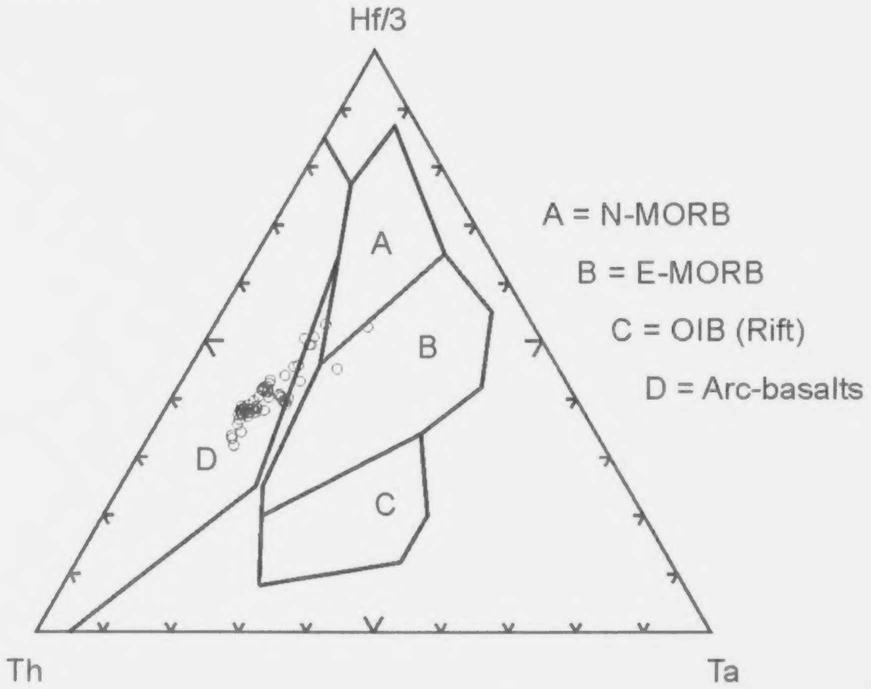

**Figure 48.** Th–Hf/3–Ta discrimination diagram for mafic rocks (*after* Wood 1980). Genex mafic metavolcanic rocks plot within the arc-basalt field.

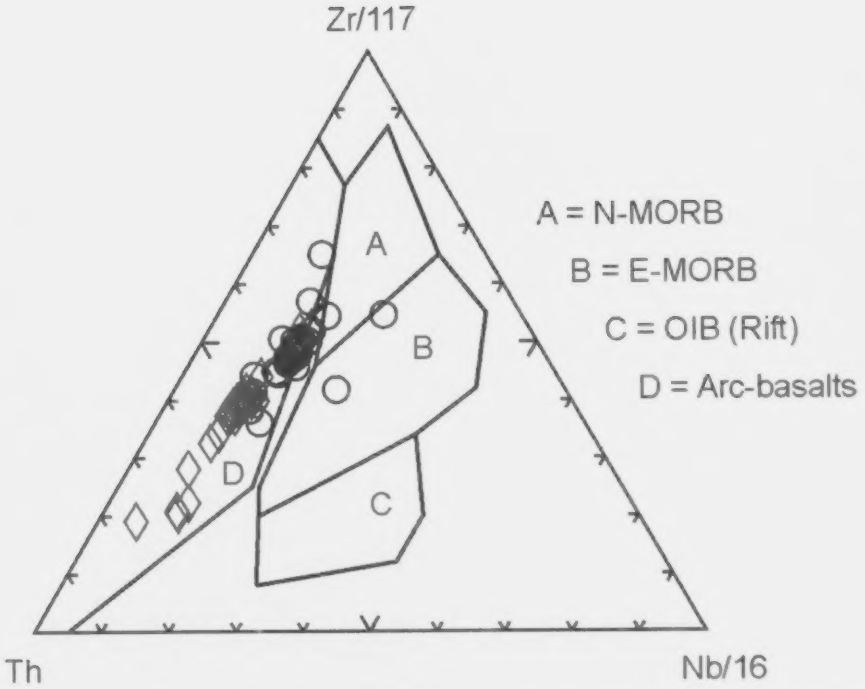

**Figure 49.** Th–Zr/117–Nb/16 discrimination diagram for intrusive rocks (*after* Wood 1980). Genex synvolcanic mafic intrusion (circles) and intermediate intrusion (diamonds) both plot in the arc-basalt field.

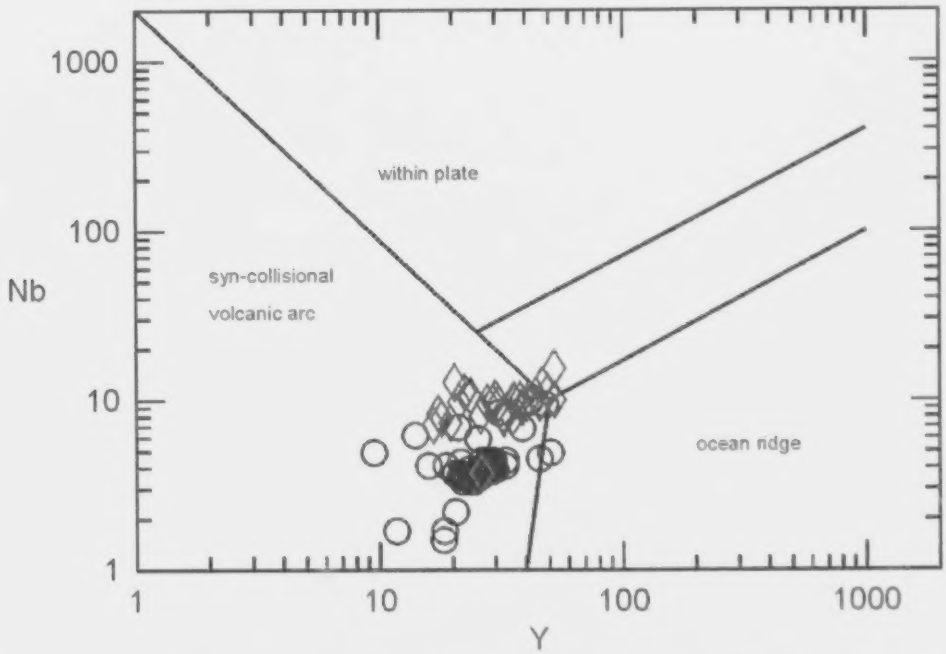

**Figure 50.** Nb versus Y tectonic discrimination diagram for intrusive rocks (*after* Pearce, Harris and Tindle 1984). Genex synvolcanic mafic intrusion (circles) and intermediate intrusion (diamonds) both plot in the syncollisional volcanic arc field.

**Table 6.** Classification of Abitibi belt igneous rocks (*from* Barrie, Ludden and Green 1993; Kerrich and Wyman 1996; Genex data from this study).

| | Group 1 (Kamiskotia) | Group 2 (Noranda) | Group 3 (Selbaie) | Group 4 (Upper Skead) | Group 5 (Timiskaming) | Genex |
|---|---|---|---|---|---|---|
| **Tectonic Environment** | Oceanic rift | Rifted island arc (plots within plate field on Th/Yb vs. Ta/Yb) | Arc | Arc (plot in continental arc-alkalic arc on Th/Yb vs. Ta/Yb) | Arc (plot in continental arc-alkalic arc on Th/Yb vs. Ta/Yb) | |
| **Geochemical Affinity** | Bimodal tholeiitic basalt/basaltic andesite and high silica rhyolite | Bimodal transitional tholeiitic-calc-alkaline andesite and dacite-rhyolite | Calc-alkalic andesite-dacite-rhyolite | Transitional calc-alkalic-alkaline rocks and alkalic (arc) rocks | Timiskaming transitional calc-alkalic-alkaline rocks and alkalic (arc rocks | Bimodal tholeiitic basaltic andesite and high silica rhyolite |
| **VMS Potential** | Economic | Economic | Economic | Barren | Barren | Sub-economic |
| **REE and HFSE Contents** | High, pronounced Eu anomaly | Intermediate HFSE | Low REE and HFSE | Low HFSE Strongly fractionated REE | Low HFSE Strongly fractionated REE | High, pronounced Eu anomaly |
| **$\mathrm{La_{CN}/Yb_{CN}}$ mafic** | <2 | 2.3-3.6 | 3-4 | >8 | >8 | 6.96 (avg) |
| **$\mathrm{La_{CN}/Yb_{CN}}$ felsic** | <3.5 | <3 | 3-9 | >8 | >8 | 8.5 (avg) |
| **$\mathrm{Yb_{CN}}$ mafic** | 16-50 | 15-20 | 10-15 | 2-20 | 2-20 | 11.5 (avg) |
| **$\mathrm{Yb_{CN}}$ felsic** | >40 | 20-45 | 10-20 | 2-25 | 2-25 | 12 (avg) |
| **Th/Yb mafic** | <0.4 | 0.4-0.6 | 0.6-0.8 | >1.5 | >1.5 | 0.55 (avg) |
| **Th/Yb felsic** | <1 | <0.6 | 0.6-2.5 | >1 | >1 | 0.92 (avg) |
| **Zr/Y mafic** | <6 | <5 | <6 | >5 | >5 | 6.63 (avg) |
| **Zr/Y felsic** | <4 | <6 | <10 | >10 | >10 | 6.77 (avg) |
| **Y (ppm) mafic** | >25 | 20-30 | 20-25 | 4-40 | 4-40 | 35.72 (avg) |
| **Y(ppm) felsic** | >70 | 30-60 | 15-35 | 5-40 | 5-40 | 42.75 (avg) |

After completing work in the Abitibi greenstone belt, Barrie, Ludden and Green (1993) created a classification scheme for Abitibi belt igneous rocks, which has been amended by Kerrich and Wyman (1996) (Table 6). According to Table 6, the Genex igneous rocks should fall within the Group 1 classification (typified by the Kamiskotia (Tisdale assemblage) igneous rocks). Group 1 rocks, therefore, should have an oceanic rift affinity. The Genex igneous rocks, however, plot exclusively in the volcanic arc fields on preceding diagrams (*see* Figures 43 to 50). Further analysis of geochemical trends in the Genex igneous rocks (*see* last column in Table 6) reveal that the Genex igneous rocks are most similar to those in Group 2 (typified by the Noranda (Blake River assemblage) igneous rocks). This discrepancy again suggests that the Genex rocks are more similar to rocks of the Blake River assemblage than they are to the Tisdale assemblage.

# Hydrothermal Alteration

## INTRODUCTION

Hydrothermal alteration in VMS systems is the result of seawater, and evolved seawater, to rock interactions (reactions) at various temperatures and water-to-rock ratios in subseafloor hydrothermal systems. The circulation system is driven by a high thermal gradient, commonly in the form of a high-level (2–4 km below seafloor) synvolcanic intrusion (i.e., the Kamiskotia gabbroic complex) (Franklin 1993; Franklin 1996; Galley 1993; Hudak et al. 2003). The hot seawater leaches base metals from the wall rocks, and from the synvolcanic intrusion (Figure 51). The fluid buoyantly rises back toward the seafloor along synvolcanic fault zones and fractures and is expelled from subaqueous hot springs (black and/or white smoker vents). The temperature difference between the hot hydrothermal fluid and the cold seawater causes the fluid to precipitate its dissolved metal load at or just beneath the seafloor, to form a massive sulphide deposit.

Throughout the hydrothermal system, numerous metasomatic reactions take place between the wall rock and the evolving hydrothermal fluid (*see* Figure 51). A zonation of alteration mineral assemblages and mineral chemistry is commonly observed both laterally from upflow zones (synvolcanic structures), and vertically, with changes in fluid temperature (Galley 1993). An understanding of these variations is critical in defining upflow zones, and potential areas of VMS mineralization (Galley 1993).

In areas of greenschist metamorphism, upflow zones are generally characterized by Fe-chlorite, quartz, siderite-ankerite, sericite, and talc alteration mineral assemblages. Semiconformable alteration zones (broad recharge zones where seawater is drawn into the hydrothermal cell) are generally characterized by Mg-chlorite, quartz, epidote, sericite, albite, and ankerite alteration mineral phases. Further discussion can be found in the following subsection.

Evidence of hydrothermal alteration is prevalent throughout the Genex area, and is conformable without a well-defined zonation of alteration mineral assemblages. Alteration types present in felsic metavolcanic rocks include sericitization, chloritization, and silicification. Alteration types present in mafic extrusive rocks, the mafic synvolcanic intrusion and the intermediate synvolcanic intrusion include Fe-carbonate alteration, silicification, chloritization, and epidotization.

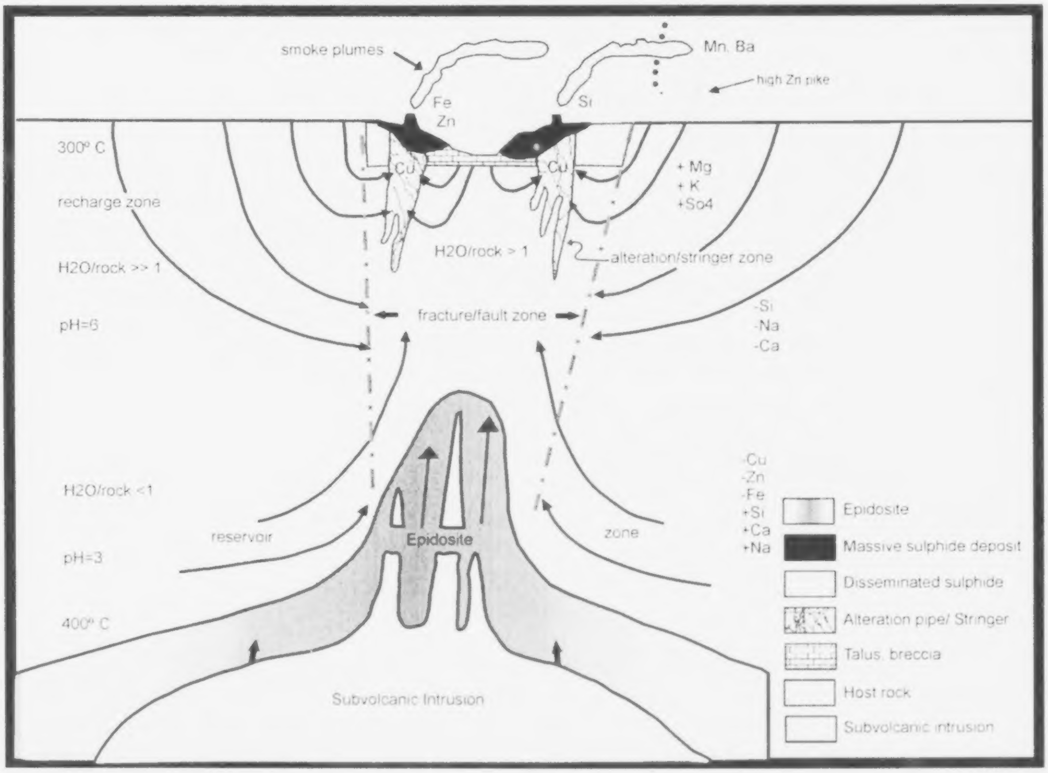

**Figure 51.** Generalized model of a hydrothermal system associated with the genesis of VMS deposits (*modified from* Franklin 1993; Franklin 1996; Hudak et al. 2003).

and/or white smoker vents). The temperature difference between the hot hydrothermal fluid and the cold seawater causes the fluid to precipitate its dissolved metal load at or just beneath the seafloor, to form a massive sulphide deposit.

Throughout the hydrothermal system, numerous metasomatic reactions take place between the wall rock and the evolving hydrothermal fluid (*see* Figure 51). A zonation of alteration mineral assemblages and mineral chemistry is commonly observed both laterally from upflow zones (synvolcanic structures), and vertically, with changes in fluid temperature (Galley 1993). An understanding of these variations is critical in defining upflow zones, and potential areas of VMS mineralization (Galley 1993).

In areas of greenschist metamorphism, upflow zones are generally characterized by Fe-chlorite, quartz, siderite-ankerite, sericite, and talc alteration mineral assemblages. Semiconformable alteration zones (broad recharge zones where seawater is drawn into the hydrothermal cell) are generally characterized by Mg-chlorite, quartz, epidote, sericite, albite, and ankerite alteration mineral phases. Further discussion can be found in the following subsection.

Evidence of hydrothermal alteration is prevalent throughout the Genex area, and is conformable without a well-defined zonation of alteration mineral assemblages. Alteration types present in felsic metavolcanic rocks include sericitization, chloritization, and silicification. Alteration types present in mafic extrusive rocks, the mafic synvolcanic intrusion and the intermediate synvolcanic intrusion include Fe-carbonate alteration, silicification, chloritization, and epidotization.

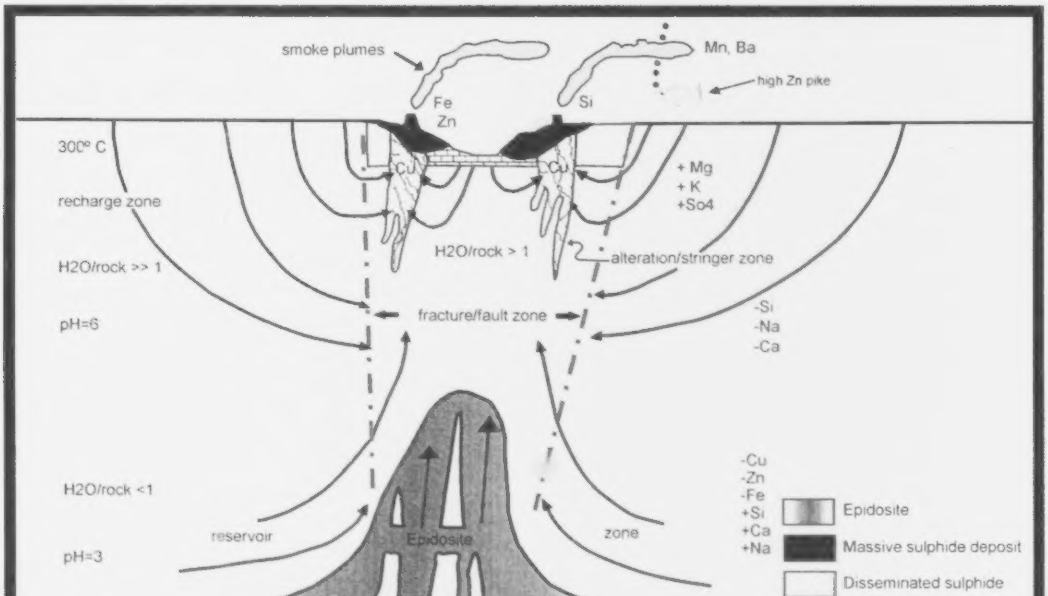

**Figure 51.** Generalized model of a hydrothermal system associated with the genesis of VMS deposits (*modified from* Franklin 1993; Franklin 1996; Hudak et al. 2003).

## SERICITIZATION

All felsic rocks are sericitized, but to varying degrees. In outcrop and in drill core, sericite alteration occurs in the matrix of fragmental rocks, and as alteration of felsic fragments. In thin section, sericite is visible as disseminated grains, and appears to be replacing volcanic ash, and felsic volcanic fragments. The tan-light green colouration of felsic rocks in outcrop both on fresh and weathered surfaces is due to sericite alteration (Photos 30 and 31). Footwall felsic rocks tend to be more sericite altered than hanging-wall felsic rocks, possibly indicating a waning in the intensity of hydrothermal alteration after the mineralizing event. Mafic rocks do not display sericite alteration.

In bimodal-felsic VMS deposits, sericite alteration is common in both pipe and semiconformable alteration assemblages (*see* "Controls on Mineralization"); this is also the case in the Genex area.

**Photo 30.** Sericite alteration if felsic lapilli-tuff giving the rock a tan colouration (03-SMH-0056).

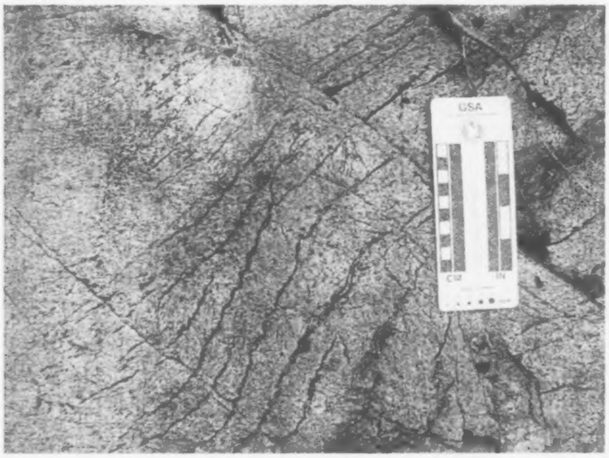

**Photo 31.** Sericite alteration in felsic-tuff (04-SMH-0056).

## CHLORITIZATION

Minor chloritization is present in most felsic rocks (Figure 52), giving the rocks an overall green colour, on a fresh surface. In more chloritized zones, it can be difficult to distinguish between felsic and mafic rocks, except by the presence of quartz phenocrysts in felsic units and amygdules in mafic units.

The intensity of chloritization in the Genex area is shown on the alteration box plots presented in Figures 52 and 53. The alteration box plot, developed by Large et al. (2001), is a graphical approach to portray alteration trends. The box plot uses two alteration indices: the Ishikawa alteration index (alteration index = $100*[(MgO+K_2O)/(MgO+K_2O+CaO+Na_2O)]$) and the chlorite-carbonate-pyrite index (CCP index = $100 * [(MgO+FeO)/(MgO+FeO+K_2O+Na_2O)]$ (Large et al. 2001). Least altered samples plot in the boxes in the centre of the diagram, whereas hydrothermally altered samples plot based on the principal hydrothermal minerals present. A sample that has experienced sericite alteration, for example, will plot toward the bottom right corner of the box plot. Samples that have experienced diagenesis plot toward the bottom left of the diagram (in the diagenetic field). In Figure 52, for example, mafic metavolcanic rocks plot either in the basalt least altered box or in a cluster by the chlorite/pyrite corner. Thus, the principal alteration minerals present in the mafic metavolcanic rocks is chlorite + pyrite, which has been confirmed petrographically.

Chloritization is present in mafic rocks throughout the Genex area where it occurs as disseminated grains of chlorite and as rare amygdule infillings. In altered zones of the mafic metavolcanic rocks, the blue green colour of the rock is due to disseminated chlorite alteration (Photo 32). In pillowed mafic metavolcanic rocks, chlorite alteration is concentrated in the more permeable pillow hyaloclastite (Photo 33). In the mafic and intermediate intrusion, chlorite is present as disseminated grains.

Like sericite alteration, chlorite is common in both pipe and semiconformable alteration styles in bimodal-felsic VMS deposits, with little zonation in chlorite amount throughout the area.

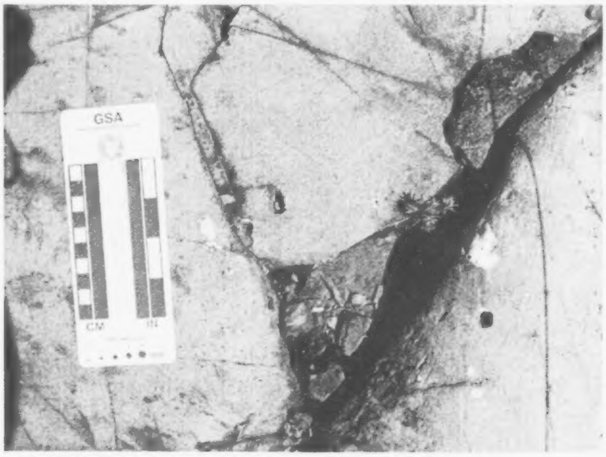

**Photo 32.** Chlorite alteration in pillowed mafic metavolcanic rocks giving the rock a blue green colour (03-SMH-0001).

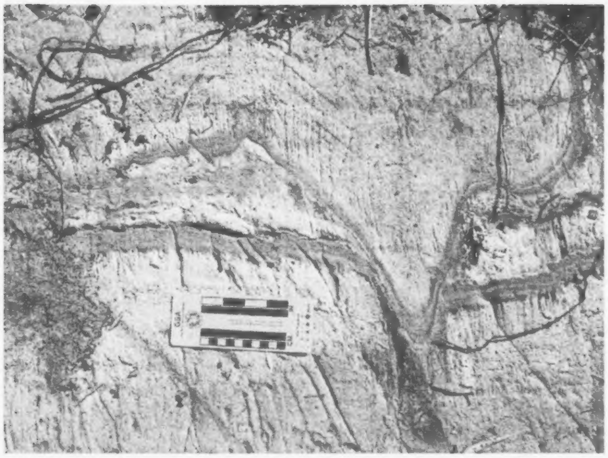

**Photo 33.** Chlorite alteration concentrated in pillow selvages (03-SMH-0167).

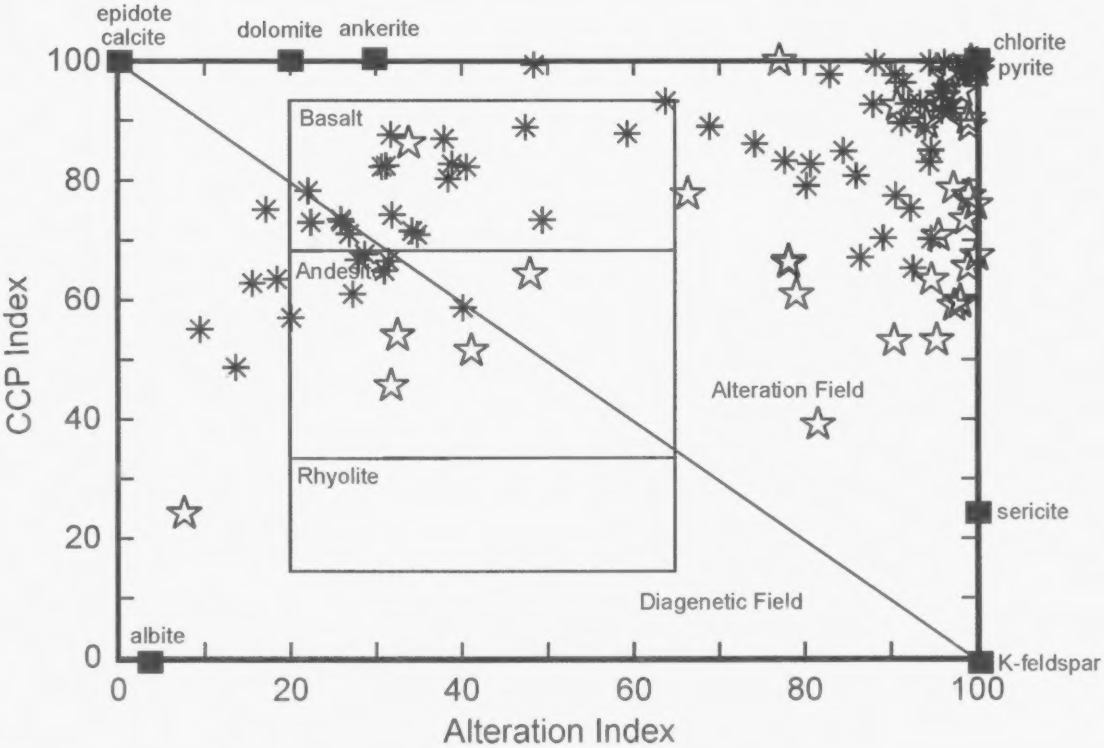

**Figure 52.** Alteration box plot of felsic metavolcanic rocks (stars) and mafic metavolcanic rocks (asterisks) (*after* Large et al. 2001). Mafic rocks trend toward chlorite/pyrite alteration and ankerite alteration. Felsic rocks trend toward chlorite/pyrite alteration and sericite alteration.

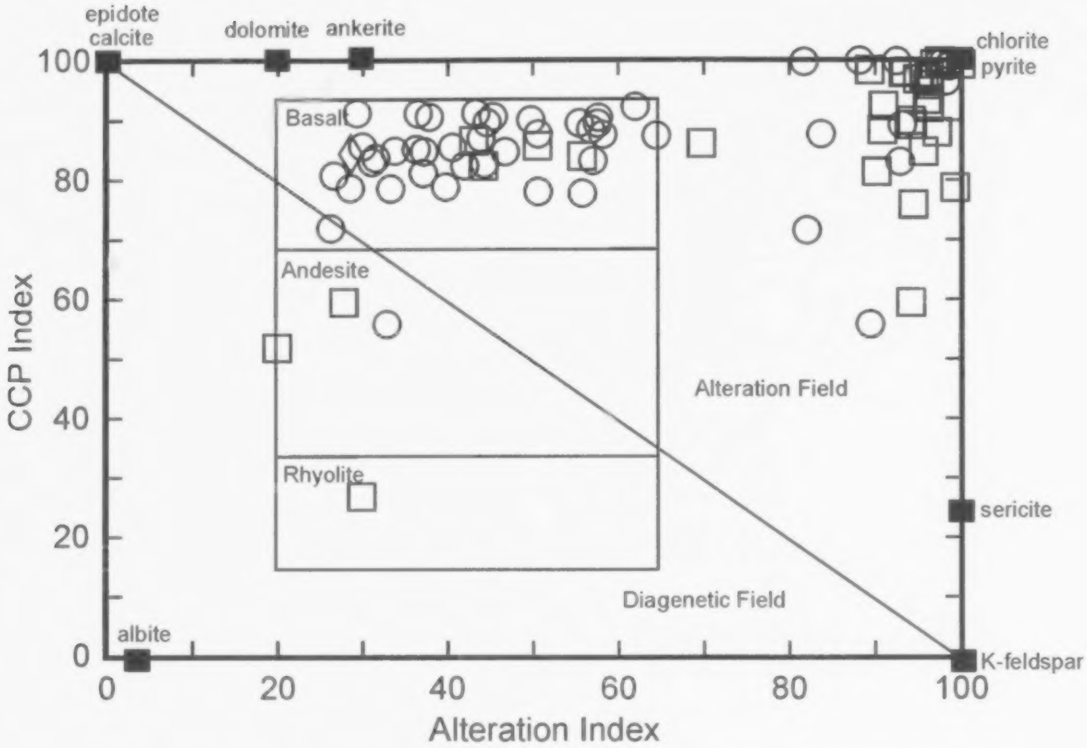

**Figure 53.** Alteration box plot of mafic synvolcanic intrusion (circles), intermediate synvolcanic intrusion (squares) and Matachewan diabase dike (diamond) (*after* Large et al. 2001). Mafic intrusive rocks are less altered, and trend toward ankerite and chlorite/pyrite alteration. Intermediate rocks trend toward chlorite/pyrite and ankerite alteration. Matachewan diabase dike is relatively unaltered.

## EPIDOTIZATION

Epidotization is present in the mafic intrusion, and to a lesser extent, in the mafic metavolcanic rocks. The synvolcanic intermediate intrusion is devoid of epidote alteration. Of all rock types in the Genex area, epidote is most abundant in the mafic synvolcanic intrusion as disseminated grains, most easily seen in thin section (*see* Appendix 1 for a selection of petrographic descriptions). In outcrop and in drill core, the mafic intrusion has a green to bluish green colour on a fresh surface due to the presence of disseminated epidote. Overall, epidote is rare in mafic metavolcanic rocks except for a metre-scale zone immediately underlying the C-zone mineralization, in pillowed mafic metavolcanic rocks. In this locality, abundant epidote is closely associated with quartz and magnetite, in the hyaloclastite and margins of the pillows. Minor epidote-filled amygdules are also present (Photo 34).

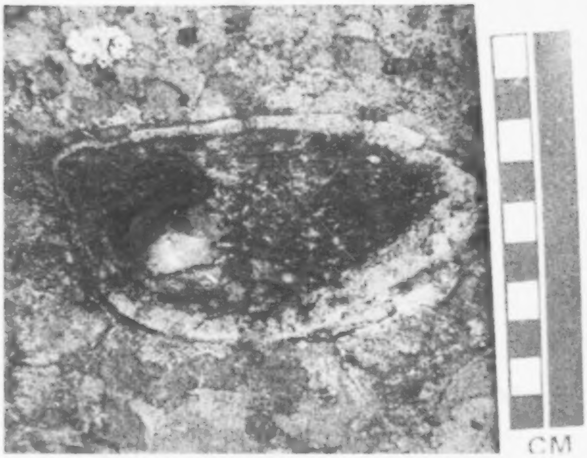

**Photo 34.** Epidote-filled amygdule in pillowed mafic metavolcanic rock (03-SMH-0001).

## SILICIFICATION

Silicification is the process by which quartz replaces the primary mineralogy of the rock. Quartz dumping, on the other hand, is infilling of void space, and is characterized by amygdule and fracture infillings (Gibson, Watkinson and Comba 1983).

Overall, felsic rocks in the Genex area are highly silicified. Silicification is manifested as replacement of the matrices in volcaniclastic rocks, replacement of ash-rich rocks, and felsic fragments. Silicification is not as prominent in the mafic metavolcanic rocks in the Genex area. Mafic rocks are instead marked by quartz dumping in the form of amygdule infillings (Photo 35) and as minor quartz veins (Photo 36). Concentric cooling cracks within pillows are preferentially quartz filled, which causes the cracks to weather positive in relief, making them easily distinguishable in outcrop. In the mafic and intermediate intrusion, quartz-dumping is manifested as amygdule infillings (Photo 37) and as “lacy” silicification, infilling fractures in the rock (Photo 38).

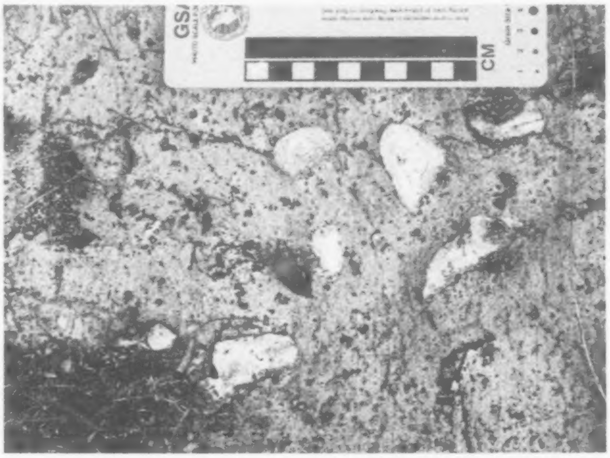

**Photo 35.** Quartz-filled amygdules in pillowed metavolcanic rock (outcrop 03-SMH-0073).

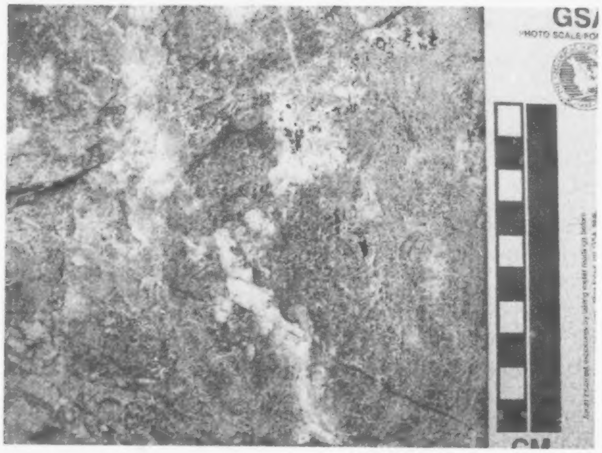

**Photo 36.** Quartz veins and epidote alteration in pillowed mafic metavolcanic rock (outcrop 03-SMH-0075).

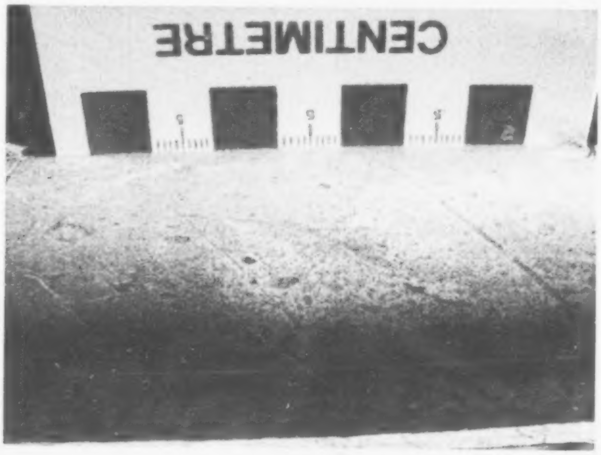

**Photo 37.** Quartz-filled amygdules in intermediate intrusion from Falconbridge drill hole G22-15 (04-SMH-0003).

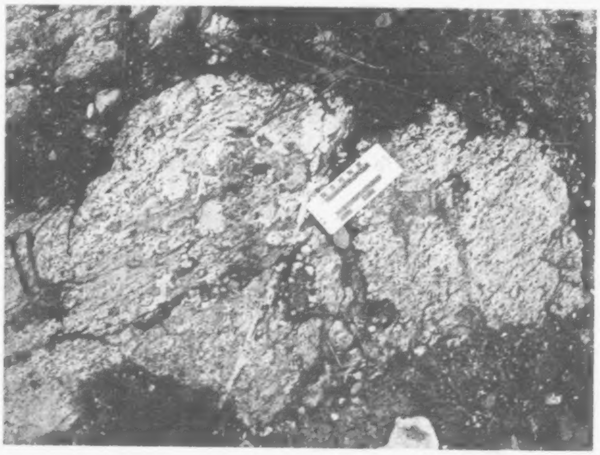

**Photo 38.** "Lacy" silicification in intermediate intrusion (03-SMH-0036).

# FE-CARBONATE ALTERATION

Fe-carbonate alteration is present throughout the footwall and hanging-wall mafic rocks, and represents the youngest alteration type, as it overprints all other alteration assemblages. Felsic rocks are relatively devoid of Fe-carbonate alteration due to the primary iron-poor mineralogy of the felsic rocks, relative to the mafic rocks. The Fe-carbonate is visible in outcrop, drill core and in thin section as weathered rusty cubes and rhombs ranging in size from <1 to 3 mm and comprising <1 to 55% of the rock (Photos 39 and 40) and also as Fe-carbonate veins (Photo 41). In drill core, massive zones of Fe-carbonate (up to 90%) are also present (Photo 42). The intermediate intrusion has a much greater degree of Fe-carbonate alteration than the surrounding units. As is the case in the Genex area, bimodal-felsic VMS deposits (*see* "Controls on Mineralization") are commonly characterized by broad, semi-conformable zones of carbonate alteration, with carbonate zonation controlled by the composition of the rock hosting the alteration (Galley 1993).

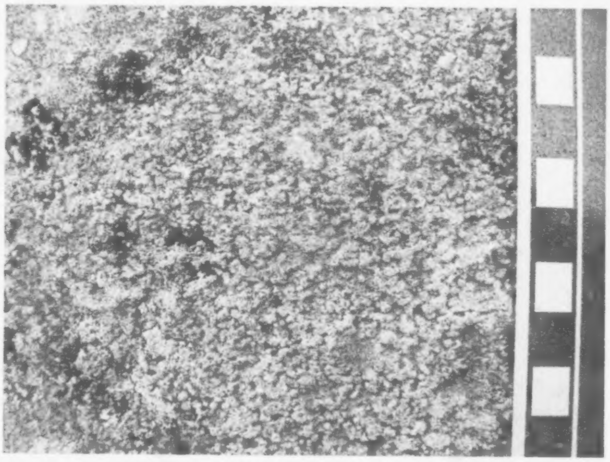

**Photo 39.** Outcrop appearance of Fe-carbonate alteration in massive mafic unit (03-SMH-0127).

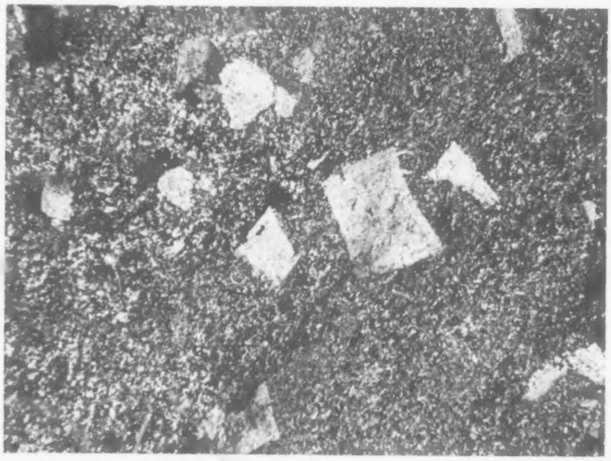

**Photo 40.** Photomicrograph of Fe-carbonate rhombs (03-SMH-0073: field of view is approximately 22 mm).

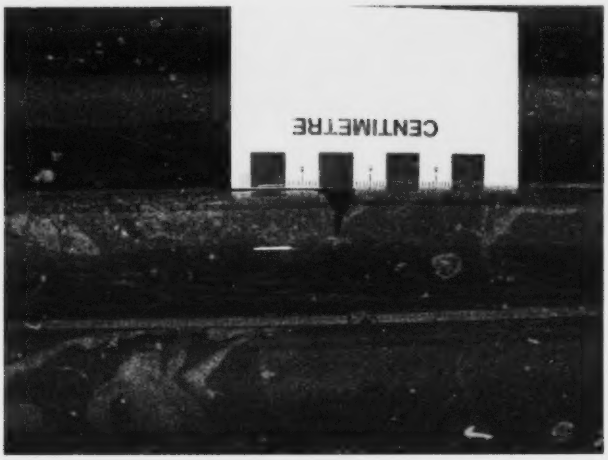
**Photo 41.** Fe-carbonate veins in mafic unit from Falconbridge drill hole G22-14 (04-SMH-0002).

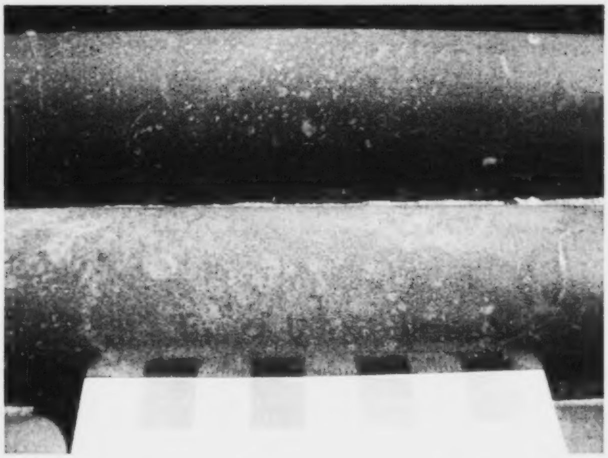
**Photo 42.** Massive Fe-carbonate alteration in mafic intrusion from Falconbridge drill hole G22-15 (04-SMH-0003).

## ALTERATION CHEMISTRY

Major element chemical variations (*see* Appendix 3 for geochemical data) are useful in the recognition of hydrothermal upflow zones (zones in which evolved fluids have risen buoyantly toward the seafloor, *see* Figure 51) and potential VMS mineralization (Franklin 1993, 1996; Galley 1993). In some VMS deposits, hydrothermal upflow zones can be poorly defined and difficult to distinguish (Franklin 1993, 1996; Morton and Franklin 1987). However, these zones are proximal to synvolcanic structures, and are enriched in Mg, Fe, K, Zn, and Cu and depleted in Si, Na, Ca relative to the surrounding rocks (which represent zones of downwelling) (Franklin 1993, 1996; Larson 1984). Vertical variations in alteration mineral chemistry can also be recognized and are manifested as decreases in Mg/Ca, Mg/Na, and Na/Ca ratios (Galley 1993). These vertical variations are related to temperature gradients in the hydrothermal cell.

Based on a major element plot using $Na_2O$ and $K_2O$ (Figure 54), element mobility (i.e., alteration) in the Genex felsic metavolcanic rocks is due to hydrothermal alteration reactions, and not to diagenesis. Further spatial analysis of Genex geochemical data, reveals the presence of lateral variations in major element geochemistry with increasing distance from the fault zones, in the footwall of the deposit.

The relative abundances of MgO, $K_2O$, and to a lesser extent, FeO, increase in proximity to the faults in the Genex area. $Na_2O$, CaO and, to a lesser extent, $SiO_2$, decrease in proximity to the aforementioned faults (geochemical data and outcrop UTM locations are in Appendixes 3 and 5, respectively). Although none of the trends are pronounced, they are best developed within the mafic metavolcanic rocks in the hanging wall of the deposit. These lateral variations are interpreted to indicate that the faults (synvolcanic structures) in the Genex area served as conduits for the upwelling hydrothermal fluids. Lateral variations in major element geochemistry are expected in a hydrothermally altered area (Larson 1984).

Vertical variations are also expected in the footwall of a hydrothermal cell. In the Genex area, vertical variations in major element geochemistry are most visible in the mafic metavolcanic rocks (i.e., footwall versus hanging-wall trends). The strongest trends are in MgO and $SiO_2$ (Figure 55), but weak trends are also visible in CaO, $K_2O$, and MnO. CaO and MnO increase in the hanging wall, whereas MgO, $SiO_2$ and $K_2O$ decrease in the hanging wall, relative to the footwall. The overall weak geochemical trends are due to the relatively small size of the study area (these changes are observed over several kilometres vertical distance: Galley 1993). However, it is impossible to tell if these variations are due to chemical variations within the hydrothermal cell, or if they are due to primary chemical differences between the footwall and hanging-wall rocks.

Overall, MgO trends are most prominent in the Genex area, and are manifested as both lateral and vertical variations.

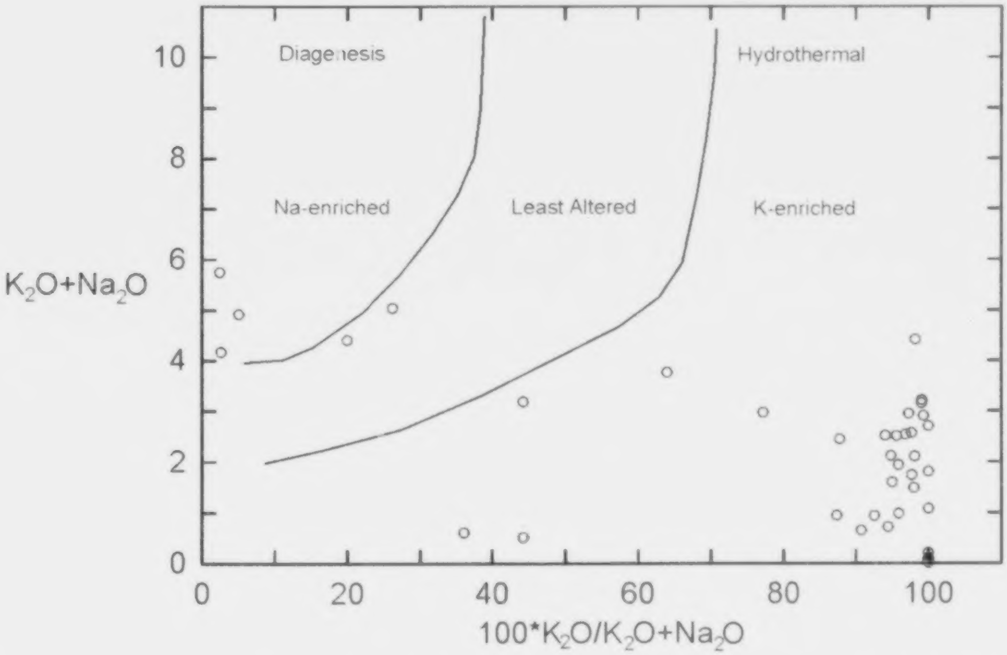

**Figure 54.** $K_2O + Na_2O$ versus $(100^* K_2O)/(K_2O + Na_2O)$ Harker diagram showing alteration of felsic metavolcanic rocks in the Genex area (from Bromley-Challenor 1988; Galley 1993).

In the Genex area, the product of hydrothermal alteration—the resultant VMS mineralization—has already been recognized, as has the presence of numerous synvolcanic structures (*see* "Deformation") along which the hydrothermal fluids rose to the seafloor. Major element geochemical trends have supported these interpretations, although the lack of significant mineralization in the Genex area, and the overall weak geochemical trends are most likely due to one of two factors: a) the hydrothermal system was short lived (Cathles, Erendi and Barrie 1997) or b) the study area is located in the distal part of a large hydrothermal system (currently unidentified) (Franklin 1996).

# Controls on Mineralization

## INTRODUCTION

The Genex deposit is a copper-zinc massive sulphide deposit that consists of 3 lenses of mineralization (the C-zone, H-zone, and A-zone) that were mined from 1964 to 1966. Over this time, approximately 242 tonnes (218 tons) of copper concentrate containing 21 to 27% Cu were produced; zinc was not recovered (*The Northern Miner*, September 1, 1966, p.13; Middleton 1975; Binney and Barrie 1991). At the time the mine closed, the ore reserves were estimated at 42 000 tons (38 000 t) grading 2.5% Cu (*The Northern Miner*, November 10, 1966, p.13, 20). Mineralization is contained within the matrix of a thin (approximately 0.5 to 3 m wide on surface) pillow breccia (C-zone) and a lapilli-tuff (H- and A-zones) units that are in contact with a portion of the north-trending fine-grained upper synvolcanic mafic intrusion (*see* Figure 56, back pocket). Numerous zones of shear-hosted mineralization are also present throughout the area in both mafic and felsic lithologies and they tend to contain a higher zinc content. Further discussion of the mineralization present in the Genex area can be found in Legault (1985) and Middleton (1975).

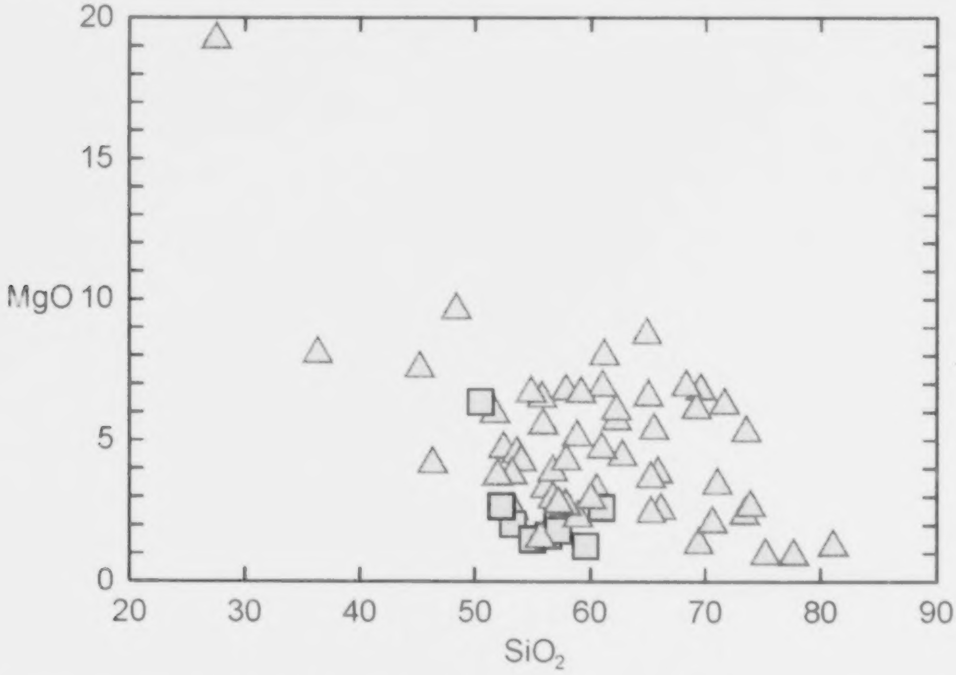

**Figure 55.** MgO versus $SiO_2$ plot of footwall (triangles) and hanging-wall (squares) mafic metavolcanic rocks in the Genex area.

## CONTROLS ON C-ZONE MINERALIZATION

C-zone mineralization is contained within the matrix of a north-trending pillow breccia unit (Photo 43) from which Genex Mines Ltd. extracted 47 000 tons of ore at 2.92% Cu (zinc was not recovered). All of the mill feed while the mine was in production came from the C-zone (*The Northern Miner*, September 1, 1966, p.13; Legault 1985). The C-zone is distinct from the A- and H-zones in that it is hosted in a mafic pillow breccia and is north trending. According to mine plans compiled by Legault (1985), the mineralized zone has a strike length of approximately 60 m, extends approximately 80 m vertically, and is less than 8 m wide. Stringer mineralization is present only to the west of the C-zone (stratigraphically below) where it extends approximately 30 m from the C-zone proper. The stringers are localized within pillow selvages and amygdules (Photo 44). To the east (stratigraphically above), the mineralization is cut by the upper synvolcanic mafic intrusion, and does not occur above the intrusion. The mineralization is dominantly pyrite-chalcopyrite.

The C-zone mineralization is contained entirely within a zone of higher permeability (matrix of pillow breccia, pillow hyaloclastite) with no true massive sulphide present. This mode of mineralization is suggestive of subseafloor deposition where sulphides are deposited within zones of higher permeability (Doyle and Allen 2003; Lydon 1988; Stix et al. 2003). One possible explanation as to the higher grade and tonnage of sulphide mineralization in the C-zone (mafic hosted) compared to the H- and A-zones (felsic hosted), is the greater percentage of ferromagnesian minerals and magmatic sulphides (preferentially enriched in copper), which are then available for leaching to the hydrothermal fluids (Barrie and Hannington 1999). The presence of disseminated and minor fracture-controlled sulphides in the lower mafic intrusion (footwall) indicates that the sulphide-bearing fluids were present after the intrusion was emplaced. The upper fine-grained synvolcanic mafic intrusions (hanging wall) are barren of mineralization, suggesting that the intrusions were emplaced post mineralization.

**Photo 43.** Mineralized pillow breccia in the C-zone (outcrop 03-SMH-0003).

**Photo 44.** C-zone stringer sulphide mineralization contained within a pillow selvage (outcrop 03-SMH-0001).

## CONTROLS ON H-ZONE AND A-ZONE MINERALIZATION

The A-zone and H-zone mineralization is contained within the matrix of a felsic lapilli-tuff breccia, and, to a lesser extent, the surrounding synvolcanic intermediate intrusion. The lens-shaped mineralization zones trend approximately east-west, perpendicular to stratigraphy.

Although there is very little surface exposure of the H-zone, mine plans indicate that the mineralized zone plunges steeply to the southwest (Middleton 1975) and is approximately 120 m in strike length (Legault 1985). According to Middleton (1975), the mineralization in the H-zone occurs both within the felsic-tuff (Photo 45) and at the contact of the tuff with the surrounding intermediate intrusion. Occasionally, the mineralization is known to occur in the intrusion, but without exception, occurs no more than 100 feet (30 m) from the contact. The mineralization is dominantly pyrite-chalcopyrite.

The A-zone is a small east-trending zone of massive to stringer pyrite, chalcopyrite, and sphalerite located directly adjacent to the H-zone, but hosted dominantly in the intermediate intrusion (Photo 46), with some mineralization occurring in the felsic lapilli-tuff (Legault 1985; Middleton 1975). On the 38 m level, the zone has been traced for approximately 75 m (Legault 1985). The zone has no surface exposure due to the debris and rock of the mine workings. Although sphalerite-rich, the A-zone was largely ignored during mining operations due to the fact that the ore was milled exclusively through a copper-circuit and the mine was not interested in zinc ore (Legault 1985).

Diamond drilling prior to production at the mine concluded that, although the zones do contain a higher grade section, the mineralization is too erratic to produce a significant tonnage of ore (Middleton 1975). Both of the sulphide lenses are disconformable and east trending, approximately parallel to faults in the area, indicating that, like the C-zone mineralization, the mineralization is the result of subseafloor replacement of sulphides in zones of higher permeability (Doyle and Allen 2003; Lydon 1988; Stix et al. 2003). However, in this case, the sulphides appear to have also been deposited along fault zones, which likely represent conduits for not only the intermediate intrusion but also for the hydrothermal fluids (Eddy et al. 1998; Stix et al. 2003).

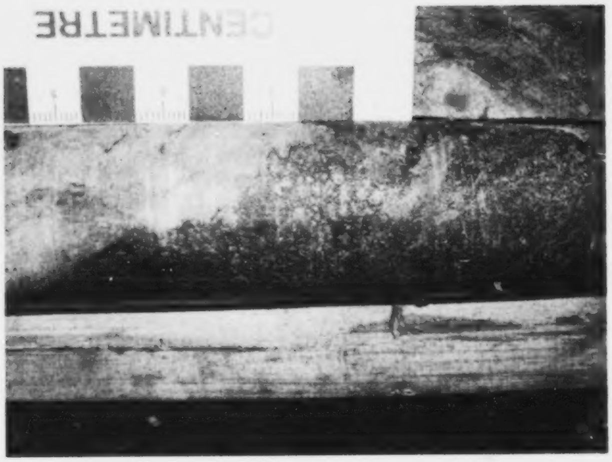

**Photo 45.** H-zone sulphide mineralization in felsic lapilli-tuff from Explorers Alliance drill hole EGG32-36 (04-SMH-0006).

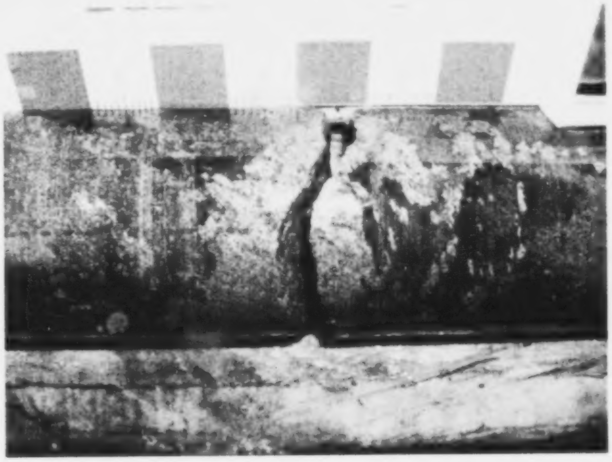

**Photo 46.** A-zone sulphide mineralization in intermediate synvolcanic intrusions from Explorers Alliance drill hole EGG32-35 (04-SMH-0007).

## SHEAR ZONE MINERALIZATION

Pyrite-chalcopyrite-sphalerite mineralization is contained within numerous east-trending shears present throughout the area in both mafic and felsic rock types. The greater abundance of black sphalerite in some shear zones, relative to the pyrite chalcopyrite rich C-, A-, and H-zones, may indicate a lower temperature hydrothermal fluid (Lydon 1988). Perhaps the best example of zinc-rich shear zone-hosted mineralization lies near the southern shore of Aconda Lake, approximately 400 m north of the former mine workings at the "Claim Post zone" (Photos 47 and 48). Hosted in sheared mafic pillows, this zone was the focus of exploration work by Explorers Alliance in 2001. The company completed 4 diamond drill holes in the area that returned assays up to 12 770 ppm (1.28%) Cu, 59 824 ppm (5.98%) Zn, 2375 ppm Pb, 10.9 g/t Ag and 1090 ppb (1.09 g/t) Au (L. Bonhomme, Explorers Alliance, personal communication, July 9, 2003). Although Explorers Alliance hoped to find significant high-grade zinc mineralization in this area, no economically viable zones have yet been discovered.

# INTRUSIONS AND MINERALIZATION

The Genex mineralization is dominantly contained in the porous matrices of pillow breccias, and felsic lapilli-tuffs. Minor stringer and fracture controlled mineralization is present in pillow basalts, the lower fine-grained synvolcanic mafic intrusion, and in the synvolcanic intermediate intrusion. The presence of mineralization in the lower fine-grained synvolcanic mafic intrusion as well as in the synvolcanic intermediate intrusion suggests that the two intrusions were emplaced before the mineralizing event took place. However, the medium-grained mafic intrusion and the upper fine-grained mafic intrusions are entirely void of mineralization which suggests that they may have been emplaced post-mineralization.

The heat from the synvolcanic intrusions was not great enough to drive the hydrothermal system responsible for the formation of the Genex deposit and associated alteration, but the intrusions may indicate the present of a high-temperature thermal corridor (Cathles, Erendi and Barrie 1997; Galley 2003). Mapping of the spatial extent of the intrusions has been important in defining synvolcanic structures which served as conduits for the mineralizing hydrothermal fluids and for the intrusions themselves.

**Photo 47.** Shear-hosted mineralization in claim post zone (outcrop 03-SMH-0082).

**Photo 48.** Black sphalerite mineralization in "Claim Post zone" from Explorers Alliance drill hole EGG32-32A (04-SMH-0013).

# DISCUSSION OF THE GENEX MINERALIZATION

Sulphide emplacement can be broadly divided into two major processes: mobilization or replacement, and remobilization. Subseafloor replacement (a type of mobilization) is defined as "translocation resulting in increased concentration of the metallic constituents originally dispersed or disseminated in 'ordinary rocks' " whereas remobilization is defined as "translocation resulting in modified concentration and distribution of pre-existing massive and semimassive mineralization" (Marshall and Gilligan 1993). The Genex mineralization is the result of subseafloor replacement in zones of higher permeability and is not the daughter product of remobilization of a source deposit due to tectonism (Marshall and Spry 2000; Marshall, Vokes and Larocque 2000). Evidence against syntectonic or posttectonic remobilization includes 1) the occurrence of a stringer zone stratigraphically below the C-zone mineralization, 2) the occurrence of sulphides in areas of high primary permeability, such as pillow hyaloclastite and the matrices of pillow breccias and lapilli-tuffs, and 3) the stratiform nature of the major zone of mineralization (the C-zone). If the C-zone mineralization had in fact resulted from syntectonic or posttectonic remobilization, the mineralization zone would be concentrated along faults and/or shear zones oblique to stratigraphy, the stringer zone would be absent, and the primary textures and structures in the host rocks would have been destroyed (Marshall and Spry 2000). The A- and H-zones are oblique to stratigraphy and do follow a fault; however, original textures in the host lapilli-tuff are preserved.

The Genex Cu-Zn mineralization can be characterized as a bimodal-felsic type according to the VMS classification scheme developed by Barrie and Hannington (1999) (Table 7). The abundance of felsic rocks in the footwall of the deposit (*see* "Stratigraphy in the Genex Area"), the tectonic setting, and the felsic and mafic host rock compositions (*see* "Geochemistry") are all indicative of a bimodal-felsic deposit.

**Table 7.** Classification of VMS deposits based on host rock composition (*modified from* Barrie and Hannington 1999). Rocks ~3 km into the footwall, ~1 km in to the hanging wall, and up to 5 km along strike are considered host rock.

| | **Mafic** | **Bimodal-Mafic** | **Mafic-Siliciclastic** | **Bimodal-Felsic** | **Bimodal-Siliciclastic** |
|---|---|---|---|---|---|
| **Host Rock** | >75% mafic rocks<br><1% felsic rocks<br><10% siliciclastic, ultramafic rocks | >50% mafic rocks<br>>3% felsic rocks<br>minor siliciclastic rocks | Subequal proportions of mafic volcanic or intrusive rocks and turbiditic siliciclastic rocks<br>Minor or absent felsic rocks | >50% felsic rocks<br><15% siliciclastic rocks<br>remainder is mafic volcanic and intrusive rocks | Equal proportions of volcanic and siliciclastic rocks<br>Felsic rocks > mafic rocks |
| **Tectonic Settings** | Ophiolites, ocean ridges, advanced back-arc rifts, supra-subduction zone nascent arcs | Primitive volcanic arcs, rifted primitive volcanic arcs | Rifted continental margins, oceanic rifts | Mature volcanic arcs, rifted volcanic arcs | Continental arcs, rifted continental arcs |
| **Mafic Host Rock Composition** | Tholeiitic, locally boninitic | Tholeiitic, may be transitional to calc-alkalic | N/A | Calc-alkalic or transitional tholeiitic | Tholeiitic, may be mildly alkalic |
| **Felsic Host Rock Composition** | N/A | Calc-alkalic | N/A | Principally calc-alkalic, may be transitional or high-silica rhyolite | Calc-alkalic |
| **Average Tonnage** | 2.8 MT | 5.1 MT | 11.0 MT | 5.2 MT | 23.7 MT |
| **Ore Composition** | Cu- and Au-rich and Pb-poor | Cu- and Zn-rich | Pb- and Cu-rich | Zn- and Ag-rich | Pb- and Ag-rich, Cu-poor |
| **Examples** | Potter Mine (Ontario), Coronation Mine (Saskatchewan) | Noranda District (Quebec), Flin Flon (Manitoba), United Verde mine (Arizona) | Besshi Deposits (Japan), Windy Craggy deposit (British Columbia) | Hokuroku district (Japan), Izok Lake deposit (Northwest Territories) | Iberian Pyrite Belt (Portugal, Spain), Bathurst camp (New Brunswick) |

# Summary

The Genex VMS deposit is hosted in a bimodal sequence of metavolcanic rocks and associated synvolcanic intrusions, overlain by a unit of volcaniclastic and epiclastic rocks. The base of the Genex stratigraphy (footwall) is composed of a thick felsic metavolcanic unit which ranges from felsic-tuff breccias, lapilli-tuffs, and tuffs with minor flows and flow breccias, forming a generally fining-upward succession. The overall lack of bedding, and the substantial thickness of the felsic breccias, suggests that the breccias may be the result of a large collapse event (i.e., caldera collapse). Although no coherent domes have been identified, the shape and packing of the fragments in the flow breccias indicate a proximal environment with little transport. Fractionation and geochemical trends in the Genex felsic metavolcanic rocks suggest that the felsic rocks are derived from fractionation of plagioclase, from a magma with A-type crustal affinity. Based on REE, the Genex felsic metavolcanic rocks are classified as FIIIa rhyolites, using the classification scheme of Lesher et al. (1986).

The basal felsic metavolcanic unit is cut by synvolcanic dikes and sills of mafic and intermediate compositions. The earlier intrusive units, the fine-grained mafic synvolcanic intrusions, are north-trending sills with numerous small apophyses stemming from the main intrusive bodies. The lower contact is brecciated with chilled and chloritized irregularly shaped fragments and local development of pillows. The upper contact is also irregular with numerous amoeboid dikes and peperite where they intrude overlying unconsolidated felsic volcaniclastic rocks. Near the upper part of the intrusions, felsic volcaniclastic rocks are incorporated in the intrusion. The presence of peperite, a pillowed base, irregular contacts, amoeboid dikes, and incorporation of felsic volcaniclastic rocks all indicates that the intrusions are high level synvolcanic sills. The lower fine-grained mafic intrusions are cut by a medium-grained intrusion, of similar composition. Fractionation trends indicate that the mafic synvolcanic intrusions are derived from fractionation of olivine ± plagioclase ± clinopyroxene, and are derived from a relatively primitive melt. The Genex mafic synvolcanic intrusions are oceanic tholeiitic basalts, and are derived from a primitive melt, without evidence of crustal contamination.

The younger intermediate synvolcanic intrusion forms a north-trending sill with numerous east-trending dikes stemming from the main intrusive body, parallel to faults in the Genex area. The lower contact of the sill is characterized by numerous apophyses which intrude the underlying volcanic rocks and the lower mafic intrusion. The upper contact of the north-trending sill, as well as the contacts of the east-trending dikes, contains a 25 m wide mixed zone in which the intrusion and the overlying rocks are chaotically mixed. However, blocks of felsic-tuff caught up in the intrusion are intact, suggesting that they were lithified prior to incorporation, indicating that the intermediate intrusion is synvolcanic, but slightly later than the mafic intrusion. In the immediate footwall of the Genex deposit, the east-trending dikes are shattered against the host rock (a felsic lapilli-tuff) with fragments of the intrusion in an altered, originally glass, matrix. The presence of a mixed zone, abundant spherulites and amygdules, and the utilization of the faults as conduits all indicate that the intermediate intrusion is a high level synvolcanic intrusion, but is slightly later than the mafic intrusions. Pearce element ratios indicate that the intermediate synvolcanic intrusion underwent olivine + clinopyroxene fractionation, and trace element data suggest it is a more evolved melt than the mafic intrusion. The intermediate synvolcanic intrusion is also an oceanic basaltic tholeiite, and is derived from either a crustal contaminated source, or a crustal-derived magma. Both the mafic and intermediate synvolcanic intrusions are chemically similar to the upper zone of the Kamiskotia gabbroic complex.

The intermediate intrusion can be physically distinguished from the mafic intrusions by a smaller degree of epidotization, a higher degree of carbonitization, a greater abundance of quartz, and a greater abundance of spherulites. Geochemically, the intermediate intrusion has a more evolved REE pattern, and a higher degree of crustal contamination.

Overlying the basal felsic unit is a massive basalt flow which has transitional contacts with a pillowed unit. Within the footwall pillowed units, there is variability in pillow size, pillow hyaloclastite thickness, amygdule percentage and degree of alteration. However, variations in pillow morphology, size, strike, and flow direction in the immediate footwall of the Genex deposit near the C-zone indicate that the pillowed flows were erupted onto a moderately to steeply dipping slope, with the crest of the slope near the C-zone. Disconformable massive mafic units are also present in the Genex area and are in close proximity to the east-trending faults. These units represent feeders for the mafic flows in the area, and are utilizing the faults as conduits. Mafic-tuffs, although rare, are found in proximity to pillowed and massive flows, and range from fine-grained tuffs to lapilli-tuffs, with evidence of bedding and cross-bedding. Fractionation trends in the mafic metavolcanic rocks indicate that the mafic rocks are a product of olivine + plagioclase + clinopyroxene fractionation. Trace element trends suggest that the footwall mafic metavolcanic rocks are oceanic tholeiitic basalts, and are derived from either a crustal-contaminated source, or a crustal-derived source.

Two fine-grained north-trending synvolcanic mafic sills define the immediate hanging wall of the deposit. The lower contact of the intrusions is a peperite, with chilled and irregularly shaped intrusion fragments in felsic lapilli-tuff. The upper contact is irregular with numerous, amoeboid dikes stemming from the main intrusive bodies. Although the intrusions are synvolcanic, they do not incorporate felsic material, which suggests that the upper fine-grained intrusions are slightly later than the fine-grained synvolcanic mafic intrusions in the footwall of the deposit. Geochemically and mineralogically, these synvolcanic sills are identical to the mafic synvolcanic intrusions in the footwall of the Genex deposit.

Overlying the hanging-wall mafic synvolcanic sills is a thin lens of felsic-tuff and lapilli-tuff overlain by a pillowed flow. Hanging-wall pillowed flows are physically similar to their footwall counterparts, but are chemically distinguished by a depletion in MgO, relative to the footwall mafic metavolcanic rocks. Pearce element ratios indicate that the hanging-wall mafic metavolcanic rocks are a product of plagioclase + olivine + minor clinopyroxene fractionation. Based on trace element trends, the hanging-wall mafic metavolcanic rocks in the Genex area are oceanic tholeiitic basalts, derived from either a crustal-contaminated source, or a crustal-derived source.

Immediately overlying the hanging-wall pillowed flow unit is a volcaniclastic and epiclastic unit composed of numerous depositional units grading from tuff-breccia and lapilli-tuff to tuff to mudstone and graphitic argillite. The volcaniclastic and epiclastic unit suggests volcanic quiescence characterized by mass flow sedimentation of volcanic-derived detritus. Mudstone beds reveal a hiatus in mass flow sedimentation that allowed relatively calm suspension deposition and pelagic background sedimentation. Felsic flows, mafic pillowed flows, and intrusions commonly disrupt the volcaniclastic sequences. The entire Genex stratigraphy is cut by several Proterozoic diabase dike of the Matachewan swarm.

Synvolcanic faulting in the Genex area occurred after emplacement of the lower synvolcanic mafic intrusion, but prior to emplacement of the intermediate synvolcanic intrusion. The synvolcanic faults formed conduits for the intermediate synvolcanic intrusion and for the hydrothermal fluids responsible for the mineralization and alteration at Genex. The late faults in the Genex area offset all Archean rock types, possibly during continued subsidence. The latest fault identified in the Genex area is the post-Proterozoic east-trending Aconda Lake fault.

Hydrothermal alteration is prevalent in all rock type in the Genex area, and is manifested as sericitization, chloritization, epidotization, silicification, and Fe-carbonitization. Although the heat from the synvolcanic intrusions in the Genex area was not great enough to drive the hydrothermal system responsible for the formation of the Genex deposit and associated alteration, the intrusions do indicate the presence of a high-temperature thermal corridor.

The mineralization in the Genex area is distributed in 3 major zones: the C-zone, H-zone, and A-zone. The C-zone is hosted in the matrix of a pillow breccia, conformable to bedding, with stringer mineralization contained in the pillow hyaloclastite of an underlying flow. The H-zone occurs within felsic-tuff and at the contact of the tuff with the surrounding intermediate synvolcanic intrusion. The A-zone mineralization is hosted dominantly in the intermediate intrusion with some mineralization in the matrix of a felsic lapilli-tuff. Both the H- and A-zones are disconformable to bedding, and are in close proximity to a synvolcanic fault. The Genex mineralization represents subseafloor replacement sulphides, localized in areas of higher permeability, with no massive sulphide present.

A brief geological history of the Genex area can be summarized as follows (from oldest to youngest events):

1. Bimodal volcanism in the Genex area begins as dominantly felsic volcanism, then shifts to dominantly mafic volcanism.
2. A hydrothermal system begins to develop penecontemporaneously with volcanism.
3. Synvolcanic emplacement of the lower fine-grained mafic intrusions (footwall), with associated development of peperite and brecciation.
4. Synvolcanic emplacement of upper fine-grained mafic intrusion (hanging wall).
5. Synvolcanic faulting of the Genex stratigraphy, with minor displacement. The synvolcanic faults are then utilized as conduits for focused hydrothermal activity.
6. Synvolcanic emplacement of the medium-grained mafic intrusion (footwall).
7. Synvolcanic emplacement of the intermediate intrusion along synvolcanic faults.
8. Hydrothermal alteration and VMS mineralization has occurred contemporaneous with the aforementioned processes, and then begins to wan.
9. Emplacement of volcaniclastic and epiclastic rocks in the hanging wall of the Genex stratigraphy suggests a waning or lapse in volcanism, or possibly another subsidence event.
10. Although minor, mineralization and hydrothermal alteration is still occurring along faults and shear zones, and in the volcaniclastic rocks.
11. Faulting with recognizable offset of stratigraphy. All of the Archean Genex stratigraphy is offset.
12. Emplacement of Proterozoic Matachewan diabase dikes.
13. Faulting along the Aconda Lake fault (reactivation of synvolcanic structure).

The Kamiskotia area, and the Genex stratigraphy, has traditionally been included in the Tisdale (2710–2703 Ma) and Kidd–Munro (2719–2711 Ma) assemblages (Ayer et al. 2002). However, recent work by Hathway, Hudak and Hamilton (2005) and this study have indicated that the Kamiskotia rocks, including the Genex stratigraphy, are more similar to the Blake River assemblage (2699 Ma). A recent age determination on a felsic lapilli-tuff in the Genex area, completed as part of this study, revealed an age of 2698.6±1.3 Ma. This date equates the Genex rocks with those of the Blake River assemblage, rather than the Tisdale and Kidd–Munro assemblages. The Genex felsic metavolcanic rocks have been geochemically classified as FIIIa rhyolites according to the classification scheme of Lesher et al. (1986). However, felsic rocks of the Tisdale assemblage are classified as FIIIb rhyolites. This discrepancy again suggests that the Genex stratigraphy is correlative to the Blake River assemblage. Further geochemical classification of the Abitibi belt igneous rocks using the scheme developed by Barrie, Ludden and Green (1993) and Kerrich and Wyman (1996) places the Kamiskotia rocks in Group 1. However, geochemical trends in the Genex rocks are most similar to rocks in Group 2 (which include those of the Noranda camp in the Blake River assemblage).

# Recommendations

Although no significant VMS mineralization has been found in the Genex area since the discovery of the initial deposit, the area still has potential to host significant VMS mineralization, especially along strike from the Genex deposit. Geochemically, the Genex felsic metavolcanic rocks are classified as FIIIa rhyolites, which, according to Lesher et al. (1986), are preferentially associated with Archean VMS mineralization. Furthermore, the presence of a mineralizing hydrothermal system has already been established in the area. Thus, many of the necessary components for a VMS deposit are present. Lastly, the presence of mineralized mudstone lapilli in the volcaniclastic rocks to the east of the Genex area is of interest. Not only is the volcaniclastic sequence a good marker horizon, but the presence of mineralized fragments indicates that VMS mineralization was still occurring during the evolution of the stratigraphic package. The source of the mineralized mudstone fragments is yet unidentified.

The area to the south of the Genex deposit, along strike, is very poorly explored. The lack of outcrop prohibits surface mapping, but a diamond drilling program to the south may be able to trace the Genex stratigraphy in order to examine the mineralized horizon. Work to the north of the Genex area, along strike, has thus far been limited by the Aconda Lake fault, the offset of which is unknown. Regional work by Hathway, Hudak and Hamilton (2005) was not able to trace the Genex stratigraphy across the fault, but detailed mapping of the area north of the Aconda Lake fault, as well as re-evaluation of diamond drill core may be able to identify the Genex stratigraphy.

In further exploration for VMS mineralization in the Kamiskotia area, an important feature that must be recognized is the presence of synvolcanic structures. In the Genex area, the identification of high-level synvolcanic intrusions are critical in defining the presence of synvolcanic structures. Thus, recognition of intrusions similar to the synvolcanic intermediate intrusions in the Genex area, which tend to utilize synvolcanic structures as conduits, are important in defining synvolcanic structures.

# References

Ayer, J., Amelin, Y., Corfu, F., Kamo, S., Ketchum, J., Kwok, K. and Trowell, N. 2002. Evolution of the southern Abitibi greenstone belt based on U-Pb geochronology: autochthonous volcanic construction followed by plutonism, regional deformation and sedimentation; Precambrian Research, v.115, p.63-95.

Barrett, T.J. and MacLean, W.H. 1999. Volcanic sequences, lithogeochemistry, and hydrothermal alteration in some bimodal volcanic-associated massive sulfide systems; Reviews in Economic Geology, v.8, p.101-113.

Barrie, C.T. 1992. Geology of the Kamiskotia area; Ontario Geological Survey, Open File Report 5829, 179p.

Barrie, C.T., Gorton, M.P., Naldrett, A.J. and Hart, T.R. 1991. Geochemical constraints on the petrogenesis of the Kamiskotia gabbroic complex and related basalts, western Abitibi Subprovince, Ontario, Canada; Precambrian Research, v.50, p.173-199.

Barrie, C.T. and Hannington, M.D. 1999. Classification of volcanic-associated massive sulfide deposits based on host-rock composition; *in* Volcanic-associated massive sulfide deposits: processes and examples in modern and ancient settings, Reviews in Economic Geology, v.8, p.11-12.

Barrie, C.T., Ludden, J.N. and Green, T.H. 1993. Geochemistry of volcanic rocks associated with Cu-Zn and Ni-Cu deposits in the Abitibi Subprovince; Economic Geology, v.88, p.1341-1358.

Binney, P. and Barrie, C.T. 1991. Kamiskotia area; *in* Geology and ore deposits of the Timmins District, Ontario (field trip 6), Geological Survey of Canada, Open File Report 2161, p.52-65.

Bromley-Challenor, M.D. 1988. The Falun supracrustal belt; Part 1, primary geochemical characteristics of Proterozoic metavolcanics and granites; *in* The Bergslagen Province – Central Sweden, Geologie en Mijnbouw, v.67, p.239-253.

Campbell, I.H., Coad, P., Franklin, J.M., Gorton, M.P., Scott, S.D., Sowa, J. and Thurston, P.C. 1982. Rare earth elements in volcanic rocks associated with Cu-Zn massive sulphide mineralization: A preliminary report; Canadian Journal of Earth Sciences, v.19, p.619-623.

Campbell, I.H., Franklin, J.M., Gorton, M.P., Hart, T.R. and Scott, S.D. 1981. The role of subvolcanic sills in the generation of massive sulfide deposits; Economic Geology, v.76, p.2248-2253.

Cann, J.R. 1970. Rb, Sr, Y, Zr, and Nb in some ocean floor basaltic rocks; Earth and Planetary Science Letters, v.10, p.7-11.

Cas, R.A.F. and Wright, J.V. 1988. Volcanic successions: modern and ancient; Unwin Hyman Ltd., London, 529p.

Cathles, L.M., Erendi, A.H.J. and Barrie, T. 1997. How long can a hydrothermal system be sustained by a single intrusive event?; Economic Geology, v.92, p. 66-771.

Chown, E.H., Harrap, R. and Moukhsil, A. 2002. The role of granitic intrusions in the evolution of the Abitibi belt, Canada; Precambrian Research, v.115, p.291-310.

Dimroth, E., Cousineau, P., Leduc, M. and Sanschagrin, Y. 1978. Structure and organization of Archean subaqueous basalt flows, Rouyn–Noranda area, Quebec, Canada; Canadian Journal of Earth Sciences, v.15, p.902-918.

Dostal, J. and Mueller, W.U. 1997. Komatiite flooding of a rifted Archean rhyolitic arc complex: geochemical signature and tectonic significance of the Stoughton–Roquemaure Group, Abitibi greenstone belt, Canada; The Journal of Geology, v.105, p.545-463.

Doyle, M.G. and Allen, R.L. 2003. Subsea-floor replacement in volcanic-hosted massive sulfide deposits; Ore Geology Reviews, v.23, p.183-222.

Eby, G.N. 1992. Chemical subdivision of the A-type granitoids: petrogenetic and tectonic implications; Geology, v.20, p.641-644.

Eddy, C.A., Dilek, Y., Hurst, S. and Moores, E.M. 1998. Seamount formation and associated caldera complex and hydrothermal mineralization in ancient oceanic crust, Troodos ophiolite (Cyprus); Tectonophysics, v.292, p.198-210.

Fisher, R.V. 1966. Rocks composed of volcanic fragments and their classification; Earth-Science Reviews, v.1, p.287-298.

Floyd, P.A. and Winchester, J.A. 1975. Magma-type and tectonic setting discrimination using immobile elements; Earth and Planetary Science Letters, v.27, p.211-218.

Franklin, J.M. 1993. Volcanic-associated massive sulphide deposits; *in* Mineral deposit modeling, Geological Association of Canada, Special Paper 40, p.315-334.

——— 1996. Volcanic-associated massive sulphide base metals; *in* Geology of Canadian mineral deposit types, Geological Survey of Canada, Geology of Canada, no.8, p.158-183.

Galley, A.G. 1993. Characteristics of semi-conformable alteration zones associated with volcanogenic massive sulfide districts; Journal of Geochemical Exploration, v.48, p.175-200.

——— 1996. Geochemical characteristics of subvolcanic intrusions associated with Precambrian massive sulphide districts; *in* Trace element geochemistry of volcanic rocks: applications for massive sulphide exploration, Geological Association of Canada, Short Course Notes, v.12, p.239-278.

——— 2003. Composite synvolcanic intrusions associated with Precambrian VMS-related hydrothermal systems; Mineralium Deposita, v.38, p.443-473.

Gibson, H.L., Morton, R.L. and Hudak, G.J. 1999. Submarine volcanic processes, deposits, and environments favorable for the location of volcanic-associated massive sulfide deposits; *in* Volcanic-associated massive sulfide deposits: processes and examples in modern and ancient settings, Reviews in Economic Geology, v.8, p.13-51.

Gibson, H.L., Watkinson, D.H. and Comba, C.D. A. 1983. Silicification: hydrothermal alteration in an Archean geothermal system within the Amulet rhyolite formation, Noranda, Quebec; Economic Geology, v.78, p.954-971.

Hannington, M.D. and Kjarsgaard, I.M. 2001. Mineral-chemical studies of regional-scale hydrothermal alteration in the central Blake River Group, western Abitibi Subprovince: Part II. Ben Nevis volcanic complex; Geological Survey of Canada, Open-File Report 94E07, p.77-122.

Hart, T.R. 1984. The geochemistry and petrogenesis of a metavolcanic and intrusive sequence in the Kamiskotia area, Timmins, Ontario; unpublished MSc thesis, University of Toronto, Toronto, Ontario, 179p.

Hart, T.R., Gibson, H.L. and Lesher, C.M. 2004. Trace element geochemistry and petrogenesis of felsic volcanic rocks associated with volcanogenic massive Cu-Zn-Pb sulfide deposits; Economic Geology, v.99, p.1003-1013.

Hathway, B., Hudak, G. and Hamilton, M.A. 2005. Geological setting of volcanogenic massive sulphide mineralization in the Kamiskotia area: Discover Abitibi Initiative; Ontario Geological Survey, Open File Report 6155.

Heaman, L.M. 1988. A precise U-Pb zircon age for a Hearst dike; Geological Association of Canada–Mineralogical Association of Canada, Program with Abstracts, v.13, p.A53.

Hudak, G.J., Heine, J., Newkirk, T., Odette, J. and Hauck, S. 2003. Comparative geology, stratigraphy, and lithogeochemistry of the Five Mile Lake, Quartz Hill, and Skeleton Lake VMS occurrences, Vermilion District, NE Minnesota: A report to the Mineral Coordinating Committee; Department of Natural Resources, Minerals Division, State of Minnesota.

Jackson, S.L. and Fyon, A.J. 1991. The western Abitibi Subprovince in Ontario; *in* Geology of Ontario, Ontario Geological Survey, Special Volume 4, Part 1, p.405-482.

Jenner, G.A. 1996. Trace element geochemistry of igneous rocks: geochemical nomenclature and analytical geochemistry; *in* Trace element geochemistry of volcanic rocks: applications for massive sulphide exploration, Geological Association of Canada, Short Course Notes, v.12, p.51-77.

Kerrich, R. and Wyman, D.A. 1996. The trace element systematics of igneous rocks in mineral exploration: an overview; *in* Trace element geochemistry of volcanic rocks: applications for massive sulphide exploration, Geological Association of Canada, Short Course Notes, v.12, p.1-50.

Kretz, R. 1983. Symbols for the rock-forming minerals; American Mineralogist, v.68, p.277-279.

Large, R.R., Gemmell, J.B., Paulick, H. and Huston, D.L. 2001. The alteration box plot: a simple approach to understanding the relationship between alteration mineralogy and lithogeochemistry associated with volcanic-hosted massive sulfide deposits; Economic Geology, v.96, p.957-971.

Larson, P.B. 1984. Geochemistry of the Alteration Pipe at the Bruce Cu-Zn volcanogenic massive sulfide deposit, Arizona; Economic Geology, v.79, p.1880-1896.

Le Bas, M.J., Le Maitre, R.W., Streckeisen, A. and Zannetin, B. 1986. A chemical classification of volcanic rocks based on the total alkali-silica diagram; Journal of Petrology, v.27, p.745-750.

Legault, M.H. 1985. The geology and alteration associated with the Genex volcanogenic Cu massive sulphide deposit, Godfrey Township, Timmins, Ontario; unpublished MSc thesis, Carleton University, Ottawa, Ontario, 222p.

Lesher, C.M., Goodwin, A.M., Campbell, I.H. and Gorton, M.P. 1986. Trace-element geochemistry of ore-associated and barren, felsic metavolcanic rocks in the Superior Province, Canada; Canadian Journal of Earth Sciences, v.23, p.222-237.

Lydon, J.W. 1988. Ore Deposit Models #14. Volcanogenic massive sulphide deposits, part 2: genetic models: Geoscience Canada, v.15, p.43-65.

MacDonald, P.J., Piercey, S.J. and Hamilton, M.A. 2005. An integrated study of intrusive rocks spatially associated with gold and base metal mineralization in Abitibi greenstone belt, Timmins area and Clifford Township: Discover Abitibi Initiative; Ontario Geological Survey, Open File Report 6160.

Marshall, B. and Gilligan, L.B. 1993. Remobilization, syn-tectonic processes and massive sulfide deposits; Ore Geology Reviews, v.8, p.39-64.

Marshall, B. and Spry, P.G. 2000. Discriminating between regional metamorphic remobilization and syntectonic emplacement in the genesis of massive sulfide ores; Reviews in Economic Geology, v.11, p.39-79.

Marshall, B., Vokes, F.M. and Larocque, A.C.L. 2000. Regional metamorphic remobilization: upgrading and formations of ore deposits; Reviews in Economic Geology, v.11, p.19-38.

Middleton, R.S. 1975. Geology of Turnbull and Godfrey townships, District of Cochrane; Ontario Division of Mines, Open File Report 5118, 267p.

Morton, R.L. and Franklin, J.M. 1987. Two-fold classification of Archean volcanic-associated massive sulfide deposits; Economic Geology, v.82, p.1057-1063.

Mueller, W.U. and Mortensen, J.K. 2002. Age constraints and characteristics of subaqueous volcanic construction, the Archean Hunter Mine Group, Abitibi greenstone belt; Precambrian Research, v.115, p.119-152.

Nicholls, J. 1990. Stoichiometric constraints on variations in Pearce element ratios and analytical uncertainty in hypothesis testing; *in* Theory and application of Pearce element ratios to geochemical data analysis, Geological Association of Canada, Short Course Notes, v.8, p.73-98.

Nicholls, J. and Russell, J.K. 1990. Pearce element ratios- an overview, example and bibliography; *in* Theory and application of Pearce element ratios to geochemical data analysis, Geological Association of Canada, Short Course Notes, v.8, p.11-21.

North American Commission on Stratigraphic Nomenclature 1983. North American stratigraphic code; The American Association of Petroleum Geologists Bulletin, v.67, p.841-875. [can be viewed at http://www.agiweb.org/nacsn/code2.html#anchor514748; accessed February 8, 2005]

Pearce, J.A. 1996. A user's guide to basalt discrimination diagrams; *in* Trace element geochemistry of volcanic rocks: applications for massive sulphide exploration, Geological Association of Canada, Short Course Notes, v.12, p.79-113.

Pearce, J.A. and Cann, J.R. 1973. Tectonic setting of basic volcanic rocks determined using trace element analysis; Earth and Planetary Science Letters, v 19, p.290-300.

Pearce, J.A., Harris, N.B.W. and Tindle, A.G. 1984. Trace element discrimination diagrams for the tectonic interpretation of granitic rocks; Journal of Petrology, v.25, p.956-983.

Pearce, T.H. 1968. A contribution to theory of variation diagrams; Contributions to Mineralogy and Petrology v.19, p.142-157.

——— 1990. Getting the most from your data: applications of Pearce element ratio analysis; *in* Theory and application of Pearce element ratios to geochemical data analysis, Geological Association of Canada, Short Course Notes, v.8, p.99-130.

Piercey, S.J., Murphy, D.C., Mortensen, J.K. and Paradis, S. 2001a. Boninitic magmatism in a continental margin setting, Yukon–Tanana terrane, southeastern Yukon, Canada; Geology, v.29, p.731-734.

Piercey, S.J., Paradis, S., Murphy, D.C. and Mortensen, J.K. 2001b. Geochemistry and paleotectonic setting of felsic volcanic rocks in the Finlayson Lake volcanic-hosted massive sulfide district, Yukon, Canada; Economic Geology, v.96, p.1877-1905.

Rytuba, J.J. 1994. Evolution of volcanic and tectonic features in caldera settings and their importance in the localization of ore deposits; Economic Geology, v.89, p.1687-1696.

Stanley, C.R. 1990. Error propagation and regression on Pearce element ratio diagrams; *in* Theory and application of Pearce element ratios to geochemical data analysis, Geological Association of Canada, Short Course Notes, v.8, p.179-215.

Stix, J., Kennedy, B., Hannington, M., Gibson, H., Fiske, R., Mueller, W. and Franklin, J. 2003. Caldera-forming processes and the origin of submarine volcanogenic massive sulfide deposits; Geology, v.31, p.375-378.

Sun, S-s. and McDonough, W.F. 1989. Chemical and isotopic systematics of oceanic basalts: implications for mantle composition and processes; *in* Magmatism in the ocean basins, Geological Society, Special Publication No.42, p.313-345.

Troll, V.R., Emeleus, C.H. and Donaldson, C.H. 2000. Caldera formation in the Rum Central Igneous Complex, Scotland, Bulletin of Volcanology, v.62, p.301-317.

Walker, G.P.L. 1992. Morphometric study of pillow-size spectrum among pillow lavas; Bulletin of Volcanology, v.54, p.459-474.

Weatherston, A.J. 1996. OGS editorial guide; Ontario Geological Survey, Miscellaneous Paper 165, 132p.

Winchester, J.A. and Floyd, P.A. 1976. Geochemical magma type discrimination; application to altered and metamorphosed basic igneous rocks; Earth and Planetary Science Letters, v.28, p.459-469.

——— 1977. Geochemical discrimination of different magma series and the differentiation products using immobile elements; Chemical Geology, v.20, p.325-343.

Wood, D.A. 1980. The application of a Th-Hf-Ta diagram to problems of tectonomagmatic classification and to establishing the nature of crustal contamination of basaltic lavas of the British Tertiary Volcanic Province; Earth and Planetary Science Letters, v.50, p.11-30.

Wyman, D.A., Kerrich, R. and Polat, A. 2002. Assembly of Archean cratonic mantle lithosphere and crust: plume-arc interaction in the Abitibi–Wawa subduction-accretion complex; Precambrian Research, v.115, p.37-62.

This page left blank intentionally

# Appendix 1

## Petrographic Descriptions of Samples

In this appendix, major lithologies have been subdivided into felsic metavolcanic rocks, mafic metavolcanic rocks, mafic intrusive rocks, intermediate intrusive rocks, volcaniclastic and epiclastic rocks, and late diabase intrusive (Matachewan) rocks. For each subdivision, representative samples have been selected, with photomicrographs and petrographic descriptions presented in this appendix. Complete petrographic descriptions and photomicrographs of all 183 samples are available in digital format on MRD 144.

### Abbreviations used in petrographic descriptions

(*from* Kretz (1983), and *OGS Editorial Guide* (Weatherston 1996))

ab: albite
act: actinolite
altd glass: altered glass
amygs: amygdules
ang: angular
ank: ankerite
bt: biotite
blky: blocky
cal: calcite
carbn: carbonitization
chl: chlorite
chlcn: chloritization
cp: chalcopyrite
cpx: clinopyroxene
cusp: cuspate
dis: disseminated
elong: elongate
ep: epidote
epi-qtz: epidote + quartz alteration
epicn: epidotization
fel lith: felsic lithic fragments
fract: fracture controlled
frags: fragments
hem: hematite
hyalo: hyaloclastite
ireg: irregular
kfs: potassium feldspar
maf lith: mafic lithic fragments
mag: magnetite
ms: muscovite
opx: orthopyroxene
pat: patchy
perv: pervasive
pheno: phenocrysts
pl: plagioclase
pum: pumice fragments
py: pyrite
qtz: quartz
rnd: rounded
scor: scoria fragments
ser: sericite
sercn: sericitization
silcn: silicification
sp: sphalerite
sph: spherulites
unID: unidentified
vein: vein controlled

## Felsic Metavolcanic Rocks

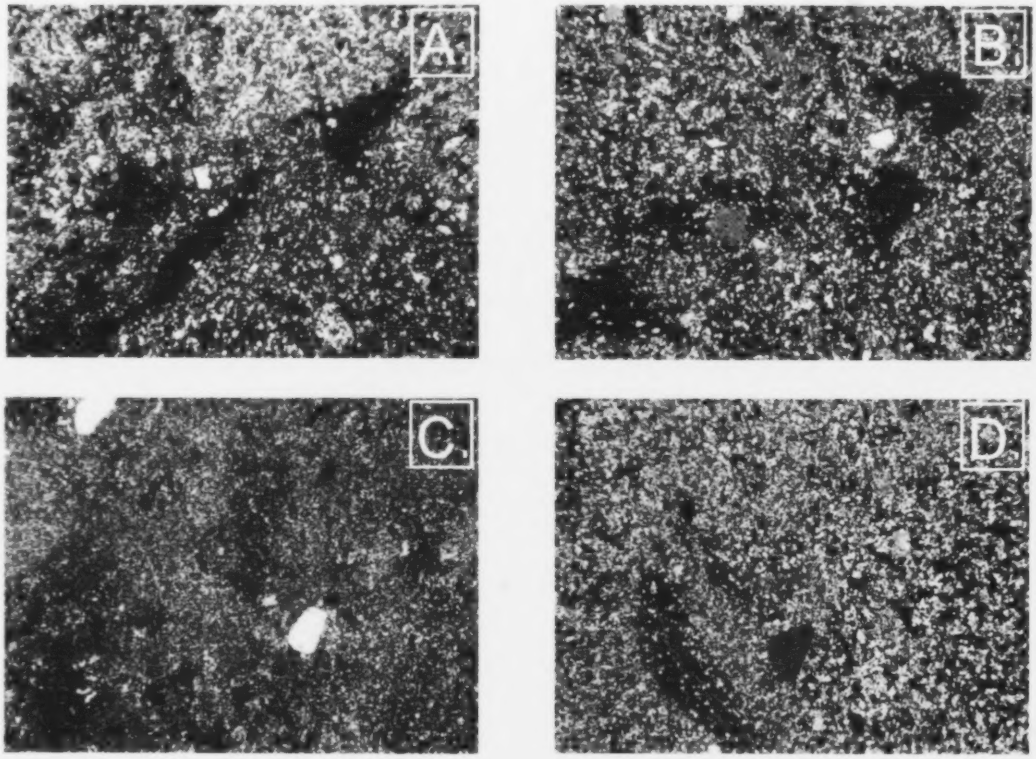

**Photo 49.** A) Photomicrograph of fragmental felsic flow in crossed polarized light. Sample 04-SMH-0023-4. B) Photomicrograph of felsic lapilli tuff in crossed polarized light. Sample 04-SMH-0001-5. C) Photomicrograph of ash-rich felsic lapilli tuff in crossed polarized light. Sample 03-SMH-0034-1. D) Photomicrograph of felsic lapilli tuff with pumice and felsic fragments in crossed polarized light. Sample 03-SMH-0025. Field of view is approximately 22 mm.

| Sample | Major Unit | Rock type |
|---|---|---|
| 03-SMH- | felsic | lapilli |
| 0025 | volcanic | tuff |

| Primary Features | | | | | | | | | |
|---|---|---|---|---|---|---|---|---|---|
| Texture | Structure | Mineralogy (phenocrysts) | | | | | Mineralogy (matrix) | | |
| polymict | | pl | kfs | qtz | opx | cpx | pl | kfs | qtz |
| | | | | 3-5% | | | | | 70% |

| Fragments | | | | | | | | | | | | |
|---|---|---|---|---|---|---|---|---|---|---|---|---|
| Fragments | | | | | | | Morphology | | | | | |
| fel lith | maf lith | pheno | pum | scor | altd glass | unID | ireg | blky | rnd | ang | cusp | elong |
| 5-10% | | | 1% | | | | | x | | | | x |

| Secondary Features | | | | | | | | | | | | | |
|---|---|---|---|---|---|---|---|---|---|---|---|---|---|
| Texture | Structure | Mineralogy (porphyroblasts) | | | | | Mineralogy (matrix) | | | | | | |
| fractured | | qtz | chl | ank | cal | act | ab | bt | ep | qtz | chl | ank | ser |
| | | | | | | | | | | | | | 25-27% |

| Comments |
|---|
| large, euhedral qtz phenocrysts with microfractures |

| Alteration | | | | | Mineralization | | | | | | | | | |
|---|---|---|---|---|---|---|---|---|---|---|---|---|---|---|
| Assemblage | | | | | Minerals | | | | | Form | | | | |
| sercn | chlcn | silcn | epi-qtz | epicn | mag | py | cp | hem | unID | dis | fract | vein | perv | pat |
| x | | x | | | | | | | | | | | | |

| Sample | Major Unit | Rock type |
|---|---|---|
| 03-SMH- | felsic | lapilli tuff |
| 0034-1 | volcanic | |

| Primary Features | | | | | | | | | |
|---|---|---|---|---|---|---|---|---|---|
| Texture | Structure | Mineralogy (phenocrysts) | | | | | Mineralogy (matrix) | | |
| polymict | brecciated | pl | kfs | qtz | opx | cpx | pl | kfs | qtz |
| | | | | 3-5% | | | | | 80-85% |

| Fragments | | | | | | | | | | | | |
|---|---|---|---|---|---|---|---|---|---|---|---|---|
| Fragments | | | | | | | Morphology | | | | | |
| fel lith | maf lith | pheno | pum | scor | altd glass | unID | ireg | blky | rnd | ang | cusp | elong |
| | | | 10-15% | | 5% | | x | | | | x | |

| Secondary Features | | | | | | | | | | | | | |
|---|---|---|---|---|---|---|---|---|---|---|---|---|---|
| Texture | Structure | Mineralogy (porphyroblasts) | | | | | Mineralogy (matrix) | | | | | | |
| fractured | | qtz | chl | ank | cal | act | ab | bt | ep | qtz | chl | ank | ser |
| | | | | | | | | | | | | | 15-20% |

| Comments |
|---|
| large qtz phenocrysts with microfractures |
| pumice is highly altered, y-shaped shards |
| matrix is microcrystalline qtz |

| Alteration | | | | | Mineralization | | | | | | | | | |
|---|---|---|---|---|---|---|---|---|---|---|---|---|---|---|
| Assemblage | | | | | Minerals | | | | | Form | | | | |
| sercn | chlcn | silcn | epi-qtz | epicn | mag | py | cp | hem | unID | dis | fract | vein | perv | pat |
| | | x | | | | | | | | | | | | |

| Sample | Major Unit | Rock type |
|---|---|---|
| 03-SMH- | felsic | lapilli |
| 0112-4 | volcanic | tuff |

| Primary Features | | | | | | | | | |
|---|---|---|---|---|---|---|---|---|---|
| Texture | Structure | Mineralogy (phenocrysts) | | | | | Mineralogy (matrix) | | |
| mono | | pl | kfs | qtz | opx | cpx | pl | kfs | qtz |
| lithic | | | | 5% | | | | | 50% |

| Fragments | | | | | | | | | | | | |
|---|---|---|---|---|---|---|---|---|---|---|---|---|
| Fragments | | | | | | | Morphology | | | | | |
| fel lith | maf lith | pheno | pum | scor | altd glass | unID | ireg | blky | rnd | ang | cusp | elong |
| | | | 10% | | | | | | | x | | |

| Secondary Features | | | | | | | | | | | | | |
|---|---|---|---|---|---|---|---|---|---|---|---|---|---|
| Texture | Structure | Mineralogy (porphyroblasts) | | | | | Mineralogy (matrix) | | | | | | |
| | | qtz | chl | ank | cal | act | ab | bt | ep | qtz | chl | ank | ser |
| | | | | 5% | | | | | | | | | 30% |

| Comments |
|---|
| fragments are very irregular, altered, broken |

| Alteration | | | | | Mineralization | | | | | | | | | |
|---|---|---|---|---|---|---|---|---|---|---|---|---|---|---|
| Assemblage | | | | | Minerals | | | | | Form | | | | |
| sercn | chlcn | silcn | epi-qtz | epicn | mag | py | cp | hem | unID | dis | fract | vein | perv | pat |
| x | | x | | | | | | | | | | | | |

| Sample | Major Unit | Rock type |
|---|---|---|
| 04-SMH- | felsic | lapilli |
| 0001-5 | volcanic | tuff |
| | | |

| Primary Features | | | | | | | | | |
|---|---|---|---|---|---|---|---|---|---|
| Texture | Structure | Mineralogy (phenocrysts) | | | | | Mineralogy (matrix) | | |
| mono | | pl | kfs | qtz | opx | cpx | pl | kfs | qtz |
| lithic | | | | 1-3% | | | | | 75% |
| | | | | | | | | | |

| Fragments | | | | | | | | | | | | |
|---|---|---|---|---|---|---|---|---|---|---|---|---|
| Fragments | | | | | | | Morphology | | | | | |
| fel lith | maf lith | pheno | pum | scor | altd glass | unID | mtx | blky | rnd | ang | cusp | elong |
| 3-5% | | | 3-5% | | | | | | | x | | x |

| Secondary Features | | | | | | | | | | | | |
|---|---|---|---|---|---|---|---|---|---|---|---|---|
| Texture | Structure | Mineralogy (porphyroblasts) | | | | | | Mineralogy (matrix) | | | | |
| | | qtz | chl | ank | act | ab | bt | ep | qtz | chl | ank | ser |
| | | | | | | | | | | | | 10-15% |

| Comments |
|---|
| felsic fragments are same composition as matrix |
| but are more sericite altered |
| |

| Alteration | | | | | Mineralization | | | | | | | | | |
|---|---|---|---|---|---|---|---|---|---|---|---|---|---|---|
| Assemblage | | | | | Minerals | | | | | Form | | | | |
| sercn | chlcn | silcn | epi-qtz | epicn | mag | py | cp | hem | unID | dis | fract | vein | perv | pat |
| x | | x | | | | | | | | | | | | |

| Sample | Major Unit | Rock type |
|---|---|---|
| 04-SMH- | felsic | ash |
| 0005-5 | volcanic | tuff |
| | | |

| Primary Features | | | | | | | | | |
|---|---|---|---|---|---|---|---|---|---|
| Texture | Structure | Mineralogy (phenocrysts) | | | | | Mineralogy (matrix) | | |
| fine | | pl | kfs | qtz | opx | cpx | pl | kfs | qtz |
| grained | | | | 1% | | | | | 1-3% |
| 50-55% sph | | | | | | | | | |

| Fragments | | | | | | | | | | | | |
|---|---|---|---|---|---|---|---|---|---|---|---|---|
| Fragments | | | | | | | Morphology | | | | | |
| fel lith | maf lith | pheno | pum | scor | altd glass | unID | mtx | blky | rnd | ang | cusp | elong |
| | | | | | | | | | | | | |

| Secondary Features | | | | | | | | | | | | |
|---|---|---|---|---|---|---|---|---|---|---|---|---|
| Texture | Structure | Mineralogy (porphyroblasts) | | | | | | Mineralogy (matrix) | | | | |
| | | qtz | chl | ank | act | ab | bt | ep | qtz | chl | ank | ser |
| | | | | | | | | | | | 5-10% | 40-45% |

| Comments |
|---|
| abundance of spherulites indicates sample may have |
| been devitrified hyaloclastite |
| spherulites are radial, well defined |

| Alteration | | | | | Mineralization | | | | | | | | | |
|---|---|---|---|---|---|---|---|---|---|---|---|---|---|---|
| Assemblage | | | | | Minerals | | | | | Form | | | | |
| sercn | carbn | silcn | epi-qtz | epicn | mag | py | cp | hem | unID | dis | fract | vein | perv | pat |
| x | x | | | | | | | | | | | | | |

| Sample | Major Unit | Rock type |
|---|---|---|
| 04-SMH- | felsic | flow |
| 0023-4 | volcanic | |
| | | |

| Primary Features | | | | | | | | | |
|---|---|---|---|---|---|---|---|---|---|
| Texture | Structure | Mineralogy (phenocrysts) | | | | | Mineralogy (matrix) | | |
| fine | fragmental | pl | kfs | qtz | opx | cpx | pl | kfs | qtz |
| grained | | | | 3-5% | | | | | 80-85% |
| | | | | | | | | | |

| Fragments | | | | | | | | | | | | |
|---|---|---|---|---|---|---|---|---|---|---|---|---|
| Fragments | | | | | | | Morphology | | | | | |
| fel lith | maf lith | pheno | pum | scor | altd glass | unID | mtx | blky | rnd | ang | cusp | elong |
| 5-7% | | | 5-7% | | | | | | x | | | x |

| Secondary Features | | | | | | | | | | | | |
|---|---|---|---|---|---|---|---|---|---|---|---|---|
| Texture | Structure | Mineralogy (porphyroblasts) | | | | | | Mineralogy (matrix) | | | | |
| | | qtz | chl | ank | act | ab | bt | ep | qtz | chl | ank | ser |
| | | | | | | | | | | | | 10-15% |

| Comments |
|---|
| looks crystalline |
| |
| |

| Alteration | | | | | Mineralization | | | | | | | | | |
|---|---|---|---|---|---|---|---|---|---|---|---|---|---|---|
| Assemblage | | | | | Minerals | | | | | Form | | | | |
| sercn | chlcn | silcn | epi-qtz | epicn | mag | py | cp | hem | unID | dis | fract | vein | perv | pat |
| x | | x | | | | | | | | | | | | |

## Mafic Metavolcanic Rocks

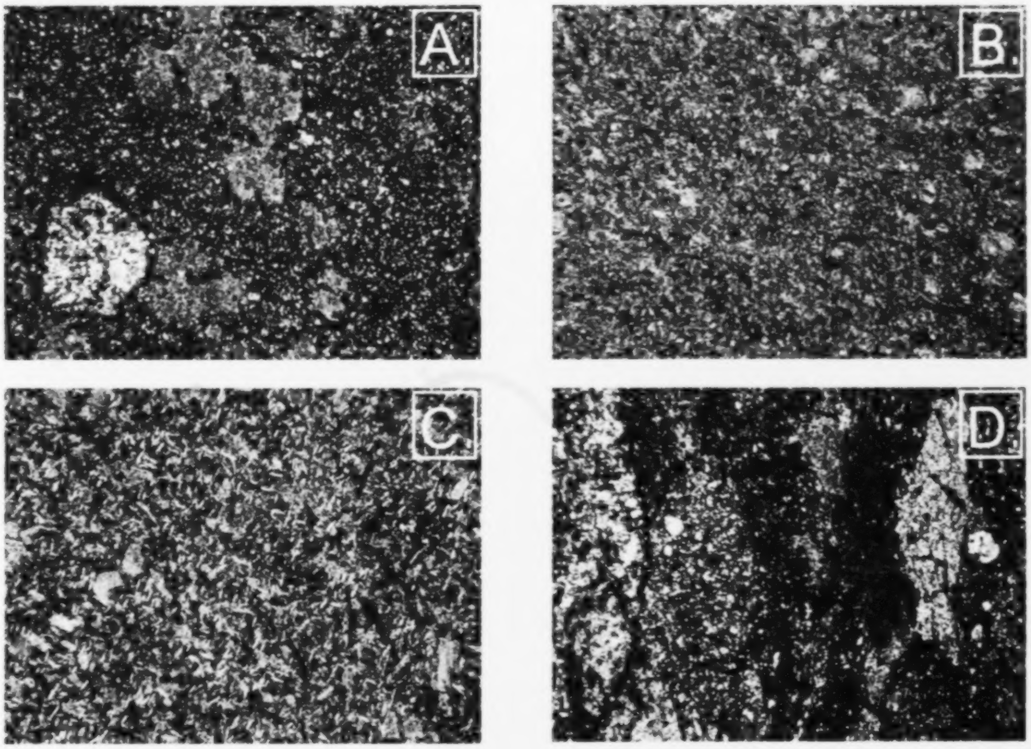

**Photo 50.** A) Photomicrograph of quartz amygdaloidal fine-grained mafic volcanic in crossed polarized light. Sample 03-SMH-0024. B) Photomicrograph of medium-grained mafic volcanic in crossed polarized light. Sample 03-SMH-0142-1. C) Photomicrograph of diabasic mafic volcanic in crossed polarized light. Sample 04-SMH-0015-2. D) Photomicrograph of pillow breccia in crossed polarized light. Sample 03-SMH-0005-1. Field of view is approximately 22 mm.

| Sample | Major Unit | Rock type |
|---|---|---|
| 03-SMH- | mafic | flow |
| 0001-8 | volcanic | |
| | | |

| Primary Features | | | | | | | | | |
|---|---|---|---|---|---|---|---|---|---|
| Texture | Structure | Mineralogy (phenocrysts) | | | | | Mineralogy (matrix) | | |
| fine | <1% | pl | kfs | qtz | opx | cpx | pl | kfs | qtz |
| grained | qtz amygs | 5% | | 5% | | | | | 5% |
| | | | | | | | | | |

| Fragments | | | | | | | | | | | | |
|---|---|---|---|---|---|---|---|---|---|---|---|---|
| Fragments | | | | | | | Morphology | | | | | |
| fel lith | maf lith | pheno | pum | scor | altd glass | unID | ireg | blky | rnd | ang | cusp | elong |
| | | | | | | | | | | | | |

| Secondary Features | | | | | | | | | | | | | |
|---|---|---|---|---|---|---|---|---|---|---|---|---|---|
| Texture | Structure | Mineralogy (porphyroblasts) | | | | | Mineralogy (matrix) | | | | | | |
| | | qtz | chl | ank | cal | act | ab | bt | ep | qtz | chl | ank | ser |
| | | | | | | | | | 60% | | 10% | 10% | |

| Comments |
|---|
| irregular shaped qtz |
| irregular shaped mag |
| |

| Alteration | | | | | Mineralization | | | | | | | | | |
|---|---|---|---|---|---|---|---|---|---|---|---|---|---|---|
| Assemblage | | | | | Minerals | | | | | Form | | | | |
| sercn | chlcn | silcn | epi-qtz | epicn | mag | py | cp | hem | unID | dis | fract | vein | perv | pat |
| | x | | x | | 5-7% | | | | | x | | | | |

---

| Sample | Major Unit | Rock type |
|---|---|---|
| 03-SMH- | mafic | massive |
| 0050-1 | volcanic | |
| | | |

| Primary Features | | | | | | | | | |
|---|---|---|---|---|---|---|---|---|---|
| Texture | Structure | Mineralogy (phenocrysts) | | | | | Mineralogy (matrix) | | |
| medium | | pl | kfs | qtz | opx | cpx | pl | kfs | qtz |
| grained | | | | 5% | | | | | |
| | | | | | | | | | |

| Fragments | | | | | | | | | | | | |
|---|---|---|---|---|---|---|---|---|---|---|---|---|
| Fragments | | | | | | | Morphology | | | | | |
| fel lith | maf lith | pheno | pum | scor | altd glass | unID | ireg | blky | rnd | ang | cusp | elong |
| | | | | | | | | | | | | |

| Secondary Features | | | | | | | | | | | | | |
|---|---|---|---|---|---|---|---|---|---|---|---|---|---|
| Texture | Structure | Mineralogy (porphyroblasts) | | | | | Mineralogy (matrix) | | | | | | |
| | | qtz | chl | ank | cal | act | ab | bt | ep | qtz | chl | ank | ser |
| | | | | | | 3% | | | | 35% | 25% | 15% | 30% |

| Comments |
|---|
| |
| |
| |

| Alteration | | | | | Mineralization | | | | | | | | | |
|---|---|---|---|---|---|---|---|---|---|---|---|---|---|---|
| Assemblage | | | | | Minerals | | | | | Form | | | | |
| sercn | chlcn | silcn | epi-qtz | epicn | mag | py | cp | hem | unID | dis | fract | vein | perv | pat |
| x | x | x | | | | | | 5% | 5% | x | x | | | |

---

| Sample | Major Unit | Rock type |
|---|---|---|
| 03-SMH- | mafic | massive |
| 0142-1 | volcanic | |
| | | |

| Primary Features | | | | | | | | | |
|---|---|---|---|---|---|---|---|---|---|
| Texture | Structure | Mineralogy (phenocrysts) | | | | | Mineralogy (matrix) | | |
| medium | | pl | kfs | qtz | opx | cpx | pl | kfs | qtz |
| grained | | | | | | | | | |
| | | | | | | | | | |

| Fragments | | | | | | | | | | | | |
|---|---|---|---|---|---|---|---|---|---|---|---|---|
| Fragments | | | | | | | Morphology | | | | | |
| fel lith | maf lith | pheno | pum | scor | altd glass | unID | ireg | blky | rnd | ang | cusp | elong |
| | | | | | | | | | | | | |

| Secondary Features | | | | | | | | | | | | | |
|---|---|---|---|---|---|---|---|---|---|---|---|---|---|
| Texture | Structure | Mineralogy (porphyroblasts) | | | | | Mineralogy (matrix) | | | | | | |
| | | qtz | chl | ank | cal | act | ab | bt | ep | qtz | chl | ank | ser |
| | | | | | | | | | 20% | 5% | | 65% | |

| Comments |
|---|
| |
| |
| |

| Alteration | | | | | Mineralization | | | | | | | | | |
|---|---|---|---|---|---|---|---|---|---|---|---|---|---|---|
| Assemblage | | | | | Minerals | | | | | Form | | | | |
| carbn | chlcn | silcn | epi-qtz | epicn | mag | py | cp | hem | unID | dis | fract | vein | perv | pat |
| x | | | | x | | | | | 10% | x | | | | |

| Sample | Major Unit | Rock type |
|---|---|---|
| 04-SMH- | mafic | basalt |
| 0015-2 | volcanic | |

| Primary Features | | | | | | | | | |
|---|---|---|---|---|---|---|---|---|---|
| Texture | Structure | Mineralogy (phenocrysts) | | | | | Mineralogy (matrix) | | |
| diabasic | | pl | kfs | qtz | opx | cpx | pl | kfs | qtz |
| medium | | 45-50% | | | | | | | |
| grained | | | | | | | | | |

| Fragments | | | | | | | | | | | | |
|---|---|---|---|---|---|---|---|---|---|---|---|---|
| Fragments | | | | | | | Morphology | | | | | |
| fel lith | maf lith | pheno | pum | scor | altd glass | unID | mtx | blky | rnd | ang | cusp | elong |
| | | | | | | | | | | | | |

| Secondary Features | | | | | | | | | | | | |
|---|---|---|---|---|---|---|---|---|---|---|---|---|
| Texture | Structure | Mineralogy (porphyroblasts) | | | | | | Mineralogy (matrix) | | | | |
| | | qtz | chl | ank | act | ab | bt | ep | qtz | chl | ank | ser |
| | | | | | | | | | | 25-30% | 20-25% | |

| Comments |
|---|
| very massive |

| Alteration | | | | | Mineralization | | | | | | | | | |
|---|---|---|---|---|---|---|---|---|---|---|---|---|---|---|
| Assemblage | | | | | Minerals | | | | | Form | | | | |
| carbn | chlcn | silcn | epi-qtz | epicn | mag | py | cp | hem | unID | dis | fract | vein | perv | pat |
| x | x | | | | | | | | 3-5% | x | | | | |

| Sample | Major Unit | Rock type |
|---|---|---|
| 03-SMH- | mafic | pillow |
| 0005-1 | volcanic | breccia |

| Primary Features | | | | | | | | | |
|---|---|---|---|---|---|---|---|---|---|
| Texture | Structure | Mineralogy (phenocrysts) | | | | | Mineralogy (matrix) | | |
| fine | <1% qtz | pl | kfs | qtz | opx | cpx | pl | kfs | qtz |
| grained | amygs | | | | | | | | 30% |
| | brecciated | | | | | | | | |

| Fragments | | | | | | | | | | | | |
|---|---|---|---|---|---|---|---|---|---|---|---|---|
| Fragments | | | | | | | Morphology | | | | | |
| fel lith | maf lith | pheno | pum | scor | altd glass | unID | ireg | blky | rnd | ang | cusp | elong |
| | | | | 1-5% | 3-5% | | x | | | | x | |

| Secondary Features | | | | | | | | | | | | | |
|---|---|---|---|---|---|---|---|---|---|---|---|---|---|
| Texture | Structure | Mineralogy (porphyroblasts) | | | | | | Mineralogy (matrix) | | | | | |
| fractured | | qtz | chl | ank | cal | act | ab | bt | ep | qtz | chl | ank | ser |
| | | | | | | | | | 50% | | 7-10% | | 1-3% |

| Comments |
|---|
| sulphide in fractures and disseminated throughout |
| quartz veins with associated mineralization |

| Alteration | | | | | Mineralization | | | | | | | | | |
|---|---|---|---|---|---|---|---|---|---|---|---|---|---|---|
| Assemblage | | | | | Minerals | | | | | Form | | | | |
| sercn | chlcn | silcn | epi-qtz | epicn | mag | py | cp | hem | unID | dis | fract | vein | perv | pat |
| x | x | | | | | 5-7% | 1-3% | | 1-3% | x | x | | | |

| Sample | Major Unit | Rock type |
|---|---|---|
| 04-SMH | mafic | peperite |
| 0001-1 | volcanic and | |
| | intrusive | |

| Primary Features | | | | | | | | | |
|---|---|---|---|---|---|---|---|---|---|
| Texture | Structure | Mineralogy (phenocrysts) | | | | | Mineralogy (matrix) | | |
| fine | <1% qtz | pl | kfs | qtz | opx | cpx | pl | kfs | qtz |
| grained | amygs | | | | | | 40% | | |
| | | | | | | | | | |

| Fragments | | | | | | | | | | | | |
|---|---|---|---|---|---|---|---|---|---|---|---|---|
| Fragments | | | | | | | Morphology | | | | | |
| fel lith | maf lith | pheno | pum | scor | altd glass | unID | mtx | blky | rnd | ang | cusp | elong |
| | | | | | | | | | | | | |

| Secondary Features | | | | | | | | | | | | |
|---|---|---|---|---|---|---|---|---|---|---|---|---|
| Texture | Structure | Mineralogy (porphyroblasts) | | | | | | Mineralogy (matrix) | | | | |
| | | qtz | chl | ank | act | ab | bt | ep | qtz | chl | ank | ser |
| | | | | | | | | 50% | | 5% | 1% | 5% |

| Comments |
|---|
| intrusion is finer grained than volcanic, but similar |
| in composition |

| Alteration | | | | | Mineralization | | | | | | | | | |
|---|---|---|---|---|---|---|---|---|---|---|---|---|---|---|
| Assemblage | | | | | Minerals | | | | | Form | | | | |
| sercn | chlcn | silcn | epi-qtz | epicn | mag | py | cp | hem | unID | dis | fract | vein | perv | pat |
| x | | | | x | | | | | 1% | x | | | | |

## Mafic Intrusive Rocks

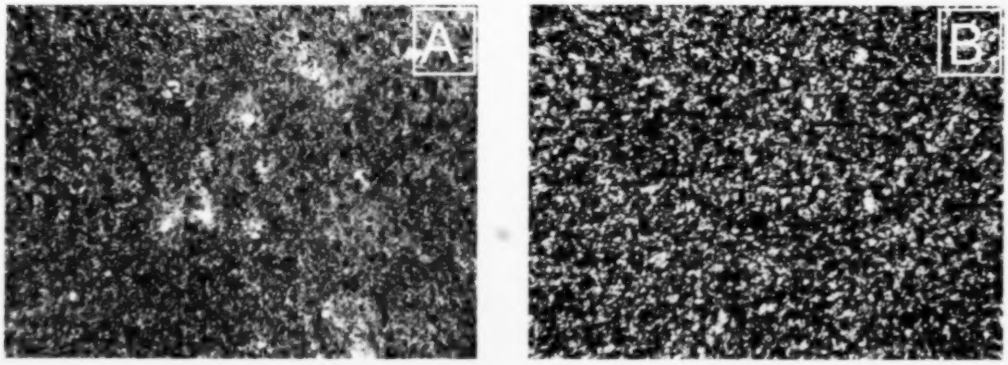

**Photo 51.** A) Photomicrograph of medium-grained mafic intrusion in crossed polarized light. Sample 03-SMH-0007. B) Photomicrograph of coarse-grained mafic intrusion in crossed polarized light. Sample 03-SMH-0107-2. Field of view is approximately 22 mm.

| Sample | Major Unit | Rock type |
|---|---|---|
| 03-SMH- | mafic | sill |
| 0007 | intrusion | |
| | | |

| Primary Features | | | | | | | | | |
|---|---|---|---|---|---|---|---|---|---|
| Texture | Structure | Mineralogy (phenocrysts) | | | | | Mineralogy (matrix) | | |
| fine | 5-10% | pl | kfs | qtz | opx | cpx | pl | kfs | qtz |
| grained | qtz | 5-10% | | 5% | | | | | |
| sph? | amygs | | | | | | | | |

| Fragments | | | | | | | | | | | | | |
|---|---|---|---|---|---|---|---|---|---|---|---|---|---|
| Fragments | | | | | | | Morphology | | | | | | |
| fel lith | maf lith | pheno | pum | scor | altd glass | unID | ireg | blky | rnd | ang | cusp | elong |
| | | | | | | | | | | | | | |

| Secondary Features | | | | | | | | | | | | | |
|---|---|---|---|---|---|---|---|---|---|---|---|---|---|
| Texture | Structure | Mineralogy (porphyroblasts) | | | | | | Mineralogy (matrix) | | | | | |
| | | qtz | chl | ank | cal | act | ab | bt | ep | qtz | chl | ank | ser |
| | | | | | | | | | 30% | | 10% | 45% | |

| Comments |
|---|
| feldspars highly carbonate altered |
| carbonate partly altered to hematite |
| possible spherulites (5%) |

| Alteration | | | | | Mineralization | | | | | | | | | |
|---|---|---|---|---|---|---|---|---|---|---|---|---|---|---|
| Assemblage | | | | | Minerals | | | | | Form | | | | |
| carbn | chlcn | silcn | epi-qtz | epicn | mag | py | cp | hem | unID | dis | fract | vein | perv | pat |
| x | | x | | x | | | | | 1-3% | x | | | | |

| Sample | Major Unit | Rock type |
|---|---|---|
| 03-SMH- | mafic | dikes/ |
| 0107-2 | intrusion | sills |
| | | gabbro |

| Primary Features | | | | | | | | | |
|---|---|---|---|---|---|---|---|---|---|
| Texture | Structure | Mineralogy (phenocrysts) | | | | | Mineralogy (matrix) | | |
| medium | | pl | kfs | qtz | opx | cpx | pl | kfs | qtz |
| grained | | 1-5% | | 3% | | | | | 5% |
| 1-3% sph | | | | | | | | | |

| Fragments | | | | | | | | | | | | | |
|---|---|---|---|---|---|---|---|---|---|---|---|---|---|
| Fragments | | | | | | | Morphology | | | | | | |
| fel lith | maf lith | pheno | pum | scor | altd glass | unID | ireg | blky | rnd | ang | cusp | elong |
| | | | | | | | | | | | | | |

| Secondary Features | | | | | | | | | | | | | |
|---|---|---|---|---|---|---|---|---|---|---|---|---|---|
| Texture | Structure | Mineralogy (porphyroblasts) | | | | | | Mineralogy (matrix) | | | | | |
| | | qtz | chl | ank | cal | act | ab | bt | ep | qtz | chl | ank | ser |
| | | | | | | | | | 30% | | 10-12% | 50% | |

| Comments |
|---|
| most primary minerals are altered |
| anhedral qtz phenocrysts |
| |

| Alteration | | | | | Mineralization | | | | | | | | | |
|---|---|---|---|---|---|---|---|---|---|---|---|---|---|---|
| Assemblage | | | | | Minerals | | | | | Form | | | | |
| carbn | chlcn | silcn | epi-qtz | epicn | mag | py | cp | hem | unID | dis | fract | vein | perv | pat |
| x | | | | x | | 3-5% | | | | x | | | | |

| Sample | Major Unit | Rock type |
|---|---|---|
| 04-SMH- | mafic | gabbro |
| 0050-1 | intrusion | |
| | | |

| Primary Features | | | | | | | | | |
|---|---|---|---|---|---|---|---|---|---|
| Texture | Structure | Mineralogy (phenocrysts) | | | | | Mineralogy (matrix) | | |
| coarse | | pl | kfs | qtz | opx | cpx | pl | kfs | qtz |
| grained | | 40% | | | | | | | |
| | | | | | | | | | |

| Fragments | | | | | | | | | | | | | |
|---|---|---|---|---|---|---|---|---|---|---|---|---|---|
| Fragments | | | | | | | Morphology | | | | | | |
| fel lith | maf lith | pheno | pum | scor | altd glass | unID | mtx | blky | rnd | ang | cusp | elong |
| | | | | | | | | | | | | | |

| Secondary Features | | | | | | | | | | | | | |
|---|---|---|---|---|---|---|---|---|---|---|---|---|---|
| Texture | Structure | Mineralogy (porphyroblasts) | | | | | | Mineralogy (matrix) | | | | | |
| | | qtz | chl | ank | act | ab | bt | ep | qtz | chl | ank | ser |
| | | | | 30% | | | | 30% | | | | |

| Comments |
|---|
| |
| |
| |

| Alteration | | | | | Mineralization | | | | | | | | | |
|---|---|---|---|---|---|---|---|---|---|---|---|---|---|---|
| Assemblage | | | | | Minerals | | | | | Form | | | | |
| sercn | chlcn | silcn | epi-qtz | epicn | mag | py | cp | hem | unID | dis | fract | vein | perv | pat |
| | | | | x | | 3% | | | | x | | | | |

## Intermediate Intrusive Rocks

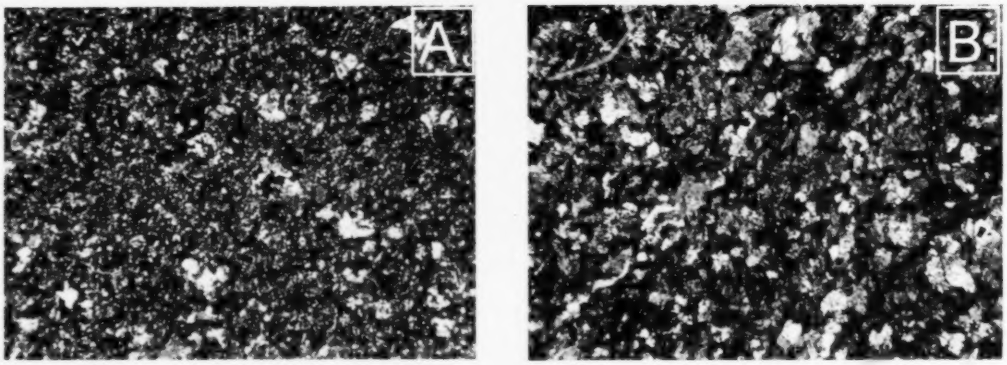

**Photo 52.** A) Photomicrograph of medium-grained intermediate intrusion in crossed polarized light. Sample 03-SMH-0089-2. B) Photomicrograph of coarse-grained intermediate intrusion in crossed polarized light. Sample 04-SMH-0023-2. Field of view is approximately 22 mm.

| Sample | Major Unit | Rock type |
|---|---|---|
| 03-SMH- | ntermediat | dikes/sills |
| 0087-1 | intrusive | |
| | | |

| Primary Features | | | | | | | | | |
|---|---|---|---|---|---|---|---|---|---|
| Texture | Structure | Mineralogy (phenocrysts) | | | | | Mineralogy (matrix) | | |
| medium | | pl | kfs | qtz | opx | cpx | pl | kfs | qtz |
| grained | | 10-15% | | 35-40% | | | | | |
| 5-7% sph | | | | | | | | | |

| Fragments | | | | | | | | | | | | |
|---|---|---|---|---|---|---|---|---|---|---|---|---|
| Fragments | | | | | | | Morphology | | | | | |
| fel lith | maf lith | pheno | pum | scor | altd glass | unID | ireg | blky | rnd | ang | cusp | elong |
| | | | | | | | | | | | | |

| Secondary Features | | | | | | | | | | | | | |
|---|---|---|---|---|---|---|---|---|---|---|---|---|---|
| Texture | Structure | Mineralogy (porphyroblasts) | | | | | | Mineralogy (matrix) | | | | | |
| | | qtz | chl | ank | cal | act | ab | bt | ep | qtz | chl | ank | ser |
| | | | | | | | | | | 5% | 40% | 5% | 5% |

| Comments |
|---|
| sericitized and chloritized feldspar phenocrysts |
| highly fractured, anhedral qtz phenocrysts |
| |

| Alteration | | | | | Mineralization | | | | | | | | | |
|---|---|---|---|---|---|---|---|---|---|---|---|---|---|---|
| Assemblage | | | | | Minerals | | | | | Form | | | | |
| sercn | chlcn | silcn | epi-qtz | epicn | mag | py | cp | hem | unID | dis | fract | vein | perv | pat |
| | x | x | | | | | | | | | | | | |

| Sample | Major Unit | Rock type |
|---|---|---|
| 03-SMH- | ntermediat | dike/sill |
| 0089-2 | intrusion | |
| | | |

| Primary Features | | | | | | | | | |
|---|---|---|---|---|---|---|---|---|---|
| Texture | Structure | Mineralogy (phenocrysts) | | | | | Mineralogy (matrix) | | |
| fine to | 5% qtz | pl | kfs | qtz | opx | cpx | pl | kfs | qtz |
| medium | amygs | | | | | | | | 45% |
| grained | | | | | | | | | |

| Fragments | | | | | | | | | | | | |
|---|---|---|---|---|---|---|---|---|---|---|---|---|
| Fragments | | | | | | | Morphology | | | | | |
| fel lith | maf lith | pheno | pum | scor | altd glass | unID | ireg | blky | rnd | ang | cusp | elong |
| | | | | | | | | | | | | |

| Secondary Features | | | | | | | | | | | | | |
|---|---|---|---|---|---|---|---|---|---|---|---|---|---|
| Texture | Structure | Mineralogy (porphyroblasts) | | | | | | Mineralogy (matrix) | | | | | |
| | | qtz | chl | ank | cal | act | ab | bt | ep | qtz | chl | ank | ser |
| | | | | | | | | | | | 20% | | 30% |

| Comments |
|---|
| |
| |
| |

| Alteration | | | | | Mineralization | | | | | | | | | |
|---|---|---|---|---|---|---|---|---|---|---|---|---|---|---|
| Assemblage | | | | | Minerals | | | | | Form | | | | |
| sercn | chlcn | silcn | epi-qtz | epicn | mag | py | cp | hem | unID | dis | fract | vein | perv | pat |
| x | x | | | | | | | | | | | | | |

| Sample | Major Unit | Rock type |
|---|---|---|
| 04-SMH- | ntermediat | quartz |
| 0023-2 | intrusion | diorite |
| | | |

| Primary Features | | | | | | | | | |
|---|---|---|---|---|---|---|---|---|---|
| Texture | Structure | Mineralogy (phenocrysts) | | | | | Mineralogy (matrix) | | |
| coarse | | pl | kfs | qtz | opx | cpx | pl | kfs | qtz |
| grained | | 10-15% | | 25-30% | 5-10% | | | | |
| | | | | | | | | | |

| Fragments | | | | | | | | | | | | |
|---|---|---|---|---|---|---|---|---|---|---|---|---|
| Fragments | | | | | | | Morphology | | | | | |
| fel lith | maf lith | pheno | pum | scor | altd glass | unID | mtx | blky | rnd | ang | cusp | elong |
| | | | | | | | | | | | | |

| Secondary Features | | | | | | | | | | | | |
|---|---|---|---|---|---|---|---|---|---|---|---|---|
| Texture | Structure | Mineralogy (porphyroblasts) | | | | | | Mineralogy (matrix) | | | | |
| | | qtz | chl | ank | act | ab | bt | ep | qtz | chl | ank | ser |
| | | | | | | | | | | 25-30% | | 30-35% |

| Comments |
|---|
| most plagioclase of pyroxene has been altered |
| |
| |

| Alteration | | | | | Mineralization | | | | | | | | | |
|---|---|---|---|---|---|---|---|---|---|---|---|---|---|---|
| Assemblage | | | | | Minerals | | | | | Form | | | | |
| sercn | chlcn | silcn | epi-qtz | epicn | mag | py | cp | hem | unID | dis | fract | vein | perv | pat |
| | | | | | | 1-3% | | | | x | | | | |

## Volcaniclastic and Epiclastic Rocks

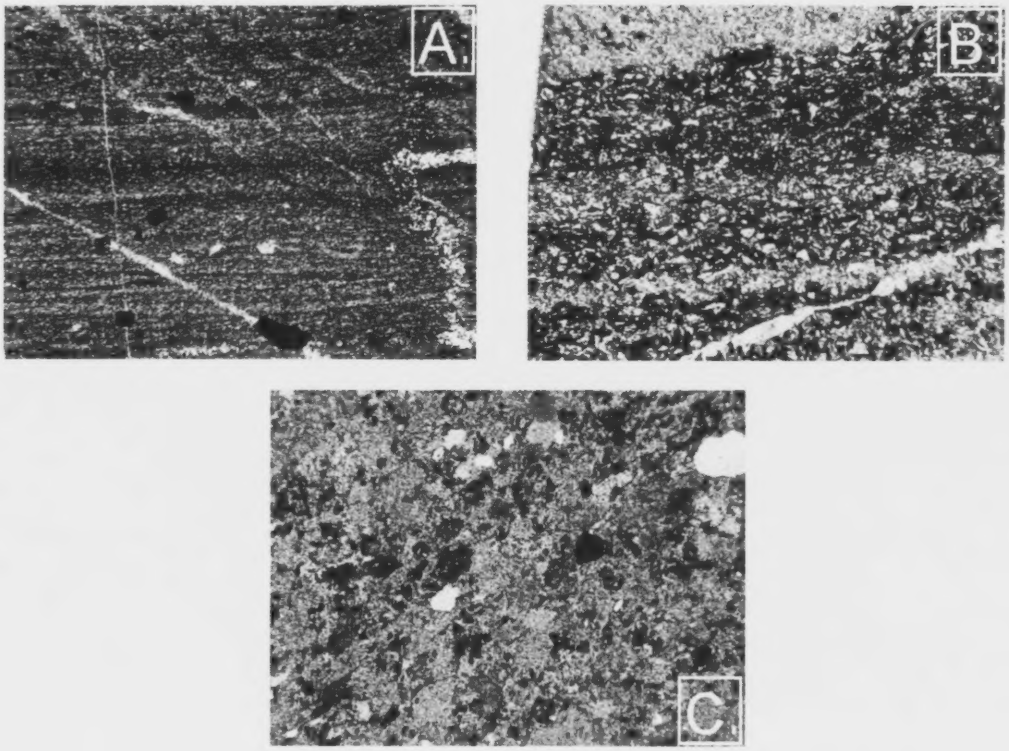

**Photo 53.** A) Photomicrograph of finely laminated mudstone in plane polarized light. Sample 04-SMH-0017-4. B) Photomicrograph of bedded tuff in plane polarized light. Sample 04-SMH-0005-3. C) Photomicrograph of polymict lapilli-tuff in crossed polarized light. Sample 04-SMH-0026-1. Field of view is approximately 22 mm.

| Sample | Major Unit | Rock type |
|---|---|---|
| 04-SMH- | epiclastic | mudstone |
| 0017-4 | sediments | |
| | | |

| Primary Features | | | | | | | | | | |
|---|---|---|---|---|---|---|---|---|---|---|
| Texture | Structure | Mineralogy (phenocrysts) | | | | | Mineralogy (matrix) | | |
| | | pl | kfs | qtz | opx | cpx | ash | mud | qtz |
| fine | laminated | | | | | | | | |
| grained | normally | | | | | | 75-80% | 20-25% | |
| | graded | | | | | | | | |

| Fragments | | | | | | | | | | | | |
|---|---|---|---|---|---|---|---|---|---|---|---|---|
| Fragments | | | | | | | Morphology | | | | | |
| fel lith | maf lith | pheno | pum | scor | altd glass | unID | mtx | blky | rnd | ang | cusp | elong |
| | | | | | | | | | | | | |

| Secondary Features | | | | | | | | | | | | |
|---|---|---|---|---|---|---|---|---|---|---|---|---|
| Texture | Structure | Mineralogy (porphyroblasts) | | | | | | Mineralogy (matrix) | | | | |
| | | qtz | chl | ank | act | ab | bt | ep | qtz | chl | ank | ser |
| | | | | | | | | | | | | |

| Comments |
|---|
| layers have different proportions of ash/mud |
| each lamination is graded from ash to mud |
| |

| Alteration | | | | | Mineralization | | | | | | | | | |
|---|---|---|---|---|---|---|---|---|---|---|---|---|---|---|
| Assemblage | | | | | Minerals | | | | | Form | | | | |
| sercn | chlcn | silcn | epi-qtz | epicn | mag | py | cp | hem | unID | dis | fract | vein | perv | pat |
| | | | | | | 1-5% | | | | x | | | | |

| Sample | Major Unit | Rock type |
|---|---|---|
| 04-SMH- | volcaniclastic | lapilli |
| 0005-3 | sediment | tuff |
| | | |

| Primary Features | | | | | | | | | |
|---|---|---|---|---|---|---|---|---|---|
| Texture | Structure | Mineralogy (phenocrysts) | | | | | Mineralogy (matrix) | | |
| | | pl | kfs | qtz | opx | cpx | mud | kfs | qtz |
| fine | bedded | | | | | | | | |
| grained | graded | | | | | | 5-10% | | |
| | | | | | | | | | |

| Fragments | | | | | | | | | | | | |
|---|---|---|---|---|---|---|---|---|---|---|---|---|
| Fragments | | | | | | | Morphology | | | | | |
| fel lith | maf lith | pheno | pum | scor | altd glass | unID | mtx | blky | rnd | ang | cusp | elong |
| 90-95% | | 1-3% | | | | | | x | | x | x | |

| Secondary Features | | | | | | | | | | | | |
|---|---|---|---|---|---|---|---|---|---|---|---|---|
| Texture | Structure | Mineralogy (porphyroblasts) | | | | | | Mineralogy (matrix) | | | | |
| | | qtz | chl | ank | act | ab | bt | ep | qtz | chl | ank | ser |
| | | | | | | | | | | | | |

| Comments |
|---|
| laminations are felsic ash in mud matrix |
| layers vary by composition, % frags, size of frags |
| |

| Alteration | | | | | Mineralization | | | | | | | | | |
|---|---|---|---|---|---|---|---|---|---|---|---|---|---|---|
| Assemblage | | | | | Minerals | | | | | Form | | | | |
| sercn | chlcn | silcn | epi-qtz | epicn | sph | py | cp | hem | unID | dis | fract | vein | perv | pat |
| | | | | | <1% | | | | | x | | | | |

| Sample | Major Unit | Rock type |
|---|---|---|
| 04-SMH- | volcaniclastic | lapilli |
| 0026-1 | sediments | tuff |
| | | |

| Primary Features | | | | | | | | | |
|---|---|---|---|---|---|---|---|---|---|
| Texture | Structure | Mineralogy (phenocrysts) | | | | | Mineralogy (matrix) | | |
| | | pl | kfs | qtz | opx | cpx | pl | kfs | qtz |
| poly | | | | | | | | | |
| mict | | | | 5-10% | | | | | |
| | | | | | | | | | |

| Fragments | | | | | | | | | | | | |
|---|---|---|---|---|---|---|---|---|---|---|---|---|
| Fragments | | | | | | | Morphology | | | | | |
| fel lith | maf lith | pheno | pum | scor | altd glass | unID | mtx | blky | rnd | ang | cusp | elong |
| 5-10% | 25-30% | | | | | | | x | x | | | |

| Secondary Features | | | | | | | | | | | | |
|---|---|---|---|---|---|---|---|---|---|---|---|---|
| Texture | Structure | Mineralogy (porphyroblasts) | | | | | | Mineralogy (matrix) | | | | |
| | | qtz | chl | ank | act | ab | bt | ep | qtz | chl | ank | ser |
| | | | | | | | | | | | | 60-65% |

| Comments |
|---|
| |
| |
| |

| Alteration | | | | | Mineralization | | | | | | | | | |
|---|---|---|---|---|---|---|---|---|---|---|---|---|---|---|
| Assemblage | | | | | Minerals | | | | | Form | | | | |
| sercn | chlcn | silcn | epi-qtz | epicn | mag | py | cp | hem | unID | dis | fract | vein | perv | pat |
| x | | | | | | 1-3% | | | | x | | | | |

## Late Diabase Intrusive (Matachewan) Rocks

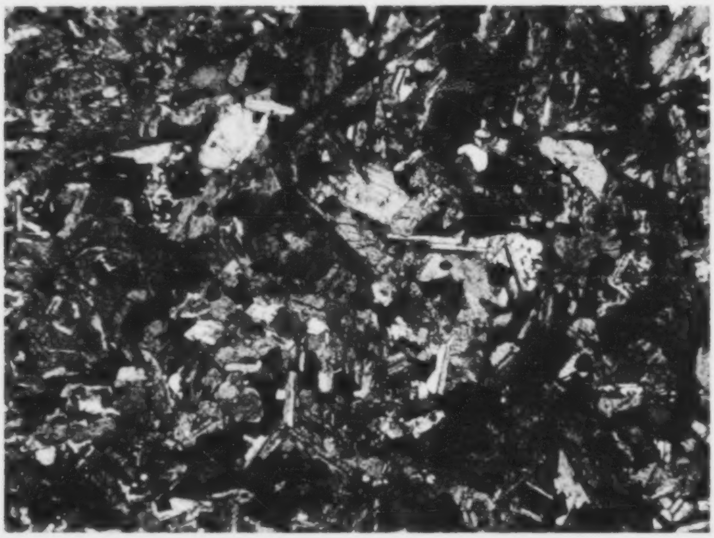

**Photo 54.** Photomicrograph of coarse-grained Matachewan diabase intrusion in crossed polarized light. Sample 03-SMH-0022. Field of view is approximately 22 mm.

| Sample | Major Unit | Rock type |
|---|---|---|
| 03-SMH-0022 | diabase | dikes/sills |

| Primary Features | | | | | | | | | |
|---|---|---|---|---|---|---|---|---|---|
| Texture | Structure | Mineralogy (phenocrysts) | | | | | Mineralogy (matrix) | | |
| | | pl | kfs | qtz | opx | cpx | pl | kfs | qtz |
| coarse grained | | 50-55% | | 5-7% | | 20-25% | | | |

| Fragments | | | | | | | | | | | | |
|---|---|---|---|---|---|---|---|---|---|---|---|---|
| Fragments | | | | | | | Morphology | | | | | |
| fel lith | maf lith | pheno | pum | scor | altd glass | unID | ireg | blky | rnd | ang | cusp | elong |
| | | | | | | | | | | | | |

| Secondary Features | | | | | | | | | | | | | |
|---|---|---|---|---|---|---|---|---|---|---|---|---|---|
| Texture | Structure | Mineralogy (porphyroblasts) | | | | | Mineralogy (matrix) | | | | | | |
| | | qtz | chl | ank | cal | act | ab | bt | ep | qtz | chl | ank | ser |
| | | | | | | | | | 3% | | 3% | | 10% |

| Comments |
|---|
| pl partially altered to ser |
| Matachewan dike |

| Alteration | | | | | Mineralization | | | | | | | | | |
|---|---|---|---|---|---|---|---|---|---|---|---|---|---|---|
| Assemblage | | | | | Minerals | | | | | Form | | | | |
| sercn | chlcn | silcn | epi-qtz | epicn | mag | py | cp | hem | unID | dis | fract | vein | perv | pat |
| x | | | | | | x | | | 5-10% | | | | | |

This page left blank intentionally

# Appendix 2

## Drill Hole Identifications

During the course of this project, 18 diamond drill holes from Falconbridge Ltd. and 9 diamond drill holes from Explorers Alliance were examined. Descriptions of these holes are available on MRD 144, as are accompanying digital photographs.

**Appendix 2.** Original drill hole ID and new drill hole ID for this project.

| Company | Original Hole ID | New Hole ID for This Project |
|---|---|---|
| Falconbridge | G32-25 | 04-SMH-0001 |
| Falconbridge | G22-14 | 04-SMH-0002 |
| Falconbridge | G22-15 | 04-SMH-0003 |
| Falconbridge | G32-29 | 04-SMH-0004 |
| Falconbridge | G22-12 | 04-SMH-0005 |
| Explorers Alliance | EGG32-36 | 04-SMH-0006 |
| Explorers Alliance | EGG32-35 | 04-SMH-0007 |
| Explorers Alliance | EGG32-34 | 04-SMH-0008 |
| Explorers Alliance | EGG32-33 | 04-SMH-0009 |
| Explorers Alliance | EGG32-30 | 04-SMH-0010 |
| Explorers Alliance | EGG32-31 | 04-SMH-0011 |
| Explorers Alliance | EGG32-32 | 04-SMH-0012 |
| Explorers Alliance | EGG32-32A | 04-SMH-0013 |
| Explorers Alliance | EGG51-26 | 04-SMH-0014 |
| Falconbridge | G22-11 | 04-SMH-0015 |
| Falconbridge | G32-28 | 04-SMH-0016 |
| Falconbridge | G22-16 | 04-SMH-0017 |
| Falconbridge | G33-15 | 04-SMH-0018 |
| Falconbridge | G22-13 | 04-SMH-0019 |
| Falconbridge | G33-13 | 04-SMH-0020 |
| Falconbridge | G32-27 | 04-SMH-0021 |
| Falconbridge | G33-14 | 04-SMH-0022 |
| Falconbridge | G32-26 | 04-SMH-0023 |
| Falconbridge | G32-10 | 04-SMH-0024 |
| Falconbridge | G23-02 | 04-SMH-0025 |
| Falconbridge | G23-03 | 04-SMH-0026 |
| Falconbridge | G22-01 | 04-SMH-0027 |
| Explorers Alliance | 6G-04-2 | 04-SMH-0085 |

# Appendix 3

## Listing of Geochemical Data from the Genex Mine Area

All analyses by Geoscience Laboratories, Ontario Geological Survey and by Activation Laboratories Limited. Digital versions of geochemical data are available on MRD 144. Precision and accuracy information can be found in MacDonald, Piercey and Hamilton (2005).

**Appendix 3**. Listing of geochemical data from the Genex mine area.

| Sample No. | Description | $SiO_2$ wt % | $TiO_2$ wt % | $Al_2O_3$ wt % | $Fe_2O_3$ wt % | FeO wt % | MnO wt % | MgO wt % |
|---|---|---|---|---|---|---|---|---|
| **03-SMH-0001H** | **Footwall Mafic Volcanic** | 60.52 | 1.85 | 12.50 | 7.09 | 6.38 | 0.12 | 3.22 |
| **03-SMH-0001I** | **Footwall Mafic Volcanic** | 56.09 | 2.06 | 14.84 | 11.54 | 10.38 | 0.17 | 3.28 |
| **03-SMH-0003D** | **Footwall Mafic Volcanic** | 73.55 | 1.26 | 6.69 | 8.81 | 7.93 | 0.07 | 5.27 |
| **03-SMH-0005A** | **Footwall Mafic Volcanic** | 51.72 | 1.45 | 10.20 | 23.40 | 21.06 | 0.17 | 5.93 |
| **03-SMH-0008C** | **Footwall Mafic Volcanic** | 81.08 | 1.46 | 6.20 | 4.83 | 4.35 | 0.07 | 1.23 |
| **03-SMH-0008G** | **Footwall Mafic Volcanic** | 52.48 | 1.71 | 11.80 | 15.16 | 13.64 | 0.15 | 4.69 |
| **03-SMH-0009-1** | **Footwall Mafic Volcanic** | 58.81 | 1.61 | 10.84 | 18.99 | 17.09 | 0.08 | 5.11 |
| **03-SMH-0011A** | **Footwall Mafic Volcanic** | 71.66 | 0.81 | 9.56 | 6.82 | 6.14 | 0.06 | 6.25 |
| **03-SMH-0011C** | **Footwall Mafic Volcanic** | 69.58 | 0.83 | 10.77 | 5.19 | 4.67 | 0.12 | 6.77 |
| **03-SMH-0012** | **Footwall Mafic Volcanic** | 48.39 | 1.39 | 13.43 | 13.52 | 12.17 | 0.07 | 9.61 |
| **03-SMH-0016** | **Footwall Mafic Volcanic** | 36.33 | 2.31 | 16.66 | 23.14 | 20.82 | 0.29 | 8.05 |
| **03-SMH-0020-2** | **Footwall Mafic Volcanic** | 71.05 | 1.57 | 11.69 | 5.31 | 4.78 | 0.04 | 3.42 |
| **03-SMH-0021-1** | **Footwall Mafic Volcanic** | 65.86 | 1.30 | 16.19 | 4.73 | 4.26 | 0.03 | 3.82 |
| **03-SMH-0050-1** | **Footwall Mafic Volcanic** | 61.17 | 1.06 | 14.71 | 11.67 | 10.50 | 0.09 | 7.99 |
| **03-SMH-0057-2** | **Footwall Mafic Volcanic** | 53.34 | 2.24 | 14.60 | 11.57 | 10.41 | 0.22 | 2.52 |
| **03-SMH-0057-3** | **Footwall Mafic Volcanic** | 53.63 | 1.90 | 13.29 | 14.20 | 12.78 | 0.22 | 4.52 |
| **03-SMH-0060** | **Footwall Mafic Volcanic** | 56.73 | 1.76 | 12.40 | 10.83 | 9.74 | 0.26 | 2.92 |
| **03-SMH-0064-2** | **Footwall Mafic Volcanic** | 65.02 | 1.06 | 12.88 | 9.52 | 8.57 | 0.04 | 6.54 |
| **03-SMH-0068-1** | **Footwall Mafic Volcanic** | 69.22 | 0.98 | 12.72 | 4.84 | 4.36 | 0.05 | 6.09 |
| **03-SMH-0069** | **Footwall Mafic Volcanic** | 54.01 | 2.21 | 15.17 | 11.22 | 10.10 | 0.21 | 4.23 |
| **03-SMH-0073** | **Footwall Mafic Volcanic** | 56.72 | 0.96 | 12.89 | 8.88 | 7.99 | 0.13 | 3.87 |
| **03-SMH-0075-1** | **Footwall Mafic Volcanic** | 69.42 | 1.82 | 12.39 | 4.62 | 4.16 | 0.06 | 1.31 |
| **03-SMH-0076** | **Footwall Mafic Volcanic** | 66.14 | 0.93 | 12.21 | 13.56 | 12.20 | 0.10 | 2.53 |
| **03-SMH-0082-2** | **Footwall Mafic Volcanic** | 61.03 | 0.99 | 13.02 | 9.38 | 8.44 | 0.18 | 6.88 |
| **03-SMH-0083-1** | **Footwall Mafic Volcanic** | 57.85 | 1.63 | 12.62 | 9.18 | 8.26 | 0.19 | 6.74 |
| **03-SMH-0084-2** | **Footwall Mafic Volcanic** | 55.77 | 1.73 | 13.02 | 16.52 | 14.86 | 0.07 | 6.48 |
| **03-SMH-0093** | **Footwall Mafic Volcanic** | 73.40 | 1.21 | 10.28 | 6.99 | 6.29 | 0.04 | 2.35 |
| **03-SMH-0095-1** | **Footwall Mafic Volcanic** | 62.75 | 1.59 | 11.20 | 15.09 | 13.58 | 0.07 | 4.42 |
| **03-SMH-0128** | **Footwall Mafic Volcanic** | 70.62 | 1.71 | 13.04 | 5.58 | 5.02 | 0.02 | 2.06 |
| **03-SMH-0153** | **Footwall Mafic Volcanic** | 54.84 | 1.34 | 17.32 | 10.64 | 9.57 | 0.15 | 6.66 |
| **03-SMH-0154-2** | **Footwall Mafic Volcanic** | 55.89 | 1.21 | 12.51 | 10.29 | 9.26 | 0.29 | 5.53 |
| **03-SMH-0156-1** | **Footwall Mafic Volcanic** | 65.52 | 0.71 | 9.63 | 7.32 | 6.59 | 0.11 | 5.36 |
| **03-SMH-0164** | **Footwall Mafic Volcanic** | 73.93 | 0.72 | 9.98 | 9.42 | 8.48 | 0.05 | 2.64 |
| **03-SMH-0167** | **Footwall Mafic Volcanic** | 58.90 | 1.37 | 11.82 | 9.33 | 8.40 | 0.34 | 2.25 |
| **03-SMH-0175-3** | **Footwall Mafic Volcanic** | 65.24 | 1.47 | 11.72 | 12.74 | 11.46 | 0.05 | 3.65 |
| **03-SMH-077-1** | **Footwall Mafic Volcanic** | 68.31 | 0.81 | 10.37 | 8.56 | 7.70 | 0.05 | 6.89 |
| **04-SMH-0002-7** | **Footwall Mafic Volcanic** | 57.88 | 1.55 | 12.72 | 11.98 | 10.78 | 0.24 | 4.26 |
| **04-SMH-0002-8** | **Footwall Mafic Volcanic** | 55.67 | 0.98 | 13.02 | 6.58 | 5.92 | 0.21 | 1.52 |
| **04-SMH-0003-6** | **Footwall Mafic Volcanic** | 53.22 | 1.98 | 13.58 | 13.10 | 11.79 | 0.21 | 3.77 |
| **04-SMH-0006-1** | **Footwall Mafic Volcanic** | 62.25 | 1.81 | 13.34 | 6.98 | 6.28 | 0.12 | 5.69 |
| **04-SMH-0009-2** | **Footwall Mafic Volcanic** | 64.87 | 1.11 | 10.50 | 8.10 | 7.29 | 0.05 | 8.74 |
| **04-SMH-0009-3** | **Footwall Mafic Volcanic** | 27.52 | 0.45 | 22.86 | 18.21 | 16.39 | 0.08 | 19.22 |
| **04-SMH-0009-5** | **Footwall Mafic Volcanic** | 62.23 | 1.14 | 15.30 | 8.93 | 8.04 | 0.05 | 6.05 |
| **04-SMH-0010-2** | **Footwall Mafic Volcanic** | 59.15 | 1.69 | 12.91 | 12.26 | 11.03 | 0.14 | 6.65 |
| **04-SMH-0014-1** | **Footwall Mafic Volcanic** | 45.22 | 1.22 | 12.68 | 14.03 | 12.62 | 0.24 | 7.53 |

**Abbreviations:** N.D. = not detected. N.M. = not measured/analyzed.

**Appendix 3**. Listing of geochemical data from the Genex mine area -- continued.

| Sample No. | CaO wt % | $Na_2O$ wt % | $K_2O$ wt % | $P_2O_5$ wt % | LOI wt % | Total wt % | Ti ppm | Mn ppm | Na ppm | K ppm |
|---|---|---|---|---|---|---|---|---|---|---|
| **03-SMH-0001H** | 5.07 | 3.92 | 0.91 | 0.20 | 4.87 | 100.27 | 11343 | 1033 | 29926 | 7585 |
| **03-SMH-0001I** | 4.50 | 4.97 | 0.04 | 0.22 | 2.57 | 100.28 | 12008 | 1532 | 40680 | 277 |
| **03-SMH-0003D** | 0.50 | 0.08 | 0.25 | 0.07 | 3.35 | 99.90 | 7094 | 593 | 64.0 | 1990 |
| **03-SMH-0005A** | 0.81 | N.D. | 0.12 | 0.11 | 6.10 | 100.01 | 7759 | 1343 | 394 | 873 |
| **03-SMH-0008C** | 0.02 | 0.22 | 1.61 | 0.02 | 2.60 | 99.34 | 8411 | 527 | 1220 | 12082 |
| **03-SMH-0008G** | 4.99 | 2.72 | 0.03 | 0.14 | 6.70 | 100.57 | 9278 | 1226 | 16229 | 266 |
| **03-SMH-0009-1** | 0.25 | 0.05 | 0.04 | 0.12 | 4.47 | 100.37 | N.M. | N.M. | N.M. | N.M. |
| **03-SMH-0011A** | 0.14 | 0.07 | 1.01 | 0.09 | 4.25 | 100.72 | 4996 | 496 | 469 | 8182 |
| **03-SMH-0011C** | 0.90 | 0.61 | 1.43 | 0.10 | 4.55 | 100.85 | 5171 | 1069 | 3988 | 11707 |
| **03-SMH-0012** | 4.37 | 1.28 | 0.31 | 0.10 | 9.33 | 101.80 | 8354 | 595 | 3106 | 2378 |
| **03-SMH-0016** | 8.43 | 0.17 | 0.03 | 0.18 | 5.81 | 101.40 | 13877 | 2599 | 1481 | 252 |
| **03-SMH-0020-2** | 0.39 | N.D. | 3.48 | 0.13 | 3.24 | 100.32 | 10110 | 332 | 151 | >13500 |
| **03-SMH-0021-1** | 0.46 | 0.18 | 4.11 | 0.29 | 3.55 | 100.52 | 8322 | 316 | 1824 | >13500 |
| **03-SMH-0050-1** | 0.36 | 0.29 | 1.15 | 0.27 | 1.63 | 100.39 | N.M. | N.M. | N.M. | N.M. |
| **03-SMH-0057-2** | 8.32 | 4.21 | 0.07 | 0.24 | 3.88 | 101.21 | 12281 | 1906 | 36657 | 628 |
| **03-SMH-0057-3** | 7.34 | 2.42 | 0.02 | 0.17 | 4.40 | 102.11 | 10611 | 1923 | 19870 | 231 |
| **03-SMH-0060** | 5.65 | 4.64 | 0.05 | 0.20 | 3.96 | 99.40 | 9727 | 2029 | 33832 | 412 |
| **03-SMH-0064-2** | 0.34 | N.D. | 1.40 | 0.23 | 4.23 | 101.26 | 6416 | 353 | N.D. | 11579 |
| **03-SMH-0068-1** | 0.57 | 0.35 | 2.69 | 0.17 | 3.18 | 100.86 | 6246 | 462 | 2706 | >13500 |
| **03-SMH-0069** | 4.65 | 4.78 | 0.19 | 0.23 | 3.48 | 100.38 | 11181 | 1709 | 33269 | 1484 |
| **03-SMH-0073** | 4.36 | 5.83 | 0.08 | 0.20 | 5.79 | 99.71 | 5561 | 1016 | 43261 | 685 |
| **03-SMH-0075-1** | 3.27 | 5.66 | 0.10 | 0.22 | 1.55 | 100.42 | N.M. | N.M. | N.M. | N.M. |
| **03-SMH-0076** | 0.38 | 0.03 | 1.69 | 0.24 | 3.23 | 101.04 | 4913 | 850 | 300 | >13500 |
| **03-SMH-0082-2** | 4.48 | 1.02 | 1.11 | 0.22 | 2.99 | 101.30 | 5906 | 1452 | 3948 | 8791 |
| **03-SMH-0083-1** | 2.04 | 0.86 | 1.57 | 0.51 | 5.77 | 98.96 | N.M. | N.M. | N.M. | N.M. |
| **03-SMH-0084-2** | 0.61 | 0.07 | 0.76 | 0.49 | 5.43 | 100.95 | 10048 | 595 | N.D. | 6250 |
| **03-SMH-0093** | 0.71 | 0.01 | 2.05 | 0.45 | 2.68 | 100.17 | 6881 | 356 | 421 | >13500 |
| **03-SMH-0095-1** | 0.08 | 0.15 | 0.90 | 0.08 | 4.19 | 100.52 | N.M. | N.M. | N.M. | N.M. |
| **03-SMH-0128** | 0.72 | 0.13 | 3.34 | 0.47 | 2.81 | 100.50 | 9660 | 200 | 144 | >13500 |
| **03-SMH-0153** | 1.30 | 1.13 | 3.17 | 0.23 | 4.06 | 100.84 | 8196 | 1310 | 3582 | >13500 |
| **03-SMH-0154-2** | 8.82 | 1.84 | 1.25 | 0.13 | 3.62 | 101.38 | 7414 | 2408 | 9516 | 10406 |
| **03-SMH-0156-1** | 2.95 | 0.10 | 1.38 | 0.19 | 6.76 | 100.03 | N.M. | N.M. | N.M. | N.M. |
| **03-SMH-0164** | 0.23 | 0.03 | 1.37 | 0.16 | 2.75 | 101.28 | 4351 | 437 | 303 | 12240 |
| **03-SMH-0167** | 6.36 | 2.87 | 0.97 | 0.47 | 6.08 | 100.76 | 7188 | 2674 | 20241 | 8630 |
| **03-SMH-0175-3** | 0.60 | 0.06 | 1.14 | 0.40 | 3.91 | 100.98 | 9059 | 468 | N.D. | 9478 |
| **03-SMH-077-1** | 0.24 | 0.08 | 0.74 | 0.19 | 3.79 | 100.03 | N.M. | N.M. | N.M. | N.M. |
| **04-SMH-0002-7** | 1.64 | 0.11 | 3.03 | 0.48 | 5.63 | 99.52 | N.M. | N.M. | N.M. | N.M. |
| **04-SMH-0002-8** | 8.37 | 4.02 | 1.59 | 0.22 | 8.16 | 100.34 | N.M. | N.M. | N.M. | N.M. |
| **04-SMH-0003-6** | 5.46 | 3.17 | 0.14 | 0.23 | 4.99 | 99.85 | N.M. | N.M. | N.M. | N.M. |
| **04-SMH-0006-1** | 1.78 | 0.43 | 1.98 | 0.43 | 5.43 | 100.24 | N.M. | N.M. | N.M. | N.M. |
| **04-SMH-0009-2** | 0.27 | 0.07 | 0.39 | 0.14 | 4.71 | 98.95 | N.M. | N.M. | N.M. | N.M. |
| **04-SMH-0009-3** | 0.16 | 0.06 | 0.70 | 0.09 | 9.93 | 99.28 | N.M. | N.M. | N.M. | N.M. |
| **04-SMH-0009-5** | 0.35 | 0.13 | 2.36 | 0.27 | 4.13 | 100.94 | N.M. | N.M. | N.M. | N.M. |
| **04-SMH-0010-2** | 0.60 | 0.09 | 1.29 | 0.44 | 4.32 | 99.54 | N.M. | N.M. | N.M. | N.M. |
| **04-SMH-0014-1** | 6.24 | 2.33 | 0.20 | 0.12 | 8.86 | 98.67 | N.M. | N.M. | N.M. | N.M. |

**Abbreviations:** N.D. = not detected. N.M. = not measured/analyzed.

**Appendix 3**. Listing of geochemical data from the Genex mine area -- continued.

| Sample No. | P<br>ppm | Cr<br>ppm | Co<br>ppm | Ni<br>ppm | Cu<br>ppm | Sc<br>ppm | V<br>ppm | Pb<br>ppm | Zn<br>ppm | As<br>ppm |
|---|---|---|---|---|---|---|---|---|---|---|
| **03-SMH-0001H** | 843 | 36.0 | 29.0 | 12.0 | 27.0 | 63.0 | 405 | N.D. | 142 | 17.0 |
| **03-SMH-0001I** | 979 | 28.0 | 51.0 | 17.0 | 59.0 | 60.0 | 444 | N.D. | 126 | 19.0 |
| **03-SMH-0003D** | 218 | 27.0 | 38.0 | 9.0 | 3.0 | 34.0 | 211 | 239 | 369 | 20.0 |
| **03-SMH-0005A** | 503 | 41.0 | 50.0 | 15.0 | 574 | 36.0 | 222 | 28.0 | 1531 | 18.0 |
| **03-SMH-0008C** | 31.0 | 19.0 | 44.0 | 7.0 | 421 | 43.0 | 130 | 375 | >3000 | 118 |
| **03-SMH-0008G** | 584 | 49.0 | 29.0 | 11.0 | 34.0 | 61.0 | 404 | 5.0 | 121 | 5.0 |
| **03-SMH-0009-1** | N.M. | -8.0 | N.M. | -4.0 | N.M. | N.M. | 406 | N.M. | N.M. | N.M. |
| **03-SMH-0011A** | 347 | 20.0 | N.D. | 6.0 | 18.0 | 36.0 | 49.0 | 9.0 | 165 | 1.0 |
| **03-SMH-0011C** | 432 | 15.0 | 21.0 | 9.0 | 77.0 | 45.0 | 50.0 | 6.0 | 1062 | 1.0 |
| **03-SMH-0012** | 420 | 124 | 53.0 | 36.0 | 82.0 | 65.0 | 318 | 7.0 | 94.0 | N.D. |
| **03-SMH-0016** | 728 | 61.0 | 67.0 | 22.0 | 32.0 | 86.0 | 515 | 6.0 | 247 | 17.0 |
| **03-SMH-0020-2** | 557 | 42.0 | N.D. | 6.0 | 61.0 | 58.0 | 271 | 8.0 | 236 | N.D. |
| **03-SMH-0021-1** | 1400 | 30.0 | N.D. | 14.0 | 9.0 | 58.0 | 96.0 | 8.0 | 130 | N.D. |
| **03-SMH-0050-1** | N.M. | 36.0 | N.M. | 12.0 | N.M. | N.M. | 137 | N.M. | N.M. | N.M. |
| **03-SMH-0057-2** | 989 | 26.0 | 52.0 | 28.0 | 16.0 | 56.0 | 497 | 6.0 | 121 | 14.0 |
| **03-SMH-0057-3** | 776 | 14.0 | 33.0 | 15.0 | 23.0 | 49.0 | 398 | N.D. | 121 | 6.0 |
| **03-SMH-0060** | 888 | 11.0 | 37.0 | 13.0 | 26.0 | 46.0 | 307 | N.D. | 87.0 | 2.0 |
| **03-SMH-0064-2** | 990 | N.D. | 17.0 | 16.0 | 15.0 | 32.0 | 118 | N.D. | 204 | 3.0 |
| **03-SMH-0068-1** | 710 | 25.0 | N.D. | 11.0 | 5.0 | 32.0 | 50.0 | 15.0 | 88.0 | 2.0 |
| **03-SMH-0069** | 975 | 28.0 | 50.0 | 15.0 | 37.0 | 40.0 | 468 | N.D. | 141 | 2.0 |
| **03-SMH-0073** | 765 | 23.0 | 60.0 | 19.0 | 33.0 | 31.0 | 56.0 | 15.0 | 83.0 | 5.0 |
| **03-SMH-0075-1** | N.M. | -8.0 | N.M. | 7.0 | N.M. | N.M. | 326 | N.M. | N.M. | N.M. |
| **03-SMH-0076** | 1061 | 23.0 | 14.0 | 16.0 | 31.0 | 30.0 | 68.0 | 8.0 | 569 | 6.0 |
| **03-SMH-0082-2** | 929 | 29.0 | 25.0 | 18.0 | 20.0 | 22.0 | 60.0 | 7.0 | 131 | 2.0 |
| **03-SMH-0083-1** | N.M. | -8.0 | N.M. | -4.0 | N.M. | N.M. | 97.0 | N.M. | N.M. | N.M. |
| **03-SMH-0084-2** | 2195 | 6.0 | 20.0 | 6.0 | 29.0 | 29.0 | 12.0 | 79.0 | 384 | 18.0 |
| **03-SMH-0093** | 1920 | N.D. | N.D. | 4.0 | 14.0 | 35.0 | 31.0 | 8.0 | 119 | 1.0 |
| **03-SMH-0095-1** | N.M. | 8.0 | N.M. | 5.0 | N.M. | N.M. | 331 | N.M. | N.M. | N.M. |
| **03-SMH-0128** | 2822 | 15.0 | N.D. | 5.0 | 3.0 | 55.0 | 46.0 | 6.0 | 84.0 | 5.0 |
| **03-SMH-0153** | 1251 | 44.0 | 34.0 | 22.0 | 49.0 | 47.0 | 95.0 | N.D. | 302 | 7.0 |
| **03-SMH-0154-2** | 643 | 102 | 44.0 | 23.0 | 80.0 | 76.0 | 319 | 6.0 | 68.0 | N.D. |
| **03-SMH-0156-1** | N.M. | -8.0 | N.M. | 10.0 | N.M. | N.M. | 105 | N.M. | N.M. | N.M. |
| **03-SMH-0164** | 911 | 38.0 | 18.0 | 9.0 | 167 | 35.0 | 58.0 | 9.0 | 192 | 12.0 |
| **03-SMH-0167** | 2733 | N.D. | 33.0 | 7.0 | 21.0 | 48.0 | N.D. | 7.0 | 98.0 | 2.0 |
| **03-SMH-0175-3** | 2341 | 15.0 | N.D. | 4.0 | 26.0 | 45.0 | N.D. | 8.0 | 141 | 27.0 |
| **03-SMH-077-1** | N.M. | 18.0 | N.M. | 9.0 | N.M. | N.M. | 106 | N.M. | N.M. | N.M. |
| **04-SMH-0002-7** | N.M. | <8 | N.M. | <4 | N.M. | N.M. | 57.0 | N.M. | N.M. | N.M. |
| **04-SMH-0002-8** | N.M. | -8.0 | N.M. | 7.0 | N.M. | N.M. | 115 | N.M. | N.M. | N.M. |
| **04-SMH-0003-6** | N.M. | 14.0 | N.M. | 9.0 | N.M. | N.M. | 438 | N.M. | N.M. | N.M. |
| **04-SMH-0006-1** | N.M. | <8 | N.M. | <4 | N.M. | N.M. | 102 | N.M. | N.M. | N.M. |
| **04-SMH-0009-2** | N.M. | 31.0 | N.M. | 26.0 | N.M. | N.M. | 227 | N.M. | N.M. | N.M. |
| **04-SMH-0009-3** | N.M. | 35.0 | N.M. | 41.0 | N.M. | N.M. | 166 | N.M. | N.M. | N.M. |
| **04-SMH-0009-5** | N.M. | 10.0 | N.M. | 14.0 | N.M. | N.M. | 130 | N.M. | N.M. | N.M. |
| **04-SMH-0010-2** | N.M. | <8 | N.M. | <4 | N.M. | N.M. | 100 | N.M. | N.M. | N.M. |
| **04-SMH-0014-1** | N.M. | 108 | N.M. | 52.0 | N.M. | N.M. | 334 | N.M. | N.M. | N.M. |

**Abbreviations:** N.D. = not detected. N.M. = not measured/analyzed.

**Appendix 3**. Listing of geochemical data from the Genex mine area -- continued.

| Sample No. | Rb<br>ppm | Cs<br>ppm | Ba<br>ppm | Sr<br>ppm | Ga<br>ppm | Ta<br>ppm | Nb<br>ppm | Hf<br>ppm | Zr<br>ppm | Y<br>ppm |
|---|---|---|---|---|---|---|---|---|---|---|
| **03-SMH-0001H** | 23.07 | 0.271 | 374 | 30.6 | 21.0 | 0.65 | 7.1 | 4.6 | 171.2 | 39.95 |
| **03-SMH-0001I** | 0.43 | 0.030 | 41.0 | 196.8 | 24.0 | 0.66 | 7.8 | 5.0 | 188.6 | 37.0 |
| **03-SMH-0003D** | 6.90 | 0.315 | 56.0 | 5.2 | 26.0 | 0.46 | 4.9 | 3.1 | 114.7 | 66.22 |
| **03-SMH-0005A** | 2.75 | 0.256 | N.D. | 9.0 | 28.0 | 0.49 | 4.8 | 3.4 | 128.8 | 24.26 |
| **03-SMH-0008C** | 35.62 | 0.387 | 328 | 3.8 | 25.0 | 0.53 | 6.0 | 3.7 | 137.8 | 75.5 |
| **03-SMH-0008G** | 0.79 | 0.052 | 36.0 | 99.1 | 23.0 | 0.56 | 6.4 | 4.0 | 150.8 | 30.87 |
| **03-SMH-0009-1** | 2.38 | 0.107 | N.M. | 5.6 | N.M. | 0.42 | 6.6 | 4.2 | 159.3 | 41.5 |
| **03-SMH-0011A** | 20.83 | 0.267 | 203 | 6.2 | 17.0 | 0.63 | 7.2 | 4.9 | 198.5 | 16.14 |
| **03-SMH-0011C** | 30.88 | 0.396 | 264 | 14.0 | 17.0 | 0.65 | 7.7 | 5.1 | 209.3 | 25.56 |
| **03-SMH-0012** | 7.25 | 0.105 | 59.0 | 38.9 | 17.0 | 0.42 | 3.9 | 2.6 | 94.4 | 22.75 |
| **03-SMH-0016** | 1.49 | 0.118 | 50.0 | 392.9 | 45.0 | 0.74 | 9.0 | 5.8 | 217.1 | 64.21 |
| **03-SMH-0020-2** | 65.98 | 0.991 | 497 | 5.2 | 22.0 | 0.61 | 8.1 | 4.2 | 155.8 | 9.93 |
| **03-SMH-0021-1** | 50.83 | 0.805 | 982 | 15.5 | 25.0 | 0.97 | 12.3 | 8.4 | 332.5 | 27.03 |
| **03-SMH-0050-1** | 22.52 | 0.454 | N.M. | 9.2 | N.M. | 0.72 | 10.7 | 7.6 | 309.7 | 48.5 |
| **03-SMH-0057-2** | 1.12 | 0.037 | 69.0 | 267 | 26.0 | 0.73 | 8.7 | 5.7 | 210.6 | 50.25 |
| **03-SMH-0057-3** | 0.45 | 0.034 | N.D. | 187.2 | 22.0 | 0.65 | 7.6 | 4.9 | 179.7 | 43.51 |
| **03-SMH-0060** | 1.25 | 0.375 | N.D. | 65.6 | 19.0 | 0.49 | 6.9 | 4.5 | 165.9 | 38.38 |
| **03-SMH-0064-2** | 21.57 | 0.149 | 476 | 5.0 | 19.0 | 0.70 | 9.9 | 6.7 | 273.2 | 45.57 |
| **03-SMH-0068-1** | 47.71 | 0.707 | 414 | 24.2 | 19.0 | 0.68 | 9.6 | 6.4 | 256 | 34.81 |
| **03-SMH-0069** | 4.70 | 0.223 | 110 | 108.1 | 26.0 | 0.58 | 8.1 | 5.4 | 203.5 | 47.21 |
| **03-SMH-0073** | 1.48 | 0.034 | 33.0 | 137.3 | 16.0 | 0.65 | 9.0 | 6.1 | 240.7 | 39.91 |
| **03-SMH-0075-1** | 1.22 | 0.048 | N.M. | 43.8 | N.M. | 0.47 | 7.4 | 4.6 | 184.7 | 36.2 |
| **03-SMH-0076** | 29.37 | 0.329 | 275 | 8.6 | 18.0 | 0.62 | 8.7 | 6.0 | 235.8 | 32.26 |
| **03-SMH-0082-2** | 23.55 | 0.650 | 246 | 64.3 | 20.0 | 0.68 | 9.4 | 6.3 | 245.5 | 35.1 |
| **03-SMH-0083-1** | 30.46 | 0.310 | N.M. | 40.5 | N.M. | 0.63 | 9.4 | 5.6 | 226.6 | 43.32 |
| **03-SMH-0084-2** | 10.56 | 0.105 | 107 | 8.8 | 22.0 | 0.68 | 10.0 | 5.7 | 228.1 | 46.53 |
| **03-SMH-0093** | 32.33 | 0.291 | 329 | 10.4 | 20.0 | 0.58 | 8.1 | 4.9 | 191.3 | 34.36 |
| **03-SMH-0095-1** | 16.68 | 0.200 | N.M. | 4.0 | N.M. | 0.40 | 6.2 | 3.9 | 151.3 | 35.38 |
| **03-SMH-0128** | 30.91 | 0.504 | 486 | 19.4 | 23.0 | 0.73 | 10.1 | 6.2 | 236.6 | 26.99 |
| **03-SMH-0153** | 42.27 | 1.285 | 350 | 88.2 | 26.0 | 0.85 | 12.2 | 8.1 | 313.2 | 39.59 |
| **03-SMH-0154-2** | 31.75 | 0.907 | 483 | 123.3 | 16.0 | 0.28 | 3.7 | 2.6 | 94.9 | 36.04 |
| **03-SMH-0156-1** | 40.58 | 0.549 | N.M. | 60.4 | N.M. | 0.43 | 6.2 | 4.3 | 170.7 | 24.24 |
| **03-SMH-0164** | 24.96 | 0.325 | 275 | 8.0 | 21.0 | 0.57 | 7.3 | 4.6 | 171.8 | 21.17 |
| **03-SMH-0167** | 41.79 | 0.788 | 841 | 116.1 | 17.0 | 0.63 | 9.0 | 5.4 | 212.3 | 35.67 |
| **03-SMH-0175-3** | 14.85 | 0.120 | 274 | 6.1 | 23.0 | 0.58 | 8.5 | 5.1 | 195.9 | 29.58 |
| **03-SMH-077-1** | 15.16 | 0.243 | N.M. | 5.4 | N.M. | 0.52 | 7.9 | 5.3 | 217.8 | 50.24 |
| **04-SMH-0002-7** | 57.79 | 1.200 | N.M. | 48.0 | N.M. | 0.65 | 9.9 | 5.8 | 230.5 | 23.41 |
| **04-SMH-0002-8** | 53.80 | 0.762 | N.M. | 127.3 | N.M. | 0.64 | 9.0 | 5.7 | 232.1 | 40.89 |
| **04-SMH-0003-6** | 3.07 | 0.288 | N.M. | 173.8 | N.M. | 0.50 | 7.7 | 4.9 | 185 | 40.4 |
| **04-SMH-0006-1** | 40.04 | 0.603 | N.M. | 45.9 | N.M. | 0.67 | 10.3 | 6.0 | 237 | 27.91 |
| **04-SMH-0009-2** | 7.37 | 0.235 | N.M. | 5.4 | N.M. | 0.40 | 6.2 | 3.5 | 133.3 | 14.04 |
| **04-SMH-0009-3** | 14.18 | 0.359 | N.M. | 3.7 | N.M. | 1.49 | 15.0 | 11.0 | 375.1 | 28.74 |
| **04-SMH-0009-5** | 44.98 | 0.522 | N.M. | 8.7 | N.M. | 0.72 | 10.8 | 7.2 | 295 | 36.57 |
| **04-SMH-0010-2** | 27.07 | 0.335 | N.M. | 13.7 | N.M. | 0.63 | 9.6 | 5.7 | 226.5 | 31.06 |
| **04-SMH-0014-1** | 4.58 | 0.460 | N.M. | 78.4 | N.M. | 0.24 | 3.8 | 2.5 | 94.3 | 26.96 |

**Abbreviations:** N.D. = not detected. N.M. = not measured/analyzed.

**Appendix 3**. Listing of geochemical data from the Genex mine area -- continued.

| Sample No. | Th<br>ppm | U<br>ppm | La<br>ppm | Ce<br>ppm | Pr<br>ppm | Nd<br>ppm | Sm<br>ppm | Eu<br>ppm | Gd<br>ppm | Tb<br>ppm |
|---|---|---|---|---|---|---|---|---|---|---|
| **03-SMH-0001H** | 1.69 | 0.461 | 14.88 | 34.31 | 4.709 | 21.07 | 5.58 | 1.782 | 6.692 | 1.125 |
| **03-SMH-0001I** | 1.80 | 0.491 | 14.61 | 35.66 | 4.89 | 22.04 | 5.94 | 1.926 | 6.867 | 1.163 |
| **03-SMH-0003D** | 1.15 | 0.495 | >100.00 | >200.00 | >25.000 | >100.00 | >30.00 | 1.825 | >20.000 | 3.564 |
| **03-SMH-0005A** | 1.24 | 0.35 | 10.65 | 25.46 | 3.449 | 15.44 | 4.1 | 0.992 | 4.675 | 0.769 |
| **03-SMH-0008C** | 1.31 | 0.744 | 22.22 | 53.7 | 7.056 | 31.32 | 8.45 | 0.675 | 11.241 | 2.1 |
| **03-SMH-0008G** | 1.46 | 0.39 | 10.56 | 25.44 | 3.451 | 15.87 | 4.47 | 1.905 | 5.38 | 0.906 |
| **03-SMH-0009-1** | 1.51 | 0.412 | 13.42 | 31.98 | 4.331 | 19.56 | 5.3 | 1.429 | 6.527 | 1.105 |
| **03-SMH-0011A** | 2.03 | 0.565 | 2.65 | 6.33 | 0.895 | 4.23 | 1.25 | 0.335 | 1.774 | 0.331 |
| **03-SMH-0011C** | 2.60 | 0.631 | 7.14 | 16.17 | 2.298 | 10.66 | 2.83 | 0.676 | 3.239 | 0.563 |
| **03-SMH-0012** | 0.63 | 0.169 | 10.12 | 24.92 | 3.438 | 15.32 | 3.88 | 1.222 | 4.092 | 0.666 |
| **03-SMH-0016** | 2.06 | 0.593 | 18.49 | 43.45 | 5.999 | 27.45 | 7.31 | 3.088 | 9.077 | 1.559 |
| **03-SMH-0020-2** | 0.66 | 0.458 | 2.72 | 6.48 | 0.896 | 4.38 | 1.26 | 0.299 | 1.604 | 0.267 |
| **03-SMH-0021-1** | 2.34 | 0.937 | 4.52 | 11.44 | 1.675 | 8.03 | 2.32 | 0.539 | 3.276 | 0.616 |
| **03-SMH-0050-1** | 3.28 | 0.831 | 27.62 | 64.0 | 8.435 | 36.18 | 8.34 | 1.3 | 8.713 | 1.398 |
| **03-SMH-0057-2** | 2.05 | 0.543 | 17.37 | 42.0 | 5.842 | 26.71 | 6.91 | 2.209 | 8.329 | 1.412 |
| **03-SMH-0057-3** | 1.76 | 0.476 | 13.3 | 32.34 | 4.525 | 20.76 | 5.65 | 1.817 | 6.809 | 1.169 |
| **03-SMH-0060** | 1.64 | 0.442 | 12.79 | 31.57 | 4.282 | 19.88 | 5.21 | 1.434 | 6.516 | 1.096 |
| **03-SMH-0064-2** | 3.04 | 0.757 | 13.26 | 32.99 | 4.512 | 20.02 | 5.2 | 0.551 | 6.77 | 1.222 |
| **03-SMH-0068-1** | 2.84 | 0.74 | 20.34 | 48.15 | 6.301 | 26.88 | 6.0 | 1.701 | 6.301 | 1.017 |
| **03-SMH-0069** | 1.94 | 0.502 | 16.66 | 39.81 | 5.401 | 25 | 6.54 | 2.032 | 7.845 | 1.317 |
| **03-SMH-0073** | 2.78 | 0.773 | 20.38 | 49.36 | 6.506 | 28.05 | 6.53 | 1.642 | 7.206 | 1.169 |
| **03-SMH-0075-1** | 1.66 | 0.488 | 14.75 | 35.27 | 4.749 | 21.4 | 5.44 | 1.64 | 6.235 | 1.021 |
| **03-SMH-0076** | 2.42 | 0.682 | 19.73 | 46.74 | 6.166 | 26.43 | 6.11 | 1.855 | 6.386 | 0.979 |
| **03-SMH-0082-2** | 2.98 | 0.764 | 21.67 | 50.79 | 6.694 | 28.95 | 6.8 | 1.75 | 6.903 | 1.056 |
| **03-SMH-0083-1** | 2.38 | 0.614 | 20.98 | 49.18 | 6.589 | 29.73 | 7.08 | 1.784 | 8.017 | 1.253 |
| **03-SMH-0084-2** | 3.06 | 0.646 | 40.6 | 95.59 | 12.759 | 55.64 | 12.16 | 4.988 | 10.759 | 1.489 |
| **03-SMH-0093** | 2.13 | 0.605 | 27.18 | 65.66 | 8.704 | 37.59 | 8.62 | 2.134 | 8.634 | 1.226 |
| **03-SMH-0095-1** | 1.41 | 0.372 | 12.19 | 29.43 | 4.015 | 17.87 | 4.36 | 1.173 | 5.237 | 0.924 |
| **03-SMH-0128** | 2.33 | 0.666 | 19.05 | 44.9 | 6.053 | 26.38 | 6.0 | 0.866 | 5.85 | 0.878 |
| **03-SMH-0153** | 3.13 | 0.917 | 25.91 | 58.58 | 7.513 | 31.84 | 7.38 | 1.693 | 7.659 | 1.195 |
| **03-SMH-0154-2** | 0.61 | 0.16 | 7.02 | 17.39 | 2.511 | 12.35 | 3.69 | 1.278 | 5.052 | 0.901 |
| **03-SMH-0156-1** | 1.90 | 0.551 | 6.64 | 15.89 | 2.179 | 10.3 | 2.86 | 0.77 | 3.569 | 0.599 |
| **03-SMH-0164** | 2.51 | 0.636 | 18.8 | 41.13 | 5.179 | 21.73 | 4.79 | 0.838 | 4.585 | 0.699 |
| **03-SMH-0167** | 2.26 | 0.631 | 17.07 | 40.03 | 5.405 | 24.61 | 6.04 | 1.676 | 6.87 | 1.112 |
| **03-SMH-0175-3** | 2.16 | 0.585 | 21.83 | 50.45 | 6.607 | 28.32 | 6.65 | 0.631 | 6.824 | 1.002 |
| **03-SMH-077-1** | 2.36 | 0.829 | 40.33 | 96.94 | 12.423 | 52.56 | 11.38 | 1.018 | 11.063 | 1.646 |
| **04-SMH-0002-7** | 1.66 | 0.644 | 20.07 | 47.03 | 6.236 | 27.0 | 5.81 | 1.501 | 5.101 | 0.717 |
| **04-SMH-0002-8** | 2.80 | 0.708 | 22.38 | 50.96 | 6.605 | 27.97 | 6.52 | 1.623 | 7.185 | 1.186 |
| **04-SMH-0003-6** | 1.80 | 0.462 | 14.49 | 35.21 | 4.857 | 22.29 | 5.85 | 1.767 | 6.889 | 1.184 |
| **04-SMH-0006-1** | 1.87 | 0.838 | 10.91 | 26.5 | 3.666 | 16.59 | 3.79 | 0.963 | 4.302 | 0.745 |
| **04-SMH-0009-2** | 1.45 | 0.368 | 2.25 | 5.98 | 0.886 | 4.4 | 1.4 | 0.382 | 1.908 | 0.334 |
| **04-SMH-0009-3** | 3.36 | 1.756 | 2.1 | 5.42 | 0.816 | 4.04 | 1.24 | 0.186 | 1.934 | 0.421 |
| **04-SMH-0009-5** | 2.43 | 0.826 | 22.45 | 56.07 | 7.523 | 32.25 | 6.98 | 0.797 | 6.824 | 1.073 |
| **04-SMH-0010-2** | 2.08 | 0.6 | 20.5 | 48.34 | 6.462 | 28.2 | 6.33 | 0.835 | 6.203 | 0.938 |
| **04-SMH-0014-1** | 0.58 | 0.148 | 7.48 | 17.9 | 2.619 | 12.53 | 3.45 | 1.25 | 4.324 | 0.717 |

**Abbreviations:** N.D. = not detected. N.M. = not measured/analyzed.

**Appendix 3**. Listing of geochemical data from the Genex mine area -- continued.

| Sample No. | Dy<br>ppm | Ho<br>ppm | Er<br>ppm | Tm<br>ppm | Yb<br>ppm | Lu<br>ppm |
|---|---|---|---|---|---|---|
| **03-SMH-0001H** | 7.126 | 1.479 | 4.35 | 0.626 | 3.97 | 0.594 |
| **03-SMH-0001I** | 7.289 | 1.492 | 4.259 | 0.617 | 4.05 | 0.592 |
| **03-SMH-0003D** | 16.607 | 2.785 | 6.591 | 0.793 | 4.7 | 0.617 |
| **03-SMH-0005A** | 4.728 | 0.968 | 2.828 | 0.426 | 2.84 | 0.424 |
| **03-SMH-0008C** | 14.173 | 3.004 | 8.362 | 1.126 | 6.64 | 0.882 |
| **03-SMH-0008G** | 5.723 | 1.209 | 3.563 | 0.526 | 3.52 | 0.528 |
| **03-SMH-0009-1** | 7.265 | 1.564 | 4.563 | 0.668 | 4.42 | 0.67 |
| **03-SMH-0011A** | 2.491 | 0.612 | 2.132 | 0.358 | 2.62 | 0.425 |
| **03-SMH-0011C** | 3.907 | 0.944 | 3.121 | 0.507 | 3.58 | 0.554 |
| **03-SMH-0012** | 4.132 | 0.88 | 2.655 | 0.388 | 2.54 | 0.383 |
| **03-SMH-0016** | 10.328 | 2.272 | 6.874 | 1.015 | 6.52 | 0.961 |
| **03-SMH-0020-2** | 1.712 | 0.396 | 1.335 | 0.22 | 1.61 | 0.27 |
| **03-SMH-0021-1** | 4.432 | 1.064 | 3.483 | 0.546 | 3.73 | 0.589 |
| **03-SMH-0050-1** | 8.638 | 1.769 | 5.246 | 0.778 | 5.14 | 0.776 |
| **03-SMH-0057-2** | 8.999 | 1.921 | 5.866 | 0.88 | 5.9 | 0.905 |
| **03-SMH-0057-3** | 7.507 | 1.627 | 4.871 | 0.725 | 4.71 | 0.721 |
| **03-SMH-0060** | 7.033 | 1.491 | 4.349 | 0.634 | 4.15 | 0.615 |
| **03-SMH-0064-2** | 7.918 | 1.695 | 5.156 | 0.761 | 4.9 | 0.753 |
| **03-SMH-0068-1** | 6.278 | 1.33 | 3.942 | 0.583 | 3.77 | 0.558 |
| **03-SMH-0069** | 8.377 | 1.785 | 5.288 | 0.766 | 4.94 | 0.738 |
| **03-SMH-0073** | 7.22 | 1.495 | 4.459 | 0.666 | 4.43 | 0.684 |
| **03-SMH-0075-1** | 6.546 | 1.365 | 3.919 | 0.586 | 3.79 | 0.56 |
| **03-SMH-0076** | 5.995 | 1.227 | 3.661 | 0.54 | 3.63 | 0.555 |
| **03-SMH-0082-2** | 6.367 | 1.334 | 3.984 | 0.6 | 4.04 | 0.619 |
| **03-SMH-0083-1** | 7.735 | 1.586 | 4.646 | 0.674 | 4.43 | 0.664 |
| **03-SMH-0084-2** | 8.423 | 1.708 | 4.971 | 0.723 | 4.81 | 0.737 |
| **03-SMH-0093** | 7.054 | 1.376 | 3.865 | 0.548 | 3.53 | 0.523 |
| **03-SMH-0095-1** | 6.084 | 1.296 | 3.888 | 0.567 | 3.72 | 0.567 |
| **03-SMH-0128** | 5.344 | 1.099 | 3.187 | 0.474 | 3.12 | 0.461 |
| **03-SMH-0153** | 7.261 | 1.527 | 4.49 | 0.675 | 4.48 | 0.691 |
| **03-SMH-0154-2** | 6.082 | 1.325 | 4.043 | 0.601 | 3.84 | 0.593 |
| **03-SMH-0156-1** | 4.029 | 0.901 | 2.932 | 0.449 | 3.07 | 0.478 |
| **03-SMH-0164** | 4.127 | 0.826 | 2.494 | 0.376 | 2.51 | 0.373 |
| **03-SMH-0167** | 6.86 | 1.403 | 4.124 | 0.598 | 3.81 | 0.559 |
| **03-SMH-0175-3** | 5.918 | 1.204 | 3.57 | 0.534 | 3.54 | 0.533 |
| **03-SMH-077-1** | 9.705 | 1.886 | 5.227 | 0.733 | 4.71 | 0.67 |
| **04-SMH-0002-7** | 4.219 | 0.845 | 2.541 | 0.369 | 2.52 | 0.384 |
| **04-SMH-0002-8** | 7.297 | 1.499 | 4.351 | 0.632 | 4.11 | 0.603 |
| **04-SMH-0003-6** | 7.442 | 1.59 | 4.645 | 0.704 | 4.58 | 0.693 |
| **04-SMH-0006-1** | 4.882 | 1.046 | 3.014 | 0.449 | 2.85 | 0.418 |
| **04-SMH-0009-2** | 2.34 | 0.523 | 1.689 | 0.278 | 2.0 | 0.321 |
| **04-SMH-0009-3** | 3.604 | 0.992 | 3.723 | 0.678 | 5.3 | 0.913 |
| **04-SMH-0009-5** | 6.632 | 1.335 | 3.85 | 0.551 | 3.44 | 0.479 |
| **04-SMH-0010-2** | 5.709 | 1.153 | 3.356 | 0.484 | 3.07 | 0.445 |
| **04-SMH-0014-1** | 4.627 | 0.971 | 2.908 | 0.429 | 2.8 | 0.42 |

**Abbreviations:** N.D. = not detected. N.M. = not measured/analyzed.

**Appendix 3**. Listing of geochemical data from the Genex mine area -- continued.

| Sample No. | Description | $SiO_2$ wt% | $TiO_2$ wt% | $Al_2O_3$ wt% | $Fe_2O_3$ wt% | FeO wt% | MnO wt% | MgO wt% |
|---|---|---|---|---|---|---|---|---|
| **04-SMH-0015-1** | **Footwall Mafic Volcanic** | 57.85 | 1.03 | 13.19 | 9.99 | 8.99 | 0.14 | 2.68 |
| **04-SMH-0015-2** | **Footwall Mafic Volcanic** | 57.22 | 1.14 | 14.42 | 7.95 | 7.15 | 0.09 | 2.74 |
| **04-SMH-0015-4** | **Footwall Mafic Volcanic** | 60.03 | 1.90 | 13.14 | 7.60 | 6.84 | 0.10 | 2.90 |
| **04-SMH-0016-1** | **Footwall Mafic Volcanic** | 65.26 | 0.97 | 12.19 | 8.02 | 7.22 | 0.11 | 2.41 |
| **04-SMH-0016-2** | **Footwall Mafic Volcanic** | 46.34 | 1.73 | 12.52 | 13.86 | 12.47 | 0.25 | 4.15 |
| **04-SMH-0016-3** | **Footwall Mafic Volcanic** | 51.97 | 1.86 | 12.38 | 12.11 | 10.90 | 0.27 | 3.73 |
| **04-SMH-0017-2** | **Footwall Mafic Volcanic** | 75.23 | 0.33 | 9.87 | 5.29 | 4.76 | 0.22 | 0.93 |
| **04-SMH-0019-4** | **Footwall Mafic Volcanic** | 60.95 | 0.97 | 13.31 | 10.41 | 9.37 | 0.05 | 4.69 |
| **03-SMH-0010-1** | **Footwall Mafic Volcanic** | 77.67 | 0.56 | 7.49 | 8.85 | 7.96 | 0.17 | 0.92 |
| | | | | | | | | |
| **03-SMH-0019-1** | **Hanging Wall Mafic Volcanic** | 57.14 | 1.48 | 11.14 | 21.74 | 19.56 | 0.48 | 2.61 |
| **03-SMH-0113** | **Hanging Wall Mafic Volcanic** | 53.30 | 1.60 | 12.33 | 11.51 | 10.36 | 0.41 | 2.04 |
| **03-SMH-0119-1** | **Hanging Wall Mafic Volcanic** | 54.96 | 0.78 | 10.70 | 6.35 | 5.71 | 0.26 | 1.50 |
| **03-SMH-0136** | **Hanging Wall Mafic Volcanic** | 50.50 | 1.56 | 16.06 | 13.96 | 12.56 | 0.30 | 6.36 |
| **03-SMH-0140-2** | **Hanging Wall Mafic Volcanic** | 52.31 | 1.59 | 16.08 | 11.74 | 10.56 | 0.42 | 2.67 |
| **03-SMH-0142-1** | **Hanging Wall Mafic Volcanic** | 56.38 | 1.86 | 14.00 | 10.70 | 9.63 | 0.30 | 1.64 |
| **03-SMH-0146** | **Hanging Wall Mafic Volcanic** | 57.21 | 1.04 | 13.72 | 7.99 | 7.19 | 0.18 | 1.81 |
| **03-SMH-0152** | **Hanging Wall Mafic Volcanic** | 59.57 | 0.98 | 12.90 | 6.97 | 6.27 | 0.17 | 1.26 |
| **04-SMH-0005-1** | **Hanging Wall Mafic Volcanic** | 60.95 | 1.09 | 13.38 | 10.30 | 9.27 | 0.16 | 2.62 |
| | | | | | | | | |
| **03-SMH-0014** | **Felsic Volcanic** | 75.48 | 0.27 | 12.18 | 2.97 | 2.67 | 0.02 | 3.20 |
| **03-SMH-0019-4** | **Felsic Volcanic** | 58.66 | 1.23 | 9.87 | 20.76 | 18.68 | 0.48 | 2.91 |
| **03-SMH-0025** | **Felsic Volcanic** | 80.31 | 0.16 | 8.58 | 2.49 | 2.24 | 0.01 | 3.47 |
| **03-SMH-0034-1** | **Felsic Volcanic** | 78.96 | 0.36 | 7.95 | 4.54 | 4.09 | 0.04 | 4.68 |
| **03-SMH-0034-2** | **Felsic Volcanic** | 87.25 | 0.15 | 6.39 | 1.78 | 1.60 | N.D. | 0.90 |
| **03-SMH-0037-1** | **Felsic Volcanic** | 81.63 | 0.18 | 8.65 | 1.73 | 1.56 | 0.01 | 1.31 |
| **03-SMH-0037-2** | **Felsic Volcanic** | 51.90 | 1.35 | 13.70 | 13.91 | 12.52 | 0.06 | 10.71 |
| **03-SMH-0040** | **Felsic Volcanic** | 52.60 | 1.27 | 12.42 | 16.44 | 14.79 | 0.10 | 9.78 |
| **03-SMH-0046-1** | **Felsic Volcanic** | 83.85 | 0.22 | 5.79 | 3.98 | 3.58 | 0.01 | 3.07 |
| **03-SMH-0056-1** | **Felsic Volcanic** | 84.46 | 0.22 | 8.05 | 2.46 | 2.21 | 0.01 | 0.93 |
| **03-SMH-0056-2** | **Felsic Volcanic** | 76.06 | 0.27 | 6.29 | 9.49 | 8.54 | 0.03 | 3.22 |
| **03-SMH-0063** | **Felsic Volcanic** | 71.69 | 0.47 | 12.82 | 5.72 | 5.15 | 0.04 | 3.61 |
| **03-SMH-0091** | **Felsic Volcanic** | 82.17 | 0.23 | 9.42 | 2.39 | 2.15 | 0.03 | 1.58 |
| **03-SMH-0102-2** | **Felsic Volcanic** | 78.09 | 0.35 | 6.81 | 6.78 | 6.10 | 0.02 | 5.93 |
| **03-SMH-0102-3** | **Felsic Volcanic** | 59.86 | 1.31 | 13.06 | 10.26 | 9.23 | 0.03 | 8.74 |
| **03-SMH-0104-2** | **Felsic Volcanic** | 79.02 | 0.19 | 6.96 | 5.66 | 5.09 | 0.03 | 5.84 |
| **03-SMH-0106-2** | **Felsic Volcanic** | 73.04 | 0.30 | 12.08 | 3.50 | 3.15 | 0.02 | 5.64 |
| **03-SMH-0108-1** | **Felsic Volcanic** | 79.10 | 0.19 | 9.78 | 3.04 | 2.74 | 0.05 | 3.32 |
| **03-SMH-0109-2** | **Felsic Volcanic** | 76.08 | 0.26 | 11.02 | 3.75 | 3.37 | 0.09 | 0.86 |
| **03-SMH-0110-1** | **Felsic Volcanic** | 78.56 | 0.22 | 10.03 | 3.12 | 2.81 | 0.02 | 1.88 |
| **03-SMH-0111-1** | **Felsic Volcanic** | 81.16 | 0.16 | 9.97 | 1.67 | 1.50 | N.D. | 0.33 |
| **03-SMH-0112-1** | **Felsic Volcanic** | 75.87 | 0.18 | 8.18 | 3.57 | 3.21 | 0.11 | 2.53 |
| **03-SMH-0112-4** | **Felsic Volcanic** | 73.71 | 0.24 | 10.93 | 3.59 | 3.23 | 0.06 | 2.56 |
| **03-SMH-0115-1** | **Felsic Volcanic** | 89.17 | 0.13 | 6.11 | 1.05 | 0.94 | 0.04 | 0.30 |
| **03-SMH-0122-2** | **Felsic Volcanic** | 79.73 | 0.19 | 9.86 | 5.04 | 4.54 | 0.04 | 0.99 |

**Abbreviations:** N.D. = not detected. N.M. = not measured/analyzed.

**Appendix 3**. Listing of geochemical data from the Genex mine area -- continued.

| Sample No. | CaO<br>wt % | $Na_2O$<br>wt % | $K_2O$<br>wt % | $P_2O_5$<br>wt % | LOI<br>wt % | Total<br>wt % | Ti<br>ppm | Mn<br>ppm | Na<br>ppm | K<br>ppm |
|---|---|---|---|---|---|---|---|---|---|---|
| **04-SMH-0015-1** | 5.30 | 4.01 | 0.74 | 0.24 | 3.73 | 98.90 | N.M. | N.M. | N.M. | N.M. |
| **04-SMH-0015-2** | 3.55 | 5.62 | 0.70 | 0.26 | 5.57 | 99.26 | N.M. | N.M. | N.M. | N.M. |
| **04-SMH-0015-4** | 4.09 | 4.37 | 0.90 | 0.24 | 3.00 | 98.27 | N.M. | N.M. | N.M. | N.M. |
| **04-SMH-0016-1** | 2.40 | 1.80 | 1.69 | 0.26 | 4.96 | 100.07 | N.M. | N.M. | N.M. | N.M. |
| **04-SMH-0016-2** | 6.02 | 3.51 | 0.07 | 0.20 | 10.20 | 98.85 | N.M. | N.M. | N.M. | N.M. |
| **04-SMH-0016-3** | 6.10 | 1.62 | 1.54 | 0.22 | 7.35 | 99.15 | N.M. | N.M. | N.M. | N.M. |
| **04-SMH-0017-2** | 2.19 | 2.07 | 1.93 | 0.05 | 1.93 | 100.04 | N.M. | N.M. | N.M. | N.M. |
| **04-SMH-0019-4** | 0.83 | 0.42 | 5.50 | 0.21 | 3.46 | 100.80 | N.M. | N.M. | N.M. | N.M. |
| **03-SMH-0010-1** | 0.09 | 0.11 | 1.70 | 0.10 | 2.55 | 100.21 | N.M. | N.M. | N.M. | N.M. |
| | | | | | | | | | | |
| **03-SMH-0019-1** | 0.58 | 0.06 | 0.49 | 0.43 | 3.30 | 99.45 | N.M. | N.M. | N.M. | N.M. |
| **03-SMH-0113** | 7.75 | 2.57 | 0.88 | 0.43 | 8.11 | 100.93 | 8085 | 3342 | 17266 | 8145 |
| **03-SMH-0119-1** | 11.33 | 3.11 | 1.16 | 0.22 | 10.70 | 101.07 | 4874 | 2094 | 24372 | 11315 |
| **03-SMH-0136** | 6.21 | 4.40 | 0.26 | 0.14 | 1.91 | 101.66 | 8665 | 2442 | 25686 | 1943 |
| **03-SMH-0140-2** | 7.44 | 2.67 | 2.59 | 0.20 | 3.19 | 100.90 | 7820 | 3135 | 17362 | >13500 |
| **03-SMH-0142-1** | 4.17 | 2.62 | 1.99 | 0.47 | 6.41 | 100.54 | N.M. | N.M. | N.M. | N.M. |
| **03-SMH-0146** | 7.31 | 4.35 | 0.82 | 0.23 | 6.20 | 100.86 | 6226 | 1494 | 31717 | 7183 |
| **03-SMH-0152** | 6.53 | 6.08 | 0.06 | 0.21 | 6.39 | 101.12 | 5359 | 1406 | 43592 | 521 |
| **04-SMH-0005-1** | 2.51 | 5.19 | 0.48 | 0.23 | 2.25 | 99.16 | N.M. | N.M. | N.M. | N.M. |
| | | | | | | | | | | |
| **03-SMH-0014** | 0.13 | 1.36 | 2.41 | 0.02 | 2.94 | 100.98 | 1721 | 148 | 9230 | >13500 |
| **03-SMH-0019-4** | 0.87 | N.D. | 0.01 | 0.31 | 3.94 | 99.04 | 6383 | 3931 | N.D. | 71.0 |
| **03-SMH-0025** | 0.01 | N.D. | 1.81 | 0.02 | 2.51 | 99.37 | 1027 | 111 | 676 | >13500 |
| **03-SMH-0034-1** | 0.05 | N.D. | 1.08 | 0.05 | 2.98 | 100.69 | 2136 | 318 | 238 | 8943 |
| **03-SMH-0034-2** | 0.03 | 0.04 | 1.70 | 0.03 | 1.61 | 99.88 | 901 | 35.0 | 1059 | 12802 |
| **03-SMH-0037-1** | 0.03 | 0.15 | 2.37 | 0.03 | 2.51 | 98.60 | 1088 | 64.0 | 993 | >13500 |
| **03-SMH-0037-2** | 0.02 | 0.39 | 0.22 | 0.11 | 6.53 | 98.90 | 7967 | 538 | 1856 | 1978 |
| **03-SMH-0040** | 0.04 | 0.29 | 0.23 | 0.10 | 5.66 | 98.93 | 7578 | 849 | 1222 | 1972 |
| **03-SMH-0046-1** | N.D. | 0.04 | 0.68 | 0.02 | 3.17 | 100.83 | 1255 | 90.0 | 46.0 | 5084 |
| **03-SMH-0056-1** | 0.02 | 0.04 | 2.07 | 0.02 | 2.42 | 100.70 | N.M. | N.M. | N.M. | N.M. |
| **03-SMH-0056-2** | N.D. | N.D. | 0.09 | 0.02 | 3.25 | 98.72 | N.M. | N.M. | N.M. | N.M. |
| **03-SMH-0063** | 0.06 | 0.03 | 3.13 | 0.04 | 2.95 | 100.56 | 2921 | 304 | 780 | >13500 |
| **03-SMH-0091** | N.D. | 0.08 | 2.46 | 0.03 | 2.15 | 100.54 | 1280 | 244 | 378 | >13500 |
| **03-SMH-0102-2** | 0.04 | N.D. | 0.02 | 0.03 | 3.13 | 101.20 | 1929 | 175 | N.D. | 206 |
| **03-SMH-0102-3** | 0.14 | 0.04 | 0.94 | 0.09 | 5.02 | 99.49 | 7879 | 294 | 180 | 8005 |
| **03-SMH-0104-2** | N.D. | N.D. | 0.21 | 0.03 | 3.08 | 101.02 | 1095 | 218 | N.D. | 1788 |
| **03-SMH-0106-2** | 0.02 | 0.06 | 2.51 | 0.04 | 3.51 | 100.72 | 1713 | 207 | 465 | >13500 |
| **03-SMH-0108-1** | 0.16 | 0.11 | 2.40 | 0.03 | 2.88 | 101.06 | N.M. | N.M. | N.M. | N.M. |
| **03-SMH-0109-2** | 0.96 | 3.72 | 1.32 | 0.04 | 2.11 | 100.21 | 1568 | 704 | 31549 | 10838 |
| **03-SMH-0110-1** | 0.42 | 3.53 | 0.88 | 0.03 | 1.88 | 100.57 | 1241 | 141 | 30294 | 7508 |
| **03-SMH-0111-1** | 0.08 | 5.61 | 0.14 | 0.03 | 0.76 | 99.91 | 945 | 48.0 | 49274 | 1134 |
| **03-SMH-0112-1** | 2.50 | 1.78 | 1.41 | 0.03 | 4.68 | 100.84 | 1150 | 887 | 12896 | 11959 |
| **03-SMH-0112-4** | 1.16 | 4.67 | 0.25 | 0.03 | 2.85 | 100.05 | N.M. | N.M. | N.M. | N.M. |
| **03-SMH-0115-1** | 0.41 | 0.08 | 1.86 | 0.03 | 1.33 | 100.51 | 780 | 266 | 2140 | >13500 |
| **03-SMH-0122-2** | 0.02 | 0.02 | 2.89 | 0.03 | 1.99 | 100.80 | 1181 | 315 | 299 | >13500 |

**Abbreviations:** N.D. = not detected. N.M. = not measured/analyzed.

**Appendix 3**. Listing of geochemical data from the Genex mine area -- continued.

| Sample No. | P | Cr | Co | Ni | Cu | Sc | V | Pb | Zn | As |
|---|---|---|---|---|---|---|---|---|---|---|
| | ppm | ppm | ppm | ppm | ppm | ppm | ppm | ppm | ppm | ppm |
| **04-SMH-0015-1** | N.M. | 23.0 | N.M. | 12.0 | N.M. | N.M. | 99.0 | N.M. | N.M. | N.M. |
| **04-SMH-0015-2** | N.M. | 15.0 | N.M. | 15.0 | N.M. | N.M. | 138 | N.M. | N.M. | N.M. |
| **04-SMH-0015-4** | N.M. | 15.0 | N.M. | 6.0 | N.M. | N.M. | 363 | N.M. | N.M. | N.M. |
| **04-SMH-0016-1** | N.M. | <8 | N.M. | 10.0 | N.M. | N.M. | 108 | N.M. | N.M. | N.M. |
| **04-SMH-0016-2** | N.M. | 20.0 | N.M. | 11.0 | N.M. | N.M. | 482 | N.M. | N.M. | N.M. |
| **04-SMH-0016-3** | N.M. | 20.0 | N.M. | 9.0 | N.M. | N.M. | 456 | N.M. | N.M. | N.M. |
| **04-SMH-0017-2** | N.M. | <8 | N.M. | <4 | N.M. | N.M. | 11.0 | N.M. | N.M. | N.M. |
| **04-SMH-0019-4** | N.M. | 11.0 | N.M. | 12.0 | N.M. | N.M. | 95.0 | N.M. | N.M. | N.M. |
| **03-SMH-0010-1** | N.M. | 43.0 | N.M. | -4.0 | N.M. | N.M. | 75.0 | N.M. | N.M. | N.M. |
| | | | | | | | | | | |
| **03-SMH-0019-1** | N.M. | -8.0 | N.M. | -4.0 | N.M. | N.M. | 96.0 | N.M. | N.M. | N.M. |
| **03-SMH-0113** | 2444 | N.D. | 26.0 | 4.0 | 27.0 | 59.0 | 64.0 | N.D. | 120 | N.D. |
| **03-SMH-0119-1** | 1069 | 30.0 | N.D. | 11.0 | 14.0 | 42.0 | 61.0 | 6.0 | 57.0 | N.D. |
| **03-SMH-0136** | 697 | 136 | 47.0 | 44.0 | 103 | 75.0 | 371 | 5.0 | 198 | N.D. |
| **03-SMH-0140-2** | 1090 | 100 | 36.0 | 27.0 | 104 | 84.0 | 338 | 8.0 | 86.0 | 2.0 |
| **03-SMH-0142-1** | N.M. | -8.0 | N.M. | -4.0 | N.M. | | 140 | N.M. | N.M. | N.M. |
| **03-SMH-0146** | 1136 | 40.0 | 24.0 | 17.0 | 14.0 | 43.0 | 66.0 | N.D. | 97.0 | N.D. |
| **03-SMH-0152** | 1159 | 28.0 | 18.0 | 15.0 | 38.0 | 24.0 | 86.0 | 5.0 | 81.0 | N.D. |
| **04-SMH-0005-1** | N.M. | 9.0 | N.M. | 10.0 | N.M. | N.M. | 110 | N.M. | N.M. | N.M. |
| | | | | | | | | | | |
| **03-SMH-0014** | 54.0 | N.D. | N.D. | N.D. | N.D. | 28.0 | N.D. | N.D. | 89.0 | N.D. |
| **03-SMH-0019-4** | 1415 | 15.0 | 21.0 | 9.0 | 7.0 | 56.0 | N.D. | N.D. | 383 | N.D. |
| **03-SMH-0025** | 10.0 | 6.0 | N.D. | N.D. | 3.0 | 37.0 | N.D. | N.D. | 21.0 | N.D. |
| **03-SMH-0034-1** | 142 | 17.0 | 12.0 | 8.0 | 199 | 33.0 | 68.0 | N.D. | 184 | 4.0 |
| **03-SMH-0034-2** | 23.0 | 5.0 | N.D. | N.D. | 9.0 | 22.0 | N.D. | N.D. | 41.0 | N.D. |
| **03-SMH-0037-1** | 37.0 | N.D. | N.D. | N.D. | 4.0 | 26.0 | N.D. | N.D. | 46.0 | N.D. |
| **03-SMH-0037-2** | 396 | 55.0 | N.D. | 29.0 | 36.0 | 64.0 | 264 | N.D. | 338 | 1.0 |
| **03-SMH-0040** | 408 | 38.0 | 41.0 | 32.0 | 17.0 | 60.0 | 190 | 9.0 | 444 | 10.0 |
| **03-SMH-0046-1** | 16.0 | 14.0 | N.D. | N.D. | 13.0 | 23.0 | N.D. | N.D. | 85.0 | N.D. |
| **03-SMH-0056-1** | N.M. | N.M. | N.M. | N.M. | N.M. | N.M. | N.M. | N.M. | N.M. | N.M. |
| **03-SMH-0056-2** | N.M. | N.M. | N.M. | N.M. | N.M. | N.M. | N.M. | N.M. | N.M. | N.M. |
| **03-SMH-0063** | 127 | 69.0 | 20.0 | 37.0 | N.D. | 19.0 | 28.0 | N.D. | 186 | 3.0 |
| **03-SMH-0091** | 13.0 | 9.0 | N.D. | 3.0 | N.D. | 19.0 | N.D. | 6.0 | 47.0 | N.D. |
| **03-SMH-0102-2** | 83.0 | 38.0 | 18.0 | 8.0 | 4.0 | 21.0 | 36.0 | N.D. | 174 | N.D. |
| **03-SMH-0102-3** | 319 | 25.0 | 32.0 | 16.0 | 2.0 | 27.0 | 120 | N.D. | 57.0 | N.D. |
| **03-SMH-0104-2** | N.D. | 13.0 | 13.0 | 4.0 | N.D. | 19.0 | 24.0 | N.D. | 25.0 | N.D. |
| **03-SMH-0106-2** | 71.0 | N.D. | N.D. | N.D. | N.D. | 27.0 | 35.0 | N.D. | 75.0 | N.D. |
| **03-SMH-0108-1** | N.M. | N.M. | N.M. | N.M. | N.M. | N.M. | N.M. | N.M. | N.M. | N.M. |
| **03-SMH-0109-2** | 56.0 | 7.0 | N.D. | 2.0 | 4.0 | 22.0 | 10.0 | N.D. | 73.0 | N.D. |
| **03-SMH-0110-1** | N.D. | 13.0 | N.D. | N.D. | 6.0 | 23.0 | N.D. | 14.0 | 77.0 | N.D. |
| **03-SMH-0111-1** | N.D. | 13.0 | N.D. | N.D. | 1.0 | 22.0 | N.D. | 12.0 | 56.0 | N.D. |
| **03-SMH-0112-1** | 26.0 | 12.0 | N.D. | N.D. | 2.0 | 40.0 | N.D. | 6.0 | 62.0 | N.D. |
| **03-SMH-0112-4** | N.M. | 14.0 | N.M. | -4.0 | N.M. | N.M. | 11.0 | N.M. | N.M. | N.M. |
| **03-SMH-0115-1** | 18.0 | 14.0 | N.D. | N.D. | N.D. | 18.0 | N.D. | N.D. | 54.0 | N.D. |
| **03-SMH-0122-2** | 28.0 | 20.0 | N.D. | 3.0 | N.D. | 25.0 | N.D. | N.D. | 18.0 | N.D. |

**Abbreviations:** N.D. = not detected. N.M. = not measured/analyzed.

***Appendix 3***. Listing of geochemical data from the Genex mine area -- continued.

| Sample No. | Rb<br>ppm | Cs<br>ppm | Ba<br>ppm | Sr<br>ppm | Ga<br>ppm | Ta<br>ppm | Nb<br>ppm | Hf<br>ppm | Zr<br>ppm | Y<br>ppm |
|---|---|---|---|---|---|---|---|---|---|---|
| **04-SMH-0015-1** | 18.80 | 0.792 | N.M. | 150.3 | N.M. | 0.62 | 9.3 | 6.1 | 242.2 | 40.84 |
| **04-SMH-0015-2** | 19.15 | 0.585 | N.M. | 137.3 | N.M. | 0.68 | 10.3 | 6.7 | 268.6 | 42.31 |
| **04-SMH-0015-4** | 18.05 | 0.437 | N.M. | 98.7 | N.M. | 0.50 | 7.5 | 4.8 | 181.9 | 38.59 |
| **04-SMH-0016-1** | 39.61 | 1.024 | N.M. | 52.0 | N.M. | 0.59 | 8.8 | 5.9 | 232.8 | 37.61 |
| **04-SMH-0016-2** | 1.14 | 0.119 | N.M. | 141.3 | N.M. | 0.41 | 6.3 | 4.0 | 150.6 | 35.91 |
| **04-SMH-0016-3** | 47.50 | 1.103 | N.M. | 69.2 | N.M. | 0.49 | 7.1 | 4.7 | 179.8 | 38.23 |
| **04-SMH-0017-2** | 39.21 | 1.637 | N.M. | 43.3 | N.M. | 1.14 | 18.0 | 8.3 | 296.8 | 38.2 |
| **04-SMH-0019-4** | 96.38 | 3.329 | N.M. | 14.9 | N.M. | 0.65 | 9.8 | 6.5 | 272.2 | 41.16 |
| **03-SMH-0010-1** | 32.84 | 0.361 | N.M. | 5.6 | N.M. | 0.40 | 5.9 | 4.0 | 157.1 | 25.22 |
| | | | | | | | | | | |
| **03-SMH-0019-1** | 7.80 | 0.116 | N.M. | 11.2 | N.M. | 0.54 | 7.9 | 4.7 | 190.7 | 34.31 |
| **03-SMH-0113** | 27.64 | 0.442 | 211 | 99.1 | 18.0 | 0.64 | 9.0 | 5.3 | 206 | 39.2 |
| **03-SMH-0119-1** | 47.84 | 0.765 | 300 | 156.2 | 14.0 | 0.55 | 7.3 | 5.1 | 199.4 | 41.39 |
| **03-SMH-0136** | 3.73 | 0.189 | 128 | 88.0 | 21.0 | 0.33 | 4.4 | 3.1 | 109.9 | 31.67 |
| **03-SMH-0140-2** | 60.69 | 0.801 | 508 | 90.3 | 23.0 | 0.34 | 4.8 | 3.3 | 129.4 | 15.32 |
| **03-SMH-0142-1** | 54.46 | 1.177 | N.M. | 85.8 | N.M. | 0.66 | 10.1 | 5.9 | 236.5 | 39.35 |
| **03-SMH-0146** | 31.52 | 0.619 | 246 | 169.5 | 17.0 | 0.69 | 9.8 | 6.8 | 266.8 | 38.93 |
| **03-SMH-0152** | 1.89 | 0.047 | 34.0 | 102.5 | 15.0 | 0.65 | 9.0 | 6.3 | 238.1 | 11.44 |
| **04-SMH-0005-1** | 10.86 | 0.626 | N.M. | 46.4 | N.M. | 0.67 | 10.2 | 6.7 | 265.3 | 39.28 |
| | | | | | | | | | | |
| **03-SMH-0014** | 55.62 | 1.072 | 595 | 27.7 | 20.0 | 1.72 | 22.7 | 12.0 | 407.7 | 21.07 |
| **03-SMH-0019-4** | 0.26 | 0.011 | N.D. | 10.8 | 18.0 | 0.57 | 6.2 | 3.8 | 148.6 | 47.78 |
| **03-SMH-0025** | 33.93 | 0.386 | 478 | 6.4 | 13.0 | 1.37 | 17.0 | 8.0 | 257.6 | 56.26 |
| **03-SMH-0034-1** | 19.99 | 0.236 | 253 | 3.5 | 14.0 | 1.00 | 11.3 | 5.8 | 188.7 | 28.3 |
| **03-SMH-0034-2** | 31.73 | 0.293 | 340 | 5.8 | 10.0 | 1.02 | 12.2 | 6.6 | 228.8 | 46.13 |
| **03-SMH-0037-1** | 37.22 | 0.509 | 615 | 9.4 | 16.0 | 1.42 | 17.7 | 8.3 | 275.5 | 52.95 |
| **03-SMH-0037-2** | 3.91 | 0.098 | 56.0 | 7.6 | 25.0 | 0.80 | 9.8 | 5.3 | 191.9 | 49.84 |
| **03-SMH-0040** | 5.58 | 0.510 | 28.0 | 5.4 | 30.0 | 0.74 | 8.8 | 4.8 | 168.8 | 35.33 |
| **03-SMH-0046-1** | 12.96 | 0.160 | 101 | 3.0 | 12.0 | 0.89 | 10.2 | 5.5 | 196.7 | 32.34 |
| **03-SMH-0056-1** | 35.89 | 0.287 | N.M. | 6.8 | N.M. | 1.22 | 16.2 | 6.7 | 222 | 55.09 |
| **03-SMH-0056-2** | 1.89 | 0.029 | N.M. | 1.1 | N.M. | 0.74 | 8.0 | 4.1 | 139.8 | 20.84 |
| **03-SMH-0063** | 53.79 | 1.303 | 965 | 8.5 | 18.0 | 1.38 | 18.0 | 9.0 | 301.3 | 69.77 |
| **03-SMH-0091** | 34.78 | 0.311 | 642 | 5.9 | 15.0 | 1.41 | 19.5 | 8.9 | 302.6 | 60.07 |
| **03-SMH-0102-2** | 0.60 | 0.041 | N.D. | 0.8 | 9.0 | 0.70 | 9.3 | 4.6 | 152.4 | 24.38 |
| **03-SMH-0102-3** | 14.98 | 0.119 | 260 | 3.6 | 15.0 | 0.89 | 19.7 | 6.7 | 241.7 | 33.78 |
| **03-SMH-0104-2** | 3.82 | 0.045 | N.D. | 0.9 | 9.0 | 1.04 | 14.1 | 6.8 | 225.5 | 46.23 |
| **03-SMH-0106-2** | 51.87 | 0.287 | 255 | 5.0 | 9.0 | 1.79 | 23.6 | 11.3 | 384.3 | 40.52 |
| **03-SMH-0108-1** | 48.15 | 0.233 | N.M. | 3.9 | N.M. | 1.59 | 22.2 | 9.3 | 299 | 72.76 |
| **03-SMH-0109-2** | 71.57 | 1.666 | 275 | 33.6 | 17.0 | 1.55 | 19.7 | 9.5 | 313.4 | 61.06 |
| **03-SMH-0110-1** | 42.01 | 0.967 | 159 | 47.5 | 11.0 | 1.49 | 22.1 | 9.6 | 310.9 | 48.3 |
| **03-SMH-0111-1** | 5.58 | 0.095 | 102 | 80.9 | 9.0 | 1.31 | 17.7 | 7.6 | 239.5 | 47.22 |
| **03-SMH-0112-1** | 43.85 | 0.628 | 123 | 28.3 | 11.0 | 1.06 | 15.2 | 8.2 | 284.5 | 45.01 |
| **03-SMH-0112-4** | 6.26 | 0.103 | N.M. | 27.2 | N.M. | 1.28 | 19.3 | 9.7 | 348.3 | 89.09 |
| **03-SMH-0115-1** | 45.77 | 0.589 | 376 | 13.3 | 9.0 | 0.87 | 11.8 | 5.7 | 184.3 | 30.73 |
| **03-SMH-0122-2** | 19.19 | 0.492 | 1194 | 2.7 | 16.0 | 1.41 | 20.8 | 8.8 | 289.4 | 61.81 |

**Abbreviations:** N.D. = not detected. N.M. = not measured/analyzed.

**Appendix 3**. Listing of geochemical data from the Genex mine area -- continued.

| Sample No. | Th<br>ppm | U<br>ppm | La<br>ppm | Ce<br>ppm | Pr<br>ppm | Nd<br>ppm | Sm<br>ppm | Eu<br>ppm | Gd<br>ppm | Tb<br>ppm |
|---|---|---|---|---|---|---|---|---|---|---|
| **04-SMH-0015-1** | 2.75 | 0.708 | 21.28 | 49.36 | 6.554 | 28.29 | 6.72 | 1.645 | 7.26 | 1.18 |
| **04-SMH-0015-2** | 2.93 | 0.769 | 23.75 | 55.9 | 7.462 | 32.43 | 7.62 | 1.911 | 8.008 | 1.264 |
| **04-SMH-0015-4** | 1.70 | 0.548 | 12.65 | 32.05 | 4.498 | 20.51 | 5.56 | 1.717 | 6.642 | 1.117 |
| **04-SMH-0016-1** | 2.16 | 0.675 | 20.34 | 48.07 | 6.489 | 28.04 | 6.44 | 1.601 | 6.756 | 1.063 |
| **04-SMH-0016-2** | 1.38 | 0.352 | 11.6 | 27.95 | 3.89 | 18.32 | 4.79 | 1.463 | 5.793 | 0.985 |
| **04-SMH-0016-3** | 1.73 | 0.443 | 13.87 | 33.45 | 4.678 | 21.37 | 5.53 | 1.642 | 6.299 | 1.065 |
| **04-SMH-0017-2** | 4.73 | 1.176 | 28.93 | 66.22 | 8.34 | 33.86 | 7.56 | 1.411 | 7.466 | 1.209 |
| **04-SMH-0019-4** | 2.97 | 0.768 | 25.66 | 58.67 | 7.632 | 32.9 | 7.41 | 1.746 | 7.461 | 1.196 |
| **03-SMH-0010-1** | 1.74 | 0.454 | 13.44 | 30.0 | 3.812 | 16.47 | 3.9 | 0.797 | 4.61 | 0.767 |
| | | | | | | | | | | |
| **03-SMH-0019-1** | 2.13 | 0.526 | 19.18 | 45.34 | 6.185 | 27.24 | 6.38 | 1.263 | 6.485 | 0.995 |
| **03-SMH-0113** | 2.27 | 0.585 | 21.28 | 49.9 | 6.727 | 29.52 | 7.05 | 1.829 | 7.766 | 1.183 |
| **03-SMH-0119-1** | 2.20 | 0.592 | 18.61 | 43.88 | 5.858 | 25.84 | 6.1 | 1.622 | 7.109 | 1.171 |
| **03-SMH-0136** | 0.73 | 0.189 | 7.64 | 19.28 | 2.785 | 13.33 | 3.88 | 1.17 | 5.076 | 0.878 |
| **03-SMH-0140-2** | 0.64 | 0.25 | 5.89 | 14.3 | 2.108 | 10.05 | 2.64 | 0.645 | 2.9 | 0.471 |
| **03-SMH-0142-1** | 2.59 | 0.636 | 20.02 | 48.6 | 6.484 | 28.57 | 6.79 | 1.777 | 7.212 | 1.147 |
| **03-SMH-0146** | 2.86 | 0.766 | 18.85 | 42.96 | 5.806 | 25.61 | 6.35 | 1.718 | 7.132 | 1.159 |
| **03-SMH-0152** | 1.39 | 0.674 | 9.18 | 20.48 | 2.684 | 11.73 | 2.68 | 0.567 | 2.387 | 0.366 |
| **04-SMH-0005-1** | 2.90 | 0.739 | 22.6 | 53.92 | 7.235 | 30.74 | 7.13 | 1.382 | 7.35 | 1.198 |
| | | | | | | | | | | |
| **03-SMH-0014** | 3.57 | 1.739 | 13.62 | 31.44 | 3.983 | 16.47 | 3.61 | 0.519 | 3.473 | 0.566 |
| **03-SMH-0019-4** | 1.79 | 0.447 | 15.64 | 37.1 | 4.96 | 22.51 | 5.8 | 1.532 | 7.392 | 1.274 |
| **03-SMH-0025** | 6.15 | 1.51 | 24.19 | 57.25 | 7.308 | 30.45 | 6.66 | 0.383 | 7.541 | 1.369 |
| **03-SMH-0034-1** | 3.66 | 0.931 | 8.41 | 19.44 | 2.528 | 11 | 2.73 | 0.647 | 3.32 | 0.617 |
| **03-SMH-0034-2** | 4.06 | 0.959 | 27.24 | 64.4 | 8.168 | 34.06 | 7.44 | 0.974 | 7.737 | 1.276 |
| **03-SMH-0037-1** | 5.90 | 1.389 | 35.57 | 85.49 | 10.896 | 45.28 | 10.08 | 1.155 | 9.815 | 1.582 |
| **03-SMH-0037-2** | 2.64 | 0.638 | 23.34 | 56.34 | 7.363 | 31.98 | 7.26 | 0.984 | 8.567 | 1.416 |
| **03-SMH-0040** | 2.31 | 0.591 | 21.0 | 42.06 | 5.085 | 20.8 | 5.03 | 0.893 | 6.025 | 1.041 |
| **03-SMH-0046-1** | 3.21 | 0.805 | 19.36 | 46.49 | 6.099 | 26.17 | 6.29 | 0.693 | 6.389 | 1.009 |
| **03-SMH-0056-1** | 4.56 | 1.3 | 29.64 | 67.73 | 8.582 | 35.68 | 7.77 | 1.081 | 8.732 | 1.533 |
| **03-SMH-0056-2** | 2.63 | 0.71 | 19.04 | 42.82 | 5.348 | 22.44 | 4.98 | 0.814 | 4.896 | 0.745 |
| **03-SMH-0063** | 6.35 | 1.578 | 45.14 | 103.75 | 12.867 | 53.19 | 11.81 | 1.665 | 12.229 | 2.002 |
| **03-SMH-0091** | 6.16 | 1.542 | 40.11 | 93.45 | 11.666 | 47.32 | 10.08 | 1.304 | 10.605 | 1.76 |
| **03-SMH-0102-2** | 2.92 | 0.663 | 4.48 | 10.81 | 1.461 | 6.25 | 1.78 | 0.193 | 2.699 | 0.533 |
| **03-SMH-0102-3** | 3.73 | 0.967 | 24.01 | 57.66 | 7.563 | 32.04 | 7.14 | 0.572 | 6.705 | 1.008 |
| **03-SMH-0104-2** | 4.47 | 1.12 | 29.0 | 67.31 | 8.592 | 35.1 | 7.55 | 0.758 | 7.909 | 1.281 |
| **03-SMH-0106-2** | 8.10 | 1.757 | 35.58 | 87.9 | 11.65 | 48.11 | 9.86 | 0.5 | 7.563 | 1.063 |
| **03-SMH-0108-1** | 6.85 | 1.395 | 40.0 | 88.53 | 12.304 | 50.12 | 11.46 | 0.395 | 12.025 | 2.003 |
| **03-SMH-0109-2** | 6.88 | 1.67 | 41.6 | 93.59 | 11.656 | 46.72 | 10.11 | 1.375 | 10.724 | 1.781 |
| **03-SMH-0110-1** | 6.21 | 1.585 | 48.7 | 108.91 | 13.992 | 56.38 | 12.49 | 1.778 | 12.47 | 1.911 |
| **03-SMH-0111-1** | 5.85 | 1.29 | 44.32 | 97.77 | 12.084 | 48.38 | 10.44 | 1.372 | 10.444 | 1.611 |
| **03-SMH-0112-1** | 4.60 | 1.121 | 33.05 | 74.96 | 9.462 | 39.01 | 8.58 | 1.387 | 8.456 | 1.323 |
| **03-SMH-0112-4** | 5.86 | 1.504 | 40.21 | 88.63 | 11.102 | 45.91 | 10.44 | 1.735 | 11.808 | 2.108 |
| **03-SMH-0115-1** | 4.10 | 1.005 | 58.51 | 112.01 | 13.059 | 45.83 | 7.36 | 1.239 | 6.779 | 0.963 |
| **03-SMH-0122-2** | 5.70 | 1.497 | 39.4 | 90.82 | 11.519 | 46.62 | 10.45 | 0.895 | 11.481 | 1.91 |

**Abbreviations:** N.D. = not detected. N.M. = not measured/analyzed.

**Appendix 3**. Listing of geochemical data from the Genex mine area -- continued.

| **Sample No.** | **Dy** | **Ho** | **Er** | **Tm** | **Yb** | **Lu** |
|---|---|---|---|---|---|---|
| | **ppm** | **ppm** | **ppm** | **ppm** | **ppm** | **ppm** |
| **04-SMH-0015-1** | 7.3 | 1.487 | 4.41 | 0.656 | 4.29 | 0.639 |
| **04-SMH-0015-2** | 7.775 | 1.575 | 4.632 | 0.679 | 4.46 | 0.663 |
| **04-SMH-0015-4** | 7.117 | 1.466 | 4.271 | 0.634 | 4.14 | 0.606 |
| **04-SMH-0016-1** | 6.54 | 1.37 | 4.132 | 0.62 | 4.14 | 0.638 |
| **04-SMH-0016-2** | 6.462 | 1.365 | 4.074 | 0.606 | 3.98 | 0.609 |
| **04-SMH-0016-3** | 6.869 | 1.476 | 4.508 | 0.671 | 4.47 | 0.67 |
| **04-SMH-0017-2** | 7.492 | 1.524 | 4.508 | 0.689 | 4.6 | 0.687 |
| **04-SMH-0019-4** | 7.496 | 1.549 | 4.6 | 0.692 | 4.52 | 0.67 |
| **03-SMH-0010-1** | 4.899 | 0.965 | 2.753 | 0.403 | 2.71 | 0.405 |
| | | | | | | |
| **03-SMH-0019-1** | 6.061 | 1.249 | 3.637 | 0.525 | 3.41 | 0.502 |
| **03-SMH-0113** | 7.177 | 1.477 | 4.292 | 0.629 | 4.02 | 0.62 |
| **03-SMH-0119-1** | 7.32 | 1.518 | 4.529 | 0.676 | 4.32 | 0.655 |
| **03-SMH-0136** | 5.646 | 1.216 | 3.623 | 0.538 | 3.52 | 0.531 |
| **03-SMH-0140-2** | 2.936 | 0.599 | 1.741 | 0.244 | 1.52 | 0.226 |
| **03-SMH-0142-1** | 7.049 | 1.478 | 4.361 | 0.642 | 4.24 | 0.639 |
| **03-SMH-0146** | 7.091 | 1.482 | 4.376 | 0.649 | 4.18 | 0.614 |
| **03-SMH-0152** | 2.227 | 0.468 | 1.348 | 0.199 | 1.25 | 0.178 |
| **04-SMH-0005-1** | 7.42 | 1.477 | 4.29 | 0.634 | 4.13 | 0.622 |
| | | | | | | |
| **03-SMH-0014** | 3.607 | 0.823 | 2.62 | 0.426 | 2.98 | 0.472 |
| **03-SMH-0019-4** | 8.207 | 1.78 | 5.169 | 0.724 | 4.61 | 0.69 |
| **03-SMH-0025** | 9.292 | 2.117 | 6.481 | 0.985 | 6.46 | 0.984 |
| **03-SMH-0034-1** | 4.441 | 1.053 | 3.567 | 0.567 | 3.98 | 0.621 |
| **03-SMH-0034-2** | 8.01 | 1.69 | 5.032 | 0.739 | 4.75 | 0.703 |
| **03-SMH-0037-1** | 9.785 | 2.029 | 6.063 | 0.883 | 5.62 | 0.831 |
| **03-SMH-0037-2** | 8.965 | 1.881 | 5.477 | 0.777 | 5.0 | 0.744 |
| **03-SMH-0040** | 6.556 | 1.353 | 4.011 | 0.586 | 3.9 | 0.597 |
| **03-SMH-0046-1** | 6.051 | 1.248 | 3.696 | 0.543 | 3.59 | 0.528 |
| **03-SMH-0056-1** | 9.74 | 2.016 | 5.992 | 0.877 | 5.62 | 0.833 |
| **03-SMH-0056-2** | 4.206 | 0.847 | 2.47 | 0.365 | 2.44 | 0.37 |
| **03-SMH-0063** | 12.376 | 2.552 | 7.611 | 1.124 | 7.34 | 1.087 |
| **03-SMH-0091** | 11.208 | 2.289 | 6.605 | 0.954 | 5.98 | 0.853 |
| **03-SMH-0102-2** | 3.827 | 0.9 | 2.926 | 0.451 | 3.05 | 0.461 |
| **03-SMH-0102-3** | 5.98 | 1.285 | 4.004 | 0.623 | 4.23 | 0.662 |
| **03-SMH-0104-2** | 8.141 | 1.749 | 5.332 | 0.778 | 5.03 | 0.743 |
| **03-SMH-0106-2** | 6.499 | 1.474 | 5.007 | 0.837 | 5.94 | 0.963 |
| **03-SMH-0108-1** | 12.646 | 2.687 | 7.817 | 1.126 | 7.11 | 1.042 |
| **03-SMH-0109-2** | 11.159 | 2.347 | 7.036 | 1.035 | 6.55 | 0.971 |
| **03-SMH-0110-1** | 10.749 | 2.039 | 5.541 | 0.789 | 5.09 | 0.752 |
| **03-SMH-0111-1** | 9.476 | 1.902 | 5.589 | 0.873 | 6.05 | 0.898 |
| **03-SMH-0112-1** | 8.152 | 1.709 | 5.098 | 0.77 | 5.05 | 0.76 |
| **03-SMH-0112-4** | 14.405 | 3.156 | 9.54 | 1.413 | 9.08 | 1.337 |
| **03-SMH-0115-1** | 5.898 | 1.239 | 3.765 | 0.582 | 3.87 | 0.583 |
| **03-SMH-0122-2** | 11.856 | 2.397 | 7.04 | 1.011 | 6.41 | 0.91 |

**Abbreviations:** N.D. = not detected. N.M. = not measured/analyzed.

**Appendix 3**. Listing of geochemical data from the Genex mine area -- continued.

| Sample No. | Description | $SiO_2$ wt % | $TiO_2$ wt % | $Al_2O_3$ wt % | $Fe_2O_3$ wt % | $FeO$ wt % | $MnO$ wt % | $MgO$ wt % |
|---|---|---|---|---|---|---|---|---|
| **03-SMH-0129-2** | **Felsic Volcanic** | 67.91 | 1.65 | 11.35 | 10.41 | 9.37 | *0.03* | *4.21* |
| **03-SMH-0130** | **Felsic Volcanic** | 70.46 | 0.46 | 14.10 | 6.99 | 6.29 | 0.07 | 1.35 |
| **03-SMH-0131** | **Felsic Volcanic** | 80.01 | 0.31 | 9.48 | 4.69 | 4.22 | 0.07 | 1.39 |
| **03-SMH-0132-1** | **Felsic Volcanic** | 81.96 | 0.21 | 9.14 | 2.00 | 1.80 | 0.07 | 1.54 |
| **03-SMH-0140-1** | **Felsic Volcanic** | 81.27 | 0.19 | 9.07 | 3.36 | 3.02 | 0.04 | 1.84 |
| **03-SMH-0141** | **Felsic Volcanic** | 64.33 | 0.60 | 11.94 | 10.71 | 9.64 | 0.07 | 8.41 |
| **03-SMH-0157** | **Felsic Volcanic** | 73.11 | 0.34 | 11.17 | 4.08 | 3.67 | 0.10 | 2.62 |
| **03-SMH-0160-1** | **Felsic Volcanic** | 78.55 | 0.29 | 9.19 | 3.59 | 3.23 | 0.03 | 2.04 |
| **03-SMH-0165-1** | **Felsic Volcanic** | 78.94 | 0.28 | 8.95 | 5.42 | 4.88 | 0.03 | 2.92 |
| **03-SMH-0168** | **Felsic Volcanic** | 69.16 | 0.94 | 10.48 | 9.10 | 8.19 | 0.32 | 2.18 |
| **04-SMH-0001-5** | **Felsic Volcanic** | 73.17 | 0.20 | 9.25 | 5.31 | 4.78 | 0.03 | 6.84 |
| **04-SMH-0007-2** | **Felsic Volcanic** | 27.30 | 0.52 | 23.51 | 18.84 | 16.95 | 0.08 | 19.57 |
| **04-SMH-0023-4** | **Felsic Volcanic** | 69.37 | 0.18 | 10.27 | 9.73 | 8.76 | 0.06 | 5.63 |
| | | | | | | | | |
| **03-SMH-0007** | **Mafic Intrusion** | 49.98 | 1.29 | 13.56 | 14.42 | 12.98 | 0.24 | 6.57 |
| **03-SMH-0013** | **Mafic Intrusion** | 52.15 | 1.41 | 14.01 | 12.65 | 11.38 | 0.19 | 7.62 |
| **03-SMH-0023** | **Mafic Intrusion** | 51.45 | 1.33 | 13.75 | 12.39 | 11.15 | 0.18 | 7.92 |
| **03-SMH-0030** | **Mafic Intrusion** | 50.19 | 1.34 | 13.74 | 14.72 | 13.25 | 0.14 | 8.13 |
| **03-SMH-0031** | **Mafic Intrusion** | 51.33 | 1.33 | 13.87 | 13.29 | 11.96 | 0.23 | 6.00 |
| **03-SMH-0082-1** | **Mafic Intrusion** | 78.08 | 1.04 | 7.88 | 3.14 | 2.83 | 0.00 | 0.55 |
| **03-SMH-0105-1** | **Mafic Intrusion** | 40.35 | 2.57 | 15.30 | 16.92 | 15.22 | 0.19 | 9.33 |
| **03-SMH-0107-2** | **Mafic Intrusion** | 46.94 | 1.31 | 12.86 | 15.28 | 13.75 | 0.14 | 7.29 |
| **03-SMH-0112-2** | **Mafic Intrusion** | 55.16 | 1.25 | 13.05 | 11.96 | 10.76 | 0.08 | 5.62 |
| **03-SMH-0018-1** | **Mafic Intrusion** | 49.28 | 1.36 | 13.28 | 12.62 | 11.36 | 0.12 | 8.03 |
| **03-SMH-0094-1** | **Mafic Intrusion** | 46.81 | 1.21 | 13.25 | 14.25 | 12.82 | 0.19 | 6.32 |
| **03-SMH-0112-5** | **Mafic Intrusion** | 43.85 | 1.17 | 13.64 | 12.41 | 11.17 | 0.21 | 4.72 |
| **03-SMH-0116-1** | **Mafic Intrusion** | 49.29 | 1.25 | 13.14 | 13.54 | 12.18 | 0.19 | 6.25 |
| **04-SMH-0001-13** | **Mafic Intrusion** | 37.18 | 1.24 | 19.31 | 15.38 | 13.84 | 0.12 | 16.74 |
| **04-SMH-0001-21** | **Mafic Intrusion** | 46.67 | 1.39 | 14.38 | 13.92 | 12.53 | 0.13 | 7.82 |
| **04-SMH-0001-22** | **Mafic Intrusion** | 48.73 | 1.34 | 14.44 | 14.00 | 12.60 | 0.27 | 6.86 |
| **04-SMH-0001-3** | **Mafic Intrusion** | 28.16 | 1.24 | 20.92 | 16.30 | 14.67 | 0.05 | 23.10 |
| **04-SMH-0001-9** | **Mafic Intrusion** | 48.76 | 1.40 | 13.25 | 13.73 | 12.35 | 0.07 | 13.82 |
| **04-SMH-0002-4** | **Mafic Intrusion** | 43.75 | 1.21 | 12.20 | 12.85 | 11.56 | 0.23 | 5.13 |
| **04-SMH-0003-1** | **Mafic Intrusion** | 45.83 | 1.27 | 13.56 | 14.95 | 13.45 | 0.37 | 5.29 |
| **04-SMH-0003-3** | **Mafic Intrusion** | 51.72 | 1.13 | 13.87 | 12.14 | 10.92 | 0.16 | 2.93 |
| **04-SMH-0003-7** | **Mafic Intrusion** | 50.82 | 1.33 | 13.65 | 11.36 | 10.22 | 0.25 | 4.72 |
| **04-SMH-0004-1** | **Mafic Intrusion** | 50.97 | 1.43 | 14.72 | 12.04 | 10.83 | 0.27 | 6.28 |
| **04-SMH-0004-3** | **Mafic Intrusion** | 46.13 | 1.33 | 12.99 | 14.58 | 13.12 | 0.61 | 6.71 |
| **04-SMH-0008-1** | **Mafic Intrusion** | 42.82 | 1.20 | 11.80 | 12.36 | 11.12 | 0.19 | 7.14 |
| **04-SMH-0017-1** | **Mafic Intrusion** | 49.16 | 1.26 | 14.05 | 10.18 | 9.16 | 0.28 | 4.91 |
| **04-SMH-0018-2** | **Mafic Intrusion** | 49.25 | 2.59 | 16.20 | 9.38 | 8.44 | 0.24 | 3.60 |
| **04-SMH-0019-1** | **Mafic Intrusion** | 47.20 | 0.58 | 21.39 | 8.20 | 7.38 | 0.12 | 5.31 |
| **04-SMH-0023-1** | **Mafic Intrusion** | 60.69 | 0.84 | 13.63 | 11.52 | 10.37 | 0.15 | 5.48 |
| **04-SMH-0023-3** | **Mafic Intrusion** | 42.35 | 0.71 | 20.53 | 16.42 | 14.77 | 0.13 | 10.07 |

**Abbreviations:** N.D. = not detected. N.M. = not measured/analyzed.

**Appendix 3**. Listing of geochemical data from the Genex mine area -- continued.

| **Sample No.** | **CaO** wt % | **$Na_2O$** wt % | **$K_2O$** wt % | **$P_2O_5$** wt % | **LOI** wt % | **Total** wt % | **Ti** ppm | **Mn** ppm | **Na** ppm | **K** ppm |
|---|---|---|---|---|---|---|---|---|---|---|
| **03-SMH-0129-2** | 0.28 | 0.08 | 1.52 | 0.20 | 3.29 | 100.93 | 9730 | 259 | N.D. | 13283 |
| **03-SMH-0130** | 0.24 | 0.08 | 4.34 | 0.07 | 2.58 | 100.74 | 2571 | 593 | 272 | >13500 |
| **03-SMH-0131** | N.D. | N.D. | 2.71 | 0.04 | 2.71 | 101.41 | 1892 | 536 | N.D. | >13500 |
| **03-SMH-0132-1** | 0.39 | 0.08 | 2.87 | 0.03 | 2.19 | 100.48 | 1423 | 574 | 412 | >13500 |
| **03-SMH-0140-1** | 0.82 | 0.30 | 2.15 | 0.03 | 2.09 | 101.16 | 1167 | 321 | 1500 | >13500 |
| **03-SMH-0141** | 0.98 | 0.03 | 1.46 | 0.07 | 3.36 | 101.96 | 3715 | 575 | 790 | 11916 |
| **03-SMH-0157** | 1.60 | 0.03 | 3.19 | 0.05 | 3.93 | 100.22 | 2031 | 826 | 691 | >13500 |
| **03-SMH-0160-1** | 0.33 | 4.06 | 0.11 | 0.05 | 1.75 | 99.99 | 1642 | 230 | 31161 | 852 |
| **03-SMH-0165-1** | 0.03 | 0.11 | 2.01 | 0.04 | 2.34 | 101.07 | 1568 | 236 | 657 | >13500 |
| **03-SMH-0168** | 1.60 | 0.68 | 2.30 | 0.09 | 3.84 | 100.69 | 5698 | 2781 | 3816 | >13500 |
| **04-SMH-0001-5** | 0.21 | 0.12 | 0.83 | 0.03 | 3.80 | 99.79 | N.M. | N.M. | N.M. | N.M. |
| **04-SMH-0007-2** | 0.03 | 0.06 | 0.59 | 0.02 | 9.83 | 100.35 | N.M. | N.M. | N.M. | N.M. |
| **04-SMH-0023-4** | 0.20 | 0.07 | 0.87 | 0.02 | 3.73 | 100.13 | N.M. | N.M. | N.M. | N.M. |
| | | | | | | | | | | |
| **03-SMH-0007** | 8.68 | 3.20 | 0.20 | 0.09 | 3.33 | 101.56 | 7035 | 1984 | 19929 | 1500 |
| **03-SMH-0013** | 5.79 | 3.89 | 0.09 | 0.12 | 3.27 | 101.19 | 8321 | 1548 | 24949 | 685 |
| **03-SMH-0023** | 7.08 | 3.98 | 0.09 | 0.11 | 2.98 | 101.26 | 7662 | 1425 | 23345 | 695 |
| **03-SMH-0030** | 5.56 | 3.78 | 0.07 | 0.12 | 4.16 | 101.95 | 7646 | 1201 | 22651 | 529 |
| **03-SMH-0031** | 8.77 | 3.13 | 0.07 | 0.13 | 3.42 | 101.57 | 7574 | 1916 | 19885 | 572 |
| **03-SMH-0082-1** | 0.38 | 0.00 | 2.67 | 0.25 | 2.24 | 96.23 | 6043 | 87.0 | 2127 | >13500 |
| **03-SMH-0105-1** | 4.38 | 1.62 | 0.45 | 0.40 | 10.11 | 101.62 | 14279 | 1653 | 4904 | 3638 |
| **03-SMH-0107-2** | 7.65 | 1.97 | 0.06 | 0.12 | 8.35 | 101.97 | 7165 | 1219 | 9093 | 410 |
| **03-SMH-0112-2** | 3.39 | 1.90 | 1.40 | 0.12 | 6.26 | 100.19 | 7559 | 674 | 9099 | 11989 |
| **03-SMH-0018-1** | 5.05 | 1.79 | 0.48 | 0.12 | 8.08 | 100.21 | N.M. | N.M. | N.M. | N.M. |
| **03-SMH-0094-1** | 8.52 | 1.95 | 0.05 | 0.44 | 7.54 | 100.53 | N.M. | N.M. | N.M. | N.M. |
| **03-SMH-0112-5** | 10.17 | 2.33 | 0.92 | 0.11 | 10.85 | 100.38 | N.M. | N.M. | N.M. | N.M. |
| **03-SMH-0116-1** | 7.47 | 3.22 | 0.09 | 0.12 | 5.59 | 100.15 | N.M. | N.M. | N.M. | N.M. |
| **04-SMH-0001-13** | 0.22 | 0.02 | 0.28 | 0.14 | 8.57 | 99.20 | N.M. | N.M. | N.M. | N.M. |
| **04-SMH-0001-21** | 3.87 | 1.33 | 1.60 | 0.14 | 9.55 | 100.80 | N.M. | N.M. | N.M. | N.M. |
| **04-SMH-0001-22** | 6.40 | 2.85 | 2.62 | 0.12 | 2.83 | 100.46 | N.M. | N.M. | N.M. | N.M. |
| **04-SMH-0001-3** | 0.22 | 0.03 | 0.03 | 0.08 | 10.44 | 100.57 | N.M. | N.M. | N.M. | N.M. |
| **04-SMH-0001-9** | 1.11 | 0.01 | 0.03 | 0.12 | 7.90 | 100.20 | N.M. | N.M. | N.M. | N.M. |
| **04-SMH-0002-4** | 9.49 | 2.71 | 0.09 | 0.11 | 11.54 | 99.31 | N.M. | N.M. | N.M. | N.M. |
| **04-SMH-0003-1** | 7.75 | 1.69 | 0.14 | 0.14 | 9.37 | 100.36 | N.M. | N.M. | N.M. | N.M. |
| **04-SMH-0003-3** | 4.60 | 0.48 | 3.48 | 0.23 | 8.67 | 99.41 | N.M. | N.M. | N.M. | N.M. |
| **04-SMH-0003-7** | 10.07 | 1.40 | 0.04 | 0.13 | 5.91 | 99.68 | N.M. | N.M. | N.M. | N.M. |
| **04-SMH-0004-1** | 6.66 | 3.90 | 0.69 | 0.13 | 1.74 | 98.83 | N.M. | N.M. | N.M. | N.M. |
| **04-SMH-0004-3** | 6.36 | 0.06 | 2.04 | 0.13 | 8.86 | 99.80 | N.M. | N.M. | N.M. | N.M. |
| **04-SMH-0008-1** | 7.87 | 2.08 | 0.65 | 0.12 | 13.64 | 99.87 | N.M. | N.M. | N.M. | N.M. |
| **04-SMH-0017-1** | 11.74 | 2.94 | 0.41 | 0.11 | 4.17 | 99.21 | N.M. | N.M. | N.M. | N.M. |
| **04-SMH-0018-2** | 6.69 | 4.37 | 0.33 | 0.39 | 6.65 | 99.69 | N.M. | N.M. | N.M. | N.M. |
| **04-SMH-0019-1** | 11.13 | 3.08 | 0.36 | 0.06 | 2.91 | 100.34 | N.M. | N.M. | N.M. | N.M. |
| **04-SMH-0023-1** | 0.76 | 0.62 | 1.61 | 0.15 | 5.45 | 100.90 | N.M. | N.M. | N.M. | N.M. |
| **04-SMH-0023-3** | 0.67 | 0.27 | 2.74 | 0.07 | 6.42 | 100.38 | N.M. | N.M. | N.M. | N.M. |

**Abbreviations:** N.D. = not detected. N.M. = not measured/analyzed.

**Appendix 3**. Listing of geochemical data from the Genex mine area -- continued.

| **Sample No.** | **P**<br>**ppm** | **Cr**<br>**ppm** | **Co**<br>**ppm** | **Ni**<br>**ppm** | **Cu**<br>**ppm** | **Sc**<br>**ppm** | **V**<br>**ppm** | **Pb**<br>**ppm** | **Zn**<br>**ppm** | **As**<br>**ppm** |
|---|---|---|---|---|---|---|---|---|---|---|
| **03-SMH-0129-2** | 1009 | 29.0 | 25.0 | 11.0 | 34.0 | 48.0 | 344 | N.D. | 195 | 25.0 |
| **03-SMH-0130** | 230 | 14.0 | N.D. | 5.0 | 27.0 | 21.0 | N.D. | N.D. | 80.0 | N.D. |
| **03-SMH-0131** | 90.0 | 48.0 | N.D. | 5.0 | 9.0 | 27.0 | 48.0 | 15.0 | 314 | 5.0 |
| **03-SMH-0132-1** | 88.0 | 14.0 | N.D. | 3.0 | N.D. | 25.0 | N.D. | N.D. | 79.0 | N.D. |
| **03-SMH-0140-1** | 101 | 12.0 | N.D. | 4.0 | 2.0 | 35.0 | N.D. | 5.0 | 69.0 | N.D. |
| **03-SMH-0141** | 328 | 388 | 32.0 | 104 | 19.0 | 38.0 | 119 | N.D. | 152 | N.D. |
| **03-SMH-0157** | 125 | 18.0 | N.D. | N.D. | 19.0 | 34.0 | N.D. | 7.0 | 130 | N.D. |
| **03-SMH-0160-1** | 177 | 19.0 | N.D. | 3.0 | 4.0 | 41.0 | N.D. | N.D. | 41.0 | N.D. |
| **03-SMH-0165-1** | 105 | N.D. | N.D. | 3.0 | 6.0 | 18.0 | N.D. | 5.0 | 199 | N.D. |
| **03-SMH-0168** | 429 | 39.0 | 31.0 | 19.0 | 64.0 | 64.0 | 225 | 12.0 | 87.0 | 16.0 |
| **04-SMH-0001-5** | N.M. | 29.0 | N.M. | 18.0 | N.M. | N.M. | 6.0 | N.M. | N.M. | N.M. |
| **04-SMH-0007-2** | N.M. | <8 | N.M. | 28.0 | N.M. | N.M. | 56.0 | N.M. | N.M. | N.M. |
| **04-SMH-0023-4** | N.M. | 42.0 | N.M. | 24.0 | N.M. | N.M. | 28.0 | N.M. | N.M. | N.M. |
| | | | | | | | | | | |
| **03-SMH-0007** | 431 | 126 | 53.0 | 43.0 | 105 | 57.0 | 270 | N.D. | 100 | N.D. |
| **03-SMH-0013** | 509 | 130 | 46.0 | 42.0 | 116 | 76.0 | 323 | N.D. | 96.0 | N.D. |
| **03-SMH-0023** | 477 | 128 | 47.0 | 40.0 | 81.0 | 64.0 | 308 | N.D. | 99.0 | N.D. |
| **03-SMH-0030** | 448 | 121 | 49.0 | 44.0 | 106 | 67.0 | 315 | N.D. | 96.0 | N.D. |
| **03-SMH-0031** | 534 | 116 | 51.0 | 44.0 | 116 | 69.0 | 339 | N.D. | 92.0 | 3.0 |
| **03-SMH-0082-1** | 1111 | 14.0 | 13.0 | 8.0 | >7000 | 30.0 | N.D. | 86.0 | >3000 | 38.0 |
| **03-SMH-0105-1** | 1503 | 197 | 70.0 | 90.0 | 25.0 | 72.0 | 337 | N.D. | 260 | N.D. |
| **03-SMH-0107-2** | 470 | 114 | 52.0 | 41.0 | 4.0 | 70.0 | 332 | N.D. | 49.0 | N.D. |
| **03-SMH-0112-2** | 545 | 107 | 44.0 | 39.0 | 163 | 66.0 | 209 | 17.0 | 163 | N.D. |
| **03-SMH-0018-1** | N.M. | 93.0 | N.M. | 38.0 | N.M. | N.M. | 376 | N.M. | N.M. | N.M. |
| **03-SMH-0094-1** | N.M. | 103 | N.M. | 38.0 | N.M. | N.M. | 319 | N.M. | N.M. | N.M. |
| **03-SMH-0112-5** | N.M. | 110 | N.M. | 74.0 | N.M. | N.M. | 356 | N.M. | N.M. | N.M. |
| **03-SMH-0116-1** | N.M. | 105 | N.M. | 36.0 | N.M. | N.M. | 338 | N.M. | N.M. | N.M. |
| **04-SMH-0001-13** | N.M. | 1028 | N.M. | 254 | N.M. | N.M. | 341 | N.M. | N.M. | N.M. |
| **04-SMH-0001-21** | N.M. | 109 | N.M. | 41.0 | N.M. | N.M. | 407 | N.M. | N.M. | N.M. |
| **04-SMH-0001-22** | N.M. | 96.0 | N.M. | 50.0 | N.M. | N.M. | 337 | N.M. | N.M. | N.M. |
| **04-SMH-0001-3** | N.M. | 1156 | N.M. | 368 | N.M. | N.M. | 324 | N.M. | N.M. | N.M. |
| **04-SMH-0001-9** | N.M. | 94.0 | N.M. | 37.0 | N.M. | N.M. | 371 | N.M. | N.M. | N.M. |
| **04-SMH-0002-4** | N.M. | 88.0 | N.M. | 39.0 | N.M. | N.M. | 379 | N.M. | N.M. | N.M. |
| **04-SMH-0003-1** | N.M. | 87.0 | N.M. | 35.0 | N.M. | N.M. | 337 | N.M. | N.M. | N.M. |
| **04-SMH-0003-3** | N.M. | 10.0 | N.M. | 15.0 | N.M. | N.M. | 149 | N.M. | N.M. | N.M. |
| **04-SMH-0003-7** | N.M. | 95.0 | N.M. | 40.0 | N.M. | N.M. | 303 | N.M. | N.M. | N.M. |
| **04-SMH-0004-1** | N.M. | 98.0 | N.M. | 40.0 | N.M. | N.M. | 385 | N.M. | N.M. | N.M. |
| **04-SMH-0004-3** | N.M. | 73.0 | N.M. | 35.0 | N.M. | N.M. | 385 | N.M. | N.M. | N.M. |
| **04-SMH-0008-1** | N.M. | 85.0 | N.M. | 31.0 | N.M. | N.M. | 311 | N.M. | N.M. | N.M. |
| **04-SMH-0017-1** | N.M. | 129 | N.M. | 52.0 | N.M. | N.M. | 290 | N.M. | N.M. | N.M. |
| **04-SMH-0018-2** | N.M. | 23.0 | N.M. | 67.0 | N.M. | N.M. | 239 | N.M. | N.M. | N.M. |
| **04-SMH-0019-1** | N.M. | 82.0 | N.M. | 67.0 | N.M. | N.M. | 147 | N.M. | N.M. | N.M. |
| **04-SMH-0023-1** | N.M. | 114 | N.M. | 76.0 | N.M. | N.M. | 297 | N.M. | N.M. | N.M. |
| **04-SMH-0023-3** | N.M. | 99.0 | N.M. | 68.0 | N.M. | N.M. | 192 | N.M. | N.M. | N.M. |

**Abbreviations:** N.D. = not detected. N.M. = not measured/analyzed.

**Appendix 3**. Listing of geochemical data from the Genex mine area -- continued.

| Sample No. | Rb<br>ppm | Cs<br>ppm | Ba<br>ppm | Sr<br>ppm | Ga<br>ppm | Ta<br>ppm | Nb<br>ppm | Hf<br>ppm | Zr<br>ppm | Y<br>ppm |
|---|---|---|---|---|---|---|---|---|---|---|
| **03-SMH-0129-2** | 22.79 | 0.256 | 209 | 7.3 | 23.0 | 0.46 | 6.3 | 4.1 | 151.4 | 20.13 |
| **03-SMH-0130** | 63.77 | 1.273 | 1409 | 8.2 | 22.0 | 1.68 | 23.4 | 13.2 | 470.5 | 44.75 |
| **03-SMH-0131** | 17.21 | 0.522 | 565 | 4.2 | 17.0 | 1.37 | 17.5 | 7.5 | 247.9 | 24.07 |
| **03-SMH-0132-1** | 37.08 | 0.725 | 336 | 6.4 | 14.0 | 1.22 | 16.5 | 9.6 | 337.6 | 39.02 |
| **03-SMH-0140-1** | 41.89 | 0.849 | 254 | 21.3 | 14.0 | 1.13 | 13.7 | 7.5 | 239.8 | 39.81 |
| **03-SMH-0141** | 32.55 | 1.857 | 366 | 43.8 | 16.0 | 0.68 | 10.0 | 4.3 | 142.5 | 31.24 |
| **03-SMH-0157** | 78.50 | 0.549 | 311 | 7.0 | 18.0 | 1.35 | 18.6 | 9.9 | 348.2 | 57.56 |
| **03-SMH-0160-1** | 1.75 | 0.023 | 46.0 | 25.3 | 10.0 | 1.13 | 14.5 | 8.1 | 290.2 | 45.45 |
| **03-SMH-0165-1** | 36.17 | 0.909 | 299 | 9.6 | 16.0 | 1.12 | 15.4 | 8.0 | 285.9 | 33.16 |
| **03-SMH-0168** | 93.54 | 2.106 | 317 | 43.1 | 16.0 | 0.31 | 4.8 | 2.6 | 95.1 | 10.83 |
| **04-SMH-0001-5** | 19.39 | 0.212 | N.M. | 4.2 | N.M. | 1.22 | 17.5 | 7.8 | 266.4 | 62.75 |
| **04-SMH-0007-2** | 10.00 | 0.490 | N.M. | 4.0 | N.M. | 3.51 | 46.6 | 23.5 | 816.6 | 34.55 |
| **04-SMH-0023-4** | 18.02 | 0.221 | N.M. | 5.5 | N.M. | 1.39 | 17.1 | 8.3 | 268.5 | 63.32 |
| | | | | | | | | | | |
| **03-SMH-0007** | 3.38 | 0.186 | 72.0 | 101.6 | 17.0 | 0.35 | 3.5 | 2.2 | 83.8 | 24.08 |
| **03-SMH-0013** | 2.42 | 0.385 | 204 | 179.4 | 18.0 | 0.41 | 4.3 | 2.8 | 103.7 | 28.33 |
| **03-SMH-0023** | 1.64 | 0.269 | 101 | 156.6 | 17.0 | 0.38 | 3.9 | 2.6 | 93.0 | 27.7 |
| **03-SMH-0030** | 1.28 | 0.233 | 72.0 | 119.4 | 20.0 | 0.38 | 3.9 | 2.6 | 93.4 | 26.83 |
| **03-SMH-0031** | 1.18 | 0.060 | 42.0 | 147.1 | 18.0 | 0.42 | 4.4 | 2.9 | 103.9 | 29.39 |
| **03-SMH-0082-1** | 50.24 | 0.522 | 421 | 9.9 | 20.0 | 0.43 | 5.9 | 3.6 | 142.3 | 25.46 |
| **03-SMH-0105-1** | 6.89 | 0.123 | 80.0 | 61.1 | 22.0 | 0.62 | 9.4 | 5.7 | 230.8 | 48.05 |
| **03-SMH-0107-2** | 1.25 | 0.049 | 34.0 | 77.0 | 19.0 | 0.30 | 4.1 | 2.8 | 101 | 28.6 |
| **03-SMH-0112-2** | 45.50 | 0.735 | 179 | 37.8 | 20.0 | 0.28 | 4.1 | 2.6 | 93.0 | 26.99 |
| **03-SMH-0018-1** | 9.29 | 0.172 | N.M. | 76.4 | N.M. | 0.26 | 4.1 | 2.7 | 100.8 | 29.48 |
| **03-SMH-0094-1** | 0.29 | 0.045 | N.M. | 243.5 | N.M. | 0.24 | 3.8 | 2.6 | 93.1 | 27.64 |
| **03-SMH-0112-5** | 30.87 | 0.482 | N.M. | 111.5 | N.M. | 0.22 | 3.5 | 2.3 | 86.0 | 23.76 |
| **03-SMH-0116-1** | 0.86 | 0.128 | N.M. | 129.2 | N.M. | 0.24 | 3.9 | 2.6 | 94.6 | 26.29 |
| **04-SMH-0001-13** | 6.31 | 0.312 | N.M. | 2.2 | N.M. | 0.23 | 4.1 | 1.8 | 65.9 | 15.95 |
| **04-SMH-0001-21** | 31.60 | 1.003 | N.M. | 62.7 | N.M. | 0.27 | 4.1 | 2.7 | 100.7 | 18.81 |
| **04-SMH-0001-22** | 42.82 | 0.427 | N.M. | 98.6 | N.M. | 0.29 | 4.3 | 2.6 | 97.4 | 27.72 |
| **04-SMH-0001-3** | 0.67 | 0.261 | N.M. | 2.7 | N.M. | 0.24 | 4.9 | 1.7 | 61.9 | 9.48 |
| **04-SMH-0001-9** | 0.26 | 0.124 | N.M. | 7.2 | N.M. | 0.27 | 4.4 | 2.7 | 102.7 | 33.1 |
| **04-SMH-0002-4** | 0.52 | 0.106 | N.M. | 126.5 | N.M. | 0.21 | 3.3 | 2.2 | 79.6 | 24.47 |
| **04-SMH-0003-1** | 3.14 | 0.199 | N.M. | 119.6 | N.M. | 0.24 | 3.9 | 2.6 | 94.9 | 29.92 |
| **04-SMH-0003-3** | 73.81 | 3.050 | N.M. | 144.2 | N.M. | 0.62 | 9.7 | 6.1 | 246.9 | 41.49 |
| **04-SMH-0003-7** | 0.44 | 0.215 | N.M. | 302.2 | N.M. | 0.25 | 4.0 | 2.7 | 100.5 | 28.52 |
| **04-SMH-0004-1** | 6.43 | 0.366 | N.M. | 65.1 | N.M. | 0.25 | 4.1 | 3.5 | 134.5 | 27.68 |
| **04-SMH-0004-3** | 32.16 | 0.528 | N.M. | 50.7 | N.M. | 0.25 | 3.9 | 2.8 | 104.4 | 23.43 |
| **04-SMH-0008-1** | 13.31 | 0.212 | N.M. | 66.4 | N.M. | 0.23 | 3.7 | 2.4 | 89.1 | 20.48 |
| **04-SMH-0017-1** | 9.37 | 0.356 | N.M. | 141.6 | N.M. | 0.24 | 3.8 | 2.5 | 91.8 | 28.87 |
| **04-SMH-0018-2** | 7.84 | 0.349 | N.M. | 236.2 | N.M. | 0.39 | 6.9 | 2.8 | 117.2 | 21.12 |
| **04-SMH-0019-1** | 6.45 | 0.166 | N.M. | 162.9 | N.M. | N.D. | 1.7 | 1.1 | 42.3 | 11.74 |
| **04-SMH-0023-1** | 3.30 | 0.135 | N.M. | 114.7 | N.M. | 0.23 | 3.8 | 2.3 | 88.0 | 26.4 |
| **04-SMH-0023-3** | 63.12 | 3.317 | N.M. | 50.8 | N.M. | N.D. | 2.2 | 1.4 | 53.3 | 20.57 |

**Abbreviations:** N.D. = not detected. N.M. = not measured/analyzed.

**Appendix 3**. Listing of geochemical data from the Genex mine area -- continued.

| **Sample No.** | **Th**<br>**ppm** | **U**<br>**ppm** | **La**<br>**ppm** | **Ce**<br>**ppm** | **Pr**<br>**ppm** | **Nd**<br>**ppm** | **Sm**<br>**ppm** | **Eu**<br>**ppm** | **Gd**<br>**ppm** | **Tb**<br>**ppm** |
|---|---|---|---|---|---|---|---|---|---|---|
| **03-SMH-0129-2** | 1.36 | 0.405 | 14.91 | 34.78 | 4.569 | 20.18 | 4.86 | 1.002 | 4.812 | 0.722 |
| **03-SMH-0130** | 6.96 | 1.875 | 38.4 | 81.58 | 11.079 | 44.44 | 9.74 | 1.75 | 8.973 | 1.392 |
| **03-SMH-0131** | 4.31 | 1.26 | 24.63 | 58.04 | 7.386 | 30.18 | 6.53 | 1.003 | 5.78 | 0.862 |
| **03-SMH-0132-1** | 4.94 | 1.289 | 33.67 | 76.87 | 9.879 | 41.21 | 9.17 | 1.545 | 8.298 | 1.209 |
| **03-SMH-0140-1** | 5.72 | 1.275 | 42.96 | 98.31 | 12.535 | 50.93 | 10.82 | 1.585 | 9.607 | 1.33 |
| **03-SMH-0141** | 2.65 | 0.623 | 18.11 | 42.18 | 5.336 | 23.05 | 5.37 | 0.924 | 5.611 | 0.906 |
| **03-SMH-0157** | 5.79 | 1.291 | 38.36 | 88.27 | 11.043 | 45.77 | 10.44 | 1.785 | 10.751 | 1.781 |
| **03-SMH-0160-1** | 4.62 | 0.995 | 34.97 | 73.99 | 9.411 | 38.5 | 8.33 | 1.701 | 8.422 | 1.317 |
| **03-SMH-0165-1** | 4.57 | 1.139 | 27.11 | 64.46 | 8.315 | 35.48 | 8.2 | 1.056 | 6.986 | 1.003 |
| **03-SMH-0168** | 0.94 | 0.289 | 4.91 | 12.31 | 1.699 | 7.79 | 2.0 | 0.426 | 2.132 | 0.342 |
| **04-SMH-0001-5** | 5.64 | 1.31 | 33.06 | 81.27 | 10.571 | 42.83 | 9.01 | 0.426 | 9.213 | 1.58 |
| **04-SMH-0007-2** | 6.80 | 3.812 | 7.93 | 19.68 | 2.631 | 11.64 | 2.66 | 0.179 | 2.501 | 0.494 |
| **04-SMH-0023-4** | 6.67 | 1.601 | 45.7 | 107.06 | 13.788 | 56.88 | 12.7 | 0.755 | 12.309 | 2.028 |
| | | | | | | | | | | |
| **03-SMH-0007** | 0.55 | 0.153 | 5.69 | 14.32 | 2.064 | 10.03 | 2.92 | 1.002 | 3.744 | 0.651 |
| **03-SMH-0013** | 0.68 | 0.174 | 6.85 | 17.48 | 2.562 | 12.3 | 3.52 | 1.192 | 4.608 | 0.776 |
| **03-SMH-0023** | 0.63 | 0.163 | 7.24 | 17.85 | 2.566 | 12.48 | 3.58 | 1.201 | 4.587 | 0.772 |
| **03-SMH-0030** | 0.65 | 0.171 | 6.85 | 16.63 | 2.396 | 11.57 | 3.29 | 1.063 | 4.318 | 0.751 |
| **03-SMH-0031** | 0.73 | 0.186 | 7.46 | 18.83 | 2.736 | 13.18 | 3.74 | 1.367 | 4.842 | 0.833 |
| **03-SMH-0082-1** | 1.49 | 0.417 | 5.26 | 13.14 | 1.821 | 8.52 | 2.51 | 0.812 | 3.708 | 0.689 |
| **03-SMH-0105-1** | 1.45 | 0.397 | 16.42 | 40.33 | 5.794 | 26.88 | 7.1 | 2.019 | 8.489 | 1.398 |
| **03-SMH-0107-2** | 0.70 | 0.174 | 6.38 | 16.58 | 2.432 | 11.6 | 3.4 | 1.105 | 4.456 | 0.78 |
| **03-SMH-0112-2** | 0.62 | 0.245 | 6.9 | 16.11 | 2.246 | 10.23 | 2.91 | 0.626 | 4.239 | 0.747 |
| **03-SMH-0018-1** | 0.67 | 0.178 | 5.79 | 14.8 | 2.175 | 10.33 | 3.17 | 1.055 | 4.293 | 0.781 |
| **03-SMH-0094-1** | 0.61 | 0.158 | 6.55 | 16.41 | 2.352 | 11.41 | 3.32 | 1.104 | 4.266 | 0.736 |
| **03-SMH-0112-5** | 0.54 | 0.139 | 5.79 | 14.21 | 2.044 | 10.03 | 2.87 | 0.719 | 3.722 | 0.626 |
| **03-SMH-0116-1** | 0.64 | 0.169 | 6.52 | 16.37 | 2.321 | 11.36 | 3.28 | 1.084 | 4.126 | 0.702 |
| **04-SMH-0001-13** | 0.21 | 0.18 | 2.37 | 6.16 | 0.897 | 4.28 | 1.46 | 0.093 | 2.241 | 0.421 |
| **04-SMH-0001-21** | 0.54 | 0.181 | 5.86 | 14.99 | 2.173 | 10.43 | 2.69 | 0.816 | 2.874 | 0.487 |
| **04-SMH-0001-22** | 0.64 | 0.168 | 7.42 | 18.56 | 2.7 | 13.38 | 3.69 | 1.112 | 4.481 | 0.765 |
| **04-SMH-0001-3** | 0.43 | 0.211 | 3.11 | 8.93 | 1.359 | 6.22 | 1.65 | 0.104 | 1.729 | 0.257 |
| **04-SMH-0001-9** | 0.68 | 0.192 | 8.63 | 22.1 | 3.309 | 16.14 | 4.4 | 0.382 | 5.103 | 0.859 |
| **04-SMH-0002-4** | 0.51 | 0.138 | 5.58 | 13.92 | 1.977 | 9.67 | 2.86 | 0.983 | 3.693 | 0.641 |
| **04-SMH-0003-1** | 0.64 | 0.169 | 6.91 | 16.98 | 2.447 | 12.03 | 3.39 | 1.1 | 4.315 | 0.751 |
| **04-SMH-0003-3** | 2.70 | 0.693 | 21.66 | 50.06 | 6.791 | 29.06 | 6.81 | 1.735 | 7.436 | 1.19 |
| **04-SMH-0003-7** | 0.63 | 0.171 | 6.86 | 16.89 | 2.551 | 12.13 | 3.48 | 1.161 | 4.4 | 0.759 |
| **04-SMH-0004-1** | 0.61 | 0.17 | 6.41 | 15.45 | 2.238 | 10.62 | 3.14 | 1.003 | 4.109 | 0.728 |
| **04-SMH-0004-3** | 0.64 | 0.176 | 6.94 | 17.15 | 2.505 | 12.02 | 3.37 | 1.253 | 4.049 | 0.691 |
| **04-SMH-0008-1** | 0.57 | 0.155 | 5.42 | 13.71 | 2.034 | 9.79 | 2.75 | 0.946 | 3.289 | 0.558 |
| **04-SMH-0017-1** | 0.57 | 0.15 | 6.47 | 15.93 | 2.378 | 11.57 | 3.38 | 1.098 | 4.483 | 0.765 |
| **04-SMH-0018-2** | 1.34 | 0.354 | 16.98 | 42.84 | 5.994 | 26.44 | 5.34 | 1.947 | 4.727 | 0.705 |
| **04-SMH-0019-1** | 0.26 | 0.075 | 2.98 | 7.46 | 1.133 | 5.52 | 1.55 | 0.622 | 1.933 | 0.333 |
| **04-SMH-0023-1** | 0.51 | 0.152 | 7.69 | 18.45 | 2.621 | 12.55 | 3.47 | 1.177 | 4.152 | 0.698 |
| **04-SMH-0023-3** | 0.42 | 0.179 | 5.64 | 12.6 | 1.725 | 7.89 | 2.3 | 0.573 | 3.183 | 0.578 |

**Abbreviations:** N.D. = not detected. N.M. = not measured/analyzed.

**Appendix 3**. Listing of geochemical data from the Genex mine area -- continued.

| Sample No. | Dy<br>ppm | Ho<br>ppm | Er<br>ppm | Tm<br>ppm | Yb<br>ppm | Lu<br>ppm |
|---|---|---|---|---|---|---|
| **03-SMH-0129-2** | 4.262 | 0.827 | 2.396 | 0.351 | 2.27 | 0.332 |
| **03-SMH-0130** | 8.584 | 1.827 | 5.768 | 0.922 | 6.3 | 0.976 |
| **03-SMH-0131** | 4.986 | 1.009 | 3.028 | 0.455 | 2.88 | 0.419 |
| **03-SMH-0132-1** | 7.356 | 1.565 | 4.776 | 0.738 | 4.84 | 0.726 |
| **03-SMH-0140-1** | 7.707 | 1.558 | 4.702 | 0.706 | 4.74 | 0.702 |
| **03-SMH-0141** | 5.698 | 1.184 | 3.548 | 0.53 | 3.48 | 0.523 |
| **03-SMH-0157** | 10.858 | 2.265 | 6.846 | 1.062 | 7.17 | 1.101 |
| **03-SMH-0160-1** | 8.054 | 1.655 | 5.027 | 0.775 | 5.16 | 0.789 |
| **03-SMH-0165-1** | 5.99 | 1.268 | 3.939 | 0.624 | 4.23 | 0.644 |
| **03-SMH-0168** | 2.094 | 0.468 | 1.502 | 0.246 | 1.84 | 0.317 |
| **04-SMH-0001-5** | 10.103 | 2.175 | 6.626 | 0.993 | 6.48 | 0.954 |
| **04-SMH-0007-2** | 4.287 | 1.211 | 4.706 | 0.89 | 6.94 | 1.206 |
| **04-SMH-0023-4** | 12.21 | 2.457 | 7.178 | 1.043 | 6.76 | 0.981 |
| | | | | | | |
| **03-SMH-0007** | 4.21 | 0.909 | 2.7 | 0.407 | 2.69 | 0.406 |
| **03-SMH-0013** | 5.059 | 1.095 | 3.298 | 0.496 | 3.27 | 0.499 |
| **03-SMH-0023** | 5.001 | 1.077 | 3.209 | 0.478 | 3.08 | 0.469 |
| **03-SMH-0030** | 4.756 | 1.035 | 3.077 | 0.462 | 2.97 | 0.446 |
| **03-SMH-0031** | 5.365 | 1.166 | 3.49 | 0.526 | 3.49 | 0.525 |
| **03-SMH-0082-1** | 4.532 | 0.969 | 2.91 | 0.426 | 2.77 | 0.424 |
| **03-SMH-0105-1** | 8.874 | 1.874 | 5.629 | 0.826 | 5.33 | 0.803 |
| **03-SMH-0107-2** | 5.169 | 1.118 | 3.336 | 0.497 | 3.22 | 0.499 |
| **03-SMH-0112-2** | 4.944 | 1.048 | 3.058 | 0.449 | 2.8 | 0.424 |
| **03-SMH-0018-1** | 5.102 | 1.073 | 3.281 | 0.478 | 3.21 | 0.486 |
| **03-SMH-0094-1** | 4.899 | 1.038 | 3.151 | 0.457 | 3.04 | 0.456 |
| **03-SMH-0112-5** | 4.248 | 0.917 | 2.759 | 0.406 | 2.68 | 0.403 |
| **03-SMH-0116-1** | 4.739 | 0.998 | 2.981 | 0.444 | 2.93 | 0.438 |
| **04-SMH-0001-13** | 2.733 | 0.55 | 1.661 | 0.242 | 1.64 | 0.255 |
| **04-SMH-0001-21** | 3.293 | 0.706 | 2.156 | 0.318 | 2.03 | 0.296 |
| **04-SMH-0001-22** | 4.934 | 1.038 | 3.13 | 0.461 | 3.04 | 0.465 |
| **04-SMH-0001-3** | 1.643 | 0.333 | 1.016 | 0.156 | 1.11 | 0.186 |
| **04-SMH-0001-9** | 5.706 | 1.206 | 3.601 | 0.537 | 3.46 | 0.522 |
| **04-SMH-0002-4** | 4.253 | 0.906 | 2.716 | 0.408 | 2.7 | 0.416 |
| **04-SMH-0003-1** | 5.015 | 1.064 | 3.292 | 0.485 | 3.22 | 0.492 |
| **04-SMH-0003-3** | 7.478 | 1.554 | 4.546 | 0.679 | 4.49 | 0.668 |
| **04-SMH-0003-7** | 5.009 | 1.084 | 3.263 | 0.481 | 3.13 | 0.476 |
| **04-SMH-0004-1** | 4.876 | 1.059 | 3.119 | 0.472 | 3.07 | 0.468 |
| **04-SMH-0004-3** | 4.471 | 0.918 | 2.684 | 0.415 | 2.85 | 0.426 |
| **04-SMH-0008-1** | 3.643 | 0.771 | 2.29 | 0.341 | 2.26 | 0.343 |
| **04-SMH-0017-1** | 5.009 | 1.077 | 3.214 | 0.471 | 3.02 | 0.453 |
| **04-SMH-0018-2** | 4.109 | 0.833 | 2.383 | 0.344 | 2.27 | 0.336 |
| **04-SMH-0019-1** | 2.112 | 0.436 | 1.274 | 0.191 | 1.24 | 0.183 |
| **04-SMH-0023-1** | 4.51 | 0.95 | 2.863 | 0.419 | 2.74 | 0.425 |
| **04-SMH-0023-3** | 3.753 | 0.792 | 2.309 | 0.328 | 2.04 | 0.292 |

**Abbreviations:** N.D. = not detected. N.M. = not measured/analyzed.

**Appendix 3**. Listing of geochemical data from the Genex mine area -- continued.

| Sample No. | Description | $SiO_2$ wt % | $TiO_2$ wt % | $Al_2O_3$ wt % | $Fe_2O_3$ wt % | FeO wt % | MnO wt % | MgO wt % |
|---|---|---|---|---|---|---|---|---|
| **04-SMH-0023-5** | **Mafic Intrusion** | 44.13 | 1.24 | 13.98 | 14.93 | 13.43 | 0.21 | 8.65 |
| **04-SMH-0024-3** | **Mafic Intrusion** | 42.65 | 1.19 | 14.60 | 15.72 | 14.15 | 0.22 | 6.73 |
| **04-SMH-0024-4** | **Mafic Intrusion** | 46.26 | 1.19 | 13.65 | 18.55 | 16.69 | 0.12 | 10.84 |
| **04-SMH-0025-1** | **Mafic Intrusion** | 40.65 | 1.07 | 13.98 | 13.90 | 12.51 | 0.17 | 7.02 |
| **04-SMH-0027-1** | **Mafic Intrusion** | 44.25 | 1.05 | 14.72 | 12.14 | 10.92 | 0.17 | 6.30 |
| **04-SMH-0033-1** | **Mafic Intrusion** | 50.33 | 1.37 | 14.00 | 15.55 | 13.99 | 0.05 | 12.24 |
| **04-SMH-0036-1** | **Mafic Intrusion** | 46.58 | 1.27 | 12.62 | 14.30 | 12.87 | 0.13 | 7.30 |
| **04-SMH-0044-1** | **Mafic Intrusion** | 47.41 | 1.24 | 13.94 | 11.38 | 10.24 | 0.26 | 8.17 |
| **04-SMH-0050-1** | **Mafic Intrusion** | 46.88 | 1.14 | 13.58 | 13.59 | 12.23 | 0.14 | 8.08 |
| **04-SMH-0052-2** | **Mafic Intrusion** | 49.66 | 1.04 | 16.17 | 16.98 | 15.28 | 0.10 | 9.47 |
| **04-SMH-0052-3** | **Mafic Intrusion** | 46.74 | 1.40 | 14.96 | 22.70 | 20.43 | 0.11 | 8.36 |
| **04-SMH-0054-1** | **Mafic Intrusion** | 48.49 | 1.36 | 13.88 | 11.51 | 10.36 | 0.25 | 4.98 |
| **04-SMH-0071-1** | **Mafic Intrusion** | 46.46 | 1.13 | 12.40 | 12.92 | 11.63 | 0.17 | 6.36 |
| **04-SMH-0071-2** | **Mafic Intrusion** | 46.56 | 1.25 | 13.52 | 12.86 | 11.57 | 0.24 | 5.10 |
| **03-SMH-0114** | **Mafic Intrusion** | 48.14 | 1.34 | 0.12 | 13.02 | 11.72 | 0.22 | 6.22 |
| **03-SMH-0086** | **Mafic Intrusion** | 46.85 | 1.49 | 13.41 | 14.94 | 13.44 | 0.11 | 12.80 |
| **03-SMH-0029-1** | **Mafic Intrusion** | 59.81 | 0.84 | 12.08 | 10.75 | 9.67 | 0.04 | 10.76 |
| **04-SMH-0062-1** | **Mafic Intrusion** | 54.04 | 1.80 | 12.38 | 18.97 | 17.07 | 0.05 | 7.16 |
| **04-SMH-0084-1** | **Mafic Intrusion** | 45.70 | 1.11 | 13.14 | 9.87 | 8.88 | 0.14 | 7.83 |
| **04-SMH-0049-1** | **Mafic Intrusion** | 50.72 | 1.39 | 14.38 | 14.73 | 13.25 | 0.07 | 11.99 |
| | | | | | | | | |
| **03-SMH-0024** | **Intermediate Intrusion** | 59.20 | 1.07 | 13.39 | 10.58 | 9.52 | 0.09 | 7.36 |
| **03-SMH-0026-1** | **Intermediate Intrusion** | 83.64 | 0.11 | 7.52 | 2.92 | 2.63 | 0.01 | 2.51 |
| **03-SMH-0026-2** | **Intermediate Intrusion** | 80.88 | 0.15 | 8.73 | 4.12 | 3.71 | 0.02 | 2.61 |
| **03-SMH-0027-2** | **Intermediate Intrusion** | 65.32 | 0.91 | 13.17 | 7.55 | 6.79 | 0.07 | 6.89 |
| **03-SMH-0028-1** | **Intermediate Intrusion** | 60.79 | 0.90 | 11.40 | 9.18 | 8.26 | 0.21 | 5.23 |
| **03-SMH-0034-3** | **Intermediate Intrusion** | 64.82 | 0.99 | 12.27 | 10.15 | 9.13 | 0.04 | 6.52 |
| **03-SMH-0034-5** | **Intermediate Intrusion** | 71.54 | 0.83 | 10.56 | 7.56 | 6.80 | 0.02 | 3.44 |
| **03-SMH-0034-7** | **Intermediate Intrusion** | 69.36 | 1.54 | 12.20 | 6.54 | 5.88 | 0.03 | 3.93 |
| **03-SMH-0039-1** | **Intermediate Intrusion** | 66.43 | 0.73 | 12.36 | 8.39 | 7.55 | 0.04 | 6.33 |
| **03-SMH-0051** | **Intermediate Intrusion** | 57.89 | 1.16 | 14.32 | 11.96 | 10.76 | 0.10 | 8.40 |
| **03-SMH-0052** | **Intermediate Intrusion** | 62.98 | 1.21 | 12.95 | 10.49 | 9.44 | 0.06 | 6.19 |
| **03-SMH-0053** | **Intermediate Intrusion** | 48.59 | 0.82 | 10.64 | 10.25 | 9.22 | 0.09 | 8.20 |
| **03-SMH-0055** | **Intermediate Intrusion** | 58.98 | 1.15 | 14.58 | 11.72 | 10.55 | 0.13 | 8.99 |
| **03-SMH-0087-1** | **Intermediate Intrusion** | 62.56 | 0.94 | 12.05 | 11.64 | 10.47 | 0.04 | 8.21 |
| **03-SMH-0088-1** | **Intermediate Intrusion** | 61.10 | 1.06 | 13.16 | 12.25 | 11.02 | 0.05 | 7.73 |
| **03-SMH-0088-3** | **Intermediate Intrusion** | 66.91 | 1.27 | 10.02 | 11.95 | 10.75 | 0.04 | 5.65 |
| **03-SMH-0089-2** | **Intermediate Intrusion** | 61.05 | 1.06 | 13.85 | 9.99 | 8.99 | 0.06 | 7.98 |
| **03-SMH-0101-1** | **Intermediate Intrusion** | 69.90 | 1.12 | 14.67 | 3.56 | 3.20 | 0.02 | 2.59 |
| **03-SMH-0102-4** | **Intermediate Intrusion** | 51.50 | 1.35 | 12.12 | 14.65 | 13.18 | 0.05 | 11.42 |
| **03-SMH-0103-2** | **Intermediate Intrusion** | 76.91 | 0.20 | 7.22 | 5.94 | 5.34 | 0.02 | 6.72 |
| **03-SMH-0111-4** | **Intermediate Intrusion** | 63.11 | 0.88 | 12.87 | 6.99 | 6.29 | 0.07 | 2.11 |
| **03-SMH-0127-1** | **Intermediate Intrusion** | 62.04 | 1.00 | 13.23 | 11.98 | 10.78 | 0.04 | 8.95 |
| **03-SMH-0161** | **Intermediate Intrusion** | 66.22 | 1.48 | 12.00 | 8.68 | 7.81 | 0.05 | 6.34 |
| **04-SMH-0001-15** | **Intermediate Intrusion** | 52.10 | 1.70 | 13.68 | 16.97 | 15.27 | 0.10 | 8.02 |

**Abbreviations:** N.D. = not detected. N.M. = not measured/analyzed.

**Appendix 3**. Listing of geochemical data from the Genex mine area -- continued.

| Sample No. | CaO<br>wt % | Na$_2$O<br>wt % | K$_2$O<br>wt % | P$_2$O$_5$<br>wt % | LOI<br>wt % | Total<br>wt % | Ti<br>ppm | Mn<br>ppm | Na<br>ppm | K<br>ppm |
|---|---|---|---|---|---|---|---|---|---|---|
| **04-SMH-0023-5** | 4.33 | 2.53 | 0.36 | 0.12 | 9.92 | 100.40 | N.M. | N.M. | N.M. | N.M. |
| **04-SMH-0024-3** | 6.13 | 2.33 | 0.09 | 0.12 | 9.52 | 99.30 | N.M. | N.M. | N.M. | N.M. |
| **04-SMH-0024-4** | 2.38 | 0.05 | 0.03 | 0.12 | 7.48 | 100.67 | N.M. | N.M. | N.M. | N.M. |
| **04-SMH-0025-1** | 9.05 | 0.11 | 2.05 | 0.08 | 11.45 | 99.53 | N.M. | N.M. | N.M. | N.M. |
| **04-SMH-0027-1** | 7.36 | 3.74 | 0.26 | 0.08 | 9.36 | 99.43 | N.M. | N.M. | N.M. | N.M. |
| **04-SMH-0033-1** | 0.22 | 0.04 | 0.04 | 0.14 | 6.38 | 100.36 | N.M. | N.M. | N.M. | N.M. |
| **04-SMH-0036-1** | 6.77 | 2.06 | 0.03 | 0.11 | 9.28 | 100.46 | N.M. | N.M. | N.M. | N.M. |
| **04-SMH-0044-1** | 6.03 | 1.00 | 1.61 | 0.12 | 9.19 | 100.34 | N.M. | N.M. | N.M. | N.M. |
| **04-SMH-0050-1** | 5.15 | 2.79 | 0.06 | 0.11 | 8.58 | 100.10 | N.M. | N.M. | N.M. | N.M. |
| **04-SMH-0052-2** | 0.11 | 0.07 | 0.83 | 0.10 | 5.90 | 100.43 | N.M. | N.M. | N.M. | N.M. |
| **04-SMH-0052-3** | 0.16 | 0.06 | 0.02 | 0.13 | 5.75 | 100.39 | N.M. | N.M. | N.M. | N.M. |
| **04-SMH-0054-1** | 6.44 | 3.97 | 0.21 | 0.14 | 9.18 | 100.42 | N.M. | N.M. | N.M. | N.M. |
| **04-SMH-0071-1** | 6.89 | 2.80 | 0.25 | 0.13 | 10.90 | 100.41 | N.M. | N.M. | N.M. | N.M. |
| **04-SMH-0071-2** | 8.02 | 3.19 | 0.06 | 0.11 | 9.40 | 100.31 | N.M. | N.M. | N.M. | N.M. |
| **03-SMH-0114** | 9.52 | 2.79 | 0.08 | 0.12 | 7.59 | 89.16 | 6917 | 1686 | 15491 | 671 |
| **03-SMH-0086** | 0.67 | 0.24 | 0.28 | 0.11 | 7.43 | 98.33 | N.M. | N.M. | N.M. | N.M. |
| **03-SMH-0029-1** | 0.31 | 0.03 | 0.11 | 0.24 | 5.36 | 100.33 | N.M. | N.M. | N.M. | N.M. |
| **04-SMH-0062-1** | 0.39 | 0.03 | 0.77 | 0.21 | 4.63 | 100.43 | N.M. | N.M. | N.M. | N.M. |
| **04-SMH-0084-1** | 6.70 | 1.14 | 2.05 | 0.11 | 12.69 | 100.48 | N.M. | N.M. | N.M. | N.M. |
| **04-SMH-0049-1** | 0.42 | 0.05 | 0.04 | 0.10 | 6.52 | 100.41 | N.M. | N.M. | N.M. | N.M. |
| | | | | | | | | | | |
| **03-SMH-0024** | 1.20 | 2.22 | 0.52 | 0.18 | 5.40 | 101.21 | 6416 | 749 | 9785 | 4212 |
| **03-SMH-0026-1** | 0.01 | 0.22 | 1.41 | 0.02 | 2.54 | 100.91 | 598 | 130 | 417 | 11198 |
| **03-SMH-0026-2** | 0.03 | N.D. | 1.71 | 0.03 | 2.68 | 100.96 | 976 | 145 | 604 | 13290 |
| **03-SMH-0027-2** | 0.24 | 0.01 | 1.86 | 0.17 | 4.56 | 100.75 | 5582 | 655 | 671 | >13500 |
| **03-SMH-0028-1** | 4.40 | 2.59 | 0.31 | 0.18 | 6.13 | 101.32 | 5436 | 1755 | 17134 | 2616 |
| **03-SMH-0034-3** | 0.26 | 0.04 | 1.32 | 0.16 | 4.66 | 101.23 | 5842 | 378 | 459 | 10711 |
| **03-SMH-0034-5** | 0.22 | 0.02 | 1.83 | 0.16 | 4.33 | 100.51 | 5259 | 181 | 506 | >13500 |
| **03-SMH-0034-7** | 0.54 | 0.12 | 2.13 | 0.40 | 3.72 | 100.51 | N.M. | N.M. | N.M. | N.M. |
| **03-SMH-0039-1** | 0.20 | 0.27 | 1.29 | 0.15 | 4.24 | 100.43 | N.M. | N.M. | N.M. | N.M. |
| **03-SMH-0051** | 0.34 | 0.04 | 1.52 | 0.23 | 5.27 | 101.23 | 7126 | 898 | 408 | 12063 |
| **03-SMH-0052** | 0.33 | 0.15 | 1.74 | 0.23 | 4.70 | 101.03 | 7405 | 502 | 734 | >13500 |
| **03-SMH-0053** | 6.29 | 2.31 | 0.60 | 0.17 | 13.33 | 101.29 | 5073 | 751 | 13144 | 5025 |
| **03-SMH-0055** | 0.74 | 0.28 | 1.33 | 0.25 | 3.90 | 102.05 | 6338 | 1078 | 1731 | 10639 |
| **03-SMH-0087-1** | 0.29 | 0.04 | 0.45 | 0.18 | 5.11 | 101.51 | 5538 | 398 | N.D. | 3662 |
| **03-SMH-0088-1** | 0.33 | 0.01 | 0.80 | 0.21 | 4.41 | 101.11 | 6028 | 426 | N.D. | 6354 |
| **03-SMH-0088-3** | 0.43 | N.D. | 0.36 | 0.24 | 3.85 | 100.72 | 7450 | 358 | 108 | 3031 |
| **03-SMH-0089-2** | 0.29 | 0.08 | 1.12 | 0.24 | 4.74 | 100.46 | N.M. | N.M. | N.M. | N.M. |
| **03-SMH-0101-1** | 0.32 | 0.08 | 3.87 | 0.22 | 3.06 | 99.41 | 7061 | 154 | 873 | >13500 |
| **03-SMH-0102-4** | 0.24 | 0.05 | N.D. | 0.10 | 6.24 | 97.72 | 7240 | 470 | N.D. | 44.0 |
| **03-SMH-0103-2** | N.D. | N.D. | 0.08 | 0.02 | 3.44 | 100.55 | 1138 | 194 | N.D. | 644 |
| **03-SMH-0111-4** | 3.11 | 4.79 | 0.93 | 0.19 | 5.25 | 100.30 | N.M. | N.M. | N.M. | N.M. |
| **03-SMH-0127-1** | 0.27 | 0.15 | 0.50 | 0.21 | 1.99 | 100.36 | N.M. | N.M. | N.M. | N.M. |
| **03-SMH-0161** | 0.65 | 0.16 | 1.71 | 0.42 | 3.69 | 101.40 | 8660 | 426 | 1428 | 13161 |
| **04-SMH-0001-15** | 0.94 | 0.05 | 0.34 | 0.65 | 5.10 | 99.65 | N.M. | N.M. | N.M. | N.M. |

**Abbreviations:** N.D. = not detected. N.M. = not measured/analyzed.

**Appendix 3**. Listing of geochemical data from the Genex mine area -- continued.

| Sample No. | P<br>ppm | Cr<br>ppm | Co<br>ppm | Ni<br>ppm | Cu<br>ppm | Sc<br>ppm | V<br>ppm | Pb<br>ppm | Zn<br>ppm | As<br>ppm |
|---|---|---|---|---|---|---|---|---|---|---|
| **04-SMH-0023-5** | N.M. | 109 | N.M. | 75.0 | N.M. | N.M. | 336 | N.M. | N.M. | N.M. |
| **04-SMH-0024-3** | N.M. | 121 | N.M. | 84.0 | N.M. | N.M. | 346 | N.M. | N.M. | N.M. |
| **04-SMH-0024-4** | N.M. | 115 | N.M. | 72.0 | N.M. | N.M. | 332 | N.M. | N.M. | N.M. |
| **04-SMH-0025-1** | N.M. | 230 | N.M. | 110 | N.M. | N.M. | 232 | N.M. | N.M. | N.M. |
| **04-SMH-0027-1** | N.M. | 224 | N.M. | 129 | N.M. | N.M. | 222 | N.M. | N.M. | N.M. |
| **04-SMH-0033-1** | N.M. | 94.0 | N.M. | 35.0 | N.M. | N.M. | 398 | N.M. | N.M. | N.M. |
| **04-SMH-0036-1** | N.M. | 91.0 | N.M. | 36.0 | N.M. | N.M. | 380 | N.M. | N.M. | N.M. |
| **04-SMH-0044-1** | N.M. | 99.0 | N.M. | 69.0 | N.M. | N.M. | 396 | N.M. | N.M. | N.M. |
| **04-SMH-0050-1** | N.M. | 105 | N.M. | 74.0 | N.M. | N.M. | 336 | N.M. | N.M. | N.M. |
| **04-SMH-0052-2** | N.M. | 113 | N.M. | 51.0 | N.M. | N.M. | 317 | N.M. | N.M. | N.M. |
| **04-SMH-0052-3** | N.M. | 104 | N.M. | 36.0 | N.M. | N.M. | 394 | N.M. | N.M. | N.M. |
| **04-SMH-0054-1** | N.M. | 93.0 | N.M. | 39.0 | N.M. | N.M. | 378 | N.M. | N.M. | N.M. |
| **04-SMH-0071-1** | N.M. | 100 | N.M. | 44.0 | N.M. | N.M. | 328 | N.M. | N.M. | N.M. |
| **04-SMH-0071-2** | N.M. | 95.0 | N.M. | 42.0 | N.M. | N.M. | 355 | N.M. | N.M. | N.M. |
| **03-SMH-0114** | 535 | 98.0 | 46.0 | 35.0 | 81.0 | 67.0 | 347 | 6.0 | 89.0 | N.D. |
| **03-SMH-0086** | N.M. | N.M. | N.M. | N.M. | N.M. | N.M. | N.M. | N.M. | N.M. | N.M. |
| **03-SMH-0029-1** | N.M. | -8.0 | N.M. | 13.0 | N.M. | N.M. | 120 | N.M. | N.M. | N.M. |
| **04-SMH-0062-1** | N.M. | 11.0 | N.M. | 4.0 | N.M. | N.M. | 446 | N.M. | N.M. | N.M. |
| **04-SMH-0084-1** | N.M. | -8.0 | N.M. | 14.0 | N.M. | N.M. | 113 | N.M. | N.M. | N.M. |
| **04-SMH-0049-1** | N.M. | 92.0 | N.M. | 45.0 | N.M. | N.M. | 320 | N.M. | N.M. | N.M. |
| | | | | | | | | | | |
| **03-SMH-0024** | 778 | 26.0 | 23.0 | 16.0 | 8.0 | 45.0 | 68.0 | 5.0 | 388 | 3.0 |
| **03-SMH-0026-1** | N.D. | 18.0 | N.D. | N.D. | 17.0 | 21.0 | 4.0 | N.D. | 27.0 | N.D. |
| **03-SMH-0026-2** | 27.0 | 26.0 | N.D. | 4.0 | 21.0 | 26.0 | N.D. | N.D. | 88.0 | N.D. |
| **03-SMH-0027-2** | 720 | 24.0 | N.D. | 8.0 | 12.0 | 53.0 | 27.0 | 14.0 | 173 | 1.0 |
| **03-SMH-0028-1** | 778 | 22.0 | 28.0 | 13.0 | 51.0 | 48.0 | 53.0 | 6.0 | 144 | 3.0 |
| **03-SMH-0034-3** | 693 | 21.0 | 19.0 | 18.0 | 146 | 40.0 | 51.0 | N.D. | 306 | 14.0 |
| **03-SMH-0034-5** | 670 | 16.0 | N.D. | 15.0 | 269 | 33.0 | 7.0 | 10.0 | 332 | 8.0 |
| **03-SMH-0034-7** | N.M. | -8.0 | N.M. | -4.0 | N.M. | N.M. | 132 | N.M. | N.M. | N.M. |
| **03-SMH-0039-1** | N.M. | -8.0 | N.M. | 7.0 | N.M. | N.M. | 86.0 | N.M. | N.M. | N.M. |
| **03-SMH-0051** | 949 | 9.0 | 41.0 | 21.0 | 7.0 | 50.0 | 60.0 | 6.0 | 105 | 2.0 |
| **03-SMH-0052** | 984 | 16.0 | 32.0 | 16.0 | 156 | 43.0 | 33.0 | 13.0 | 529 | 4.0 |
| **03-SMH-0053** | 743 | 15.0 | 15.0 | 14.0 | 36.0 | 38.0 | 37.0 | N.D. | 107 | N.D. |
| **03-SMH-0055** | 1081 | 9.0 | 28.0 | 21.0 | 6.0 | 44.0 | 71.0 | N.D. | 241 | N.D. |
| **03-SMH-0087-1** | 760 | 23.0 | 21.0 | 16.0 | 2.0 | 24.0 | 52.0 | N.D. | 224 | 1.0 |
| **03-SMH-0088-1** | 796 | 21.0 | 23.0 | 18.0 | 8.0 | 41.0 | 120 | N.D. | 128 | 2.0 |
| **03-SMH-0088-3** | 1120 | 10.0 | 29.0 | N.D. | 16.0 | 33.0 | N.D. | 13.0 | 268 | 12.0 |
| **03-SMH-0089-2** | N.M. | 16.0 | N.M. | 14.0 | N.M. | N.M. | 135 | N.M. | N.M. | N.M. |
| **03-SMH-0101-1** | 990 | 16.0 | N.D. | 15.0 | 4.0 | 44.0 | 84.0 | N.D. | 74.0 | 3.0 |
| **03-SMH-0102-4** | 361 | 126 | 49.0 | 40.0 | N.D. | 58.0 | 363 | N.D. | 370 | 14.0 |
| **03-SMH-0103-2** | N.D. | N.D. | 17.0 | 7.0 | N.D. | 22.0 | N.D. | N.D. | 202 | N.D. |
| **03-SMH-0111-4** | N.M. | -8.0 | N.M. | 7.0 | N.M. | N.M. | 106 | N.M. | N.M. | N.M. |
| **03-SMH-0127-1** | N.M. | 45.0 | N.M. | 13.0 | N.M. | N.M. | 115 | N.M. | N.M. | N.M. |
| **03-SMH-0161** | 2331 | 5.0 | 28.0 | 3.0 | 15.0 | 43.0 | 47.0 | N.D. | 385 | 35.0 |
| **04-SMH-0001-15** | N.M. | -8.0 | N.M. | -4.0 | N.M. | N.M. | 75.0 | N.M. | N.M. | N.M. |

Abbreviations: N.D. = not detected. N.M. = not measured/analyzed.

**Appendix 3**. Listing of geochemical data from the Genex mine area -- continued.

| Sample No. | Rb ppm | Cs ppm | Ba ppm | Sr ppm | Ga ppm | Ta ppm | Nb ppm | Hf ppm | Zr ppm | Y ppm |
|---|---|---|---|---|---|---|---|---|---|---|
| **04-SMH-0023-5** | 7.70 | 0.199 | N.M. | 48.3 | N.M. | 0.24 | 3.7 | 4.0 | 168.5 | 25.44 |
| **04-SMH-0024-3** | 2.26 | 1.157 | N.M. | 42.0 | N.M. | 0.23 | 3.6 | 2.4 | 91.2 | 22.83 |
| **04-SMH-0024-4** | 0.38 | 0.194 | N.M. | 13.0 | N.M. | 0.23 | 3.6 | 2.3 | 89.6 | 21.93 |
| **04-SMH-0025-1** | 64.67 | 1.943 | N.M. | 325.3 | N.M. | N.D. | 1.5 | 1.4 | 47.0 | 18.39 |
| **04-SMH-0027-1** | 6.28 | 0.302 | N.M. | 229.0 | N.M. | N.D. | 1.7 | 1.5 | 51.7 | 18.49 |
| **04-SMH-0033-1** | 0.74 | 0.056 | N.M. | 2.5 | N.M. | 0.28 | 4.4 | 3.0 | 111 | 26.4 |
| **04-SMH-0036-1** | 0.38 | 0.060 | N.M. | 84.0 | N.M. | 0.23 | 3.6 | 2.3 | 87.8 | 26.44 |
| **04-SMH-0044-1** | 35.32 | 0.334 | N.M. | 41.7 | N.M. | 0.22 | 3.6 | 2.5 | 92.5 | 22.18 |
| **04-SMH-0050-1** | 0.53 | 0.045 | N.M. | 79.7 | N.M. | 0.21 | 3.3 | 2.2 | 82.3 | 23.87 |
| **04-SMH-0052-2** | 16.40 | 0.168 | N.M. | 2.7 | N.M. | 0.20 | 3.3 | 2.1 | 75.8 | 22.13 |
| **04-SMH-0052-3** | 0.34 | 0.032 | N.M. | 1.3 | N.M. | 0.28 | 4.5 | 2.8 | 104.2 | 45.52 |
| **04-SMH-0054-1** | 8.13 | 0.235 | N.M. | 104.3 | N.M. | 0.26 | 4.1 | 2.8 | 99.2 | 27.69 |
| **04-SMH-0071-1** | 7.38 | 0.264 | N.M. | 178.3 | N.M. | 0.24 | 3.7 | 2.5 | 91.7 | 21.76 |
| **04-SMH-0071-2** | 2.16 | 0.137 | N.M. | 124.0 | N.M. | 0.23 | 3.6 | 2.4 | 87.3 | 25.03 |
| **03-SMH-0114** | 2.12 | 0.278 | 38.0 | 65.6 | 17.0 | 0.30 | 4.1 | 2.8 | 97.6 | 32.96 |
| **03-SMH-0086** | 7.84 | 0.186 | N.M. | 7.9 | N.M. | 0.32 | 4.3 | 2.9 | 103.7 | 21.61 |
| **03-SMH-0029-1** | 1.88 | 0.087 | N.M. | 5.0 | N.M. | 0.55 | 8.4 | 5.4 | 219.4 | 31.12 |
| **04-SMH-0062-1** | 18.62 | 0.119 | N.M. | 7.6 | N.M. | 0.46 | 6.8 | 4.4 | 170.1 | 38.68 |
| **04-SMH-0084-1** | 47.02 | 0.435 | N.M. | 50.2 | N.M. | 0.21 | 3.5 | 2.3 | 84.4 | 21.39 |
| **04-SMH-0049-1** | 0.84 | 0.091 | N.M. | 3.2 | N.M. | 0.26 | 4.9 | 2.7 | 101.3 | 50.49 |
| | | | | | | | | | | |
| **03-SMH-0024** | 15.15 | 0.193 | 45.0 | 32.8 | 21.0 | 0.81 | 9.9 | 6.7 | 261.7 | 35.74 |
| **03-SMH-0026-1** | 27.31 | 0.341 | 241 | 8.9 | 13.0 | 1.17 | 12.7 | 5.7 | 168.6 | 20.43 |
| **03-SMH-0026-2** | 31.34 | 0.363 | 312 | 7.7 | 15.0 | 1.42 | 15.3 | 7.2 | 214.6 | 52.35 |
| **03-SMH-0027-2** | 34.27 | 0.424 | 437 | 11.2 | 28.0 | 0.84 | 9.6 | 6.0 | 231.5 | 29.4 |
| **03-SMH-0028-1** | 5.73 | 0.164 | 75.0 | 62.7 | 15.0 | 0.70 | 7.8 | 5.2 | 202.8 | 32.49 |
| **03-SMH-0034-3** | 23.89 | 0.298 | 329 | 7.0 | 20.0 | 0.76 | 9.1 | 6.2 | 246 | 38.8 |
| **03-SMH-0034-5** | 31.40 | 0.342 | 377 | 7.1 | 25.0 | 0.68 | 7.8 | 5.4 | 211.1 | 18.08 |
| **03-SMH-0034-7** | 41.42 | 0.459 | N.M. | 15.0 | N.M. | 0.62 | 10.2 | 5.6 | 222.6 | 29.99 |
| **03-SMH-0039-1** | 25.66 | 0.323 | N.M. | 9.7 | N.M. | 0.75 | 9.8 | 5.7 | 224.5 | 36.16 |
| **03-SMH-0051** | 26.91 | 0.431 | 246 | 8.7 | 24.0 | 0.87 | 10.6 | 7.3 | 292.4 | 44.02 |
| **03-SMH-0052** | 26.50 | 0.335 | 324 | 8.6 | 20.0 | 0.82 | 10.2 | 6.8 | 266.2 | 41.44 |
| **03-SMH-0053** | 11.31 | 0.113 | 93.0 | 104.2 | 15.0 | 0.69 | 7.8 | 5.4 | 213.3 | 35.18 |
| **03-SMH-0055** | 27.02 | 0.650 | 246 | 12.2 | 22.0 | 0.89 | 11.1 | 7.7 | 306.5 | 49.36 |
| **03-SMH-0087-1** | 7.24 | 0.085 | 146 | 3.1 | 17.0 | 0.59 | 8.1 | 5.7 | 223.7 | 26.08 |
| **03-SMH-0088-1** | 13.88 | 0.330 | 286 | 5.2 | 20.0 | 0.66 | 9.5 | 6.4 | 255.1 | 30.97 |
| **03-SMH-0088-3** | 5.48 | 0.054 | 79.0 | 5.2 | 21.0 | 0.52 | 7.3 | 4.3 | 170.9 | 19.64 |
| **03-SMH-0089-2** | 18.67 | 0.154 | N.M. | 5.4 | N.M. | 0.65 | 10.0 | 6.7 | 274.6 | 38.02 |
| **03-SMH-0101-1** | 18.86 | 0.269 | 1152 | 8.0 | 21.0 | 0.81 | 10.5 | 7.4 | 288.8 | 23.79 |
| **03-SMH-0102-4** | 0.25 | 0.054 | N.D. | 3.5 | 19.0 | 0.28 | 3.7 | 2.6 | 92.9 | 26.34 |
| **03-SMH-0103-2** | 1.52 | 0.041 | N.D. | 1.0 | 9.0 | 0.88 | 12.1 | 5.1 | 165.9 | 46.74 |
| **03-SMH-0111-4** | 19.18 | 0.453 | N.M. | 108.2 | N.M. | 0.71 | 9.6 | 5.9 | 228.6 | 27.86 |
| **03-SMH-0127-1** | 8.49 | 0.258 | N.M. | 4.3 | N.M. | 0.63 | 9.6 | 6.4 | 266 | 45.71 |
| **03-SMH-0161** | 29.64 | 1.179 | 420 | 16.8 | 28.0 | 0.68 | 9.6 | 5.9 | 230 | 40.57 |
| **04-SMH-0001-15** | 6.01 | 0.114 | N.M. | 5.9 | N.M. | 0.75 | 11.1 | 6.8 | 273.9 | 22.49 |

**Abbreviations:** N.D. = not detected. N.M. = not measured/analyzed.

**Appendix 3**. Listing of geochemical data from the Genex mine area -- continued.

| **Sample No.** | **Th** | **U** | **La** | **Ce** | **Pr** | **Nd** | **Sm** | **Eu** | **Gd** | **Tb** |
|---|---|---|---|---|---|---|---|---|---|---|
| | **ppm** | **ppm** | **ppm** | **ppm** | **ppm** | **ppm** | **ppm** | **ppm** | **ppm** | **ppm** |
| **04-SMH-0023-5** | 0.54 | 0.134 | 6.29 | 15.37 | 2.259 | 11.04 | 3.27 | 1.03 | 3.922 | 0.658 |
| **04-SMH-0024-3** | 0.55 | 0.159 | 3.23 | 9.46 | 1.522 | 8.03 | 2.64 | 0.704 | 3.517 | 0.603 |
| **04-SMH-0024-4** | 0.53 | 0.124 | 6.57 | 16.1 | 2.32 | 11.3 | 2.99 | 0.849 | 3.46 | 0.584 |
| **04-SMH-0025-1** | 0.30 | 0.064 | 4.65 | 12.21 | 1.847 | 9.19 | 2.54 | 0.887 | 3.009 | 0.497 |
| **04-SMH-0027-1** | 0.45 | 0.1 | 4.79 | 12.16 | 1.783 | 8.94 | 2.53 | 0.906 | 2.988 | 0.511 |
| **04-SMH-0033-1** | 0.70 | 0.172 | 8.95 | 21.32 | 2.966 | 13.9 | 3.64 | 0.679 | 4.282 | 0.715 |
| **04-SMH-0036-1** | 0.55 | 0.152 | 5.9 | 14.94 | 2.138 | 10.46 | 3.04 | 0.93 | 3.928 | 0.688 |
| **04-SMH-0044-1** | 0.54 | 0.141 | 4.32 | 11.07 | 1.655 | 7.96 | 2.56 | 0.866 | 3.339 | 0.622 |
| **04-SMH-0050-1** | 0.50 | 0.126 | 5.84 | 14.7 | 2.149 | 10.38 | 2.98 | 0.974 | 3.687 | 0.646 |
| **04-SMH-0052-2** | 0.60 | 0.181 | 6.88 | 15.66 | 2.155 | 9.79 | 2.54 | 0.329 | 3.214 | 0.57 |
| **04-SMH-0052-3** | 0.75 | 0.24 | 6.72 | 17.27 | 2.498 | 12.01 | 3.81 | 0.583 | 6.087 | 1.181 |
| **04-SMH-0054-1** | 0.66 | 0.171 | 7.02 | 17.39 | 2.529 | 11.96 | 3.39 | 1.054 | 4.314 | 0.747 |
| **04-SMH-0071-1** | 0.60 | 0.151 | 5.68 | 13.97 | 2.061 | 10.13 | 2.8 | 0.885 | 3.483 | 0.596 |
| **04-SMH-0071-2** | 0.56 | 0.148 | 5.96 | 14.95 | 2.176 | 10.49 | 3.03 | 1.022 | 3.847 | 0.668 |
| **03-SMH-0114** | 0.65 | 0.179 | 6.58 | 16.56 | 2.391 | 11.82 | 3.52 | 1.202 | 5.052 | 0.884 |
| **03-SMH-0086** | 0.47 | 0.172 | 2.52 | 6.28 | 0.973 | 5.0 | 1.66 | 0.494 | 2.82 | 0.528 |
| **03-SMH-0029-1** | 2.34 | 0.753 | 5.09 | 13.71 | 2.026 | 10.1 | 3.12 | 0.616 | 4.258 | 0.787 |
| **04-SMH-0062-1** | 1.64 | 0.412 | 11.48 | 25.28 | 4.001 | 18.64 | 4.88 | 0.491 | 5.909 | 1.029 |
| **04-SMH-0084-1** | 0.54 | 0.133 | 7.0 | 17.66 | 2.565 | 12.48 | 3.44 | 1.075 | 3.763 | 0.613 |
| **04-SMH-0049-1** | 0.72 | 0.335 | 10.23 | 23.34 | 3.109 | 14.09 | 4.43 | 0.5 | 7.292 | 1.419 |
| | | | | | | | | | | |
| **03-SMH-0024** | 2.90 | 0.753 | 12.24 | 28.66 | 3.785 | 16.34 | 4.27 | 0.729 | 5.413 | 0.981 |
| **03-SMH-0026-1** | 4.83 | 1.175 | 22.63 | 54.28 | 6.837 | 27.79 | 5.67 | 0.264 | 4.473 | 0.649 |
| **03-SMH-0026-2** | 6.02 | 1.443 | 40.13 | 90.28 | 11.467 | 46.26 | 9.96 | 1.579 | 9.837 | 1.601 |
| **03-SMH-0027-2** | 3.19 | 0.911 | 8.93 | 20.84 | 2.784 | 12.36 | 3.33 | 0.593 | 4.202 | 0.73 |
| **03-SMH-0028-1** | 2.38 | 0.632 | 12.68 | 31.28 | 4.225 | 18.82 | 4.84 | 1.256 | 5.684 | 0.945 |
| **03-SMH-0034-3** | 2.96 | 0.725 | 21.99 | 55.54 | 7.41 | 32.3 | 7.41 | 0.827 | 7.661 | 1.205 |
| **03-SMH-0034-5** | 1.81 | 0.616 | 17.33 | 37.82 | 4.664 | 19.34 | 4.12 | 0.64 | 4.091 | 0.63 |
| **03-SMH-0034-7** | 2.23 | 0.62 | 14.86 | 35.07 | 4.591 | 20.56 | 5.04 | 0.834 | 5.4 | 0.84 |
| **03-SMH-0039-1** | 4.30 | 0.952 | 26.58 | 61.17 | 7.645 | 31.77 | 6.87 | 0.746 | 6.519 | 1.025 |
| **03-SMH-0051** | 3.17 | 0.823 | 24.81 | 58.57 | 7.662 | 33.32 | 7.72 | 1.325 | 8.173 | 1.318 |
| **03-SMH-0052** | 2.73 | 0.741 | 16.14 | 38.33 | 5.063 | 22.65 | 5.44 | 0.913 | 6.701 | 1.141 |
| **03-SMH-0053** | 2.33 | 0.615 | 15.3 | 37.73 | 5.135 | 22.49 | 5.5 | 1.448 | 6.18 | 1.019 |
| **03-SMH-0055** | 3.44 | 0.864 | 38.48 | 81.39 | 10.043 | 42.3 | 9.58 | 1.534 | 9.728 | 1.486 |
| **03-SMH-0087-1** | 2.20 | 0.626 | 9.25 | 22.49 | 2.983 | 13.38 | 3.43 | 0.357 | 4.171 | 0.693 |
| **03-SMH-0088-1** | 2.76 | 0.736 | 16.47 | 39.63 | 5.254 | 22.62 | 5.42 | 0.433 | 5.805 | 0.917 |
| **03-SMH-0088-3** | 1.74 | 0.494 | 18.24 | 41.7 | 5.472 | 23.32 | 5.13 | 0.724 | 4.766 | 0.676 |
| **03-SMH-0089-2** | 2.86 | 0.721 | 19.31 | 46.02 | 6.09 | 26.66 | 6.42 | 0.555 | 6.622 | 1.072 |
| **03-SMH-0101-1** | 1.64 | 0.738 | 13.81 | 33.84 | 4.562 | 19.76 | 4.71 | 0.532 | 4.732 | 0.72 |
| **03-SMH-0102-4** | 0.49 | 0.158 | 3.84 | 10.33 | 1.576 | 7.77 | 2.5 | 0.263 | 3.781 | 0.696 |
| **03-SMH-0103-2** | 4.20 | 0.965 | 31.9 | 75.24 | 9.541 | 39.1 | 8.24 | 0.471 | 8.086 | 1.273 |
| **03-SMH-0111-4** | 3.44 | 0.866 | 23.94 | 53.87 | 6.816 | 28.24 | 6.1 | 1.366 | 6.028 | 0.918 |
| **03-SMH-0127-1** | 2.86 | 0.71 | 28.78 | 67.91 | 8.858 | 38.09 | 8.86 | 0.606 | 8.972 | 1.403 |
| **03-SMH-0161** | 2.72 | 0.74 | 9.51 | 25.13 | 3.692 | 18.37 | 5.1 | 1.177 | 6.53 | 1.096 |
| **04-SMH-0001-15** | 2.70 | 0.738 | 4.47 | 12.45 | 1.825 | 9.61 | 3.15 | 0.345 | 4.243 | 0.685 |

**Abbreviations:** N.D. = not detected. N.M. = not measured/analyzed.

**Appendix 3**. Listing of geochemical data from the Genex mine area -- continued.

| **Sample No.** | **Dy** | **Ho** | **Er** | **Tm** | **Yb** | **Lu** |
|---|---|---|---|---|---|---|
| | **ppm** | **ppm** | **ppm** | **ppm** | **ppm** | **ppm** |
| **04-SMH-0023-5** | 4.388 | 0.941 | 2.859 | 0.42 | 2.74 | 0.406 |
| **04-SMH-0024-3** | 3.86 | 0.831 | 2.528 | 0.375 | 2.5 | 0.382 |
| **04-SMH-0024-4** | 3.78 | 0.82 | 2.522 | 0.375 | 2.48 | 0.383 |
| **04-SMH-0025-1** | 3.175 | 0.672 | 2.035 | 0.292 | 1.89 | 0.282 |
| **04-SMH-0027-1** | 3.242 | 0.677 | 2.02 | 0.296 | 1.92 | 0.284 |
| **04-SMH-0033-1** | 4.627 | 1.018 | 3.021 | 0.444 | 3.05 | 0.479 |
| **04-SMH-0036-1** | 4.481 | 0.988 | 2.986 | 0.443 | 2.89 | 0.429 |
| **04-SMH-0044-1** | 4.002 | 0.864 | 2.565 | 0.386 | 2.58 | 0.379 |
| **04-SMH-0050-1** | 4.164 | 0.902 | 2.715 | 0.403 | 2.65 | 0.399 |
| **04-SMH-0052-2** | 3.825 | 0.816 | 2.441 | 0.352 | 2.2 | 0.317 |
| **04-SMH-0052-3** | 8.083 | 1.71 | 4.932 | 0.687 | 4.28 | 0.612 |
| **04-SMH-0054-1** | 4.974 | 1.056 | 3.148 | 0.46 | 3.01 | 0.449 |
| **04-SMH-0071-1** | 3.817 | 0.833 | 2.553 | 0.381 | 2.52 | 0.383 |
| **04-SMH-0071-2** | 4.379 | 0.946 | 2.879 | 0.429 | 2.77 | 0.419 |
| **03-SMH-0114** | 5.872 | 1.281 | 3.862 | 0.566 | 3.63 | 0.554 |
| **03-SMH-0086** | 3.715 | 0.821 | 2.543 | 0.383 | 2.58 | 0.411 |
| **03-SMH-0029-1** | 5.085 | 1.111 | 3.443 | 0.525 | 3.63 | 0.554 |
| **04-SMH-0062-1** | 6.623 | 1.447 | 4.427 | 0.653 | 4.36 | 0.65 |
| **04-SMH-0084-1** | 3.884 | 0.824 | 2.493 | 0.369 | 2.48 | 0.385 |
| **04-SMH-0049-1** | 9.142 | 1.837 | 5.09 | 0.699 | 4.4 | 0.616 |
| | | | | | | |
| **03-SMH-0024** | 6.648 | 1.467 | 4.488 | 0.68 | 4.62 | 0.71 |
| **03-SMH-0026-1** | 3.889 | 0.869 | 2.879 | 0.488 | 3.6 | 0.565 |
| **03-SMH-0026-2** | 9.942 | 2.105 | 6.218 | 0.927 | 5.92 | 0.871 |
| **03-SMH-0027-2** | 4.928 | 1.116 | 3.522 | 0.552 | 3.77 | 0.582 |
| **03-SMH-0028-1** | 5.886 | 1.271 | 3.778 | 0.561 | 3.68 | 0.563 |
| **03-SMH-0034-3** | 7.371 | 1.477 | 4.396 | 0.649 | 4.26 | 0.647 |
| **03-SMH-0034-5** | 3.756 | 0.741 | 2.158 | 0.312 | 2.05 | 0.291 |
| **03-SMH-0034-7** | 5.356 | 1.109 | 3.414 | 0.514 | 3.46 | 0.525 |
| **03-SMH-0039-1** | 6.348 | 1.305 | 3.802 | 0.567 | 3.71 | 0.553 |
| **03-SMH-0051** | 8.118 | 1.664 | 4.942 | 0.729 | 4.78 | 0.702 |
| **03-SMH-0052** | 7.444 | 1.574 | 4.693 | 0.685 | 4.49 | 0.671 |
| **03-SMH-0053** | 6.284 | 1.303 | 3.846 | 0.566 | 3.82 | 0.593 |
| **03-SMH-0055** | 9.041 | 1.852 | 5.521 | 0.827 | 5.62 | 0.856 |
| **03-SMH-0087-1** | 4.442 | 0.996 | 3.08 | 0.479 | 3.36 | 0.526 |
| **03-SMH-0088-1** | 5.582 | 1.18 | 3.665 | 0.567 | 3.76 | 0.612 |
| **03-SMH-0088-3** | 3.932 | 0.806 | 2.348 | 0.352 | 2.44 | 0.374 |
| **03-SMH-0089-2** | 6.725 | 1.413 | 4.213 | 0.631 | 4.26 | 0.656 |
| **03-SMH-0101-1** | 4.3 | 0.938 | 2.943 | 0.458 | 3.13 | 0.495 |
| **03-SMH-0102-4** | 4.66 | 1.01 | 3.05 | 0.455 | 2.94 | 0.436 |
| **03-SMH-0103-2** | 8.04 | 1.703 | 5.076 | 0.736 | 4.62 | 0.689 |
| **03-SMH-0111-4** | 5.586 | 1.101 | 3.116 | 0.467 | 3.12 | 0.465 |
| **03-SMH-0127-1** | 8.391 | 1.671 | 4.861 | 0.696 | 4.6 | 0.691 |
| **03-SMH-0161** | 7.251 | 1.625 | 4.911 | 0.746 | 4.89 | 0.743 |
| **04-SMH-0001-15** | 4.14 | 0.91 | 2.854 | 0.46 | 3.35 | 0.559 |

**Abbreviations:** N.D. = not detected. N.M. = not measured/analyzed.

**Appendix 3**. Listing of geochemical data from the Genex mine area -- continued.

| Sample No. | Description | $SiO_2$ wt % | $TiO_2$ wt % | $Al_2O_3$ wt % | $Fe_2O_3$ wt % | FeO wt % | MnO wt % | MgO wt % |
|---|---|---|---|---|---|---|---|---|
| **04-SMH-0003-2** | **Intermediate Intrusion** | 65.92 | 1.01 | 12.02 | 4.50 | 4.05 | 0.14 | 1.48 |
| **04-SMH-0023-2** | **Intermediate Intrusion** | 46.01 | 1.25 | 14.98 | 14.69 | 13.22 | 0.16 | 7.18 |
| **04-SMH-0026-2** | **Intermediate Intrusion** | 73.08 | 0.33 | 12.44 | 1.66 | 1.49 | 0.06 | 0.61 |
| **04-SMH-0076-1** | **Intermediate Intrusion** | 61.12 | 0.88 | 13.46 | 9.87 | 8.88 | 0.07 | 4.20 |
| **04-SMH-0041-1** | **Intermediate Intrusion** | 66.14 | 1.02 | 12.23 | 5.85 | 5.25 | 0.05 | 7.05 |
| | | | | | | | | |
| **03-SMH-0022** | **Late Diabase Intrusion** | 50.23 | 1.98 | 13.32 | 17.59 | 15.83 | 0.25 | 3.94 |
| | | | | | | | | |
| **04-SMH-0005-4** | **Epiclastic** | 76.50 | 0.13 | 10.76 | 2.96 | 2.66 | 0.04 | 0.64 |
| **04-SMH-0017-4** | **Epiclastic** | 75.41 | 0.19 | 13.63 | 1.48 | 1.33 | 0.02 | 0.45 |
| | | | | | | | | |
| **04-SMH-0017-5** | **Volcaniclastic** | 76.60 | 0.49 | 11.12 | 2.92 | 2.63 | 0.07 | 0.96 |
| **04-SMH-0018-1** | **Volcaniclastic** | 77.45 | 0.15 | 10.75 | 2.23 | 2.01 | 0.03 | 0.33 |

| Sample No. | CaO wt % | $Na_2O$ wt % | $K_2O$ wt % | $P_2O_5$ wt % | LOI wt % | Total wt % | Ti ppm | Mn ppm | Na ppm | K ppm |
|---|---|---|---|---|---|---|---|---|---|---|
| **04-SMH-0003-2** | 4.77 | 4.34 | 0.79 | 0.22 | 4.86 | 100.05 | N.M. | N.M. | N.M. | N.M. |
| **04-SMH-0023-2** | 7.05 | 2.85 | 0.32 | 0.12 | 4.11 | 98.72 | N.M. | N.M. | N.M. | N.M. |
| **04-SMH-0026-2** | 2.88 | 3.59 | 2.15 | 0.07 | 3.01 | 99.88 | N.M. | N.M. | N.M. | N.M. |
| **04-SMH-0076-1** | 1.19 | 0.71 | 4.49 | 0.19 | 4.31 | 100.49 | N.M. | N.M. | N.M. | N.M. |
| **04-SMH-0041-1** | 0.45 | 0.11 | 2.41 | 0.24 | 4.11 | 99.66 | N.M. | N.M. | N.M. | N.M. |
| | | | | | | | | | | |
| **03-SMH-0072** | 8.39 | 3.03 | 0.63 | 0.32 | 1.35 | 101.03 | 12014 | 2015 | 25330 | 5610 |
| | | | | | | | | | | |
| **04-SMH-0005-4** | 0.91 | 2.07 | 2.76 | 0.02 | 2.70 | 99.49 | N.M. | N.M. | N.M. | N.M. |
| **04-SMH-0017-4** | 0.42 | 3.50 | 2.78 | 0.03 | 2.17 | 100.08 | N.M. | N.M. | N.M. | N.M. |
| | | | | | | | | | | |
| **04-SMH-0017-5** | 1.56 | 0.93 | 3.93 | 0.15 | 1.20 | 99.93 | N.M. | N.M. | N.M. | N.M. |
| **04-SMH-0018-1** | 1.05 | 2.19 | 3.42 | 0.02 | 1.69 | 99.31 | N.M. | N.M. | N.M. | N.M |

| Sample No. | P ppm | Cr ppm | Co ppm | Ni ppm | Cu ppm | Sc ppm | V ppm | Pb ppm | Zn ppm | As ppm |
|---|---|---|---|---|---|---|---|---|---|---|
| **04-SMH-0003-2** | N.M. | <8 | N.M. | 9.0 | N.M. | N.M. | 111 | N.M. | N.M. | N.M. |
| **04-SMH-0023-2** | N.M. | 33.0 | N.M. | 26.0 | N.M. | N.M. | 140 | N.M. | N.M. | N.M. |
| **04-SMH-0026-2** | N.M. | <8 | N.M. | <4 | N.M. | N.M. | 11.0 | N.M. | N.M. | N.M. |
| **04-SMH-0076-1** | N.M. | 105 | N.M. | 68.0 | N.M. | N.M. | 363 | N.M. | N.M. | N.M. |
| **04-SMH-0041-1** | N.M. | -8.0 | N.M. | 10.0 | N.M. | N.M. | 132 | N.M. | N.M. | N.M. |
| | | | | | | | | | | |
| **03-SMH-0022** | 1688 | 90.0 | 52.0 | 48.0 | 182 | 73.0 | 171 | 8.0 | 137 | N.D. |
| | | | | | | | | | | |
| **04-SMH-0005-4** | N.M. | <8 | N.M. | 6.0 | N.M. | N.M. | <5 | N.M. | N.M. | N.M. |
| **04-SMH-0017-4** | N.M. | <8 | N.M. | <4 | N.M. | N.M. | <5 | N.M. | N.M. | N.M. |
| | | | | | | | | | | |
| **04-SMH-0017-5** | N.M. | 21.0 | N.M. | <4 | N.M. | N.M. | 10.0 | N.M. | N.M. | N.M. |
| **04-SMH-0018-1** | N.M. | <8 | N.M. | <4 | N.M. | N.M. | <5 | N.M. | N.M. | N.M. |

**Abbreviations:** N.D. = not detected. N.M. = not measured/analyzed.

**Appendix 3**. Listing of geochemical data from the Genex mine area -- continued.

| Sample No. | Rb ppm | Cs ppm | Ba ppm | Sr ppm | Ga ppm | Ta ppm | Nb ppm | Hf ppm | Zr ppm | Y ppm |
|---|---|---|---|---|---|---|---|---|---|---|
| **04-SMH-0003-2** | 28.55 | 0.747 | N.M. | 135.9 | N.M. | 0.55 | 8.2 | 5.2 | 206.3 | 32.4 |
| **04-SMH-0023-2** | 35.36 | 0.451 | N.M. | 10.9 | N.M. | 0.58 | 8.3 | 5.3 | 212.6 | 17.49 |
| **04-SMH-0026-2** | 55.77 | 1.821 | N.M. | 144 | N.M. | 0.57 | 7.1 | 4.5 | 173.9 | 16.72 |
| **04-SMH-0076-1** | 71.22 | 1.874 | N.M. | 18.7 | N.M. | 0.67 | 9.7 | 6.6 | 260 | 21.36 |
| **04-SMH-0041-1** | 52.48 | 0.353 | N.M. | 5.5 | N.M. | 0.65 | 10.0 | 6.6 | 270.6 | 52.5 |
| | | | | | | | | | | |
| **03-SMH-0022** | 21.10 | 1.164 | 322 | 139.1 | 23.0 | 0.89 | 12.3 | 6.6 | 257.9 | 56.83 |
| | | | | | | | | | | |
| **04-SMH-0005-4** | 111.56 | 1.385 | N.M. | 40.4 | N.M. | 1.43 | 20.3 | 9.1 | 248.2 | 113.33 |
| **04-SMH-0017-4** | 70.78 | 1.084 | N.M. | 17.6 | N.M. | 1.32 | 14.9 | 8.3 | 300.5 | 59.22 |
| | | | | | | | | | | |
| **04-SMH-0017-5** | 59.98 | 1.102 | N.M. | 63.0 | N.M. | 0.51 | 7.1 | 5.3 | 216.5 | 23.84 |
| **04-SMH-0018-1** | 86.72 | 0.780 | N.M | 33.3 | N.M. | 1.84 | 27.4 | 11.1 | 340 | 115.67 |

| Sample No. | Th ppm | U ppm | La ppm | Ce ppm | Pr ppm | Nd ppm | Sm ppm | Eu ppm | Gd ppm | Tb ppm |
|---|---|---|---|---|---|---|---|---|---|---|
| **04-SMH-0003-2** | 2.30 | 0.618 | 17.98 | 41.88 | 5.694 | 24.59 | 5.74 | 1.544 | 6.088 | 0.98 |
| **04-SMH-0023-2** | 2.19 | 0.563 | 12.29 | 28.69 | 3.714 | 15.88 | 3.53 | 0.817 | 3.341 | 0.519 |
| **04-SMH-0026-2** | 5.87 | 1.319 | 28.94 | 60.97 | 6.935 | 25.07 | 4.09 | 0.725 | 3.231 | 0.476 |
| **04-SMH-0076-1** | 2.85 | 0.784 | 21.96 | 50.03 | 6.455 | 27.19 | 5.85 | 1.25 | 5.036 | 0.725 |
| **04-SMH-0041-1** | 2.88 | 0.847 | 51.1 | 110.74 | 14.38 | 61.99 | 13.78 | 1.031 | 12.113 | 1.729 |
| | | | | | | | | | | |
| **03-SMH-0022** | 3.69 | 0.954 | 24.4 | 54.32 | 7.246 | 32.31 | 8.16 | 2.452 | 9.696 | 1.605 |
| | | | | | | | | | | |
| **04-SMH-0005-4** | 8.79 | 2.001 | 70.62 | 170.84 | 22.898 | 98.33 | 22.22 | 2.483 | >20.000 | 3.438 |
| **04-SMH-0017-4** | 7.39 | 1.738 | 45.28 | 103.93 | 13.035 | 51.74 | 10.15 | 1.628 | 9.432 | 1.528 |
| | | | | | | | | | | |
| **04-SMH-0017-5** | 2.74 | 0.742 | 8.65 | 22.65 | 3.205 | 14.69 | 3.44 | 0.825 | 3.759 | 0.637 |
| **04-SMH-0018-1** | 9.61 | 2.334 | 54.37 | 120.87 | 15.756 | 67.59 | 15.7 | 2.036 | 17.17 | 2.965 |

| Sample No. | Dy ppm | Ho ppm | Er ppm | Tm ppm | Yb ppm | Lu ppm |
|---|---|---|---|---|---|---|
| **04-SMH-0003-2** | 6.033 | 1.224 | 3.619 | 0.529 | 3.45 | 0.516 |
| **04-SMH-0023-2** | 3.193 | 0.664 | 1.986 | 0.291 | 1.91 | 0.276 |
| **04-SMH-0026-2** | 2.885 | 0.589 | 1.741 | 0.257 | 1.7 | 0.259 |
| **04-SMH-0076-1** | 4.142 | 0.826 | 2.504 | 0.383 | 2.69 | 0.414 |
| **04-SMH-0041-1** | 9.931 | 1.947 | 5.402 | 0.78 | 5.02 | 0.755 |
| | | | | | | |
| **03-SMH-0022** | 10.225 | 2.182 | 6.47 | 0.95 | 6.25 | 0.96 |
| | | | | | | |
| **04-SMH-0005-4** | >20.000 | 4.309 | 12.543 | 1.85 | 11.9 | 1.692 |
| **04-SMH-0017-4** | 9.622 | 2.064 | 6.41 | 0.994 | 6.92 | 1.061 |
| | | | | | | |
| **04-SMH-0017-5** | 4.108 | 0.86 | 2.624 | 0.386 | 2.57 | 0.386 |
| **04-SMH-0018-1** | 19.524 | 4.252 | 13.402 | 2.012 | 13.21 | 1.972 |

**Abbreviations:** N.D. = not detected. N.M. = not measured/analyzed.

This page left blank intentionally

# Appendix 4

# Previous Ownership and Exploration History of the Genex Mine Area

This table represents the highlights of ownership and exploration history in the Genex Mine area up to the present. Many events up to 1985 have been compiled from Legault (1985) and references therein.

**Table 8.** Table of ownership and exploration history in the Genex mine area.

| Dates | Company or Individual's Name | Highlights of Activity |
|---|---|---|
| Prior to 1926 | Prospector Fred Steep | Noticed sulphide mineralization in the area south of Aconda Lake while trapping |
| 1926 | Fred Steep, Phillip Sheehan | Staked the area covering the "surface showings" of sulphide mineralization |
| 1927 | Aconda Mines Ltd. | Surface-trenching and diamond-drilling |
| Claims allowed to lapse | | |
| 1933 | M.J. Tinkess | Re-staked the claims in the area |
| 1937 | Charles McCaughey Alameda Mines, Ltd. | Surface diamond-drilling, dropped the option |
| 1940 | A. H. Graham | Area was re-staked |
| 1942 | Sylvanite Gold Mines Ltd. | Surface trenching, dropped the option |
| 1944–1954 | Mordey Copper Mines Ltd. | Purchased area, 5 diamond drill holes, magnetometer survey |
| 1948 | Millbren Copper Mines Ltd. | Surface diamond drilling, dropped the option |
| 1951 | New Walcoro Porcupine Mines Ltd. | Surface diamond drilling, dropped the option |
| 1954 | Consulting geologist Nelson Hogg | Detailed geologic mapping of the area (Hogg 1954) |
| 1955 | Broulan Reef Mines Ltd. | Electromagnetic survey, 3 diamond drill holes, dropped the option |
| 1956 | Kimberley Copper Mines Ltd. | Magnetic, electromagnetic and self-potential surveys, 31 diamond drill holes, dropped the option |
| 1958 | P.J. O'Neill | Surface trenching, diamond drilling |
| 1959 | Maple Bay Copper Mines Ltd. | Purchased area, electromagnetic survey and 17 diamond drill holes |
| 1960–1962 | Maple Bay Copper Mines Ltd. | Electromagnetic survey and 56 diamond drill holes |
| 1964 | P.J. O'Neill | Diamond drilling |
| 1964–1967 | Genex Mines Ltd. | Purchased area, 50 diamond drill holes, induced polarization survey. Shaft sunk to 84 m with levels at 38 and 76 m. Total 807 m of drifts, 211 m of raises, 95 m of crosscuts, and 82 m of underground drill holes. |
| 1965 | Consolidated Sannorm Mines Ltd. | Induced polarization survey, one diamond drill hole |
| September 1966 | Genex Mines Ltd. | Name changed to Irvington Mines Ltd. |
| November 1966 | Irvington Mines Ltd. | Operations ceased |
| February 1967 | | Company declared bankruptcy |
| 1967 | United Obalski Mining Company Ltd. | Purchased area, geological mapping, surface sampling, ore reserve calculations |
| 1968–1969 | Kenneco Explorations Canada Ltd. | 15 diamond drill holes and dropped the option |
| 1975 | R.S. Middleton | Geologic mapping for the Ontario Department of Mines (Middleton 1975) |
| 1981–1982 | Texasgulf Ltd. | 2 diamond drill holes, geophysics |
| 1981–1982 | Samim Canada Ltd. | Diamond drilling |
| 1985 | Campbell Resources Ltd. | Purchased the area |
| 1985 | Esso Resources | Diamond drilling, stripping |
| 1985 | Mark H. Legault | Detailed surface mapping as a masters thesis (Legault 1985) |
| 1985–1991 | Falconbridge Ltd. (Kidd) | Purchased property, diamond drilling, mechanical stripping, power stripping, geophysics |
| 1993–1999 | Property Inactive | |
| 1999 | Prospectors Alliance Corp. | Mapping, drilling |
| 2001 | Falconbridge Ltd., joint venture with Explorers Alliance, Campbell Resources | Diamond drilling, assaying of grab samples |
| 2004 | Explorers Alliance | Claims transferred |
| The claims in the Genex area are presently held by Explorers Alliance | | |

# Appendix 5

## Outcrop, Drill Hole and Waypoint UTM Locations

This appendix contains locations for all outcrops and waypoints mapped during the course of this project, as well as the collar locations for the drill holes presented in Appendix 2. The locations are provided as Universal Transverse Mercator (UTM) co-ordinates using North American Datum 1983 (NAD83).

Additionally, outcrop photographs are included on MRD 144.

**Appendix 5.** Outcrop, drill hole and waypoint locations.

| Station Number | Station Type | UTM Co-ordinates (NAD 83) | | | Comments |
|---|---|---|---|---|---|
| | | Zone | Easting (m) | Northing (m) | |
| 03-SMH-0001 | outcrop | 17 | 458775 | 5370340 | |
| 03SMH0002 | outcrop | 17 | 458785 | 5370362 | |
| 03SMH0003 | outcrop | 17 | 458800 | 5370350 | |
| 03SMH0004 | outcrop | 17 | 458770 | 5370375 | |
| 03SMH0005 | outcrop | 17 | 458790 | 5370380 | |
| 03SMH0006 | outcrop | 17 | 458800 | 5370395 | |
| 03SMH0007 | outcrop | 17 | 458810 | 5370365 | |
| 03SMH0008 | outcrop | 17 | 458800 | 5370340 | |
| 03SMH0009 | outcrop | 17 | 458785 | 5370290 | |
| 03SMH0010 | outcrop | 17 | 458780 | 5370260 | |
| 03SMH0011 | outcrop | 17 | 458820 | 5370255 | |
| 03SMH0012 | outcrop | 17 | 458837 | 5370260 | |
| 03SMH0013 | outcrop | 17 | 458845 | 5370250 | |
| 03SMH0014 | outcrop | 17 | 458860 | 5370250 | |
| 03SMH0015 | outcrop | 17 | 458885 | 5370275 | |
| 03SMH0016 | outcrop | 17 | 458760 | 5370345 | |
| 03SMH0017 | outcrop | 17 | 458765 | 5370390 | |
| 03SMH0018 | outcrop | 17 | 458790 | 5370410 | trench |
| 03SMH0019 | outcrop | 17 | 458915 | 5370620 | Aconda Zone trench |
| 03SMH0020 | outcrop | 17 | 458801 | 5370363 | |
| 03SMH0021 | outcrop | 17 | 458820 | 5370279 | |
| 03SMH0022 | outcrop | 17 | 458885 | 5370240 | |
| 03SMH0023 | outcrop | 17 | 458860 | 5370245 | |
| 03SMH0024 | outcrop | 17 | 458840 | 5370222 | |
| 03SMH0025 | outcrop | 17 | 458780 | 5370195 | |
| 03SMH0026 | outcrop | 17 | 458775 | 5370160 | |
| 03SMH0027 | outcrop | 17 | 458805 | 5370125 | |
| 03SMH0028 | outcrop | 17 | 458850 | 5370160 | |
| 03SMH0029 | outcrop | 17 | 458830 | 5370198 | |
| 03SMH0030 | outcrop | 17 | 458860 | 5370200 | |
| 03SMH0031 | outcrop | 17 | 458800 | 5370415 | |
| 03SMH0032 | outcrop | 17 | 458748 | 5370220 | |
| 03SMH0033 | outcrop | 17 | 458741 | 5370230 | |
| 03SMH0034 | outcrop | 17 | 458700 | 5370240 | |
| 03SMH0035 | outcrop | 17 | 458735 | 5370138 | |
| 03SMH0036 | outcrop | 17 | 458725 | 5370130 | |
| 03SMH0037 | outcrop | 17 | 458735 | 5370120 | |
| 03SMH0038 | outcrop | 17 | 458705 | 5370128 | |
| 03SMH0039 | outcrop | 17 | 458710 | 5370100 | |
| 03SMH0040 | outcrop | 17 | 458670 | 5370115 | |
| 03SMH0041 | outcrop | 17 | 458725 | 5370158 | |
| 03SMH0042 | outcrop | 17 | 458715 | 5370170 | |
| 03SMH0043 | outcrop | 17 | 458709 | 5370187 | very little outcrop |
| 03SMH0044 | outcrop | 17 | 458697 | 5370200 | |
| 03SMH0045 | outcrop | 17 | 458690 | 5370169 | |
| 03SMH0046 | outcrop | 17 | 458670 | 5370160 | |
| 03SMH0047 | outcrop | 17 | 458685 | 5370198 | |
| 03SMH0048 | outcrop | 17 | 458663 | 5370230 | |

**Appendix 5.** Outcrop, drill hole and waypoint locations -- continued.

| Station Number | Station Type | UTM Co-ordinates (NAD 83) | | | Comments |
|---|---|---|---|---|---|
| | | Zone | Easting (m) | Northing (m) | |
| 03SMH0049 | outcrop | 17 | 458653 | 5370200 | |
| 03SMH0050 | outcrop | 17 | 458635 | 5370165 | |
| 03SMH0051 | outcrop | 17 | 458608 | 5370255 | |
| 03SMH0052 | outcrop | 17 | 458638 | 5370261 | |
| 03SMH0053 | outcrop | 17 | 458635 | 5370300 | |
| 03SMH0054 | outcrop | 17 | 458670 | 5370275 | several small outcrops |
| 03SMH0055 | outcrop | 17 | 458570 | 5370220 | small outcrops exposed on ridge |
| 03SMH0056 | outcrop | 17 | 458513 | 5370263 | |
| 03SMH0057 | outcrop | 17 | 458740 | 5370430 | |
| 03SMH0058 | outcrop | 17 | 458730 | 5370445 | |
| 03SMH0059 | outcrop | 17 | 458690 | 5370440 | |
| 03SMH0060 | outcrop | 17 | 458665 | 5370445 | |
| 03SMH0061 | outcrop | 17 | 458630 | 5370431 | |
| 03SMH0062 | outcrop | 17 | 458547 | 5370418 | |
| 03SMH0063 | outcrop | 17 | 458513 | 5370410 | |
| 03SMH0064 | outcrop | 17 | 458512 | 5370318 | |
| 03SMH0065 | outcrop | 17 | 458530 | 5370285 | |
| 03SMH0066 | outcrop | 17 | 458548 | 5370300 | |
| 03SMH0067 | outcrop | 17 | 458612 | 5370280 | |
| 03SMH0068 | outcrop | 17 | 458580 | 5370330 | |
| 03SMH0069 | outcrop | 17 | 458562 | 5370380 | |
| 03SMH0070 | outcrop | 17 | 458575 | 5370357 | |
| 03SMH0071 | outcrop | 17 | 458617 | 5370414 | |
| 03SMH0072 | outcrop | 17 | 458623 | 5370402 | |
| 03SMH0073 | outcrop | 17 | 458617 | 5370381 | |
| 03SMH0074 | outcrop | 17 | 458608 | 5370360 | |
| 03SMH0075 | outcrop | 17 | 458750 | 5370365 | |
| 03SMH0076 | outcrop | 17 | 458761 | 5370285 | |
| 03SMH0077 | outcrop | 17 | 458757 | 5370265 | |
| 03SMH0078 | outcrop | 17 | 458710 | 5370281 | |
| 03SMH0079 | outcrop | 17 | 458721 | 5370381 | |
| 03SMH0080 | outcrop | 17 | 458660 | 5370363 | |
| 03SMH0081 | outcrop | 17 | 458702 | 5370323 | |
| 03SMH0082 | outcrop | 17 | 458748 | 5370560 | |
| 03SMH0083 | outcrop | 17 | 458610 | 5370593 | |
| 03SMH0084 | outcrop | 17 | 458560 | 5370618 | |
| 03SMH0085 | outcrop | 17 | 458338 | 5370570 | |
| 03SMH0086 | outcrop | 17 | 458365 | 5370530 | may be a very large boulder |
| 03SMH0087 | outcrop | 17 | 458450 | 5370460 | |
| 03SMH0088 | outcrop | 17 | 458550 | 5370530 | |
| 03SMH0089 | outcrop | 17 | 458590 | 5370530 | |
| 03SMH0090 | outcrop | 17 | 458640 | 5370538 | |
| 03SMH0091 | outcrop | 17 | 458680 | 5370518 | |
| 03SMH0092 | outcrop | 17 | 458703 | 5370531 | |
| 03SMH0093 | outcrop | 17 | 458710 | 5370523 | |
| 03SMH0094 | outcrop | 17 | 458780 | 5370486 | |
| 03SMH0095 | outcrop | 17 | 458745 | 5370475 | |
| 03SMH0096 | outcrop | 17 | 458705 | 5370470 | |

**Appendix 5.** Outcrop, drill hole and waypoint locations -- continued.

| Station Number | Station Type | UTM Co-ordinates (NAD 83) | | | Comments |
|---|---|---|---|---|---|
| | | Zone | Easting (m) | Northing (m) | |
| 03SMH0097 | outcrop | 17 | 458690 | 5370470 | |
| 03SMH0098 | outcrop | 17 | 458588 | 5370486 | |
| 03SMH0099 | outcrop | 17 | 458462 | 5370398 | |
| 03SMH0100 | outcrop | 17 | 458387 | 5370386 | |
| 03SMH0101 | outcrop | 17 | 458425 | 5370400 | |
| 03SMH0102 | outcrop | 17 | 458400 | 5370330 | |
| 03SMH0103 | outcrop | 17 | 458440 | 5370358 | |
| 03SMH0104 | outcrop | 17 | 458430 | 5370245 | |
| 03SMH0105 | outcrop | 17 | 458270 | 5370255 | |
| 03SMH0106 | outcrop | 17 | 458230 | 5370305 | |
| 03SMH0107 | outcrop | 17 | 458310 | 5370410 | |
| 03SMH0108 | outcrop | 17 | 458220 | 5370480 | |
| 03SMH0109 | outcrop | 17 | 458660 | 5369620 | |
| 03SMH0110 | outcrop | 17 | 458660 | 5369685 | |
| 03SMH0111 | outcrop | 17 | 458570 | 5369770 | |
| 03SMH0112 | outcrop | 17 | 458480 | 5369990 | |
| 03SMH0113 | outcrop | 17 | 458970 | 5370250 | |
| 03SMH0114 | outcrop | 17 | 458920 | 5370285 | |
| 03SMH0115 | outcrop | 17 | 458950 | 5370295 | |
| 03SMH0116 | outcrop | 17 | 458912 | 5370323 | |
| 03SMH0117 | outcrop | 17 | 458940 | 5370340 | |
| 03SMH0118 | outcrop | 17 | 459010 | 5370305 | |
| 03SMH0119 | outcrop | 17 | 459045 | 5370350 | |
| 03SMH0120 | outcrop | 17 | 459138 | 5370338 | |
| 03SMH0121 | outcrop | 17 | 458937 | 5370362 | |
| 03SMH0122 | outcrop | 17 | 458935 | 5370430 | |
| 03SMH0123 | outcrop | 17 | 459078 | 5370430 | |
| 03SMH0124 | outcrop | 17 | 458401 | 5370450 | |
| 03SMH0125 | outcrop | 17 | 458431 | 5370289 | |
| 03SMH0126 | outcrop | 17 | 458450 | 5370510 | |
| 03SMH0127 | outcrop | 17 | 458540 | 5370463 | |
| 03SMH0128 | outcrop | 17 | 458717 | 5370518 | |
| 03SMH0129 | outcrop | 17 | 458720 | 5370490 | |
| 03SMH0130 | outcrop | 17 | 458942 | 5370463 | |
| 03SMH0131 | outcrop | 17 | 458930 | 5370482 | |
| 03SMH0132 | outcrop | 17 | 458910 | 5370525 | |
| 03SMH0133 | outcrop | 17 | 459066 | 5370480 | |
| 03SMH0134 | outcrop | 17 | 459090 | 5370550 | |
| 03SMH0135 | outcrop | 17 | 458995 | 5370438 | |
| 03SMH0136 | outcrop | 17 | 458866 | 5370472 | |
| 03SMH0137 | outcrop | 17 | 459100 | 5370308 | |
| 03SMH0138 | outcrop | 17 | 459100 | 5370240 | |
| 03SMH0139 | outcrop | 17 | 459017 | 5370245 | |
| 03SMH0140 | outcrop | 17 | 458930 | 5370198 | |
| 03SMH0141 | outcrop | 17 | 458932 | 5370145 | |
| 03SMH0142 | outcrop | 17 | 458890 | 5370138 | |
| 03SMH0143 | outcrop | 17 | 459001 | 5370172 | |
| 03SMH0144 | outcrop | 17 | 459030 | 5370190 | |

**Appendix 5.** Outcrop, drill hole and waypoint locations -- continued.

| Station Number | Station Type | UTM Co-ordinates (NAD 83) | | | Comments |
|---|---|---|---|---|---|
| | | Zone | Easting (m) | Northing (m) | |
| 03SMH0145 | outcrop | 17 | 459080 | 5370202 | |
| 03SMH0146 | outcrop | 17 | 459090 | 5370170 | |
| 03SMH0147 | outcrop | 17 | 459130 | 5370095 | |
| 03SMH0148 | outcrop | 17 | 459038 | 5370075 | |
| 03SMH0149 | outcrop | 17 | 459003 | 5370040 | |
| 03SMH0150 | outcrop | 17 | 458960 | 5370020 | |
| 03SMH0151 | outcrop | 17 | 459020 | 5369930 | |
| 03SMH0152 | outcrop | 17 | 459130 | 5370020 | |
| 03SMH0153 | outcrop | 17 | 458869 | 5370137 | |
| 03SMH0154 | outcrop | 17 | 458900 | 5370011 | |
| 03SMH0155 | outcrop | 17 | 458868 | 5370103 | |
| 03SMH0156 | outcrop | 17 | 458843 | 5370011 | |
| 03SMH0157 | outcrop | 17 | 458195 | 5370030 | |
| 03SMH0158 | outcrop | 17 | 458163 | 5370065 | |
| 03SMH0159 | outcrop | 17 | 458132 | 5370067 | |
| 03SMH0160 | outcrop | 17 | 458156 | 5370088 | |
| 03SMH0161 | outcrop | 17 | 458743 | 5370070 | |
| 03SMH0162 | outcrop | 17 | 458758 | 5370056 | |
| 03SMH0163 | outcrop | 17 | 458793 | 5370065 | |
| 03SMH0164 | outcrop | 17 | 458748 | 5370040 | |
| 03SMH0165 | outcrop | 17 | 458715 | 5370045 | |
| 03SMH0166 | outcrop | 17 | 458733 | 5370033 | |
| 03SMH0167 | outcrop | 17 | 458730 | 5369960 | |
| 03SMH0168 | outcrop | 17 | 458719 | 5369920 | |
| 03SMH0169 | outcrop | 17 | 458797 | 5369950 | |
| 03SMH0170 | outcrop | 17 | 459176 | 5369868 | |
| 03SMH0171 | outcrop | 17 | 459200 | 5369866 | |
| 03SMH0172 | outcrop | 17 | 458740 | 5370700 | |
| 03SMH0173 | outcrop | 17 | 458738 | 5370680 | |
| 03SMH0174 | outcrop | 17 | 458697 | 5370648 | |
| 03SMH0175 | outcrop | 17 | 458640 | 5370690 | |
| 03SMH0176 | outcrop | 17 | 458750 | 5370620 | |
| 03SMH0177 | outcrop | 17 | 459045 | 5370683 | |
| 04SMH0001 | drill-core | 17 | 458226.6 | 5370351.8 | Falconbridge drill hole G32-25 ♦ |
| 04SMH0002 | drill-core | 17 | 458186.5 | 5369509.3 | Falconbridge drill hole G22-14 ♦ |
| 04SMH0003 | drill-core | 17 | 458386.67 | 5369361.07 | Falconbridge drill hole G22-15 ♦ |
| 04SMH0004 | drill-core | 17 | 458797.07 | 5370628.745 | Falconbridge drill hole G32-29 ♦ |
| 04SMH0005 | drill-core | 17 | 459112.61 | 5369605.83 | Falconbridge drill hole G22-12 ♦ |
| 04SMH0006 | drill-core | 17 | 458782 | 5370168 | Explorers Alliance drill hole EGG32-36 ♦ |
| 04SMH0007 | drill-core | 17 | 458769 | 5370208 | Explorers Alliance drill hole EGG32-35 ♦ |
| 04SMH0008 | drill-core | 17 | 458793 | 5370286 | Explorers Alliance drill hole EGG32-34 ♦ |
| 04SMH0009 | drill-core | 17 | 458795 | 5370341 | Explorers Alliance drill hole EGG32-33 ♦ |
| 04SMH0010 | drill-core | 17 | 458652 | 5370570 | Explorers Alliance drill hole EGG32-30 ♦ |
| 04SMH0011 | drill-core | 17 | 458637 | 5370538 | Explorers Alliance drill hole EGG32-31 ♦ |
| 04SMH0012 | drill-core | 17 | 458716 | 5370541 | Explorers Alliance drill hole EGG32-32 ♦ |
| 04SMH0013 | drill-core | 17 | 458752 | 5370551 | Explorers Alliance drill hole EGG32-32A ♦ |

♦ For detailed drill log, refer to drill hole database on MRD 144.

**Appendix 5.** Outcrop, drill hole and waypoint locations -- continued.

| Station Number | Station Type | UTM Co-ordinates (NAD 83) | | | Comments |
|---|---|---|---|---|---|
| | | Zone | Easting (m) | Northing (m) | |
| 04SMH0014 | drill-core | 17 | | | Explorers Alliance drill hole EGG51-26 ♦ |
| 04SMH0015 | drill-core | 17 | 458781.58 | 5369169.43 | Falconbridge drill hole G22-11 ♦ |
| 04SMH0016 | drill-core | 17 | 458763.24 | 5369905.21 | Falconbridge drill hole G32-28 ♦ |
| 04SMH0017 | drill-core | 17 | 458935.696 | 5368465.83 | Falconbridge drill hole G22-16 ♦ |
| 04SMH0018 | drill-core | 17 | 459519.214 | 5369938.587 | Falconbridge drill hole G33-15 ♦ |
| 04SMH0019 | drill-core | 17 | 457694.697 | 5369111.526 | Falconbridge drill hole G22-13 ♦ |
| 04SMH0020 | drill-core | 17 | 459266.559 | 5369849.778 | Falconbridge drill hole G33-13 ♦ |
| 04SMH0021 | drill-core | 17 | 459098.689 | 5370593.092 | Falconbridge drill hole G32-27 ♦ |
| 04SMH0022 | drill-core | 17 | 459210.091 | 5370398.688 | Falconbridge drill hole G33-14 ♦ |
| 04SMH0023 | drill-core | 17 | 458509.871 | 5370770.451 | Falconbridge drill hole G32-26 ♦ |
| 04SMH0024 | drill-core | 17 | 458488.547 | 5370609.101 | Falconbridge drill hole G32-10 ♦ |
| 04SMH0025 | drill-core | 17 | 459159.885 | 5369044.867 | Falconbridge drill hole G23-02 ♦ |
| 04SMH0026 | drill-core | 17 | 459252.062 | 5368247.238 | Falconbridge drill hole G23-03 ♦ |
| 04SMH0027 | drill-core | 17 | 459108.2865 | 5368745.839 | Falconbridge drill hole G22-01 ♦ |
| 04-SMH-0028 | outcrop | 17 | 458310 | 5369620 | |
| 04-SMH-0029 | outcrop | 17 | 458210 | 5369630 | |
| 04-SMH-0030 | outcrop | 17 | 458030 | 5369640 | |
| 04-SMH-0031 | outcrop | 17 | 457970 | 5369627 | |
| 04-SMH-0032 | outcrop | 17 | 458420 | 5370560 | |
| 04-SMH-0033 | outcrop | 17 | 458427 | 5370577 | |
| 04-SMH-0034 | outcrop | 17 | 458403 | 5370581 | |
| 04-SMH-0035 | outcrop | 17 | 458330 | 5370610 | |
| 04-SMH-0036 | outcrop | 17 | 458310 | 5370574 | |
| 04-SMH-0037 | outcrop | 17 | 458336 | 5370537 | |
| 04-SMH-0038 | outcrop | 17 | 458280 | 5370560 | |
| 04-SMH-0039 | outcrop | 17 | 458190 | 5370550 | |
| 04-SMH-0040 | outcrop | 17 | 458189 | 5370608 | |
| 04-SMH-0041 | outcrop | 17 | 458181 | 5370652 | |
| 04-SMH-0042 | outcrop | 17 | 458114 | 5370705 | |
| 04-SMH-0043 | outcrop | 17 | 458118 | 5370770 | |
| 04-SMH-0044 | outcrop | 17 | 457995 | 5370713 | |
| 04-SMH-0045 | outcrop | 17 | 457915 | 5370587 | |
| 04-SMH-0046 | outcrop | 17 | 457953 | 5370582 | |
| 04-SMH-0047 | outcrop | 17 | 458418 | 5369565 | |
| 04-SMH-0048 | outcrop | 17 | 458277 | 5370216 | |
| 04-SMH-0049 | outcrop | 17 | 458266 | 5370186 | |
| 04-SMH-0050 | outcrop | 17 | 458210 | 5370175 | |
| 04-SMH-0051 | outcrop | 17 | 458245 | 5370075 | |
| 04-SMH-0052 | outcrop | 17 | 458270 | 5370115 | |
| 04-SMH-0053 | outcrop | 17 | 458722 | 5370514 | |
| 04-SMH-0054 | outcrop | 17 | 458620 | 5369573 | |
| 04-SMH-0055 | outcrop | 17 | 458575 | 5369570 | |
| 04-SMH-0056 | outcrop | 17 | 458540 | 5369440 | |
| 04-SMH-0057 | outcrop | 17 | 458500 | 5369490 | |
| 04-SMH-0058 | outcrop | 17 | 458450 | 5369390 | |
| 04-SMH-0059 | outcrop | 17 | 458490 | 5369540 | |

♦ For detailed drill log, refer to drill hole database on MRD 144.

**Appendix 5.** Outcrop, drill hole and waypoint locations -- continued.

| Station Number | Station Type | UTM Co-ordinates (NAD 83) | | | Comments |
|---|---|---|---|---|---|
| | | Zone | Easting (m) | Northing (m) | |
| 04-SMH-0060 | outcrop | 17 | 458465 | 5369585 | |
| 04-SMH-0061 | outcrop | 17 | 458405 | 5369535 | |
| 04-SMH-0062 | outcrop | 17 | 458014 | 5369687 | |
| 04-SMH-0063 | outcrop | 17 | 458340 | 5369495 | |
| 04-SMH-0064 | outcrop | 17 | 458300 | 5369435 | |
| 04-SMH-0065 | outcrop | 17 | 458355 | 5369365 | |
| 04-SMH-0066 | outcrop | 17 | 458430 | 5369300 | |
| 04-SMH-0067 | outcrop | 17 | 458345 | 5369230 | |
| 04-SMH-0068 | outcrop | 17 | 458315 | 5369245 | |
| 04-SMH-0069 | outcrop | 17 | 458335 | 5369168 | |
| 04-SMH-0070 | outcrop | 17 | 458405 | 5369195 | |
| 04-SMH-0071 | outcrop | 17 | 458495 | 5369190 | |
| 04-SMH-0072 | outcrop | 17 | 458500 | 5369030 | |
| 04-SMH-0073 | outcrop | 17 | 458455 | 5368998 | |
| 04-SMH-0074 | outcrop | 17 | 458410 | 5369020 | |
| 04-SMH-0075 | outcrop | 17 | 458310 | 5368940 | |
| 04-SMH-0076 | outcrop | 17 | 458200 | 5368930 | |
| 04-SMH-0077 | outcrop | 17 | 458263 | 5369143 | |
| 04-SMH-0078 | outcrop | 17 | 458080 | 5369195 | |
| 04-SMH-0079 | outcrop | 17 | 458200 | 5369315 | |
| 04-SMH-0080 | outcrop | 17 | 458160 | 5369460 | |
| 04-SMH-0081 | outcrop | 17 | 458190 | 5369514 | |
| 04-SMH-0082 | outcrop | 17 | 458180 | 5369570 | |
| 04-SMH-0083 | outcrop | 17 | 458300 | 5369540 | |
| 04-SMH-0084 | outcrop | 17 | 458407 | 5369712 | |
| 04-SMH-0085 | drill-core | 17 | 459445 | 5370844 | Explorers Alliance drill hole 6G-04-2 ◆ |
| W001 | waypoint | 17 | 458780 | 5370227 | |
| W002 | waypoint | 17 | 458770 | 5370222 | |
| W003 | waypoint | 17 | 458689 | 5370081 | |
| W004 | waypoint | 17 | 458630 | 5370084 | |
| W005 | waypoint | 17 | 458642 | 5370109 | |
| W006 | waypoint | 17 | 458673 | 5370222 | |
| W007 | waypoint | 17 | 458603 | 5370165 | |
| W008 | waypoint | 17 | 458633 | 5370143 | |
| W009 | waypoint | 17 | 458610 | 5370117 | |
| W010 | waypoint | 17 | 458586 | 5370117 | |
| W011 | waypoint | 17 | 458591 | 5370175 | |
| W012 | waypoint | 17 | 458606 | 5370205 | |
| W013 | waypoint | 17 | 458527 | 5370169 | |
| W014 | waypoint | 17 | 458526 | 5370199 | |
| W015 | waypoint | 17 | 458587 | 5370212 | |
| W016 | waypoint | 17 | 458571 | 5370419 | |
| W017 | waypoint | 17 | 458502 | 5370384 | |
| W018 | waypoint | 17 | 458508 | 5370344 | |
| W019 | waypoint | 17 | 458512 | 5370303 | |
| W020 | waypoint | 17 | 458511 | 5370295 | |

◆ For detailed drill log, refer to drill hole database on MRD 144.

**Appendix 5.** Outcrop, drill hole and waypoint locations -- continued.

| Station Number | Station Type | UTM Co-ordinates (NAD 83) | | | Comments |
|---|---|---|---|---|---|
| | | Zone | Easting (m) | Northing (m) | |
| W021 | waypoint | 17 | 458581 | 5370280 | |
| W022 | waypoint | 17 | 458550 | 5370327 | |
| W023 | waypoint | 17 | 458552 | 5370353 | |
| W024 | waypoint | 17 | 458620 | 5370317 | |
| W025 | waypoint | 17 | 458487 | 5370570 | |
| W026 | waypoint | 17 | 458448 | 5370076 | |
| W027 | waypoint | 17 | 458942 | 5370274 | |
| W028 | waypoint | 17 | 458965 | 5370343 | |
| W029 | waypoint | 17 | 458896 | 5370345 | |
| W030 | waypoint | 17 | 458871 | 5370340 | |
| W031 | waypoint | 17 | 458418 | 5370416 | |
| W032 | waypoint | 17 | 458901 | 5370475 | |
| W033 | waypoint | 17 | 458867 | 5370535 | |
| W034 | waypoint | 17 | 458942 | 5370544 | |
| W035 | waypoint | 17 | 459014 | 5370503 | |
| W036 | waypoint | 17 | 458955 | 5370456 | |
| W037 | waypoint | 17 | 458925 | 5370458 | |
| W038 | waypoint | 17 | 458897 | 5370419 | |
| W039 | waypoint | 17 | 458871 | 5370377 | |
| W040 | waypoint | 17 | 459037 | 5370232 | |
| W041 | waypoint | 17 | 458900 | 5370175 | |
| W042 | waypoint | 17 | 458959 | 5370144 | |
| W043 | waypoint | 17 | 459135 | 5370153 | |
| W044 | waypoint | 17 | 459108 | 5370141 | |
| W045 | waypoint | 17 | 459025 | 5370043 | |
| W046 | waypoint | 17 | 459052 | 5369967 | |
| W047 | waypoint | 17 | 458900 | 5370143 | |
| W048 | waypoint | 17 | 458961 | 5369984 | |
| W049 | waypoint | 17 | 458720 | 5370027 | |
| W050 | waypoint | 17 | 458709 | 5369885 | |
| W051 | waypoint | 17 | 459232 | 5369885 | |
| W053 | waypoint | 17 | 458595 | 5369546 | |
| W054 | waypoint | 17 | 458485 | 5369334 | |
| W055 | waypoint | 17 | 458239 | 5369083 | |
| W056 | waypoint | 17 | 458218 | 5369118 | |
| W057 | waypoint | 17 | 458204 | 5369420 | |
| W058 | waypoint | 17 | 458484 | 5369648 | |

# Metric Conversion Table

| Conversion from SI to Imperial | | | Conversion from Imperial to SI | | |
|---|---|---|---|---|---|
| *SI Unit* | *Multiplied by* | *Gives* | *Imperial Unit* | *Multiplied by* | *Gives* |
| | | | LENGTH | | |
| 1 mm | 0.039 37 | inches | 1 inch | **25.4** | mm |
| 1 cm | 0.393 70 | inches | 1 inch | **2.54** | cm |
| 1 m | 3.280 84 | feet | 1 foot | **0.304 8** | m |
| 1 m | 0.049 709 | chains | 1 chain | 20.116 8 | m |
| 1 km | 0.621 371 | miles (statute) | 1 mile (statute) | **1.609 344** | km |
| | | | AREA | | |
| 1 $cm^2$ | 0.155 0 | square inches | 1 square inch | **6.451 6** | $cm^2$ |
| 1 $m^2$ | 10.763 9 | square feet | 1 square foot | **0.092 903 04** | $m^2$ |
| 1 $km^2$ | 0.386 10 | square miles | 1 square mile | 2.589 988 | $km^2$ |
| 1 ha | 2.471 054 | acres | 1 acre | 0.404 685 6 | ha |
| | | | VOLUME | | |
| 1 $cm^3$ | 0.061 023 | cubic inches | 1 cubic inch | **16.387 064** | $cm^3$ |
| 1 $m^3$ | 35.314 7 | cubic feet | 1 cubic foot | 0.028 316 85 | $m^3$ |
| 1 $m^3$ | 1.307 951 | cubic yards | 1 cubic yard | 0.764 554 86 | $m^3$ |
| | | | CAPACITY | | |
| 1 L | 1.759 755 | pints | 1 pint | 0.568 261 | L |
| 1 L | 0.879 877 | quarts | 1 quart | 1.136 522 | L |
| 1 L | 0.219 969 | gallons | 1 gallon | **4.546 090** | L |
| | | | MASS | | |
| 1 g | 0.035 273 962 | ounces (avdp) | 1 ounce (avdp) | 28.349 523 | g |
| 1 g | 0.032 150 747 | ounces (troy) | 1 ounce (troy) | **31.103 476 8** | g |
| 1 kg | 2.204 622 6 | pounds (avdp) | 1 pound (avdp) | **0.453 592 37** | kg |
| 1 kg | 0.001 102 3 | tons (short) | 1 ton (short) | **907.184 74** | kg |
| 1 t | 1.102 311 3 | tons (short) | 1 ton (short) | **0.907 184 74** | t |
| 1 kg | 0.000 984 21 | tons (long) | 1 ton (long) | **1016.046 908 8** | kg |
| 1 t | 0.984 206 5 | tons (long) | 1 ton (long) | **1.016 046 90** | t |
| | | | CONCENTRATION | | |
| 1 g/t | 0.029 166 6 | ounce (troy)/ ton (short) | 1 ounce (troy)/ ton (short) | 34.285 714 2 | g/t |
| 1 g/t | 0.583 333 33 | pennyweights/ ton (short) | 1 pennyweight/ ton (short) | 1.714 285 7 | g/t |

## OTHER USEFUL CONVERSION FACTORS

| | *Multiplied by* | |
|---|---|---|
| 1 ounce (troy) per ton (short) | 31.103 477 | grams per ton (short) |
| 1 gram per ton (short) | 0.032 151 | ounces (troy) per ton (short) |
| 1 ounce (troy) per ton (short) | 20.0 | pennyweights per ton (short) |
| 1 pennyweight per ton (short) | 0.05 | ounces (troy) per ton (short) |

*Note: Conversion factors which are in bold type are exact. The conversion factors have been taken from or have been derived from factors given in the Metric Practice Guide for the Canadian Mining and Metallurgical Industries, published by the Mining Association of Canada in co-operation with the Coal Association of Canada.*

ISSN 0826-9580
ISBN 0-7794-7614-X